SIMULATION OF THE INTERMITTENT CUTTING ACTION OF A BANDSAW BLADE

ANAND RAJ DORAISINGAM BEng (Hons)

A thesis submitted in partial fulfilment
of the requirements of
Northumbria University for the
degree of Doctor of Philosophy

in collaboration with Bahco Metal Saws AB

March 2003

DECLARATION

The candidate has not been registered for another award of a University during the research programme.

Work on the Simulation of Intermittent Cutting Action of a Bandsaw Blade has been undertaken at Northumbria University since November 1999. The candidate was employed full-time as a research student and a member of the Bandsaw Development Group under the directions of Professor M.Sarwar and supervision Mr. H. Hellbergh and Dr. P.S. Leung on Simulation of Intermittent Cutting Action of a Bandsaw Blade. Mr. M. Persson was a member of the team assigned to work on the Simulation of Intermittent Cutting Action of a Bandsaw Blade and made significant contributions by jointly carrying out the full bandsaw blade product testing with the candidate. Bahco Metal Saws AB, Sweden, financially supported this programme of work. Work carried out during the research programme has been reported in the following scientific papers:

1. Sarwar, M; Hellbergh, H; Doraisingam, A.R; Persson, M;
   "Simulation of the intermittent cutting action of a bandsaw blade",
   12 International Conference on Flexible Automation & Intelligent Manufacturing, Dresden, June 15, 2002

2. Sarwar, M; Hellbergh, H; Doraisingam, A.R; Persson, M;
   "Bandsawing of Ball Bearing steel", Fifth International Conference on the Behaviour of Materials in Machining, Chester, November 2002

3. Sarwar, M; Persson, M; Hellbergh, H; Doraisingam, A.R;
"Sawability in the band sawing process when machining Hot and Cold work tool steels", Fifth International Conference on the Behaviour of Materials in Machining, Chester, November 2002

ABSTRACT

Bandsawing is a preferred method used by steel stockholders and steel users in industry for cutting-off to size in the primary and secondary processes. The state-of-the-art features in current industrial bandsaw machines have transformed this method for cutting-off stock to size into a hi-tech operation capable of storage and handling. This method is particularly suitable for use in engineering factories involved in fast, highly automated mass-production techniques, providing the user with continuous batches of cut-to-length materials. Bandsaw machines have now superseded power hacksaws and circular saws in cutting rate and lower kerf loss due to better computer-controlled saw machines and improved blade designs (bi-metal HSS, carbide tipped).

Although, there have been some new developments in bandsaw blades (tooth geometry, band material etc.) there are continuous new demands made on the bandsaw blades by materials engineers, challenged with introducing new materials to satisfy the needs of the design engineers, e.g. aerospace industry. There is therefore a need to improve the bandsaw blade. In order to do this we need to have an understanding of the mechanics of the cutting process associated with bandsawing and the various parameters affecting cutting forces, specific cutting energy, metal removal rates etc.

One of the primary problems in evaluating metal bandsaws and developing newer variants, including new saw tooth materials, their heat treatment, or special tooth forms and quality, has been the use of costly and time consuming sawing tests. Furthermore, there are no simple ways of quantitatively evaluating the performance

and life of these bands during sawing. Traditional method used by machine operators to assess the performance of blades only give global data, which is difficult to apply to individual teeth. Therefore there is a need to develop "time compression" test methods for evaluating the performance of bandsaw blades to replace full bandsaw blade testing.

The work presented in this thesis is on the development of a single tooth testing method to simulate the intermittent cutting action of a bandsaw blade. Cutting tests have been performed to assess the testing method by comparing single tooth test results to full bandsaw blade test results. The test method developed is capable of producing scientific data for bandsawing associated with forces, metal removal rate and specific cutting energy when cutting a variety of workpiece materials at different speeds and feeds. Thus, it can be used as a substitute to full bandsaw blade testing.

The cutting data for the workpiece materials tested using the single tooth test method was obtained in 25% of the full bandsaw blade evaluation time. This represents a significant saving in time and cost, which should prove useful to design engineers when designing and testing new prototype bandsaw blades for the future needs of the steel and manufacturing industry involved in metal cutting.

ACKNOWLEDGEMENT

The author expresses his sincere gratitude to his director of studies Professor M. Sarwar, his supervisors Mr. H.Hellbergh and Dr. P.S Leung for their guidance and advice throughout this work. Particular thanks go to Mr. M.Persson for his help and support in the experimental work.

The author is extremely grateful to the authorities at Bahco Metal Saws AB, Sweden and the School of Engineering and Technology, Northumbria University for financing the research programme and for allowing the work to be carried out in their laboratories. Thanks are also due to the technical staff at Bahco Metal Saws AB, Sweden for their help in the bandsaw product tests.

The help and support from the workshop technicians in the Pandon workshop, is greatly appreciated particularly in building the experimental test rig.

Last, but not least, the author expresses his thanks to his family and friends for their encouragement and moral support during the course of the research programme.

NOMENCLATURE

A	Undeformed chip cross-sectional area (m^2)
$A_{c\text{-}FBT}$	Calculated average chip cross-sectional (Full bandsaw blade test) (m^2)
$A_{c\text{-}STT}$	Calculated chip cross-sectional area (Single tooth test) (m^2)
a	Factor relating to the varible-height tooth geometry
b	Factor relating to the setting of the teeth in the band
C_h	Chip thickness ratio
D	Average Tooth Pitch
d	Diameter (m)
E_{SP}	Specific cutting energy (GJ m^{-3})
$E_{SP\text{-}t}$	Specific cutting energy per tooth (GJ m^{-3})
F_v	Cutting force component (N)
F_p	Thrust force component (N)
F_{p0}	Thrust force component – Thrust force transducer at entry (N)
F_{p1}	Thrust force component – Thrust force transducer at exit (N)
F_{vD}	Cutting force component – Dynamometer reading (N)
F_{pD}	Thrust force component – Dynamometer reading (N)

$F_{v\text{-}fbt}$	Cutting force per tooth – Full bandsaw blade test (N)
$F_{p\text{-}fbt}$	Thrust force per tooth – Full bandsaw blade test (N)
$F_{v\text{-}STT}$	Cutting force per tooth – Single tooth test (N)
$F_{p\text{-}STT}$	Thrust force per tooth – Single tooth test (N)
h_c	Undeformed chip thickness (μm)
h_o	Deformed chip thickness (μm)
L	Length (m)
l_{arc}	Arc length of workpiece (m)
n_t	Number of teeth cutting
n	Rotational frequency of machine-tool (r.p.m)
P_m	Power required to perform machining operation (kW)
T_o	Time (s)
t_m	Machine Time (s)
V_b	Band Speed ($mmin^{-1}$)
V_w	Workpiece Speed ($mmin^{-1}$)
V_f	Feedrate ($mmmin^{-1}$)
Vol_{chip}	Volume of Chip

Vol_{mat}	Volume of Material
W	Slot width/Kerf width
W_t	Width of tooth
W_{chip}	Chip weight (g)
γ	Rake Angle
α	Clearance Angle
δas	Nominal depth of cut per tooth (μm)
δa_{STT}	Depth of Cut Per Tooth – Single tooth test (μm)
δa_{fbt}	Calculated average depth of cut per tooth–Full bandsaw blade test (μm)
ρ	Density of Workpiece Material (Kgm^{-3})

TABLE OF CONTENTS

Chapter 1 INTRODUCTION

1.1 Aims and objectives of the investigation

The aim of this investigation is to develop a single tooth time compression test method to simulate the intermittent cutting action of a bandsaw to replace full product testing of bandsaw blades, which is time consuming and expensive.

The objectives of this investigation are to develop the test rig to be capable of producing scientific data for bandsawing associated with forces, metal removal rate and specific cutting energy when cutting a variety of workpiece materials at different speeds and feeds. The method developed will significantly reduce the time required to develop new tooth geometries, which is a major concern among bandsaw blade producers as current methods used are very time consuming and expensive. The scientific data presented will add to current knowledge associated to the bandsawing simulation. The objectives of this investigation will be accomplished by carrying out the following:

i) Development of a scientific single tooth simulation test capable of achieving cutting conditions as for full product (depth of cut 4μm to 36μm)

ii) Development of a suitable tool holder and precision slide system.

iii) Conduct full product tests using bandsaw machines.

iv) Conduct simulation tests for different cutting conditions, workpiece materials and produce data to add to knowledge and to verify the simulation test.

vi) Complete test program and collect data to develop a model capable of converting single tooth test data to full product.

1.2 Literature survey

Metal cutting is an important and major activity and represents a very large segment in industries involved with metallic materials and products. It has been estimated that 75% of machine tools used in production plants are produced from some type of metal cutting process [1]. In the U.K., the cost of metal cutting was calculated to be approximately £20,000 million. As such, metal cutting is a key industrial activity, employing tens of millions people throughout the world [2].

The first metal cutting operation in most manufactured products begins life with a cut-off process more than with any other machining method. Sawing is normally the method employed to perform the cut-off function. Sawing machines that accomplish this function include bandsaws, hacksaws and circular saws. These machines cut with different metal removal rates, power consumption, kerf loss, surface finish, etc. Sawing is only one method of cutting-off materials prior to further machining. Other machining methods such as parting-off using a turning tool in a lathe, abrasive cut-off, friction sawing and wire erosion cutting can be adopted so that the same job can be accomplished. However, bandsawing has an advantage over all other kinds of machining, mainly due to the low kerf loss and the high metal removal rates associated with this process [3].

In the 1990s, the strong economy gave customers in the bandsawing industry the capital required to invest in more bandsaw machines, challenging at the same time bandsaw machine manufacturers to develop machines with better reliability at a competitive price [4]. Bandsaw machine manufacturers responded with high-tech innovations like double-column saws that provide a heavier and more rigid cutting platform, CNC capabilities, bar feeds with sophisticated top clamping, bi-directional vising that allows easier cutting of mill bundles, and more stringent requirements for length tolerances, which are standard features in most industrial bandsaw machines found today. Owing to the development of newer and more accurate bandsawing machines, it has become the preferred method used in the manufacturing industry for cutting-off to size workpieces compared to other traditional sawing methods [4]. Bandsawing currently holds a global market of $600 million USD, $ 200 million USD in US, $200 million in Europe and $200 million in Asia.

While bandsaw machine manufacturers have transformed this once simple method of cutting-off stock to size to a high-tech operation, new hard to cut materials (High Nickel, Tungsten, Vanadium, Chromium, etc.) in the market today are requiring bandsawing machines to be more rigid, have sufficient drive power and a feed system that can feed the blade into the workpiece material uniformly. In order to meet the present day requirements for high volume production and cutting different materials with high precision and speed, it has been necessary for blade manufacturers to constantly improve and develop their products to work in conjunction with bandsaw machines of today to optimise the bandsawing process. The use of new bandsaw blade materials such as carbide tipped, bi-metal, coated

blades, advanced coatings (TiN, TiAlN, TiCN and etc) to cut hard materials has resulted in bandsaws being used at higher cutting speeds (70-150 m/min). This has led to vibrations in the machine and hence shows the weakness of the current saw machines.

Studies of the literature conducted by the author relating to sawing-off processes [3,4,5,6,7,8,9,10,11,12] have revealed concern amongst bandsaw machine and blade manufacturers regarding the future of bandsawing as the preferred method for cutting-off. The main concern is the continuous advancement of circular saw technology, which in a few years will have features that could challenge the bandsawing process or perhaps even replace it. At present, bandsawing is preferred to circular sawing when sawing workpieces larger than 150 mm in diameter. Furthermore, bandsawing also provides more flexibility, so it can virtually cut different materials continuously. A circular saw, on the other hand, can't switch between materials because machine specifications differ for each material type. However, improvements to circular saw machines and blades have allowed circular saws to run at very high speeds (12,000 to 20000 sfm) and produce finishes that, in some applications, require no secondary operations [7,9].

Review of the work of researchers into bandsawing has shown that in the last 20 years most of the research has come from the study of hacksaw blades. Studies using single point cutting tools in turning have also been extensively used as a basis for understanding the effect of cutting edge geometry on performance and wear. Most of the studies performed then have provided blade designers with the knowledge to improve the performance of bandsaw blades. However, bandsaw

blade development is still in its infancy stage since there are very few studies devoted specifically to understanding mechanics of the cutting process involved in bandsawing. It is often claimed that the procedure used by bandsaw blade manufacturers to develop new prototype blades is the main cause of this. The usual sequence of work from initial development of a prototype blade design to the blade going into production involves time consuming and costly tests that inhibit bandsaw blade development.

Most of the earlier studies [13,14,15,16,17,18,19,20,21,22] concentrated on understanding the cutting action of bandsaws have been rewarding through studying the cutting mechanism of power hacksaw blades through simulation work using single point cutting tools. Although there are obvious differences between hacksaw and bandsaw blades, the geometries of the cutting edges, which primarily control the cutting performance, are very similar.

Sarwar [16] in his work on blunt tools found that the depth of cut achieved in hacksawing was smaller than the cutting edge radius of the saw tooth. As such, the cutting action of a bandsaw blade is classified as a blunt tool. The resulting cutting mechanism removes material by a complex combination of modes of chip formation. In today's bandsawing operation the edge radius of nominally sharp tools can be in the range of 7μm-20μm. The average depth of cut achieved by each blade can be between 4μm-30μm [17]. Thompson [18,19,20,21,22] confirmed this in experiments performed to study sawing rates of power hacksaw and bandsaw operations. Thompson found that the principal effect of this cutting geometry is to promote the establishment of a chip by a piling-up action. While

investigating this, Thompson found that the cutting performance of the blade was dependent on the cutting mechanism associated with the gradual increase in the cutting force component, acting on the individual blade tooth during the initial length of the cut. Therefore the cutting performance is dependent on the pitch of the blade teeth and the breadth of the work piece material.

While Sarwar and Thompson contributed significantly to the understanding of the mechanics of cutting in multipoint cutting tools, i.e. edge radius effect and chip formation etc, the main research activity of most researchers in metal cutting has been the investigation of the effects of wear. It is commonly accepted by most researchers [23,24,25,26,27,28,29,30,31,32,33] that temperature predominantly influences both the wear and failure mechanisms that develop in cutting tools. Dautzenbergh [23], investigating the effects of workpiece materials on cutting tools in turning operation, found that tool failure was due to the high temperature in the contact zone of the tool and chip as a result of friction. High temperature substantially increases the diffusion of the tool material in the chip, which changes the chemical composition of the tool. This limits the lifetime of the tool. The study found that lowering friction between chip and tool by using low friction coatings could be more effective than using a harder cutting tool material. Gillibrand et al. [25] studied cutting tool temperature by investigating the influence of low frictional coating (TiN) on cutting forces. His study showed that the use of TiN coated saw tips in experiments, gave a decreased cutting force and in turn decreased the temperature generated near the cutting tool edge. However, Sarwar [27,28,29,30,31] in his work on TiN coated bandsaws found that TiN coatings did not improve the wear resistance of the blade. It was observed that the TiN-coated

blades showed improvement in performance, which was indicated by a reduction in cutting forces and specific cutting energy but the wear lives of the coated and uncoated blades were the same. The reason for this was attributed to the poor quality of the blade manufactured prior to coating. The bandsaw blades having multi-point cutting edges and complex geometrical features and poor edge geometry, make coating difficult. Hellbergh [32] in his paper on bandsaw innovations reported that coating bandsaw blades with TiN PVD coatings was not very economical. The effectiveness of TiN coatings in reducing wear in blades was not as good as in other cutting tools. TiN coating was found to be effective in reducing friction and stopping crater wear on the rake face of the cutting edge but not flank wear, which is normally found in bandsaw blades.

In addition to studying the effects of temperature on wear, full evaluation of metal bandsaws, specifically in terms of saw tooth micro-chipping and its relation, has been the object of a long research effort. Chanderasekaran and Thoors [33] performed extensive study on tooth chipping during bandsawing. The study was aimed at the influence of heat treatment upon the chipping behaviour for high-speed steel, Bi-metal M42 bandsaw variants. The experiments conducted showed that increase in hardness of the bandsaw blade material was closely related to increase in wear, due to chipping. The study found that increase in the content of small carbides improves chipping resistance.

Tool wear has been long identified as an important factor affecting cutting performance and production optimisation [34,35,36,37]. The complex stochastic nature of tool wear is one of the obstacles in achieving manufacturing automation.

Force signals are sensitive carriers of information about the status of machining process, and hence, represent the best alternative to tool wear monitoring. Predicting cutting force in bandsawing is difficult due to the geometrical shape of the cutting edge, which varies as a result of the setting of the saw tooth [38,39,40,41]. In order to predict the cutting forces, Ko and Kim [43] developed a mechanistic cutting force model using mathematical modelling techniques used for the milling process. The mechanistic model in this study uses the instantaneous undeformed chip thickness and specific cutting energy to predict cutting force. The model was developed to include the shape of each tooth in a set. In order to validate the mechanistic model developed, the specific cutting pressure (energy) was first obtained through cutting experiments. The corresponding cutting forces were measured and used to check the cutting force model. Results from the study showed that the mechanistic model developed was able to predict cutting forces. However, the model does not include non-uniform tooth shapes, i.e. vari-pitch bandsaw blades. Choudhury and Kishore [36] developed a tool wear model as a function of force ratio in turning using Taylor's equation. The experimental results obtained showed that the measurement of ratio between the thrust force and the cutting force components was found to provide a practical method for an in-process approach, to quantification of tool wear. The mathematical model developed to predict flank wear was successful as the comparison of experimental with predicted values of tool flank wear showed very close results. The result showed that the flank wear increased linearly with the feed rate, depth of cut and diameter of the work piece material. The method devised was for single point cutting tools.

In order to have an understanding of metal removal in bandsawing operations there is a need for fundamental data associated with forces, metal removal rate and specific cutting energy to improve the process and blade design. One of the primary problems in evaluating metal bandsaws and developing newer variants, involving new saw tooth materials, their heat treatment or special tooth forms and quality, has been the costly and time consuming sawing tests. There are no simple ways of quantitatively evaluating the performance and life of these bands during sawing. Traditionally, the time per cut as well as indirect parameters, such as increase in feed (thrust) force, or the amount of deviation of the saw kerf from the vertical plane are often used as performance criteria. This only gives global data, which is difficult to apply to individual teeth. Therefore, there is a need to develop testing methods that can be representative of a full product performance of a bandsaw blade and give the fundamental data required for optimising the cutting condition. This would also provide a solution to manufacturers of bandsaw blades to decrease the time and cost involved when developing new blade variants. Furthermore, the testing method developed will also enable the acquisition of cutting data for new difficult to cut materials regularly introduced into the steel market in a shorter time.

In view of the impact a "time compression" testing method could have on the future of bandsaw blade development, Wallen [44] devised a pendulum technique testing method to simulate the cutting action of a bandsawing machine using a modified Charpy impact tester. The testing method utilised was used to study metal cutting with respect to cutting and thrust force, chip formation mechanism and finish of the cut surface. The method was successful in the study of individual cutting edge

condition. However, the technique was limited, as it did not allow the study of gradual tooth edge wear, which is vital when studying performance of bandsaw blades.

Development of other methods to evaluate bandsaws has been through the study of wear to predict performance [38]. A rapid method for saw tooth wear testing using a number of short welded lengths of test variants (patch welding) and a new method SKIM for quantifying saw tooth wear were developed. The methods were tested for statistical accuracy and reliability in evaluating saw performance differences by measuring the wear land area on the tooth flank. Measuring the area of the wear land was found to provide information on how the different set tooth was behaving during sawing. Saw tooth material and heat treatment in terms of the method used and the temperatures involved, were the variables used in the experiments. The method was able to provide a quick way to test a number of saw variants. However, the method still uses full product testing to acquire cutting data, which is expensive and time consuming. Furthermore, the results had a number of sources of error, partly due to the software used.

Andersson [45,46,47] performed comprehensive study on the cutting mechanics of individual tooth of a bandsaw blade having different tooth settings. A mechanical force model was devised to describe the variation in the cutting action of the individual tooth. The force model calculates the cutting forces in conjunction with the size of the undeformed chip thickness removed by the different tooth settings. In order to validate the force model, an experimental test rig to measure the cutting force of individual tooth during cutting was devised. The measurement equipment

for the bandsaw experiment uses a specially developed staircase-shaped workpiece adjusted to the geometry of the blade tooth. The objective of the staircase-shape workpiece was to separate the number of teeth engaged at a time during cutting to enable the measurement of cutting force of different set teeth in the bandsaw blade. The experimental study and the use of the force model showed that cutting forces vary during sawing as a result of tooth setting. The results of the test were obtained without the use of cutting fluid as this was not possible using the method devised. This represents a weakness of the test method as the use of cutting fluid can have an influence on the performance of saw blades.

Sarwar et. al. [48] developed a single tooth simulation test using a specially adopted lathe machine. The method was devised to investigate and analyse the characteristics of bandsaw blade performance and design. Data acquired from the simulation test was used to predict transient stress behaviour within bandsaw teeth using finite element models. Experiments were conducted at 10-100 μm depth of cut, and were found to be useful in studying blade performance and cutting characteristics of standard production bandsaw blades. However, the depth of cut per tooth tested was not within the normal operating range, found in actual bandsawing processes where depths of cut are between 4-30 μm.

Although useful when studying the effect of edge geometry during cutting, the methods devised to date, which have looked towards developing testing methods that can be representative of a full product performance test of a bandsaw blade, do not have the capability of studying the effects of saw tooth geometry, i.e. gullet, tooth setting etc., on performance and wear. Furthermore, these methods may not

have commercial application, for instance, used by bandsaw producers in producing scientific cutting data associated with performance when sawing different materials.

The author has conducted experiments using the single tooth test method previously developed by Sarwar et. al [48]. The aim of the test was to validate the simulation test method and to subsequently use this time compression technique to replace full bandsaw product testing to acquire cutting data (cutting forces, speed, feed and specific cutting energy) at 4μm-30μm depth of cut. Preliminary test results have shown that the method can be used in the study of cutting at fine depths of cut [49,50,51]. However, the test was found to produce inconsistent results owing to the stiffness in the lathe cross-slide system, which produced backlash and hence inconsistency when setting the depths of cut. The poor stiffness of the lathe system resulted in the test having to be repeated several times before the required depth of cut was achieved. As such, the single tooth test method therefore requires further development, particularly in the cross-slide system and tool holder. However, the experience gained from performing the test has revealed that the method has the adequate features required for a "time compression" test method.

1.3 Bandsaw evolution

1.3.1 Bandsaw machine

Leighton A. Wilkie invented and patented the first practical metal cutting bandsaw in 1933. Wilkie realised that he could increase productivity and reduce cost by modifying a wood cutting bandsaw machine to have the capability of cutting contours in metal. He adapted a wood saw making it more rigid and increased the power supplied. He built a brazer into the saw frame enabling the saw blade to be joined forming a band after passing it through a starting hole in the workpiece when making internal cuts. Further research and development work produced improved saw guides that could hold the saw blade with better rigidity at the point of cut.

The first bandsaw machine specifically for sawing metal was marketed in May 1935 [53]. The bandsaw machines sold were essentially a bench-type sawing machine mounted on a cast base. The blade life was limited to cutting an average of only 0.015 m^2 of mild steel [53]. Nevertheless, the metal cutting industry quickly realised its possible applications and potential as a fast precision method for performing cutting-off operations.

Simultaneous with saw blade developments was the improvement of machine design and construction. The variable speed drive developed in 1937 was improved to have an increased range of band speeds (0.25-4m/s) [54]. The increased speed made it possible to cut softer materials. Further improvements

continued in the following year raising the band speed to 7.6 m/s [54]. In 1943, the high-speed bandsaw machine was introduced, which was capable of running up to 76 m/s [54]. Mechanical drive system capable of running at higher bandspeed once again stressed the need for greater rigidity. Designers had already found solutions to the challenges met in 1938, by using an all welded, steel frame construction instead of the three-piece cast iron construction of earlier models. In conjunction with increased bandspeeds came an increase in the diameter of band carrier wheels to reduce band flex fatigue. The wheels used in 1937 increased from 300 mm to 400 mm. Today the size ranges up to 1000 mm.

By the end of the 1940s the development of better saw blades, more rigid construction and higher bandspeeds had extracted the full capability of machine design. Design engineers were under pressure to produce machines of greater built-in potential. The modern power-table bandsaw machine supplied the solution. It had the capability of sawing different groups of materials that previously could not be sawn efficiently. Owing to its added power and hydraulically actuated feeding force, these materials could be sawn faster and more accurately. The first of these power table machines emerged in 1949 but these prototypes were followed by more sophisticated models in 1953 [4]. As bandsaw machines became more popular the need for machines designed specifically for heavy industry arose.

Bandsawing is a continuous cutting operation that utilises an endless flexible band. The band is tensioned on two large-diameter rotating wheels mounted on parallel axes some distance apart. The cutting operation is carried out on the section

where the blade is exposed. The band travels in a continuous motion and the process is thrust force controlled with the teeth fed against the workpiece under constant feed condition. In cutting-off operations of workpiece materials, horizontal band machines are used. The machines normally used in this operation are gravity and hydraulic fed machines. Gravity fed machines exist for light duty work in which the thrust load is developed by virtue of the gravity force acting on a massive swing-arm assembly. While these machines are mechanically simple they are limited in respect of the magnitude of thrust load, which can be generated and therefore are light duty machines. Hydraulic fed machines are a type of machine where the thrust load developed is produced by the action of a hydraulic device. This type of machine is mainly used in heavy-duty operations, as the thrust load developed is very high. These machines also represent the majority of bandsaw machines used in industry today.

One of the main improvements made to bandsaw machines was to increase the ridigity of the frame. Bandsaw blades are normally stretched and tensioned to around 210 MN/m^2 in order to cut metal effectively. As such, the column that supports the idler wheel is subjected to high strain. During sawing, a thrust force is applied to the workpiece material and this exerts a downward force on the idler wheel and so imparts a further strain on the column support. Since the deflection or vibration in the column is magnified at the point of cutting, the importance of a rigid column is vital.

Another vital improvement was the use of modern CNC controls. By the end of the 1980's the use of CNC control turned the bandsaw machine into a highly

developed, computer-driven machine [7]. Computerisation of automatic bar feeders allowed the operator to cut different part lengths out of a single bar by programming multiple jobs in the memory of the computer. CNC control also enabled improved control of the hydraulic and pneumatic arm-control system allowing better band feed [7]. These improvements provided manufacturers the tool required to machine difficult to cut materials faster and more accurately, thus reducing the cost and meeting the needs of the supply chain.

1.3.2 Bandsaw Blades

Bandsaw blades used in 1935 were made from standard carbon alloy. These blades, which could cut 0.015 m^2 of mild steel, were gradually improved and by 1939 they were more than 10 times better and could cut an average of 0.20 m^2 [4,7,54]. A significant period in bandsaw blade improvement came in 1953 when research engineers came up with a solid high-speed steel saw blade.

The introduction of high-speed steel blades revolutionised bandsawing, enabling machine operators to cut conventional materials up to 10 times faster and last 30 times longer than carbon alloy blades under normal cutting conditions [4]. The significant improvement in the bandsaw blade performance was attributed to the characteristics of the material, which has a greater hot hardness, better tooth tip hardness, resistance to abrasion and tensile strength.

Bi-metal blades were introduced in 1965 and still comprise the vast majority of blades in use today [4]. These blades consist of a high-speed steel strip electron

beam welded to a tough flexible carbon alloy steel backing material. The teeth are then milled into the high-speed steel strip through to the backing material so that the finished blade has a high-speed steel cutting edge. As the high-speed steel cutting edge does not have to be flexible, it can be harder than a solid high-speed steel blade. This hardness, coupled with the flexibility, delivers a better cutting performance compared to solid high-speed steel while the carbon alloy steel back is less prone to breakage. High-speed steel bi-metal blades can cut up to 13 m^2 of metal at improved cutting rates [53].

Bandsaw blade technology has made great advances in recent years, particularly in the development of cemented carbide-tipped blades. These blades are used for cutting extremely abrasive and difficult to cut materials such as titanium or inconel compared to conventional bi-metal blades. Carbide-tipped blades are well suited to run at higher cutting speed (90-180 m/min) and last 5 times longer than high-speed steel bi-metal blades. Although these blades cost more than most conventional blades they are still preferred, as these blades provide a better finish and give higher production rates [5].

In conjunction with the advancement in bandsaw blade materials, blade designers have modified tooth geometry to improve blade performance. Most tooth geometry in the market today has a variable pitch and positive rake angles. Variable pitch coupled to positive-rake teeth was first introduced at the beginning of the 80's to cut noise and vibration by varying the distance between the cutting edges in repeated patterns. The preference of using positive rake geometry has been showing a very strong trend over recent years. Saw rake angles used to be 0°

rising to 6° in the 80's. Today blades have a positive rake 10° to 15°, normally used when sawing extremely hard steels that require high penetration. The high rake angle reduces cutting forces, thus enabling straighter cuts and longer blade life [32].

1.4 Mechanics of metal cutting

In 1906, Taylor [14] published his famous paper, which reported the effect of tool material and cutting conditions on tool life. The empirical law relating cutting speed and tool life suggested by Taylor is still used today in calculations governing machining economics. Since the publication of Taylor's work in 1906, considerable time and effort devoted to fundamental and empirical work relating to metal cutting has increased, particularly after the publication of the well-known paper by Ernst and Merchant [15] associated with the mechanics of the process. Most of the work carried out by Merchant and Taylor has been mainly concerned with single-point cutting tools.

Most practical machining involves cutting edges inclined at various angles to the cutting direction. The wedge-shaped tool is constrained to move relative to the workpiece material in such a way that the layer of metal removed is plastically deformed to form a chip. The basic cutting mechanism involved can be explained by analysing cutting with a single cutting edge. In both experimental and analytical investigation of chip formation, it has been usual to consider the relatively simple case of orthogonal machining, figure 1. In orthogonal cutting the cutting edge is perpendicular to the cutting speed vector and the feed motion. The cutting tool,

which is wedge shaped consists of two planes intersecting to form the cutting edge, figure 2. The tool cutting face along which the chip flows is known as the rake face, and the surface ground back to clear the machined workpiece surface is known as the clearance face, figure 3. The angle γ between the rake face and the normal to the cutting velocity V_w is termed the rake angle. The rake angle is one of the most important variables which has a profound effect on the chip formation process and hence on cutting forces. The angle α between the clearance face of the tool and the work surface is termed the clearance angle. The clearance angle is generally considered to be of minor importance, as it does not contribute to the process of chip removal; however, it can have an influence on the rate of clearance face wear.

Orthogonal machining conditions approximate quite closely to many practical machining processes, as such the basic mechanism of cutting has been extended and applied to multipoint cutting tools, which have not received the same amount of research attention due to the complexity of cutting mechanisms involved.

1.4.1 Chip formation process

Chip sections have been used extensively to observe the different types of material removal processes, which can take place in machining. The formation of the chip can be described as follows. Consider the wedge type of tool, figure 3, to be stationary and the workpiece approaching the tool with a velocity V_W [1,2]. The material in front of the cutting edge is heavily compressed, plastically deformed along a shear plane/shear zone AB, and continues to flow in a solid form as a chip

with a velocity V_c. The sheared material, the chip, partially deforms and moves along the rake face of the tool, which is called the secondary deformation zone. The friction over where the flank of the tool rubs the newly machined surface is called the tertiary zone. During metal removal, the chip initially sticks to the rake face of the tool. At this instant the friction stress at this point is approximately equal to the yield shear stress of the material at the sticking zone where the chip moves over the material stuck on the rake face of the tool. The chip stops sticking and starts sliding over the rake face. The chip leaves the tool, losing contact with the rake face. The chip tool contact length depends on the cutting speed, tool geometry and material properties. The layer of material removed h_o is plastically deformed into chip thickness h_c, A measure of the efficiency of the cutting process is given by the chip thickness ratio $C_h=h_c/h_o$ [2].

The nature of chip formation produced during metal cutting depends on the material being machined, the cutting conditions and the geometry of the cutting tool. In multi-point cutting edges such as sawing, there is an additional complication as the chip is restricted in flowing due to the gullet. In spite of this, the chip formation is approximately the same for orthogonal cutting. There are three basic types of chips obtained during metal cutting with nominally sharp tools.

i) Discontinuous chip (figure 4a)

ii) Continuous Chip (figure 4b)

iii) Continuous chip with built-up edge (figure 4c)

It can been seen that the machining process reaches a steady state cutting condition when continuous chip (figure 4b) is produced during the cutting process. It is this process which is assumed to apply in most machining analyses. The cutting process is not considered to be a steady state, when the chip produced is discontinuous or when a built up edge occurs.

In multi-point cutting operations such as metal bandsawing, the undeformed chip thickness of the material being removed is often small in comparison to the tooth edge radius [16], as shown in figure 5. The resulting cutting mechanism removes material by a complex combination of 'piling-up" and shearing forces, as reported in for the hacksawing operation [16]. Multi-point cutting is designed to have an enclosed gullet to accommodate the material being removed during the cutting operation. As such, the way the removed material behaves in the gullet can have a significant effect on the chip formation mechanism. With multi-point cutting tools, additional forces arise owing to chip-flow restrictions in the gullet, which leads to inefficient cutting. During cutting the efficiency of the cutting varies along the length of the cut. As the saw tooth progresses through the cut the characteristics of the chip formation and forces alter. Figure 6 shows the material being removed, curled and contained in the gullet [20]. Generally, the chip geometry is affected by many of the following factors:

1) **Workpiece material**, having specific mechanical properties and mechanical strain-rate response. The force required when cutting a chip is normally governed by tool geometry, cutting conditions and the shear yield stress of the material. The shear yield stress is affected by the

temperature in the shear plane and also by the strain-rate response of the material. Workpiece materials can have different microstructures that affect the chip formation. As an example, a material that has a carbide network in a matrix of steel can have discontinuous chip formation as the chip breaks when the cutting edge cuts or deflects on a carbide.

2) **Saw tooth geometry**, such as tooth-height precision, tooth pitch, tooth sharpness, gullet shape and size, gullet surface finish etc. Bandsaws are produced by either milling or grinding the teeth in a strip of bi-metal steel. Most bandsaws have a varying pitch (called vari-pitch) and some have varying tooth height. Bandsaw teeth are also set in different patterns. All of this naturally affects the chip formation. Variation in the accuracy of the manufacturing process, such as tooth height accuracy, tooth sharpness, gullet surface finish, loop waviness and loop weld accuracy also affect chip formation. Variation in tooth height accuracy will result in variation in chip formation with some teeth cutting deeper than they were intended and others not cutting at all [55].

3) **The use of cutting fluid.** The heat produced in the shear zone is also dependent on the heat transfer, heat capacity in both the workpiece material and the cutting tool; the cutting fluid also affects it. Generally "coolants" are used at high cutting speed operations (turning, milling) and "lubricants" are used at low cutting speed operations (broaching, gear cutting). There are a variety of cutting fluids available, such as oil emulsions (oil in water), pure oil and synthetic cutting fluids of different

brands. If applied at a sufficient rate, the cutting fluid can lubricate the cutting edge and transport some heat away from the cutting edge and cool the tool and workpiece material. Cutting fluid can affect chip formation by changing temperature and by reducing friction, but it is very difficult to quantify exactly how much it affects the cutting forces and chip formation.

4) **Cutting speed** affects the chip formation by the heat produced when cutting the material. Higher speed will produce more heat. The chip, the cutting tool, the work-piece material and the cutting fluid transport this heat. The relative rate of heat transported by each of the above is decided by the specific heat capacity and heat transfer capacity of the respective part of the cutting system. It is accepted that temperature and strain rate have a balancing and opposing effect in metal cutting, where strain rate has the effect of work hardening and hence increasing the yield stress of the workpiece material. Increase in temperature reduces the yield stress of the material. Also, the cutting speed affects the strain-rate response of the work-piece material in a direct way even if the temperature is held constant. Different work-piece materials respond in different ways to a change in strain rate, some increase their cutting resistance and some are not affected, while some decrease their cutting resistance.

Figure 7, shows chips collected from a bandsawing operation. The pictures show the variation in the chip produced when cutting stainless steel.

1.4.2 Cutting tool wear

Cutting tools are subjected to extremely severe conditions when in use because they are in metal to metal contact with the chips and the workpiece under conditions of very high stress and temperature. Tools wear by the actions of many mechanisms on both the rake and clearance faces. The effects of wear can be observed when a cutting tools is examined, the rake face and clearance face is often worn to produce a flat surface extending back from the cutting edge, known as a wear land. There are several wear mechanisms present in bandsawing, and three main wear mechanisms have been identified and they are:

i) Adhesive wear

ii) Abrasive wear

iii) Diffusion wear

In the case of adhesive wear, the chip is welded to the saw tooth material as part of the friction mechanism; when the welded junction between the chip and the saw tooth material fracture, small fragments of the saw tooth material can also be torn out leaving a cavity or crater. The form of wear known as abrasive wear involves the loss of the saw tooth material due to the rubbing action of the newly generated workpiece surface and the contact area on the tool flank. Diffusion wear occurs when atoms from the saw tooth material move to the work material [1]. This process, which takes place within a very narrow reaction zone at the interface between the two materials, causes the surface structure of the tooth cutting edge to weaken [1].

Any of the above wear characteristics in bandsawing generally have a significant influence on the performance of the blade. The initial signs of the effect of wear are the obvious increase in the cutting forces especially the thrust force. The increase in the thrust force relates to the reduced ability of the tooth edge to penetrate the workpiece material due to flank wear. In bandsawing the saw teeth are set, when the set teeth begin to wear, this causes the blade to deflect in the kerf, which leads to run-out.

1.5 Cutting parameters affecting metal removal and tool life

1.5.1 Effect of tool geometry

Tool geometry is the branch of metal cutting science that deals with the angles of the cutting tool and the way they influence cutting performance particularly in tool life, temperature, cutting forces, surface finish, vibration and hence production. The influence of rake angle on tool performance and life is well established. Studies have shown [1,2,13, 56] that increasing the normal rake angle reduces the cutting forces and heat generated in cutting. However, there is a limit to this effect; increasing the rake angle decreases the wedge angle of the tool, which can result in a weak cutting edge that can chip or fracture during cutting. Tool flank does not play any part in the process of chip formation. However, the clearance angle, the angle between the flank and the generated surface, can affect the rate at which the flank wears.

1.5.2 Effect of cutting speed and feed

In metal cutting, when the cutting speed or feed is increased, the temperature on the tool face increases. When a tool is operating at low speed, increasing the cutting speed tends to improve cutting conditions by preventing the formation of built-up edges. At high speed, increasing the tool-face temperature by increasing the cutting speed would tend to increase the rate of crater wear.

Although metal removal rate is a function of cutting speed and feed, the specific cutting energy, which is a measure of the efficiency of the cutting process, is largely affected by the depth of cut (which is directly related to the feed), figure 8. At low depth of the cut, the influence of the edge radius effect takes place giving an inefficient cutting action. As such, it is advisable to perform machining at high depths of cut to obtain efficient cutting. In multipoint tools such as bandsaws, this is difficult to achieve, since the beam strength of the band limits the thrust force that can be subjected, which limits the depth of cut.

It is a common experience, when cutting most metals and alloys, that the forces decrease as the cutting speed is raised [1]. The reduction in the forces is partly caused by the increase in temperature as the speed is increased. This causes a drop in shear strength in the flow-zone, which causes an increase in the associated shear angle and a reduction in the energy required for metal removal. Therefore, it is usual that the cutting efficiency improves when the cutting speed is increased. Furthermore, the reduction in the cutting forces, particularly the thrust force component when the cutting speed is increased, will also cause a reduction

in the depths of cut taken. Figure 9 illustrates the major forces acting on the cutting edge.

1.5.3 Bandsaw blade nomenclature and terminology

The bandsaw blades used are normally classified according to their overall dimensions, teeth geometry and the material from which they are made. The following are brief discussions of some of the more important nomenclature and terminologies of the cutting edge of the saw blades used in this thesis. More detailed information about these and other properties of saw blade can be found in the British Standards Institution publication BS 3877 [51]. Figure 10, shows the nomenclature of metal cutting saw blades:

Pitch of teeth:

Described as the number of teeth per unit length of the cutting edge. In most cases the pitch is referred to as T.P.I (Teeth Per Inch). The pitch of the teeth commonly used for metal cutting has evolved significantly in recent years from regular pitch teeth, i.e. 4 T.P.I or 6 T.P.I to blades having a vary-pitch teeth, for example 1.4/2, 2/3 T.P.I. etc. In a variable pitch blade every tooth in each blade section has a different pitch dimension. The 1.4/2 refers to the different pitches in the band, i.e. 1.4 T.P.I and 2 T.P.I.

Set pattern:

To achieve clearance between the sides of the saw blade and the kerf produced; some of the teeth are set to the left and right from the centre line of the blade. There are different set patterns used for this purpose, and these are as follows:

i) Raker set : straight (un-set)-right-left etc.

ii) Combo set : Straight (un-set)-right-left-right-left-right-left-straight etc.

iii) Alternate set : Right-left-right etc.

Besides providing side clearance, the set pattern also provides coolant access and chip removal. The overall width of the blade measure across the set teeth controls the slot width and, therefore the amount of material removed during cutting. The use of the different saw teeth patterns depends on the work characteristics for which the blade was designed. The Raker set is known to provide a better cutting action compared to the Combo Set when cutting tool steel materials. It was found that the distribution of the workload among the teeth in the band during sawing was more uniform, resulting in better wear life [55]. The Alternate set pattern is more regularly used for fine pitch teeth.

Gullet:

The space formed between adjacent teeth is called the gullet. In modern bandsaw blades the gullet shapes and sizes are adequate to contain the volume of chip removed during sawing. It is believed that the gullet has no major influence on the cutting performance of the blade, provided that clogging of the teeth does not occur. However, gullet is always a compromise between gullet capacity, tooth strength and beam strength of the band.

Kerf width:

The width of the slot formed as a result of the overall thickness of the blade measured across the set teeth. Theoretically the kerf width is measured as

Kerf width = Blade Thickness + Magnitude of the left-set from un-set tooth
+ Magnitude of the right from Un-set tooth

However, this is only true if there is no wear on the teeth, which normally happens when the blade is still new. The kerf width is usually smaller than the theoretical kerf width when the teeth are worn.

Rake angle:

The inclination of the cutting face of the teeth measured from the normal to the cutting edge is termed the rake angle. Common tooth profiles used for metal cutting bandsaw blades have positive rake angles (5°-15°).

Cutting edge sharpness:

The sharpness of cutting edges is usually referred to as the cutting edge radius. Examination of the cutting edges of saw blade teeth produced by grinding have shown to have a cutting edge radius in the range 7μm-15μm [17]

Bandsaw industrial codes:

Bandsaw blades are usually expressed in the order shown below:

Blade width (mm) - Blade thickness (mm) -Teeth per Inch (TPI) -Band length (mm)

Example **54 - 1.6 - 1.4/2 - 8800**

Chapter 2 FULL BANDSAW BLADE EVALUATION

2.1 Introduction

While the British Standard BS 3877 [57] gives specifications for bandsaw blades relating to the nomenclature, terminology, dimensions and some tolerances of bandsaw blades, the standard does not specify performance tests but rather only specifies general quality requirements. Thus, both manufacturers of bandsaw blades and users have experienced considerable difficulty in establishing testing procedures, as there are no national or international standards relating to bandsaw performance testing. Recent experience of the author working with bandsaw product performance at Bahco, Lidköping and UNN have found that evaluation of bandsaw blades using commercial bandsaw machines can produce results, which are subjective and varied. The performance and life of bandsaw blades can be influenced by the bandsaw machine characteristics (dynamics of the machine, feed rate, cutting speed etc.). This could influence test data and may contribute to one of the reasons for inconsistency in the test data. Hence, there has been a need to identify the machine characteristics under normal working conditions and to investigate the mechanics of the sawing process and parameters affecting metal removal rate.

This chapter provides full details and specification for the setting-up of a bandsaw machine and undertaking bandsaw blade evaluation using a fully instrumented commercial bandsaw machine. Details are provided on the methodology used in assessing the characteristics of the bandsaw machine, instrumentation used and

the relevant parameters measured for different workpiece materials. The derived parameters (specific cutting energy) for assessing the blade performance and the presentation of data are also explained. The full bandsaw methodology described in this chapter have been successfully implemented by the collaborating company (Bahco Metal Saws AB) for testing and evaluating bandsaw blades in their R & D centre.

Scientific cutting data (forces, specific cutting energy, etc) from the performance tests were obtained using full bandsaw blades when cutting hot work tool steel, cold work tool steel and stainless steel. These materials were selected as they represent new materials, which are commonly used in the steel market today. Besides this, they also posses different material characteristics, and hence produce different cutting data, which was required for use in the validation of the single tooth simulation test method discussed in chapter 4.

2.2 Experimental set-up

2.2.1 Bandsaw machine characteristics

The machine used was a Behringer production bandsaw machine, figure 11. The bandsaw machine is a double column vertical pillar machine, which features advancements such as precise band linear guides, hydraulic band tensioning, quick band change and material clamping on both sides of the cut. The bandsaw machine was also equipped with CNC, which is completely programmable, reduces the amount of operator handling. The CNC allows straightness and

squareness of the cut to be monitored and controlled to maintain pre-set tolerances set by the operator. Table 1, shows the bandsaw machine specification

2.2.2 Instrumentation

The bandsaw machine described in section 2.2.1 was fully instrumented to have the capabilities for measuring and monitoring cutting forces, cutting speed and feedrate.

The cutting force and the thrust force components were measured using strain gauge transducers located on the frame of the machine. The outputs from the transducers were fed into a high frequency amplifier and A/D converter (data logger) and the data was stored and processed by a computer on-line. A schematic of the experimental set-up is shown in figure 12. A detailed description will follow, discussing the instrumentations on the machine and the calibration tests for these instruments in section 2.3.

2.2.2.1 Force measurements

The cutting force (F_V) was measured in terms of an indirect force measurement. The motor that rotates the bandsaw wheels is situated on the back of the machine, where it hangs freely around its axis with the centre of rotation, behind the right wheel, as shown in figure 13. The force transducer located just below the motor measures the cutting force from the torque produced on the bandsaw carrier wheel, which develops when it is cutting.

Two transducers mounted in the band guides, figures 14 and 15, measure the thrust force (F_P). The band guides are made of tungsten-carbide inserts connected vertically to a rod, which supports the bandsaw blade. The other end of the rod is connected to a force transducer. When the band is loaded vertically, the transducers are loaded, giving the vertical forces. There are two force transducers for measuring the thrust force. The transducers measure the thrust force at entry and exit of the bandsaw blade through the workpiece material. The sum of the forces, represent the total thrust force (figure 20). On top of the band guides, there are vertical adjustment screws. They are used to ensure that the band is horizontal and not slanting in the band guides. Slanting of the band causes variation in the thrust force measured, as one transducer will register a higher force.

The outputs from the load transducers were sent to a data logger acquisition system (HBM Spider 8) figure 16, where these signals were processed. The data-logging device sends the data accumulated to the computer shown in figure 17. The computer has a data acquisition program called HBM Catman, which gives a graphical representation of the thrust force and cutting force measured by the force transducers.

2.2.2.2 Feed rate measurement

The feed-rate was set, by programming the CNC on the machine manually using the keyboard shown in figure 18. A rotary sensor positioned at the back of the bandsaw machine measures the feed rate, figure 19. The rotary sensor has a spring-loaded wire that goes from the sensor to the base of the machine. When the

bandsaw machine was fed downwards, the movement generated a specific number of electric pulses per second in the feed meter, which was sent to the data acquisition system to be transformed into the feed rate.

2.2.2.3 Cutting speed measurement

Similarly to the setting of the feed rate, the cutting speed can also be programmed into the machine. When the speed was programmed, the CNC control system had the capability of deciding the power necessary to feed the motor to rotate the bandsaw carrier wheels at the correct speed. Since there was no instrumentation on the bandsaw machine to measure the band speed, a hand held tachometer was used to determine and calibrate the band speed.

2.3 Machine calibration test

2.3.1 Dynamometer test to calibrate the load transducers

Prior to any tests, the force measuring system in the machine, i.e. load strain gauges located on the frame of the bandsaw machine was calibrated and the accuracy of the force measuring system assessed along with the feedrate measurements.

This was performed using a 3-axis force component Kistler dynamometer clamped in the vice jaws of the machine. A Stainless Steel workpiece material (Sandvik Sanmac 304L), dimensions 154 x 80 x 50 mm (width x length x height), was

mounted on top of the dynamometer using the strap holes provided. Figure 20 shows the dynamometer set-up for a range of cutting speeds (31m/min- 60 m/min) and feedrates (10mm/min-40 mm/min). The cutting force component (F_v, F_P=$F_{P\,0}$+$F_{P\,1}$) as measured by the machine load cells and the corresponding cutting force ($F_{v\,D}$ and $F_{p\,D}$) measured by the dynamometer were recorded simultaneously. The result of the test was plotted as shown in figures 21-23 for different feeds and cutting speeds.

i) F_v - Cutting force component measured by the load transducer attached to the motor plate of the Bandsaw machine

ii) F_p - (= $F_{p\,0}$ + $F_{p\,1}$) Total thrust force component measured by the load transducers located on the frame of the bandsaw machine (figure 14-15)

iii) $F_{v\,D}$ - Cutting force component measured by the Dynamometer

iv) $F_{p\,D}$ - Thrust force component measured by the Dynamometer

The graphs show only a small difference between the forces measured by the dynamometer and forces monitored by the Behringer machine transducers. The transducer for measuring the horizontal force has an error of approximately 0.9% (average value), the transducer for the vertical force has an error of approximately 0,2% (average value). Since the error was small, the force signal output from the strain gauge transducers was considered comparable to that from the Kistler dynamometer.

2.3.2 Feedrate sensor calibration test

The feedrate measured by the sensor on the machine was checked for accuracy. This was performed by recording the time taken to cut through a section of the workpiece material. The feedrate was calculated by dividing the height of the workpiece with the time recorded to cut through the workpiece. The height of the workpiece and the time were measured with a vernier and a stopwatch.

The feedrate was checked for consistency using a range of different combinations of nominal depth of cut per tooth and cutting speeds. Table 3 shows a summary of the cutting parameters used in the test. All tests performed were repeated twice. The values obtained from the tests were plotted and illustrated on graphs shown in figure 24 and 25. The result shows that the feedrate measured by the feed sensor is approximately 1.6% higher than the feedrate calculated. This error is minor and can be considered negligible.

2.4 Bandsaw blade specification

A great deal has been written and discussed about saw blades and their characteristics. However, most of the studies carried out to date on bandsaw blades have been on blades with regular pitch. Recent innovative work by saw blade manufacturers has resulted in the development of variable pitch bandsaw blades. It has been reported [3] by manufacturers that this type of blades has become the most commonly used by machine operators to saw metal workpieces to size as these blades give a marked reduction in resonance and vibration

producing a smoother and quieter cut compared to regular pitch saw blades. The consequence of this has led to the gradual phasing out of regular pitch blades.

To stay up to date with the saw blades commonly used in the market today, the author has selected a variable pitch blade for the full bandsaw product tests. The bandsaw blade used was a ground M42 HSS-54-1.6-1.4/2 (variable pitch)-8800-(variable height). Details of the blade geometry and specification are shown in figure 26. The variable height refers to the height of the teeth in the band, where every second tooth in the band has a height difference of 0.15 mm. Therefore in a 8800 mm band only half of the number of teeth is engaged in cutting. This blade was selected as it provides stability during sawing of tool steel materials. The nominal chemical composition of the band material and the hardness of the tooth are shown in table 4 and table 5.

2.4.1 Bandsaw blade specification checking procedure

Bandsaw blades often fail prematurely during cutting due to chipping and defects of the tooth edge caused by mishandling. Therefore, in order to ensure this from occurring, visual examination of the saw edges was performed using a magnifying glass. Besides this, setting of the teeth in different parts of the band was also measured and the accuracy of the set was compared to the specification supplied by the bandsaw blade manufacturer. The blades used for the tests all conformed to the specification supplied and were free from edge defects.

2.5 Workpiece material examination

2.5.1 Sample preparation for hardness and microstructure testing

Hot work tool steel, cold work tool steel and stainless steel workpiece materials were selected and used for the full bandsaw product test for their different machining characteristics. The hot work tool steel and cold work tool steel represent some of the new difficult to cut material recently introduced into the steel market. Since these materials do not have an international specification, the author has identified them as Workpiece-X for the hot work tool steel and Workpiece-Y as the cold work tool steel in this thesis. A brief discussion concerning the use and characteristics of the materials is given in the following sections.

The workpiece materials tested in full product bandsaw testing were prepared according to figure 27. Sample pieces from different positions of the workpiece were taken and the isotropy for the workpiece was investigated by measuring hardness and observing the microstructure.

For hardness and microstructure evaluation, pieces 1, 3, 5, 6, 8, 10, 11, 13 and 15 were used. Pieces 2, 4, 7, 9, 12 and 14 were saved to make further testing possible. The test pieces were mounted in Bakelite plastic using a standard laboratory hot mounting machine (Buehler). To prepare the test piece surface the plastic mount was ground using silicon carbide grinding papers (220, 600 and 1000 grit) in a laboratory wet grinding machine (Struers Knuth Rotor). The ground

surface was polished using polishing discs and diamond suspension (6, 3 and 1 μm diamond size) in a laboratory polishing machine (Struers).

2.5.1.1 Hardness testing

The hardness testing was performed with 1 kg load in a calibrated hardness-testing machine (Buehler). A minimum of 4 hardness values was taken for every test-piece, with the average hardness being stated.

2.5.1.2 Microstructure sample etching

The samples were etched to evaluate microstructure. Different etch agents were used according to table 6. The special etch agent was used to observe grain boundaries as well as general structure. Hydrochloric acid was used to observe general structure of materials that are difficult to oxidise. The microstructure was evaluated using a Nikon microscope with magnifications 50, 100, 200, 400 and 1000.

2.6 Material specifications & characteristics

2.6.1 Austenitic stainless steel

Stainless steels are selected as engineering materials mainly because of their excellent corrosion resistance, which is principally due to their high chromium contents. In order to make steels stainless, at least 12% chromium is required.

Chromium makes the iron surface passive by forming a surface oxide film that protects the underlying metal from corrosion in oxidizing media.

The addition of nickel to stainless steels improves the ductility and formability of the steel by making it possible for the austenitic structure to be retained at room temperature, keeping the steel in its soft state. Without nickel the material would harden in processing and might not have desired properties in its finished state. Some austenitic stainless steels are subjected to severe work-hardening, which is mainly an effect of unstable austenite transforming to harder phases when plastically deformed, these meta-stable steels can be made stable by further addition of nickel. Nickel also has a small effect on improving the corrosion resistance.

In stainless steel, the carbon content is very low because its chemical solubility in the steel is low. Excessive amounts of carbon will exist in its pure form (as carbon molecules or graphite) and can react with chromium, preferably in the grain boundaries where the need for energy is least. If chromium carbides form in the grain boundaries, the surrounding material is at risk of being depleted of chromium, making inter-granular corrosion possible.

The silicon content is used to deoxidise the steel before solidification, with silicon reacting with oxygen; it can also have an effect on machinability by lubrication of the cutting edge. The sulphur content is likely to have an effect on machinability by lubrication of the cutting edge rake face as well as weakening the grain boundary shear strength in the steel. It is undesired to have too much oxide in the steel since

such inclusions can make steel brittle. In steel-melts, some melting methods use refinements to remove slag such as silicon oxide.

2.6.1.1 Stainless Steel 304L

This stainless steel is used in a variety of applications, such as flanges, valves, fittings, couplings and seals in petrochemical, food and chemical industry for its improved machinibility. The improved machinability has been achieved through optimising the microstructure and non-metallic inclusion content. Stainless Steel 304L, is a stainless austenitic chrome-nickel steel with a chemical composition as shown in table 7. The addition of sulphur and phosphorus is the probable reason for the improved machinability. Table 8 shows the standard numbers of this material.

The material is delivered in solution-annealed condition. This means that it is in its softest state, all internal stresses that come from rolling and other steel mill operations have been removed by holding the material at 1040-1100 °C during approximately 1 hour, then cooling it rapidly in circulating air or water. For this particular kind of material the heat treatment results in a soft austenitic microstructure. If the cooling is too slow, carbon will have time to react with chromium to form chromium carbides in the grain boundaries, which can result in inter-granular corrosion.

Type 304L is a stable austenitic steel, and will not work-harden to the same extent as a meta-stable austenitic steel. Work hardening can therefore not be expected in any significant amount.

2.6.1.2 Discussion

The hardness (HV1) of a cut-off work-piece is shown in figure 28. The dimension of the work-piece was 155 mm wide / 107 mm high. The hardness was tested on the pieces described in section 2.5. The hardness values indicate that the material has a uniform structure with equal machinability throughout the height of the workpiece, since the hardness value is an indication of the strength of the material. Examination of the microstructure showed that the workpiece was not uniform. The microstructure, figure 29, shows particles of chromium carbides or silicon oxide embedded in an austenitic steel matrix. The austenitic structure shows a uniform grain size. Furthermore, the distribution of particles is not equal throughout the workpiece material; positions 3, 5 and 15 have smaller particles than the other positions. This can lead to varying machinability, leading to force variations throughout the cutting operation.

2.6.2 Hot work tool steels

Hot work tool steel is used in tools processing molten or heated metal or polymer, as in die casting moulds or hot extrusion nozzles and inserts, operating at high temperatures (500 °C in some extrusion operations). The required properties of a

hot work tool steel is one or more of the following, depending on the specific use of the tool:

- Adequate resistance to wear at elevated temperatures
- Enhanced hot yield strength and hot hardness
- High level of temper resistance and resistance to softening at elevated temperatures
- Good compressive and bending strength at high temperatures
- High creep strength
- Acceptable resistance to thermal fatigue
- Increased thermal conductivity and low thermal expansion to avoid thermal cracking and fatigue.

Hot work tool steels usually have a relatively low carbon content. The main reason for this is to get high ductility of the steel when hardened, which is a desired property to get shock resistance. The low carbon content will not allow the steel to get high hardness after hardening.

Chromium and molybdenum is used to increase hardenability, molybdenum also increases hot hardness and hot strength. Vanadium can be used as a grain size refinement, with vanadium carbides acting as nucleation points in solidification. But the main purpose was to prevent grain growth during hardening of a tool. Most other carbide types are dissolved in hardening. Vanadium also increases hardenability.

Silicon is used to deoxidise the steel before solidification, with silicon reacting with oxygen, but the main reason for using a relatively high amount was to achieve oxidation resistance for the tool since it is used at elevated temperatures.

2.6.2.1 Workpiece-X (Hot work tool steel)

Workpiece-X is a hot work tool steel with a chemical composition as shown in Table 7. The relatively low amount of carbon keeps carbide content at a very low level. The alloying elements increase through hardenability for large work-pieces, so that a homogeneous hardened structure can be obtained even in large workpieces. The alloying elements also increase the hot hardness so that strength can be maintained at elevated temperatures (500 °C in some extrusion operations)

Tools made from Workpiece-X are generally heat treated so that the hardness ranges from 35 to 50 HRC, and are often surface treated to increase the wear resistance. The material is delivered in a soft annealed condition. Internal stresses that come from rolling and other steel mill operations were reduced by heating the material to 850 °C, then cooling it slowly to 650 °C followed by further cooling in air. This operation also transforms the structure back to a state where it consists of a soft ferrite matrix with carbides embedded in it. Since the alloy content is relatively high, fast cooling from above 850 °C results in partial hardening that can be undesirable (resulting in a slight increase in hardness and a partial transformation to hardened structure).

2.6.2.2 Discussion

The hardness (HV1) of a cut-off work-piece is shown in figure 30. The dimension of the work-piece was 256 mm wide / 75 mm high. The hardness values indicate that the material has uniform structure with equal machinability throughout the height of the work-piece, since the hardness value is an indication of the strength of the material. The microstructure of the material, in figure 31, shows a small amount of large undissolved carbides. The structure consists of ferrite with numerous small, dispersed carbides. These carbides can be seen at magnifications 400 and 1000, at lower magnifications the small carbides have the appearance of dark fields in the structure.

The different grains have varying orientation and carbide content, which results in different coloration of the grains and different darkness. All test pieces appear to have almost equally coarse structure, which should represent equal machinability throughout the work-piece.

2.6.3 Cold work tool steels

Cold work tool steels are used in cold working (tools) operations such as forming, blanking, cold drawing, punching, cold rolling, compacting dies, cold extrusion etc. The tool operates at lower temperatures than the hot work tool steels; therefore it does not need to have high strength at elevated temperatures. Instead it has high compressive strength and high resistance against wear, but also needs to resist chipping. To achieve a high wear resistance, it has an alloying content that allows

high hardness as well as wear resistant carbides in its microstructure. The high carbon content of cold work tool steels will raise the matrix hardness of a hardened product. The carbon content is also high enough to make carbides possible, embedded in the matrix. Part of the chromium and tungsten content will dissolve in the steel matrix during hardening, increasing hardenability. The remaining part will stay in the form of carbides. Manganese will also increase the hardenability of the steel matrix. Silicon and manganese act as deoxidisers in the steel melt.

2.6.3.1 Workpiece-Y (Cold work tool steel)

The chemical composition is shown in table 10. The high amount of carbon allows some of the alloying elements to form carbides; it also raises the possible matrix hardness after hardening. The carbides will consist of chromium and tungsten carbides. Tools made from Workpiece-Y are generally heat treated so that the hardness ranges from 55 to 62 HRC, and are sometimes surface treated to increase the wear resistance. The material is soft annealed in its as delivered state. Annealing transforms the structure back to a state where it consists of a soft ferrite matrix with carbides embedded in it. Since the alloy content is relatively high, fast cooling from above 850 °C results in partial hardening.

2.6.3.2 Discussion

The hardness (HV1) of a cut-off work-piece is shown in figure 32. The dimension of the work-piece was 253 mm wide / 83 mm high. Figure 33 illustrates the microstructure of the material, which shows large undissolved carbides in a

ferrite/dispersed carbide matrix. The small, dispersed carbides can be seen at magnifications 400 and 1000. At lower magnifications the small carbides have the appearance of dark fields in the structure.

Test piece 8 has a coarser carbide structure than the other pieces. This can be expected since piece 8 is in the centre of the work-piece and will have cooled slower than the other positions. The difference in coarseness of the large carbide net may vary machinability throughout the workpiece.

2.7 Cutting test methodology

2.7.1 Mapping test to determine the cutting condition to use in the full bandsaw blade product test

Prior to running the full bandsaw program, a series of preliminary cutting test were performed on the workpiece materials to determine the cutting conditions to use for the tests, i.e. speed, feed rate and cutting depth of cut. The test is commonly known as a Mapping Test and is usually performed on materials with unknown machining data to map and identify the boundary conditions (max/min speed, max/min feed rate) for the material. The tests were carried out by using random combination of bandspeed with feed rate (depth of cut per tooth) within the limits of the machine and bandsaw blade, appendix 1. These limits are based on the following criteria:

i) A sudden and significant increase in forces

ii) Rapid wear of the cutting teeth

iii) Blade run-out

iv) Excessive heat generation (cutting fluid vaporising, blue chips)

2.7.2 Feedrate setting

The keypad control on the Behringer bandsaw machine does not allow depth of cut setting. To run a test at a given depth of cut per tooth, the feedrate had to be determined. The feedrate was calculated using the following equation below:

$$\delta as = \frac{D \cdot V_f}{V_b \cdot 1000} \qquad (2.1)$$

Derivation of δas, is shown as follow:

At T_0 (instantaneous time) the bandsaw tooth has moved a distance D, which is the distance between two teeth (pitch). In the same instant, the tooth has also been vertically fed a distance that is δas.

Therefore,

$$T_0 = \frac{D}{V_b} \qquad (2.2)$$

and also,

$$T_0 = \frac{\delta as}{V_f/1000} \qquad \text{where the 1000 is to convert mm/min into m/min} \qquad (2.3)$$

Putting Equation (1) into (2):

$$\frac{D}{V_b} = \frac{\delta as}{V_f/1000} \qquad (2.4)$$

rearranging for δas

$$V_b = \frac{D * V_f}{\delta as * 1000} \qquad (2.5)$$

Since, the cutting speed and the nominal depth of cut (set depth of cut) are known, the feedrate can be calculated using equation 2.5.

2.7.3 Cutting test conditions

The test conditions for Workpiece-X, Workpiece-Y and Stainless Steel 304L were determined by conducting the Mapping Test. In order to study the effect of different cutting parameters on the cutting force components (Fv, Fp), the cutting parameters, i.e. speed and feed, were evenly spread to cover the whole range. Table 11-13 shows a summary of the test conditions used when sawing Workpiece-X, Workpiece-Y and Stainless Steel 304L.

The full bandsaw blade test was conducted by using random combination of the cutting parameters determined from the mapping test. Since, this was a performance test for the blade in its new condition, it was vital that the forces measured were not influenced by wear. An effective method used to monitor and to ensure this from happening was to repeat the first test cut (Reference cut) performed in the test program. Normally, this was performed after the fifth test cut. The forces were then compared to see if they were the same. If the saw teeth were beginning to wear, the forces would have typically increased and would not have matched the force curves obtained from the reference cut. In this case, the bandsaw blade would have been replaced with a new blade.

2.8 Cutting test results

2.8.1 Determining the average forces during cutting

The average cutting force and average thrust force per tooth may be defined as the average force developed between the saw blade and the workpiece material during sawing at the steady state, assuming that each tooth in contact carries equal load.

Figure 34 shows a typical force-time trace recorded from the outputs of the transducers attached to the bandsaw machine. These forces were recorded during a full cut of the bandsaw blade when cutting a rectangular bar of 254 mm x 153 mm. The cutting force components Fv and Fp were obtained by taking average force values at the steady state condition, shown by the dotted lines on the force-

time trace. The cutting force and thrust force values obtained were tabulated as shown in appendix 2.

2.8.2 Specific cutting energy (E_{SP})

The efficiency of the cutting process for the workpiece materials can be measured by calculating the specific cutting energy. The specific cutting energy is defined as the energy required to remove a unit volume of material; the lower the specific cutting energy value the more efficient the cutting process [2]. The specific cutting energy E_{SP} is derived as follows:

The power required to perform a machining process P_m is the product of the cutting speed V_b and the cutting force F_v. Thus,

$$P_m = F_V . V_b \qquad \text{Watt (Nm/s)} \qquad 2.6$$

And,

Metal removal rate (MRR) for bandsawing process = $\frac{\text{Volume of material removed}}{\text{Machining time}}$

$$= \frac{Vol_{mat}}{t_m} = A_c \cdot \frac{L}{t_m}$$

$$= A_c . V_b \qquad 2.7$$

Therefore, the energy consumed per unit volume of material removed (specific cutting energy) can be obtained by dividing equation 2.1 with 2.2.

$$\frac{P_m}{MRR} = \frac{F_V}{A_c} \cdot \frac{V_b}{V_b} \qquad (Joule/m^3) \qquad 2.8$$

$\therefore$

$$\text{Specific Cutting Energy, } E_{SP} = \frac{F_V}{A_c} \qquad 2.9$$

Where, F_V - cutting force

A_c – Undeformed chip cross-sectional area

The specific cutting energy represents the rate of energy consumed during machining and can vary for different materials and is affected by changes in cutting speed, feed and saw tooth geometry. Therefore, the specific cutting energy for the bandsawing operation is a very useful parameter for determining the efficiency of the cutting action of the saw blade.

A convenient method of assessing the cutting efficiency of the blade is by means of a graph showing the specific cutting energy against the average depth of cut per tooth. A typical graph would generally show an exponential curve, where the specific cutting energy is usually reduced with an increase in cutting depth of cut per tooth. This happens as the cutting edge effect reduces (as the depth of cut is increase), thus resulting in increase in cutting efficiency. The specific cutting energy parameter is used throughout the present work for assessing the blade

performance. A sample calculation on how the specific cutting energy was calculated is shown below.

Sample calculation 2.1

Consider the cutting force value taken for Workpiece-X (hot work tool steel) material cutting at 31 m/min using a nominal depth of cut per tooth of 1 μm (appendix 2, table 18-1). The width of the chip was assumed to be the same as the kerf width, in this case was measured to be 2.6 mm.

Cutting force, Fv = 375 N

Nominal depth of cut per tooth, δas = 1 μm

Slot Width, W = 2.6 mm

Undeformed-Chip Cross-Sectional Area, $A_c = \delta as \times W$ (m^2)

$= (1 \times 10^{-6}) \times (2.6 \times 10^{-3}) = 2.6 \times 10^{-9}\ m^2$

The cutting force value was a product of the number of teeth cutting. For a 1.4/2 T.P.I pitch blade cutting a 254 mm breadth workpiece material, there will be 17 teeth cutting.

Therefore, $E_{sp} = \dfrac{F_V}{(17)A_c}$

Specific cutting energy $E_{SP} = 375 / 17(2.6 \times 10^{-9})$

$= 8.48\ GJ/m^3$

2.9 Discussion of cutting test results

Full bandsaw product tests were performed for Workpiece-X, Workpiece-Y and Stainless Steel 304L using the cutting condition shown in section 2.7. The raw data obtained from the tests were processed and presented as forces against nominal depth of cut per tooth and specific cutting energy against nominal depth of cut per tooth.

Figure 35- 46 illustrate graphs obtained by processing the raw cutting data from the full bandsaw product tests for the workpiece materials. Test results have shown that for a 1.4/2 (vari-pitch) TPI-variable height blade, the nominal depth of cut per tooth is directly proportional to the cutting force and thrust force. The graphs developed on the basis of the tests conducted show the familiar pattern of straight lines when force was plotted against the nominal depth of cut per tooth for different cutting speeds.

Figures 35-38 shows the influence of cutting speed on forces for different cutting depth of cut per tooth when cutting Workpiece-X material. The trends in the forces are typical for hotwork tool steel, i.e. forces decreased when the cutting speed was increased from 31 m/min to 90 m/min. This is also a common experience when cutting most metals and alloys, the cutting forces decrease, as the cutting speed is increased [58,60]. In the shear zone of the chip formation, increased strain rate (higher cutting speed) will normally result in increased strain hardening, giving increased shear strength of the workpiece material. Higher strain rate also produces more heat, which will soften the material and decrease the shear

strength in the flow zone. If the softening from the higher temperature is greater than the hardening from increased strain rate, the cutting force will decrease as the cutting speed is increased [1,58]. Therefore, a reduction in the specific cutting energy required for metal removal. The specific cutting energy graph reflects this; increase in cutting speed improves the cutting action of the blade (increased efficiency), figure 37. The specific cutting energy ranges between 4 GJ/m^3 to 8 GJ/m^3. The specific cutting energy curves seem to suggest that the tests could be run at higher depths of cut than the one selected. During the mapping tests it was observed that an increasing depth of cut per tooth above 4μm causes a significant increase in forces (≈700 N increase/μm). Therefore, cutting above 4 μm nominal depth of cut per tooth was found to be unsuitable for this material. The chips collected at different speeds and feeds are shown in appendix 3. The chips have a bright, shiny surface and are not burnt for the cutting conditions tested. The swarf does not agglomerate to form bundles of chips, mainly due to chips breaking off into smaller pieces during cutting. In general, there was a large variation in the chips produced. Increasing the nominal depth of cut results in a large fraction of flat and curly chips produced. This was also evident when the cutting speed was increased. The chips appeared to have work-hardened, as they were brittle. The typical length of chips (continuous and full width) was approximately 20 mm. With the cutting length being 254 mm the chip ratio was calculated to be approximately 0.08.

Figures 39-42 show results obtained for cold work steel Workpiece-Y. The results of the test show that the forces increase with the increase in cutting speed. The specific cutting energy curves (6 GJ/m^3 to 8 GJ/m^3) show that the cutting action of

the blade becomes less efficient when the cutting speed was increased, figure 41. The trend in the forces may have been caused by built up edges as the workpiece material adheres to the cutting edge at higher cutting speed. In order to ensure that this trend was a material characteristic, the test was repeated. The results of the test was consistent with the one previously conducted. This behaviour, which has not been reported anywhere else, seem to suggest that the strain hardening produced was higher than the softening from increased temperature, giving higher forces as the cutting speed was increased. There could also be other possibilities; it may be due to the friction forces or to the chemical reaction, taking place at the tool-chip and tool-work interface.

The microstructure of the material when observed revealed a structure consisting of relatively hard ferrite (appr.230 HV) due to high carbon and alloy content. A high-strength ferrite will result in lower machinability but does not explain the unusual strain-rate response. Furthermore, the microstructure of the material contains relatively large carbide clusters (up to appr. 75 μm). Abrasive alloy carbides have an adverse effect on machining characteristics, more than the higher hardness of its ferrite matrix would suggest [59]. Since the depth of cut per tooth used in the test was small, the saw teeth in the band will most probably crush or tear out the large carbide in the ferrite matrix instead of cutting, thus having to shear individual carbides, which requires a higher cutting force.

An analysis of the chips collected revealed that the material (Workpiece-Y) produces very small chips that have a curl diameter ranging from 2 mm (low speed and feed) to 8 mm. The typical length of chips was between 10 to 25 mm. With the

cutting length being 254 mm, the chip ratio calculated was between 0.04 and 0.1. The chips were predominantly a mixture of small, curly and continuous chips. The effect of increasing cutting speed was not easy to determine. It appeared that the chip length increases with cutting speed, indicating an increased chip ratio and efficiency. However, the cutting force data obtained showed the opposite. So far there have not been cutting data reported for this trend in forces, investigations of detailed explanations would seem to be a fruitful topic for future work.

Figures 43-46, shows results obtained for stainless steel. The results show that the cutting speed influences the cutting force and thrust force in a similar trend to hot work tool steel, i.e. Workpiece-X. This is also reflected in the specific cutting energy curves. The range for the specific cutting energy was between 4 GJ/m^3 to 7 GJ/m^3, figure 45. The chips produced when cutting stainless steel were predominantly long, curly and was relatively large in diameter (approximately 10 mm). The effect of increasing speed did not cause any significant difference in the appearance of the chips. The chip produced was uniformly deformed over the entire range of cutting speed used in this study, which is typical for this material [1,60]. The chip length was estimated to be approximately 30 mm. Since the workpiece breadth was 158 mm, the chip ratio was calculated as 0.2 for the chips that were cut in the most efficient way. Not every chip was cut with such a high chip ratio (efficiency).

Chapter 3 DETERMINING FORCE/TOOTH AND THE AVERAGE DEPTH OF CUT/TOOTH, IN FULL BANDSAW BLADE PRODUCT TEST

3.1 Introduction

In chapter 2, the results of the full bandsaw blade product test was presented using total force values, which were plotted against the nominal depth of cut per tooth. This method of presenting the cutting data is usually used in industry. However, for the purpose of using the cutting data in the later part of the thesis for validating and assessing the single tooth test method, the cutting force values showed in chapter 1, are presented as cutting forces per tooth in this chapter. Furthermore, the nominal depth of cut per tooth (set depth of cut) is usually referred to as an average value. This is due to the variation in the saw tooth geometry, which causes the teeth in the band to remove material at different depth of cuts. As such, in a normal sawing operation the average depth of cut achieved per tooth can sometimes be 3 times or more than the nominal depth of cut per tooth depending on the type of bandsaw blade geometry used. The average depth of cut per tooth achieved using a vari-pitch, variable-height, bandsaw blade in the full bandsaw blade product tests, was found to be influenced by the following tooth geometry:

i) The variable height tooth profile of the blade

ii) Setting of the teeth

The actual average depth of cut per tooth achieved based on the characteristics of the tooth geometry can be determined by calculation in conjunction with AutoCad drawings of the tooth profile. The method used will be shown and discussed in the following sections.

3.2 Determining the force per tooth

The force per tooth calculation depends on the number of teeth engaged on the workpiece material during sawing. The blade used in the tests had variable-height tooth geometry. This type of blade has two groups of teeth with different root- to-tip heights. The difference in height between the high-teeth to the low-teeth is 0.150 mm. The higher tooth occurs consecutively after a lower tooth in the band. The lower teeth do not engage in cutting and only function to provide stability to the cutting action of the saw blade. The sample calculation shows the method used to ascertain the force per tooth for both the cutting force and thrust force.

Sample calculation 3.1 (force per tooth)

Consider the cutting data taken (from table 18-1, appendix 2) for Workpiece-X (hot work tool steel) material below.

$Fv = 375$ N

$Fp = 322$ N

$V_b = 30$ m/min

$V_f = 2.1$ mm/min

Nominal Depth of cut/tooth (δas) = 1μm

Workpiece Breadth = 254mm

T.P.I = 1.4/2 teeth per inch (vari-pitch)

= 3.4 teeth per 2 inch

= 3.4 teeth per 50.8 mm

Since the workpiece breadth used for the tests was 254 mm, the average number of teeth engaged on the workpiece material can be calculated as follows:

n_t (no. of teeth cutting) = $\frac{3.4 \times 254\text{mm (workpiece breadth)}}{50.8\text{ mm}}$ = 17 teeth

However, the T.P.I designation (1.4/2) used does not take into account the effect of the variable-height tooth geometry. Since only the high tooth is cutting, the average number of teeth actually engaged in cutting is half of that calculated above.

Therefore, n_t (no. of teeth cutting) = 17 teeth/2 = 8.5 teeth

Thus,

$F_{v\text{-}fbt}$ (Cutting force/tooth) = Fv / (n_t)

= 375 /8.5

= 44.1 N/tooth

$F_{p\text{-}fbt}$ (Thrust force/tooth) = Fp / (n_t)

= 322/8.5

= 38 N/tooth

The force per tooth values calculated was used to determine the specific cutting energy per tooth. All the results are tabulated in appendix 2, table 18 (1-2).

3.3 Establishing the average depth of cut per tooth

3.3.1 Effect of variable-height tooth profile on the average depth of cut per tooth

In section 3.2 the variable-height tooth geometry was discussed. Since only half of the teeth in the band are cutting, the average depth of cut per tooth is therefore twice the nominal depth of cut. This can be calculated using the equation below. The derivation for the calculated average depth of cut δa_{fbt} is similar to equation 2.1, for the nominal depth of cut per tooth. δa_{fbt} is the calculated average depth of cut per tooth shown below .

Sample calculation 3.2

$$\delta a_{fbt} = \frac{D \cdot V_f}{V_b \cdot 1000} \qquad (3.1)$$

Using the calculation for the average number of teeth for a variable-height blade geometry in example 3.1, section 3.2. The pitch of the saw tooth (D) can be calculated as:

$$\text{The average tooth pitch (D)} = \frac{\text{Workpiece breadth}}{\text{Number of Teeth cutting}}$$

$$= \frac{254}{8.5} \text{ mm} = 30 \text{ mm}$$

$$= 0.03 \text{ m}$$

Putting values into equation 3.1

$$\delta a_{fbt} = (0.03)(2.1/1000)/(31)$$

$$\delta a_{fbt} = 2.0 \times 10^{-6} = 2 \ \mu m$$

The calculations have shown that due to the variable-height tooth geometry, the average depth of cut per tooth was twice the nominal depth of cut per tooth. However, the calculation above does not include the influence of the tooth setting. This will be discussed in the next section.

3.3.2 Effect of tooth setting

It was shown that the variable-height tooth geometry causes the teeth to cut at twice the nominal depth of cut per tooth. The setting of the tooth will increase the average depth of cut calculated, shown in example 3.2, by a further three times.

Figure 47 illustrates how the teeth in the band are set. Each set tooth repeats in the band after the two other set teeth have passed. For example, the right-set tooth (tooth 3 in figure 47) is the only tooth that cuts the right side of the kerf and cuts after the left set and the un-set teeth have completed its cut. Therefore, before the next right-set comes into contact with the workpiece material the tooth will need to remove 3 times the depth of cut per tooth since the material on the right kerf was not removed when the other set teeth had passed. This scenario is also true for the un-set and left set teeth.

3.3.3 Calculating the average depth of cut per tooth

The Average depth of cut per tooth can be expressed using the equation below

$$\delta a_{fbt} = a.\ b.\ \delta as \qquad (3.2)$$

Where,

a = Factor relating to the varible-height tooth geometry

b = Factor relating to the setting of the teeth in the band

δas = Nominal depth of cut per tooth set

δa_{fbt} = Calculated Average Depth of cut per tooth

The expression shown is a general equation, which can be used in calculating the average depth of cut per tooth. Values for a and b are found through calculation and simulation (AutoCad Drawings). For a Raker-set, variable height-1.4/2 T.P.I (Vari-pitch) M42 bi-Metal, ground bandsaw blade the values found are as follow:

$a = 2$

$b = 3$

For 1μm nominal depth of cut per tooth set (δas) the average depth of cut per tooth using equation 2.5 is

$\delta a_{fbt} = 2 \times 3 \times (1\mu m) = 6\mu m$

Since, the average depth of cut per tooth was 6 times the nominal depth of cut set in the full bandsaw product test. Therefore, in the single tooth test performed (chapter4), the depth of cut used in the tests was set to reflect this correlation.

3.3.4 Establishing the average chip cross-section area in full bandsaw product tests

Figure 48, illustrates an example of the effective cutting edge length for the set teeth in full bandsaw product test. The setting of the saw teeth causes a shadowing effect, where large parts of the saw teeth are blocked by the previously differently set saw teeth. This mainly applies to the regions after the neutral saw tooth where corners of other saw teeth cut instead. The shadowing effect causes each tooth to use only 54% of its cutting edge in metal removal (highlighted area shown in figure 48). This was calculated by dividing the kerf width with the number of teeth that produced it (Left-set, right-set and un-set teeth). The calculation is shown as follow:

Kerf width (slot width) was measured as 2.6 mm.

Since, the three different tooth setting was responsible for the kerf width

Therefore,

$$\text{Effective cutting edge width} = \frac{\text{Kerf width}}{3\,(\text{No. tooth setting})}$$

$$= \frac{2.6\,\text{mm}}{3} = 0.87\text{mm}$$

Since, the width of a saw (tooth) blade was 1.6 mm

Hence,

$$\text{Width of saw tooth used in cutting \%} = \frac{0.87}{1.6}$$

$$= 54\ \%$$

The chip cross-sectional area for different depth of cut per tooth can be determined by multiplying the effective cutting edge width with the calculated average depth of cut. The values of the chip cross-sectional area for different calculated average depth of cut per tooth were plotted on a graph and are shown in figure 49. The equation of the linear curve of the graph represents an expression that can be used for calculating the average chip cross–sectional area and shown as follows:

$$\text{Average Chip Cross-sectional area } A_{c\text{-}fbt} = \delta a_{fbt} \times W_t \qquad (3.3)$$

Equation for the graph in figure 111 is y = 8.64E-04x

Since, $y = A_{c\text{-}fbt}$

$x = \delta a_{fbt}$

W_t= gradient of the curve = 0.000864 m

Therefore,

Average Chip Cross-sectional area per tooth, $A_{c\text{-}fbt} = (0.000864)\delta a_{fbt}$ (3.4)

The full bandsaw blade product test results discussed in chapter 2 was re-plotted using cutting force per tooth, thrust force per tooth, specific cutting energy per tooth (using the calculated average chip cross-sectional area) and the calculated average depth of cut per tooth shown above. The graphs plotted (figures 50-61) will be compared to the single tooth test results in chapter 4.

Chapter 4 DEVELOPMENT OF A SINGLE TOOTH TEST

4.1 Introduction

It was envisioned that the use of a "time compression" test method to test bandsaw blades would help reduce significantly the time taken to develop new saw tooth geometries and also to produce cutting data associated with cutting forces and specific cutting energy when sawing different materials. The method developed would replace full bandsaw product testing, which is time consuming and expensive.

The author has built a test rig based on the work by Sarwar and Thompson [20] who adapted a commercial lathe machine to simulate the cutting action of hack saw blades. Sarwar, Bradbury and Dinsdale [48], later used this method to generate cutting data for predicting transient stress behaviour within bandsaw teeth using finite element models.

In this chapter the author presents details of the single tooth test rig used, which was previously used by Sarwar et al. [48], and the corresponding cutting test results. The experience of using the test rig was found to be vital as it allowed the author to identify problems associated with the test rig. This knowledge was used to improve the test rig to its current state. Details of the modifications and improvements to the instrumentation used to acquire cutting data are also discussed in detail. Cutting test results obtained from using the improved test rig

are also shown together with the methodology adopted when performing single tooth tests.

4.2 Single tooth test rig (STT-1)

4.2.1 Test rig design

The test rig was built using a 1609 Dean Smith & Grace lathe machine with a variable-speed control between 40 and 1600 rev/ min. For the purpose of the test, a work-piece holder and tool holder was specially designed and built, which also represents the main feature of the test rig. The workpiece holder was a disc of 155 mm diameter with four slots machined on one side to take rectangular $48 \times 40 \times 6.5$ mm workpiece samples, which were clamped to the disc using bolts, figure 62. For the cutting test the material used was standard steel with a Vickers hardness of 140 HV1. The back of the holder has a 90 mm long solid bar, diameter 45 mm connection, which was held in a 3-jaw chuck, figure 63. The components of the tool holder consist of a rectangular bar (30 mm x 20 mm x 80 mm) with a 20 mm slot machined on one end fastened to a plate (94 mm x 155 mm x 15 mm) as shown in figure 64. The tool holder was bolted to a Kistler Dynamometer, which in turn was bolted to the lathe cross-slide.

The cutting tools used in the tests to simulate the intermittent cutting process were single tooth cut out from bandsaw blades. To prepare samples, blades were cut into two-tooth sections. While maintaining the gullet, one of the tooth tips was ground off, leaving just one tooth to be used in the cutting test, figure 65. The

cutting tools used in the test were cut from standard bi-metal, HSS M42, vari-pitch (2/3 TPI) Raker set bandsaw blades produced through milling. Table 14 show the blade geometry. The cutting tools used were all unset tooth samples. Prior to starting the test, the workpiece was pre-machined on the periphery using a parting tool. This was carried out in order to provide an arc on the sample workpiece, figure 66. The diameter of the workpiece holder was of sufficient diameter to represent a linear cut.

4.2.2 Instrumentation and experimental set-up

The experimental set-up and the instrumentation used are shown in figure 67. The force was measured using a three-force component Kistler dynamometer with piezo-electric transducers. This equipment was used to measure the cutting and feed force during the metal cutting process. The piezo-electric transducers send electrical signals in the form of electrical charges to a charge amplifier. The measuring range was set on the charge amplifier to give 1 volt as force measurement of 100 N. The signal was sent to an oscilloscope where it was stored and converted from analogue to digital signal. The digital signal was fed into a computer where it was stored and presented via a program for visualisation of the oscilloscope.

4.2.3 Cutting Tests

The cutting force components Fv and Fp were monitored for each depth of cut. In order to overcome the stiffness of the tool holder cross-slide, each depth of cut was repeated 3 times and the corresponding chips were collected, weighed and

the undeformed chip thickness (h_0) calculated. The specific cutting energy (E_{SP}) was calculated from forces measured using the Kistler Dynamometer

Cutting depth per tooth h_o, was obtained by weighing the chip using a micro-balance weight machine (Sartorius Micro). As the cutting length (arc length l_{arc} measured and calculated to be 48.6 mm), slot width (W_t measured as 1.30 mm) and the density (ρ=7850 kg/m^3) of the workpiece material was known, a simple calculation was carried out to establish the depth of cut (h_o).

Using the relationship below,

$$\rho \text{ (Density of workpiece material)} = \frac{W_{chip} \text{ (Weight of Chip)}}{Vol_{chip} \text{ (Volume of Chip)}} \qquad (4.1)$$

Since,

Vol_{chip} = h_o (Depth of cut) x W_t (Slot width) x l_{arc} (Cutting length)

Equation 4.1 can be rearranged as

$$h_o = w_{chip} / (\rho * W_t * l_{arc}) \qquad (4.2)$$

Specific cutting energy can be calculated using Equation 2.4

$$E_{SP} = F_v / A_c \quad (\text{Where, } A_c = ho * W_t) \qquad (2.4)$$

Sample Calculation 4.1

The values below were obtained from the table of results in appendix 4. The calculation shows an example of the method used to determine the depth of cut per tooth using the weight of the chip collected from the single tooth test.

Sample calculation for chip 1:

w_{chip} = 0.02692 g , ρ=7850 kg/m^3 , W_t=1.30 mm, l_{arc} =48.56 mm

i) $ho = w_{chip} / (\rho * W_t * l_{arc})$ (4.2)

$ho = (0.02692 \times 10^{-3}) / (7850 \times 1.3 \times 10^{-3} \times 48.56 \times 10^{-3})$

$ho = 54.3\ \mu m$

ii) E_{SP} (Specific Cutting Energy) = F_v/A_c (2.4)

(F_v =171.5 N, $A_c = ho * W_t$)

$E_{SP} = 171.5 / (54.3 \times 10^{-6})(1.3 \times 10^{-3})$

$= 2.4\ GJ/m^3$

4.2.4 Discussion

Initial testing performed by the author using the single tooth test rig produced encouraging results, shown in figure 68 and 69. However, the cutting data produced was inconsistent and obvious from the large scatter in the result, were not repeatable [51].

The discrepancies in the results obtained during the tests, with regards to the relationship between the depth of cut and the forces recorded, was found to be attributed to two major causes:

i) The poor stiffness of the lathe cross-slide system. The backlash in the cross-slide system caused the cutting tool to rub against the surface of the workpiece material. It was found that every test had to be repeated several times before the required set depth of cut was achieved.

ii) Cutting tests were performed by manually feeding the cutting tool. Manual feed was used because the automatic feed of the lathe machine was unable to perform depth of cut less than 25μm. The inaccuracy of the manual feed, leading to the depth of cut per tooth was difficult to predict during the test. Due to the stiffness of the tool holder cross-slide system, setting the depth of cut was not possible using the cross-slide dial. Setting was carried out manually and was based on trial and error. The depth of cut for each test conducted was quantified through calculation using the weight of the chip collected. It was found that it was not always possible to collect the entire chip, especially when the chip produced was fragmented. As such, the depth of cut calculation did not reflect actual values.

The problems listed above were also reported by Sarwar et al [48] where stiffness of the machine tool system was overcome by performing repeated cuts. It was found that after the third consecutive cut, the layer of material removed was within

1% of the nominal depth of cut per tooth set. It was apparent from the test results that the test rig had limited facilities and required improvements.

4.3 Development of the single tooth test rig (STT-2)

The cutting test performed using the SST-1 test rig showed weaknesses, which required improving. The author was able to identify these problems, which were mainly the backlash produced by lathe cross-slide and the cross-slide feed system. Therefore, it was found that using a precision-cross slide electrically driven by a micro-stepper motor in place of the lathe cross-slide would solve the problem.

The tool holder previously used was also replaced as it was found to be limited when testing bandsaw blades with different width. Furthermore, there was a tendency for the single tooth sample to slip in the slot, causing it to tilt downwards. This usually happened during cutting and was caused by the clamping mechanism used for holding the single tooth samples, which was inaccurate and weak. Movement of the single tooth sample in the slot has an effect on the cutting angles, as the tooth was not fed at the height of the lathe centre-line, hence affecting the single tooth performance, i.e. cutting forces and specific cutting energy. The tool holder was redesigned to include features for holding the single tooth samples accurately and rigidly using locating pins, see figure 70. The locating pins were 6 mm diameter silver steel and ensured that the tooth was set at the correct height (lathe centre-line). A M8 bolt was added for clamping the tooth sample. The tool holder was constructed on a cross-slide specially built to enable the cutting tool (saw tooth samples) to be transverse along the breadth of the workpiece material.

The tool holder cross-slide was secured on top of a Kistler, three-axis force component dynamometer, which was in turn fastened to a precision cross-slide, figure 71. The precision cross-slide was mounted on a solid platform bolted to the lathe bed. Detailed drawings of the test rig construction are shown in appendix 6.

The workpiece material used in the tests was fastened to a faceplate having a 355 mm diameter using M10 bolts. The faceplate was held in the camlock spindle nose of the lathe. The most important feature of the faceplate design was that it allowed workpiece material with different dimension to be fastened on to it. This feature was found to be essential and useful when testing workpieces that normally come in different sizes. Since, the workpiece sample was not required in a specific size, there was no need for further fabrication, which otherwise would have been time consuming. As such, the flexibility of mounting different test-piece dimensions on the faceplate was preferred to the material holder previously used, which required the test-pieces to be prefabricated.

Cutting speed setting on the lathe could only be set in r.p.m using the spindle speed change levers. Since the speed range was set at predetermined values, it was not possible to achieve the required cutting speed for the tests using the spindle speed change on the lathe. Therefore, the cutting speed was set by using a combination of the spindle speed change setting on the lathe and varying the position of the workpiece material on the faceplate, see appendix 7. The position to place the workpiece material on the faceplate was determined by using the formula,

$V_b = \pi\, d\, n$

Where,

V_b = Cutting speed in m/min

d = Diameter m (position to mount the workpiece material on the faceplate)

n = Cutting speed in r.p.m

As the general experimental aim was to measure the magnitude of the forces in relation to the depth of cut and cutting speed, a force measurement system with the appropriate instrumentation was required to work in conjunction with the precision cross-slide system. A schematic of the test rig set-up is shown in figure 72.

4.3.1 Force measurement and instrumentation

The force was measured using a three-force component Kistler dynamometer with piezo-electric transducers. This equipment was used to measure the cutting and feed force during the metal cutting process. The piezo-electric transducers send electrical signals in the form of electrical charges to a charge amplifier when a load is applied. The signal was sent to a data acquisition card (PCI-MIO-16E National Instrument) installed in a computer, where it was stored and converted from analogue to digital signal. The digital signal was presented via a program (Labview 6.0) for visualisation.

4.3.1.1 Data Acquisition System (DAQ)

Measurement devices, such as a data acquisition device are concerned with the acquisition, analysis, and presentation of measurements. The DAQ (National Instruments) device used in the single tooth experiment was connected directly to the computer's internal bus through a plug-in slot. The DAQ device hardware only converts the incoming signal into a digital signal, which was sent to the computer. The DAQ device does not compute or calculate the final measurement. That task was left to the software that resides in the computer, in this case Labview 6.0 (National Instruments). The DAQ can be used to perform a multitude of different measurements by simply changing the software application that is reading the data. While this allows the use of just a single hardware for different tests, one needs to develop the different application for the different types of tests.

Labview is a graphical programming language that uses icons instead of lines of text to create applications. In Labview a user interface is built using a set of tools and objects. The user interface is known as the front panel. The front panel objects are controlled by using codes in the form of graphical representation. Labview programs are called virtual instruments (VIs). VIs contain three main components, the front panel, the block diagram, and the icon and connector pane.

4.3.2 Precision Cross-Slide

The precision cross-slide selected to hold and drive the cutting tool had N-rail guides with needle roller assemblies supplied by SKF (NSS 100.310.100.R0801).

The cross-slide was selected for its greater dynamic load-carrying capacity (60.9 kN) and static load carrying capacity (13 kN). Furthermore, the short stroke (100 mm) and the preloaded guide (3-10% of static load rating) achieve a high stiffness ($\approx$ 30N/μm) with no backlash, which made the cross-slide less sensitive to shocks. This was an important feature since the slide would have been subjected to impact loading when the cutting tool engages the workpiece material in the single tooth test. The slide was equipped with preloaded planetary roller screws having 1mm pitch. The drive screws were supported at the motor end by preloaded angular contact bearings in the table endplate. The cross-slide could be used for travel speeds of up to 2 m/s and with acceleration of up to 10 m/s^2. The travel speed and acceleration of the cross-slide was adequate to work with the spindle speed of the lathe used for the single tooth test.

In order to prevent damage to the leadscrew the movement of the cross-slide was limited using two inductive limit switches, which were fitted under the right-hand plate cover of the tabletop on a rail, 5 mm from the mechanical dead ends. The limit switches have an accuracy of $\pm$ 0.01mm. The limit switches are wired into an 8-pin plug on the motor side and connected to the MC3E. In addition to the limit switches an inductive reference switch was also fitted under the same cover and on the same rail as the limit switches. The inductive reference switch functions as the datum position from where the cross-slide starts. The reference switch can be adjustable by around $\pm$ 20 mm. Further details and specification for the cross-slide are given in appendix 5.

4.3.3 Precision Cross-Slide Control

The precision cross-slide and the associated control system represent the heart of the single tooth test method. As such, understanding how the different equipments and the software work is vital. Figure 73 illustrates a simple schematic diagram of the cross-slide control system.

4.3.3.1 Machine Control (MC3E) Hardware

The machine control (MC3E) hardware operates in open loop with the stepper motor to control the shaft position of the motor, figure 74. The MC3E controls the linear movement by the number of steps per unit. This parameter value is the number of drive pulses or steps from the MC3E needed to cause the machine axis to move by one whole unit movement. The unit used to represent the linear axis is in mm. For a leadscrew of 1mm pitch directly coupled to a 1000 steps/rev, there will be 1000 steps to rotate the leadscrew by one turn and move the load by 1 mm, i.e. 1000 steps/unit.

4.3.3.2 Remote Programming Software

To make the MC3E perform a sequence of operations, a program is required. The program created contains a string of commands, which causes the MC3E to perform the requested operation. The program consists of a series of blocks containing a G or M code. For the purpose of the single tooth test, the programming commands were written such that the cutting operation for a

predetermined depth of cut was continuously repeated. In order to ensure that the cutting tool was fed continuously and more importantly at the right time, both the feeding of the cutting tool and the turning operation of the lathe were required to be in the right sequence of operation. To do this the programming of the command string was written to only execute after a signal was received from a non-contact switch (proximity detector). When this condition was fulfilled the command string then instructs the MC3 to move the cross-slide by the set movement. For example, a command string may be written to move the cross-slide by 15 μm, and to continuously repeat this for 25 cuts. Before every cut, the command string waits for an ON signal from the proximity detector. When this is received the MC3 receives a command to move the cross-slide by 15 μm and stops when an OFF signal is received. This is repeated for 25 cuts. The ON and OFF signal is a result of the movement of the proximity detector over a ferrous metal plate. A detailed description of the proximity detector used is given in section 4.3.5

4.3.4 Stepper Motor

The stepper motor consist of a stator which has coils electrically connected to and driven by the motor drive, and a rotor which can be considered to be a bar magnet and is mechanically connected to the load. When there is no power applied to the motor, the shaft magnetically locks into defined mechanical positions around its rotational axis. There are normally 200 such positions per revolution of the motor shaft. The amount required to move from one position to another is known as the Detent Torque of the motor and is due to the residual magnetism within the motor. By applying current to the coils of the motor the magnetic field and therefore the

Detent torque is increased and the motor becomes more difficult to turn. Sequentially switching and controlling the amount of current in the coils changes the position of the resultant magnetic field in the motor and causes the rotor to move onto and lock into the next defined position. It is the motor drive that is responsible for sequencing the current to generate rotational motion in the motor. Links on each drive allow selection of 4000, 2000, 1000 or 400 steps per motor revolution.

For the purpose of the single tooth experiment, the motor drive was set for 1000 steps per revolution. The lead screw in the precision cross-slide has a 1mm pitch, therefore the minimum movement can be calculated as,

$$\text{Minimum movement} = \frac{\text{Leadscrew Pitch}}{\text{Steps Per Revolution of Motor Drive}}$$

$$= \frac{1 \text{ mm}}{1000} = 1 \ \mu\text{m}$$

Figure 75 shows the stepper-motor connected to the precision cross-slide.

4.3.5 Proximity Detector

A proximity detector was used with the purpose of ensuring that the cutting tool was fed at the correct time into the workpiece material during the cutting operation. The proximity detector was positioned at approximately 0.5 mm from a ferrous metal plate mounted to the back of the faceplate. The proximity detector operates as a current switch whose output current depends upon whether the ferrous metal

plate is covering the detector or not. As such, it was important that the metal plate was of sufficient length to enable the proximity detector to operate. The metal plate shown in figure 76 is 100mm in length. The proximity detector was positioned just after the workpiece so that the infeed of the saw tooth happened after the workpiece had passed. This also ensured that there was enough time for the infeed of the tooth in preparation for the next cut.

4.3.6 Precision Cross-slide Calibration Tests

In order to ensure that the precision cross-slide used was working to its capability and specifications, a series of different calibration tests were performed. The tests performed are as follows:

i) Stiffness test

ii) Laser interferometer test

4.3.6.1 Cross-slide system stiffness

The stiffness of the cross-slide in the direction of the lead screw drive was measured using a specially built jack incoporating a Kistler load washer and a Linear Displacement Transducer. The experimental set-up and the equipments used are show in figure 77. The outputs from the Kistler load washer were fed into a high frequency amplifier and A/D converter (DAQ National Instruments) where it was stored and presented via a program for visualisation. Simultaneously, the

output signal (Volts) from the linear displacement transducer was read using a voltmeter. The linear measurement transducer sensitivity was 0.6 V/mm.

To measure the stiffness of the cross-slide system, the jack was placed between the cross-slide and the chuck, illustrated in figure 77. The screw on the jack was slightly tightened against the cross-slide to prevent the jack from slipping during the test. Doing this caused the linear measuring transducer and the Kistler load washer to register values. The Kistler load washer was reset to zero. The linear measuring transducer could not be reset; as such, the test was performed with an initial deflection of 0.7 mm. Turning the screw slowly exerts a force, which pushes against the chuck and the cross-slide. The increase in force causes the cross-slide to deflect. This was detected by the linear measuring transducer, which sends a volt signal to a voltmeter where the value was directly read. The stiffness of the chuck was also measured using the stiffness jack and was measured to be approximately 1000 N/μm.

The test was performed for a range of increasing forces and the corresponding deflection was recorded. The results from the test were used to plot Force Vs Deflection graph shown in figure 78. The gradient of the graph (F/deflection) gives the stiffness of the cross-slide system. This was calculated to be 5 N/μm. This value represents the stiffness of the whole system, which includes the tool holder, dynamometer, stepper-motor and the base plates.

However, it was identified that the stiffness test was performed without the stepper-motor being powered. When the stiffness jack was tightened the force

exerted on the cross-slide caused the lead screw to turn, resulting in a large deflection. If the stepper-motor was powered during the test, the current applied to the coils of the motor increases the magnetic field and therefore the Detent torque. Subsequently, this would have caused the motor to become more difficult to turn. Hence, a higher stiffness value would have been expected.

When the cross-slide is fed forward to a pre-determined distance during cutting, the shaft magnetically locks into defined mechanical positions around its rotational axis, preventing backlash due to the impact loading developed between the cutting tool and the workpiece material. As such, the depth of cut per tooth set would be the actual depth of cut achieved. However, the stiffness test should be repeated with the stepper-motor power switch on. This would be a useful activity for future work.

4.3.6.2 Laser Interferometer

The most important feature of the single tooth test rig is the accurate feeding of the cutting tool. In the previous test rig, the depth of cut was determined through calculation using the weight of the chip collected because of the inaccuracy associated with the lathe cross-slide feed system. This method was found to be time consuming and inaccurate. Therefore, using the precision cross-slide in principal would remove the need to do this. Nevertheless, the precision cross-slide feed was calibrated using laser interferometer and the accuracy assessed. The laser interferometer uses an initial source producing two laser beams, which are polarised orthogonally. The optical polarisation of the laser beams causes the two

beams to follow different paths; one will serve for reference (fixed lense), the other for measurement (lense mounted on the precision cross-slide), figure 79. When the two are recombined, they form an interfering image, which depends on the wavelength of the ray used. The interferometer consists of three parts: the liquid crystal cell, the laser head and the measuring unit. The latter is fixed to the laser head and contains the optical elements (polarisers, lenses) and the electronic measuring instruments.

The laser interferometer test was performed by moving the cross-slide in predetermined distances using the manual control on the remote programming software for the precision cross-slide. The movement of the cross-slide set on the remote programming software was compared to the one measured by the laser interferometer. The results obtained from the test showed a 3.5% error on the graph plotted in figure 80. This value was small and considered negligible. This result, confirms the accuracy of the precision cross-slide.

4.3.7 Tooth sample

The single tooth samples used for the simulation tests were un-set (high teeth group) saw teeth samples from standard bi-metal, HSS M42, vari-pitch (1.4/2 TPI), variable height, ground, raker set bandsaw blades. These blades were identical and came from the same batch of blades used in the full bandsaw test.

Inspection of the saw tooth profile was checked by means of a shadowgraph by comparing the magnified image on the round glass screen with the saw tooth

specification shown in figure 26. The cutting edge of the saw tooth samples were inspected using an optical microscope to ensure that the samples were free from chipping due to handling which could affect the single tooth test results. Figure 81 show an example of the cutting edge of a standard saw tooth sample used in the tests taken on a scanning electron microscope.

The new tool holder used in the test had locating pins for securing the single tooth samples. In order for the tooth sample to fit into the tool holder a jig was specially built for drilling holes through the tooth samples, figure 82. The jig was used to drill two 6 mm holes for the locating pins and an 8 mm hole for the M8 bolt used for clamping the tooth sample in the tool holder, figure 83.

4.3.8 Workpiece materials and cutting conditions

The workpiece materials used in the single tooth tests were sawn sections (77 x 253 mm rectangular sections) obtained from the full bandsaw product test. In the single tooth test the workpiece material was positioned on the faceplate such that cutting was carried out on the 77 mm side of the rectangular section. The breadth of the material used was adequate to produce chips to fill the tooth gullet. Prior to any test, the workpiece material was pre-machined on the periphery using a parting tool to provide an arc on the sample workpiece, figure 84. The diameter of the workpiece holder was of sufficient diameter to represent a linear cut.

Cutting conditions used for the single tooth test were similar to that used in the full bandsaw test. The nominal depth of cut used during the cutting tests were varied

from 6 μm to 36 μm and the cutting speeds used were between 30 m/min to 90 m/min, see table 17. The depth of cut per tooth used was the average depth of cut per tooth determined in section 3.3.3. In section 2.7, the method for conducting the cutting tests was explained. The single tooth tests were conducted using the same test sequence as that used in the full bandsaw test.

4.4 Machine vibrations

Preliminary single tooth simulation tests performed using the STT-2 test rig showed results, which were effected by machine vibrations. The source of the machine vibration was identified and was caused by the impact loading developed during cutting. The impact loading caused excitation to the components of the test rig and this was found to affect the cutting force and thrust force measurements from the Kistler dynamometer, making it difficult to ascertain force values at the steady state condition, see figure 85. In order to reduce the vibrations, the stiffness of the test rig was improved as follows:

i) The bolts and other fixtures used to hold parts of the test rig together were tightened, making them more rigid.

ii) The solid platform, on which the precision cross-slide, dynamometer and the tool holder are mounted, extends 244 mm from the edge of the lathe bed. To ensure that the cantilever effect of the platform was not causing the vibrations the bottom of the platform was supported with a jack covered with rubber pads to help with the damping effect, shown in figure 87.

The improvements carried out on the test rig did not have any effect on reducing the vibrations during cutting. However, while performing the modifications to the test rig, it was observed that there was a significant improvement to the vibrations when weights were placed on top of the tool holder. The cutting force and thrust force were found to be unaffected by vibrations caused by the impact loading during cutting when a solid metal block 20 kg in weight was mounted on top of the tool holder. The results of the test shown in figure 85, when compared to the test results shown in figure 86, using the same cutting conditions but using the weight fastened to the tool holder cross-slide shows the improvement.

Since this was the only solution found to solve the vibration problem, all single tooth simulation tests were performed with the weight secured on top of the tool holder cross-slide. The use of the solid block of mild steel was a temporary measure adopted in order to complete the single tooth simulation tests and hence validate it. Therefore, a comprehensive investigation should still be performed in the future to identify the cause of the vibration. This would enable the use of tune dampers in place of the weight.

4.5 Side clearance for the single tooth cutting edge

Suppose the single tooth edge points along the axis of the lathe, and the desired feed has been applied by the precision cross-slide (along the axis of the lathe). When the tooth penetrates to any distance into the workpiece, there will be rubbing on the sides of the tooth, as the tooth has zero side clearance angle. Since there are no additional teeth which would normally widen the kerf by reason of their set,

rubbing on the sides of the single tooth will give a progressive increase in cutting force as the cut becomes deeper. One-way of avoiding this difficulty was to set the tool holder so that the cutting edge of the tooth was set at an angle to the lathe axis. The sideways setting of the tool holder prevents the sides of the tooth from rubbing against the workpiece.

In figure 88, the tooth has a cutting edge TT. Sideways setting of the tooth is shown as a simple rotation of the tooth through a small angle θ about horizontal axis AA. In the single tooth test the tooth was set at 3 °. The sideways setting was found to be adequate to avoid rubbing of the left side of the tooth against the workpiece material. Since the sideways setting was small, it did not have any effect on the cutting force and the thrust force.

4.6 Single tooth test methodology

4.6.1 Introduction

The "time compression" test method developed to replace full bandsaw blade product testing, required a methodology that was reliable and tested. The methodology used in the single tooth tests was based on the experience of the author and recommends that it be used as a standard procedure in the future. The following sections give a sequence of tasks that were performed prior and during the single tooth tests. This would prove helpful to future researchers using the single tooth test method.

4.6.2 Single tooth sample preparation and setup

The first task that was performed was to fabricate the single tooth samples. This was accomplished using the method described in section 4.3.9. During fabrication the edge of the tooth was protected from damage by covering it with a hard plastic cover. The tooth edge was examined using optical microscope to ensure that the tooth samples were free from defects that might have occurred during fabrication. A prepared tooth sample was inserted into the locating pins and secured using the M8 bolt. The tool holder was next set at an angle 3° to the lathe axis to provide the tooth with side clearance.

The workpiece material to be tested (Workpiece-X, Workpiece-Y and Stainless Steel 304L) was fastened to the faceplate and machined on the periphery using a single tooth. A new saw tooth sample was inserted into the tool holder and was positioned as shown in figure 88. The tooth was set such that the whole width of the tooth was cutting.

4.6.3 Programming the cross-slide control system

To make the MC3E perform a sequence of operation, a machining program had to be created first. The program created would have the commands, which will cause the MC3E to perform the requested operation. The program was written using G and M codes.

The MC3E remote programming software always sets the precision cross-slide to start from the Datum position when first switched on. The displacement of the cross-slide, which could be monitored on the screen of the computer, could be controlled in two ways. One was by writing a program and the other was by keying the required displacement using manual control.

Before a program could be written, the cutting tool was first moved to the starting point of the test. This was performed using manual control. The starting point of the test was the point where the cutting tool edge just touches the cutting surface of the workpiece. The distance moved to that point could be read from the digital display shown on the software and was used to write the first command string (staring point). For example, assume the starting point of the test was set up at 52.100 mm (this is the point where the single tooth edge touches the surface of the workpiece material) and that the depth of cut required was 0.010 mm (10 μm) for 20 continuous cuts. The program written would be as follow

Test Program

```
N1          G01  LINEAR
          X 52.100                                   F 100.00
N2          M17  LABEL 1
N3          M21  INPUTS
          ON 1
          OFF
```

```
N4          M21  INPUTS
          ON
          OFF 1
N5          G01  LINEAR
          X 52.110                                          F
N6          M17  LABEL 2
N7          G81  REPEAT        20 times from LABEL 1   to 2
          X 0.010                                           F
N8          G00  RAPID
          X 0.000
N9          M02  END  OF  PROGRAM
```

The first command string N1 moves the cross-slide from the Datum position to the starting point in this case at 52.100 mm. The N2 to N6 command string are used for the proximity detector. When the ON signal is received from the proximity detector the cross-slide moves by 10 μm and stops (OFF) at 52.110 mm. The whole sequence (LABEL 1 to LABEL 2) is repeated continuously for 20 times by command string N7. Once this has been completed the cross-slide returns to the datum position shown by command string N8.

4.6.4 Data acquisition

The labview program has numerous built in programs for capturing and displaying data. The program used for recording the data from the single tooth tests was a High-Speed Data Logger. The high-speed data logger receives data from any

source that is connected to an analog input channel. This example is a high-speed, hardware-timed, data logger. Data was logged to a binary file at 5000 data points/second at 10000 scan/second. The high-speed data logger does not display the data recorded in real time but saves it into the hard drive of the computer. A Graph Acquire program was used to read and display the data that was written to file by the high-speed data logger as a graph.

4.6.5 Starting a single tooth tests

When the cross-slide, single tooth sample and the data acquisition was set-up, the single tooth test was ready to start. The lathe spindle was set at the appropriate speed (r.p.m) using the speed spindle change. To start the test, the cross-slide program was run simultaneously with the data acquisition program. While the test was running, the chips produced were collected for analysis.

4.6.6 Single tooth data processing

The raw data obtained from the tests required processing. The cutting force and thrust force values were taken at the steady state. The values obtained were used to plot Cutting Forces against Depth of Cut per Tooth and Specific Cutting Energy against Depth of Cut per Tooth, figures 89-100.

The single tooth test results for the materials tested (Workpiece-X, Workpiece-Y and Stainless Steel 304L) produced cutting data with similar trend to that obtained from the full bandsaw product test (Chapter 2 section 2.9). This was encouraging

as it showed the potential of the test method. However, the cutting force per tooth and the thrust force per tooth values were higher than that obtained from the full bandsaw blade product test. This was expected, as it was apparent that the saw teeth in the full bandsaw blade test were not using the full width of the cutting edge compared to the single tooth test during cutting. The results of the single tooth test also showed that the efficiency of the cutting process improved at higher cutting speed, which was typical when cutting most alloy steels [1]. This trend was also found when cutting Workpiece-Y. In the full bandsaw blade product test, the characteristics of the forces when cutting this material showed decrease efficiency when the cutting speed was increased. The reason for this variation may be due to the test rig in particular to the tool holder. It was observed that when a test was performed using low cutting speeds and depth of cut per tooth, i.e. 30-40 m/min and 6-15 μm, the cutting tool seemed to scrape against the surface of the material, which caused the tool to chatter. This cutting action was found to produce fragmented chips. In some case, the chips produced at low cutting speed and depth of cut per tooth, were long and flat. However, the surface of the chips when examined showed a serrated surface compared to a smooth surface obtained at higher cutting speeds (appendix 9). The cutting action of the single tooth sample may have caused the variation in the cutting data when compared to the cutting data obtained from the full bandsaw blade product test. Detailed examination of the thrust force curves showed that the curves were similar to the characteristics of the material; discussed in chapter 2, section 2.9. Therefore, by comparing the results for Workpiece-Y obtained in the single tooth test method to the full bandsaw blade test, it was possible to conclude that the cutting force and the thrust force curves shown in figure 89 and 90 was influenced by the characteristics

of the single tooth sample and holder at low cutting speeds and depth of cut per tooth.

In order to study the effect of the test rig components in particular the tool holder cross-slide on the test results, the cutting data (cutting force and thrust force) obtained for all the test materials from both testing methods were plotted on the same graph, figures 101–124. As expected, the graphs in general show the cutting force and thrust force values obtained from the single tooth tests to be approximately twice that of obtained from the full bandsaw blade test. The specific cutting energy values were higher compared to the specific cutting energy values for the full bandsaw tests at low cutting speeds (31-50 m/min). At higher cutting speeds (60-90 m/min) the specific cutting energy curve for both methods of testing was similar. Pictures of the chips collected during the single tooth tests are presented in appendix 9. The chips collected, give a very good reflection of the efficiency of the cutting action of the saw tooth at different cutting conditions.

For Workpiece-X, there was a distinctive difference in the specific cutting energy curves shown in figures 105-108. The curves from both tests when compared start with a difference of 3-4 GJ/m^3 at 6μm for test run at 31-70 m/min. As the depth of cut was increased the curves start to converge and cross over at 15-24μm. When the test was run at 90 m/min the curves were comparable. The trend in the specific cutting energy curves was reflected in the characteristics of the chip produced (single tooth test). Fragmented/serrated chips were produced when the cutting operation was inefficient, in the case shown at 31-70 m/min. At 90 m/min the chips were long and flat. The chips produced when cutting Stainless Steel

304L for all cutting speeds produced similar chips, appendix 9. The effect of inefficient cutting was not visible in the chips when cutting Stainless Steel 304L. This was consistent with the chips collected in the full bandsaw blade test. At 60 m/min, the curves matched each other.

The specific cutting energy curves for Workpiece-Y showed the same effects of cutting at lower cutting speed, i.e. inefficient cutting at low speed, figure 113-116. The chips produced do not show this trend. In general for all cutting speeds used the chips produced were small, fragmented and brittle. This was not surprising as the chips obtained from the full bandsaw blade exhibited similar characteristics. The main reason for this was partly the carbide content, which made it brittle.

Micrographs of the single tooth sample used in the single tooth test were taken, see figures 125-127. The main wear mechanism acting on the tooth was abrasive wear, partly from the carbides and chipped off pieces of the saw tooth edges. Figure 125 shows the tooth sample used for cutting Stainless Steel 304L. The picture shows mild adhesive wear with material sticking to the edge of the tooth. This is a common experience when cutting stainless steel, where it is known that this material bonds very strongly to the tool during cutting [1,60]. Figure 126 shows the effect of adhesive wear that may have caused the chipped edge. However, the main wear mechanism acting on the tooth edge was abrasive in nature. This was clear from the smooth and flat surface of the flank. Tooth sample used for cutting Workpiece-Y showed a lot of material sticking on the tooth edge. Picture of the tooth edge illustrated in figure 127, show material adhering to the rake face. The pictures show signs relating to high temperature and softening. It could be possible

that this material was prone to forming built up edges. However, the flat and smooth surface of the flank show the presences of abrasive wear. This was more likely caused by the high carbide content of this material.

The cutting force and thrust force values obtained from the single tooth test does not match the cutting data obtained from the full bandsaw blade product tests. The high cutting force and thrust force values obtained for the single tooth test was due to the way the cutting edge removed material. It was shown in chapter 2 that the saw teeth only used 54 % of its cutting edge to remove material. In the single tooth test, the saw tooth used 100% of its cutting edge in metal removal. As such, based on the simple relationship, it was predicted that the cutting force and thrust force obtained would be comparable to the full bandsaw product test results if the force values obtained from the single tooth test was re-plotted using a correction factor of 0.54. The graphs plotted and a simple conversion model to relate the single tooth test results to full bandsaw blade product test is discussed in chapter 5.

Chapter 5 MODELLING THE SINGLE TOOTH TEST TO REPRESENT FULL BANDSAW BLADE PRODUCT TESTS

5.1 Relating the single tooth test results to full bandsaw test

One of the objectives of the single tooth tests was to relate the results obtained to the full bandsaw test results acquired for Workpiece-X, Workpiece-Y and Stainless Steel 304L are shown in chapter 2. It was found that the results of the single tooth test was representative to the full bandsaw product tests when the cutting data was adjusted by relating the cutting force and thrust force to the chip cross-sectional area removed during the test. In the full bandsaw test, cross-sectional area of the chip produced was difficult to measure due to the variation in teeth qeometry, i.e. setting of the tooth, which produced chip of different cross-section area. Therefore an average chip cross-sectional area was used. In the single tooth test the width of the chip was the width of the single saw tooth used in the test.

Since it is assumed that the width of the chip produced was the width of the saw tooth sample used. The chip cross-sectional area can be represented using the following relationship:

$A_{c\text{-}STT}$ = Chip Cross-Sectional Area in single tooth test

= δa_{STT} (Depth of cut) x W_t (slot width) (4.1)

Since, W_t = width of tooth sample

= 0.0016 m

Therefore,

$$A_{c\text{-}STT} = (0.0016)\delta a_{STT} \quad (4.2)$$

Now that an expression for the chip cross-sectional area has been established, a relationship to convert the single tooth test results to the full bandsaw product test can be determined: Using the cutting force per tooth as an example,

$$\frac{F_{v\text{-}STT}}{A_{c\text{-}STT}} = \frac{F_{v-fbt}}{A_{c-fbt}} \quad (4.3)$$

Rearranging for $F_{v\text{-}fbt}$

$$F_{v\text{-}STT} = F_{v\text{-}fbt}\,(A_{c\text{-}STT} / A_{c\text{-}fbt}) \quad (4.4)$$

Since,

$A_{c\text{-}fbt} = (0.00087)\delta a_{fbt}$ (Equation 3.4)

$A_{c\text{-}STT} = (0.0016)\delta a_{STT}$ (Equation 4.2)

Substituting equation 3.4 and 4.2 into equation 4.4

$$F_{v\text{-}STT} = F_{v\text{-}fbt} ((0.0016)\delta a_{STT} / (0.0087)\delta a_{fbt}) \quad (4.5)$$

When $\delta a_{STT} = \delta a_{fbt}$

therefore,

$$F_{v\text{-}STT} = 1.85 \, . \, F_{v\text{-}fbt} \quad (4.6)$$

and

$$F_{p\text{-}STT} = 1.85 \, . \, F_{p\text{-}fbt}$$

Equation 4.5 shows that the cutting forces measured in the single tooth tests should be 1.85 times the forces measured in the full bandsaw test. This prediction was based on the ratio of the width of the chip produced in single tooth to that of the full bandsaw tests. The result from the single tooth tests (shown in table 22-24 appendix 8), when compared to the results from the full bandsaw product test (table 18 – 20, appendix 2) does show this correlation. Equation 4.5 represents the mathematical conversion required to relate the cutting force and thrust force obtained from the single tooth test method to the full bandsaw product test.

5.2 Discussion of Results

The cutting forces obtained from the single tooth test was adjusted according to the expression shown in equation 4.5, where it was established that the cutting forces were comparable to the cutting forces obtained from the full bandsaw

product test by a correction factor of 0.54. The correction factor based on the cutting-edge length of the saw tooth engaged in metal removal or the width of the chip was applied to the cutting forces obtained from the single tooth tests and plotted on the same graph as the full bandsaw tests.

Figure 128-131, shows the results plotted for Workpiece-X material using correction factor applied to the cutting force and thrust force values obtained from the single tooth tests. The graphs of cutting forces against average depth of cut per tooth were plotted individually for different cutting speed together with the force values obtained from the full bandsaw blade product tests. The curves in general are similar in shape and follow similar trend where the cutting forces decrease with increase in cutting speed. Observing the curves on the graphs one can see that as the cutting speed was increased, the curves tend to get closer to each other, which seem to indicate an increase in accuracy of the single tooth method in simulating the cutting forces obtained from the full bandsaw tests. Single tooth tests for Workpiece-Y material (figure 132-135) and stainless steel (figure 136-139) when modified using the correction factor produced comparable force trace to that obtained from full bandsaw blade product test results. The specific cutting energy values however, remains unchanged. In chapter 4 the specific cutting values obtained from the single tooth test and full bandsaw blade product test for the three materials were plotted on the same graph, see figure 106-108 (Workpiece-X), figure 113-116 (Workpiece-Y) and figure 121-124 (Stainless Steel). The specific cutting energy curves from the single tooth tests showed good correlation. Applying a correction factor to the cutting force does not alter the specific cutting energy values since the same correction factor must also be applied to the chip

width (as the force must correspond to the width of the chip removed). The correction factor therefore cancels out and the specific cutting energy remains the same.

It was very clear from the single tooth simulation test method, the test rig characteristics had an influence on the cutting data at low cutting speeds. In the entire test, the cutting data at low cutting speeds produced the same trend. However, at higher cutting speeds the influence of the test machine on the cutting data was minimal and in all cases showed very good comparable results. In general the single tooth test rig produced cutting data, which were acceptable and comparable to the cutting data obtained from the full bandsaw blade test. The cutting data obtained for the workpiece materials through the single tooth simulation test method was produced in 25 % of the full product evaluation time. This represents a significant saving in cost and evaluation time. Thus, reflects the potential and capability of the "Time compression" test method devised.

Chapter 6 CONCLUSIONS & FURTHER WORK

6.1 Conclusions

1) A methodology for assessing bandsaw blade performance using a fully instrumented commercial bandsaw machine, based on specific cutting energy values calculated using cutting force and the undeformed chip thickness was proposed. The methodology has been used successfully for assessing the accuracy of the instrumentation for measuring the relevant parameters and has been found to be useful in establishing the machine characteristics ensuring the cutting data obtained was accurate.

2) The bandsaw cutting data obtained for hot Workpiece-X, Workpiece-Y and Stainless Steel 304L presented in this thesis has shown that while for most alloy steels (Workpiece-Y, stainless steel 304L etc.) previously reported the cutting forces decrease with increasing cutting speed, cold work tool steel (Workpiece-Y) have an opposing effect, where the cutting forces increases with an increase in cutting speed.

3) In normal sawing operation the average depth of cut achieved per tooth can sometimes be 3 times or more than the nominal depth of cut per tooth depending on the type of bandsaw blade geometry used. A useful empirical relationship between the average depth of cut per tooth and the geometry of the saw teeth was presented. The average depth of cut per tooth achieved with a vari-pitch, variable-height, bandsaw blade used in the full

bandsaw blade product tests, was shown to be 6 times the nominal depth of cut per tooth.

4) AutoCAD drawings of the tooth setting have shown that the setting of the saw teeth causes a shadowing effect, where large parts of the saw teeth are blocked by the previously differently set saw teeth. The shadowing effect causes each tooth to only use 54% of its cutting edge for metal removal.

5) An experimental test rig was successfully built to assess the performance of bandsaw blades using a single saw tooth cut from a band. The single tooth test method devised has the necessary capabilities to produce scientific data (Forces, Esp etc) for different cutting conditions (depth of cut, cutting speed), and tool geometry (Rake angle, Clearance angle, Gullet geometry etc) when cutting different workpiece materials.

6) Simulation test results agree well with the results obtained from the full bandsaw product tests. Experimental observation when performing single tooth simulation tests show that the simulated results increase in accuracy with increase in cutting speed. Chips collected at lower cutting speed were fragmented indicating inefficient cutting. This was also reflected in the specific cutting energy values.

7) The cutting forces per tooth measured using the single tooth simulation test method fall into a simple pattern where it was found to be 1.85 times the cutting forces per tooth obtained from the full bandsaw test. The results

obtained from the single tooth simulation test, was found to be comparable to the full bandsaw test by adjusting the results using a correction factor of 0.54.

8) The tests performed to obtain cutting data for the 3 workpiece materials took 20 hours to complete using the single tooth simulation test method compared to 80 hours using the full bandsaw test. This represents a 75% saving in cutting time. This represents a major cost savings to the bandsaw blade manufacturing industry

6.2 Suggestions for future work

Development of the single tooth test rig (STT-2) should be continued to improve the test method. The test rig should be improved as follows:

(i) The speed change using the spindle chuck should be replace with a variable speed control. This will remove constraints to cutting speed setting caused by preset spindle speed change lever.

(ii) Dynamic stability at lower cutting speeds should be investigated. Identifying the cause of the vibration would enable the use of tune dampers instead of the weights currently used.

(iii) Single tooth sample holder should be improved to enable the fixture of different bandsaw blade samples.

(iv) Locking bolts for the tool holder cross-slide has been found to be cumbersome and should be replaced.

(v) Stiffness test should be performed to access the stiffness of the single tooth test rig system.

(vi) Quick stops capabilities should be added to the test rig. This will enable the study of chip formation.

(vii) To carry out simulation tests using different workpiece materials and saw blade samples. This would provide comprehensive data that would further validate the single tooth test method and hence enable performance tests associated with wear.

(viii) Labview program used should be developed to have the capability to analyse and process cutting data automatically to reduce data processing time.

(ix) Saw blade performance test when cutting cold work tool steel should be investigated. This may provide explanation for behaviour of the cutting forces associated with cutting speed, which has been found to be unusual.

REFERENCES

[1] Trent, EM; "Metal Cutting", Butterworth Heinemann Book Company, 1991

[2] Boothroyd G; "Fundamentals of Metal Machining and Machine Tools", McGraw Hill Book Company, 1975

[3] Owen, J V; "Bandsaws join the mainstream", Manufacturing Engineering, Feb. 1997, pp 28-39

[4] Harris, D; "Better bandsawing Technology", Manufacturing Engineering, Feb. 2001

[5] Hogan, J B; "Cutting the tough stuff", Manufacturing Engineering, 2, 1999, pp 62-68

[6] Rozzi, R; "Choosing the right blade for your job", Manufacturing Engineering, 126 (2001), 2, 56-60

[7] Pritchard, B; "The sophisticated cinderellas", Machinery, December 2001, pp.37-38

[8] Harris, R G; "Bandsawing", Tooling & Production, March 1996, pp 81-89

[9] Bates, C; "Band or circular", American Machinist, April 2002, pp. 54-58

[10] Powel, L; "Sawing and cutting-off: Why is investment such a sore point", Machinery and Production Engineering, 17 March, 1995

[11] Anon; "Systems supersede stand-alone saws", Machinery and Production Engineering, 3 July, 1992

[12] Hales, F; "Circular sawing and bandsawing of tube", TPQ, March 1996, pp 16-22

[13] Kronenberg, M; "Machining science and application", Pergamon Press, 1966

[14] Taylor, F W; "The art of cutting metals", Trans. A.S.M.E, 28, 1906, pp.204

[15] Merchant, M E; "Mechanics of metal cutting process", J. Appl. Phys., Vol 16, 1945

[16] Sarwar, M; Thompson, P J; "Cutting action of blunt tools", International MTDR Conference, Manchester,1981

[17] Sarwar, M; "The mechanics of power hacksawing and the cutting action of blunt tools", Ph.D. thesis at Dept. of Mech. and Prod. Eng., Sheffield City Polytechnic, April 1982

[18] Thompson, P J; "Factors influencing the sawing rate of hard ductile metals during power hacksaw and bandsaw operations", Metals Technology, 1974, pp 437-443

[19] Thompson, P J; "A theoretical study of the cutting action of power hacksaw blades", Int. J. Mach. Des. Res. Vol 14, 1974, pp 199-209

[20] Sarwar,M; Thompson, P J; "Simulation of the cutting action of a single hacksaw blade tooth", The Production Engineer, June 1974

[21] Thompson, P J; Taylor, R W; "A computer simulation of the power hacksaw operation and its use in estimating blade life, cutting rate and cost", The Production Engineer, Jan. 1976

[22] Taylor, R W; Thompson, P J; "A study of bandsaw blade wear and its effects on cutting rates and economics", 17 MTDR conf. Birmingham, 1976

[23] Dautzenberg, J H; Jasper, S P F C; Taminiau, D A; "The workpiece material in machining", Int. J. Adv. Manuf. Technol, 15, 1999, pp 383-386

[24] Plamai, Z; "Cutting temperature in intermittent cutting", Int. J. Mach. Tools Manufact. Vol 27, No. 2, 1987, pp 261-274

[25] Gillibrand, D; Bradbury, S R; Yazdanpanah, A; Mobayyen, S; "A simplified approach to evaluating the thermal behaviour of surface engineering cutting tools", Surface an Coatings Technology, 82, 1996, pp 344-351

[26] Saubi, R M; Lebrun, J L; Changeux, B; "A new method for cutting tool temperature measurements using CCP infrared technique: Influence of tool and coating", machining Science and Technology, 2(2), 1998, pp365-382

[27] Sarwar, M; Gillibrand, D; Bradbury, S R; "Forces, surface finish and friction characteristics in surface engineered single-and multiple-point cutting edges", Surface and Coatings Technology, 49, 1991, pp 443-450

[28] Sarwar, M; Xi-yang Zhang; Gillibrand, D; "Performance of titanium nitride-coated carbide-tipped circular saws when cutting stainless steel and mild steel", Surface and Coatings Technology, 94-95 (1997), pp. 617-621

[29] Sarwar, M; "Performance characteristics of Titanium-Nitride coated bandsaws", IITT-International, 1986

[30] Dugdale, D S; Sarwar, M; "Fatigue strength of bandsaws with hard coatings", J. Materials Processing Tech. 56 (1996), pp 729-732

[31] Sarwar, M; "Application of advance surface engineering treatments to multi-point cutting edges", Surface and Coatings Technology, 108-109 (1998), pp. 612-619

[32] Hellbergh, H; "Bandsaw blades show-The sharp end of technology", Bandsaw Blade Technology, 1994, pp17-19

[33] Thoors, H; Chandrasekaran, H; "Tooth chipping during bandsawing of steel", Swedish Institute for Metal Research, Jan. 1992

[34] Archer, P M; Bradbury, S R; Sarwar,M; "Evaluation of performance and wear characteristics of bandsaw blades",

[35] Che Haron, C H; Ginting, A; Goh, J H; "Wear of coated and uncoated carbides in turning tool steel", J. Materials Processing Tech. 116 (2001), pp 49-54

[36] Choudhury, S K; Kishore, K K; "Tool wear measurement in turning using force ratio", Int. J. Mach. Tools Manufact. Vol. 40, 2000, pp 899-909

[37] Lee, J H; Lee, S J; "One-step-ahead prediction of flank wear using cutting force", Int. J. Mach. Tools Manufact. 39 (1999), pp 1747-1760

[38] Thoors, H; Chandrasekaran, H; "Evaluation of metal bandsaws-Development of a rapid method for saw tooth wear testing", Swedish Institute for Metals Research, 6 Aug. 1992

[39] Astakhov, V P; Osman, M O M; "Correlations amongst process parameters in metal cutting and their use for establishing the optimum cutting speed", J. Materials Processing Tech. 62 (1996), pp 175-179

[40] Ahmad, M M; Hogan, B; Goode, E; "Effect of machine parameters and workpiece shape on a bandsawing process", Int. J. Mach. Tools Manufact. Vol. 29, No. 2, 1989, pp 173-183.

[41] Mackown, G M; "Get your basic right", Metal Production, Nov. 1980, pp. 255-263

[42] Zheleznov, G S; "Determining the forces acting on the back surface of a cutting tool", Russian Engineering Research, Vol.19, No.12, pp.78-79, 1999

[43] Tae Jo Ko; Hee Sool Kim; "Mechanistic cutting force model in bandsawing", Machine Tools & Manufacture, 39 (1999), pp 1185-1197

[44] Wallen, P; "Simulation on intermittent metal cutting", Ph.D thesis at Institute of Physics, Uppsla University, May 12, 1989

[45] Andersson, C; Andersson, M.T; Ståhl, J.-E; "Bandsawing. Part I: Cutting force model including effects of positionsl errors, tool dynamics and wear", Int. J. Mach. Tools Manufact. 41 (2001), pp 227-236

[46] Andersson, C; Ståhl, J.-E; Hellbergh, H; "Bandsawing. Part II: detecting positional errors, tool dynamics and wear by cutting force measurement", Int. J. Mach. Tools Manufact. 41 (2001), pp 237-253

[47 Andersson, C; "Bandsawing. Part III: stress analysis of saw tooth microgeometry", Int. J. Mach. Tools Manufact. 41 (2001), pp 254

[48] Sarwar, M; Bradbury, S R; Dinsdale, M; "An approach to computer aided bandsaw teeth testing and design", 4th NCPR Conference on Computer-Aided Production Engineering, University of Edinburgh, November 1988.

[49] Doraisingam, A.R; Persson, M; Sarwar, M; Confidential Internal Report "Evaluating the single tooth simulation test", Industrial Research and Consultancy Centre, University of Northumbria at Newcastle U.K, (Jan 2000)

[50] Doraisingam, A.R; Persson, M; Sarwar, M; Confidential Internal Report "Evaluating the single tooth simulation test II", Industrial Research and Consultancy Centre, University of Northumbria at Newcastle U.K, (Jan 2000)

[51] Sarwar, M; Hellbergh, H; Doraisingam, A.R; Persson, M; "Simulation of the intermittent cutting action of a bandsaw blade",12 International Conference on Flexible Automation & Intelligent Manufacturing, Dresden, June 15, 2002

[52] Schneider, G; "Cutting tool applications", Tooling & Production, March 2002, pp. 20-25

[53] Bradley, I; "Saws & Sawing", Argus Books, 1986

[54] Taylor, R W; "An investigation into the wear characteristics of bandsaw blades and their influence on the sawing rates and costs of bandsaw operations", M.Phil. Dissertation, Sheffield City Polytechnic, December 1976.

[55] Sarwar, M; Hellbergh, H; Doraisingam, A.R; Persson, M; "Bandsawing of Ball Bearing steel", Fifth International Conference on the Behaviour of Materials in Machining, Chester, November 2002

[56] Zorev, N N; "Metal cutting mechanics", Pergamon Press, 1966

[57] British Standard Specification for metal cutting bandsaw blade, BS 3877, 1979

[58] Strafford, K N; Audy, J; "Indirect monitoring of machinibility in carbon steels by measurement of cutting forces", J. Materials Processing Tech. 67 (1997), pp 150-156

[59] ASM Specialty Handbook, 1995, Machining of tool steels, pp. 352-376

[60] Agrawal, S; Chakrabarti, A K; Chattopadhyay, A B; "A study of the machining of cast austenitic stainless-steel with carbide tools", J. Materials Processing Tech. 52 (1995), pp 610-620

[61] Sarwar, M; Persson, M; Hellbergh, H; Doraisingam, A.R; "Sawability in the band sawing process when machining Hot and Cold work tool steels", Fifth International Conference on the Behaviour of Materials in Machining, Chester, November 2002

APPENDIX B

List of figures

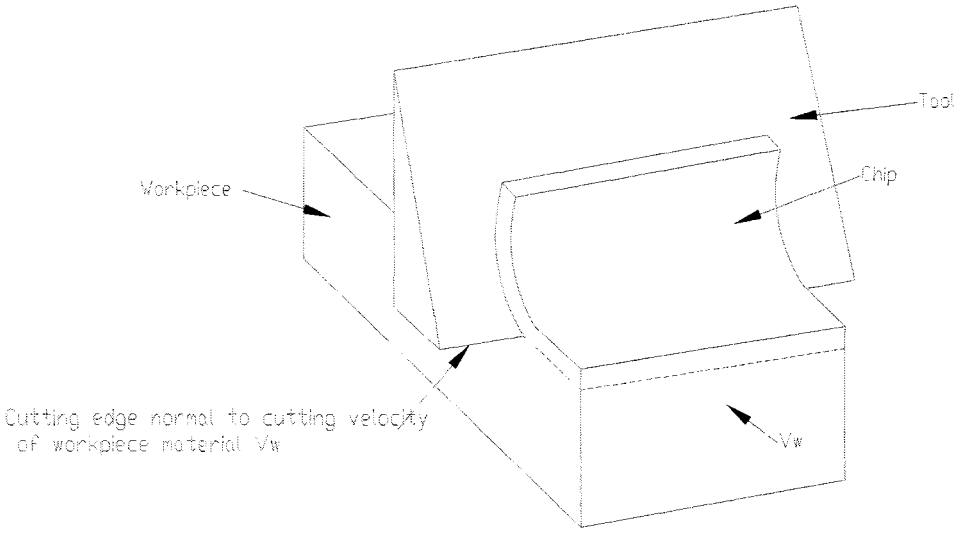

Figure 1 Orthogonal machining process

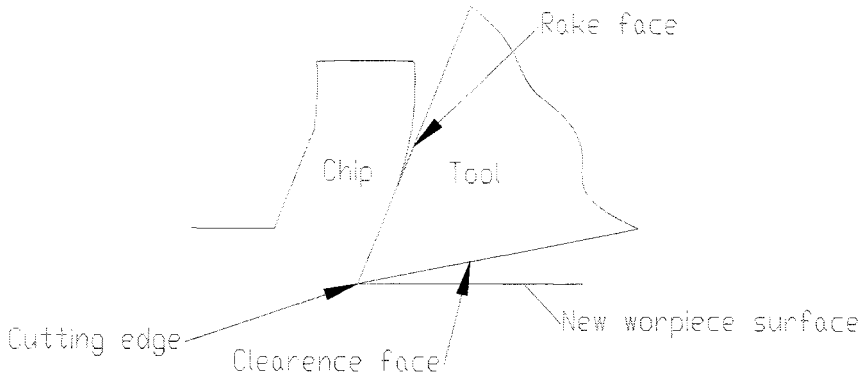

Figure 2 Terms used in metal cutting

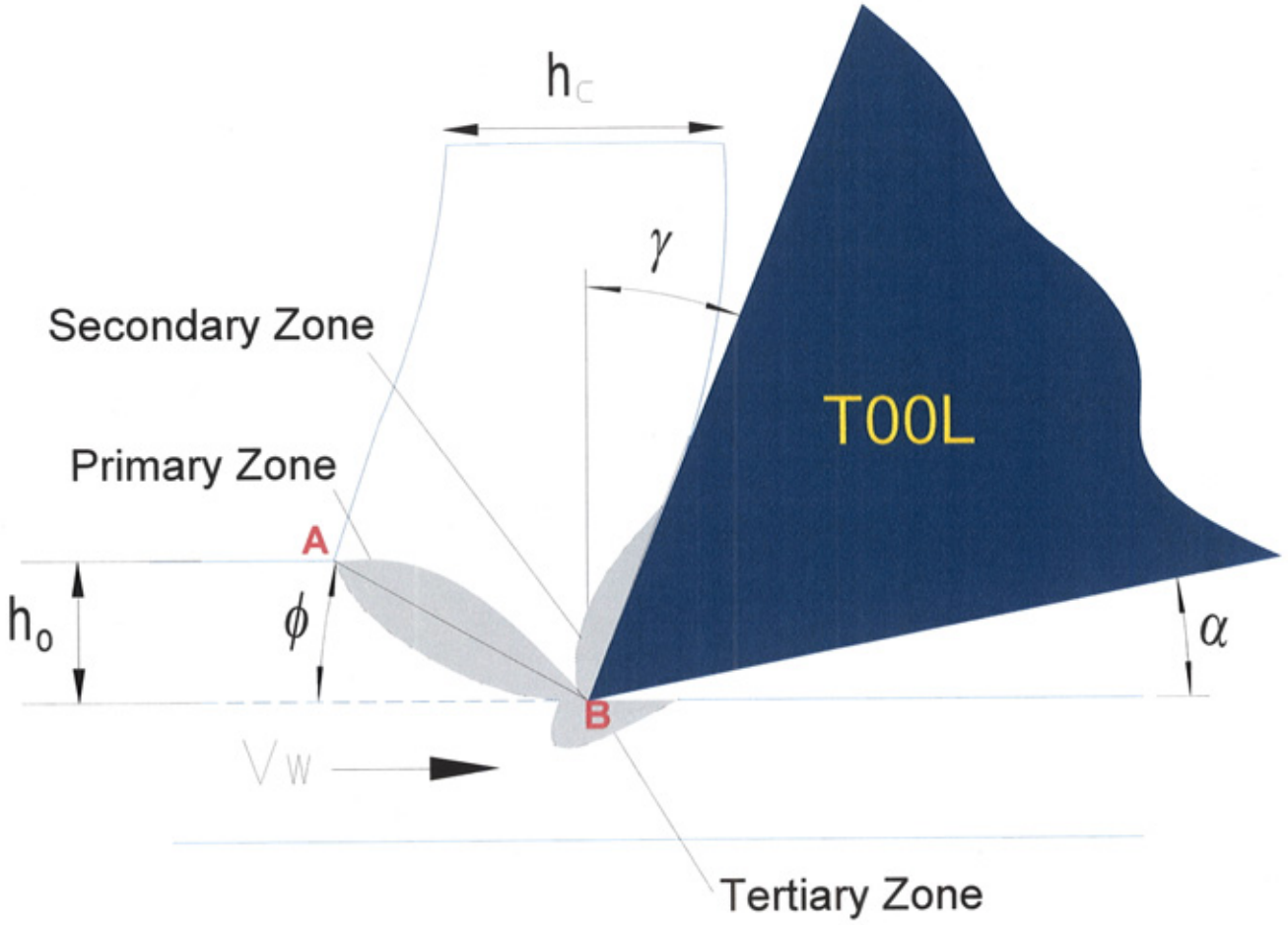

Figure 3 Deformation zones and distribution of load on the rake face

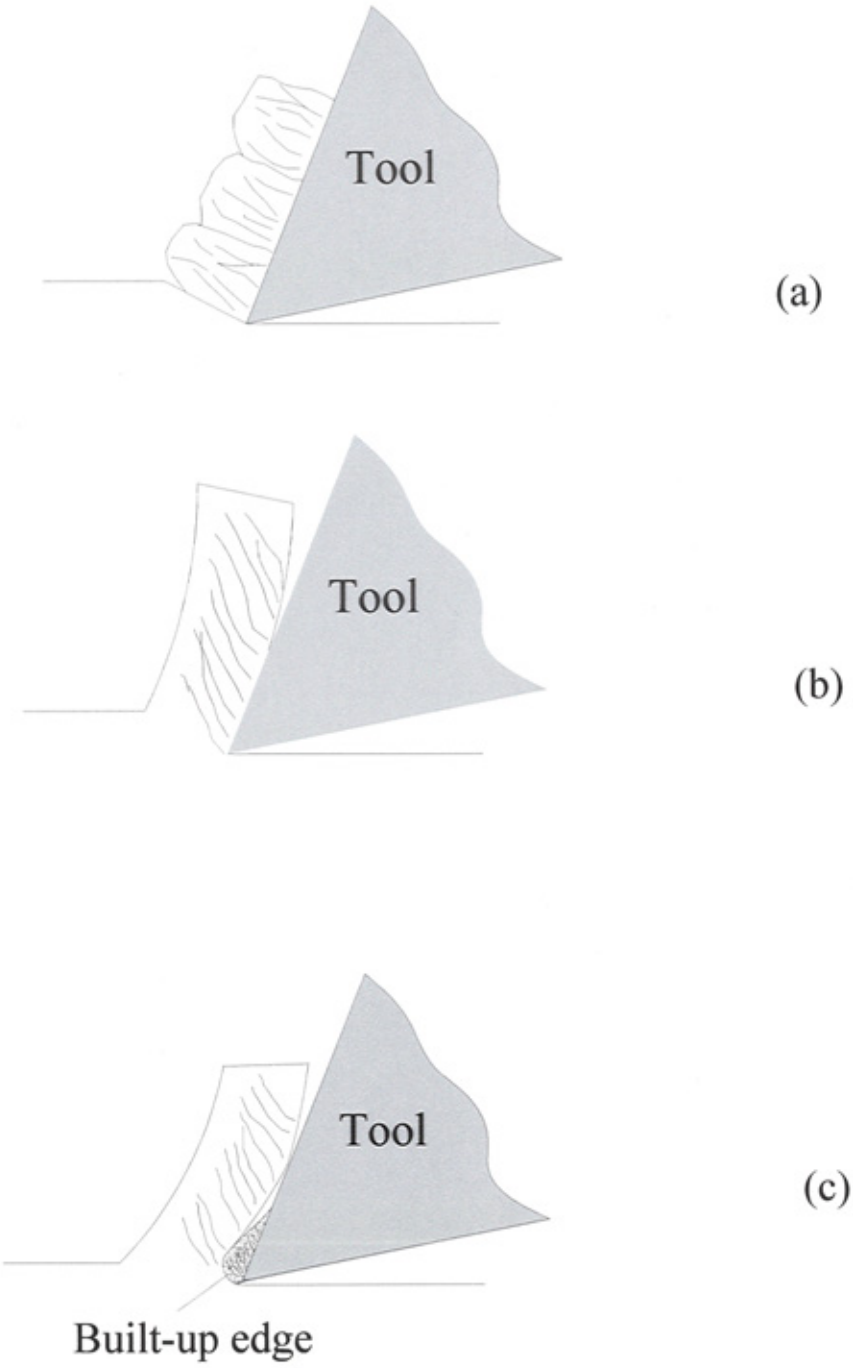

Figure 4 Sketches of different chip types: (a) discontinuous; (b) continuous;(c)continuous with built-up edge.

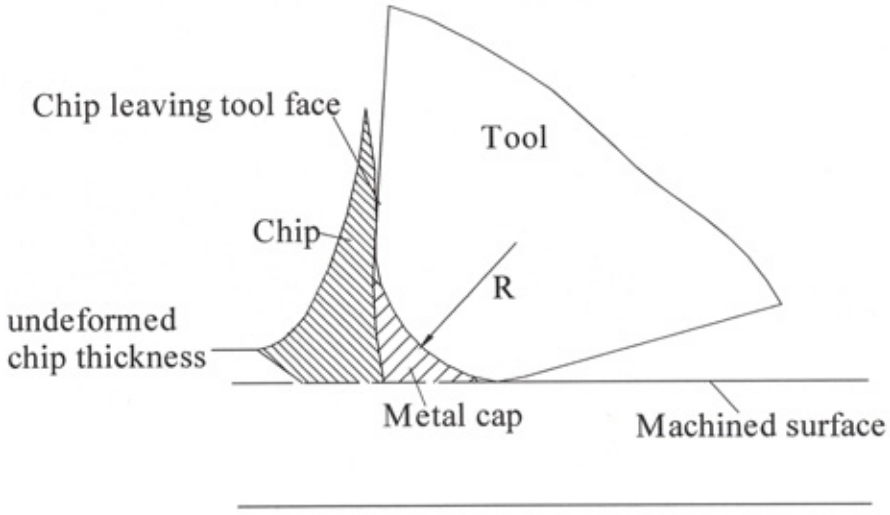

Figure 5 The effect of tooth edge radius on undeformed chip thickness [27]

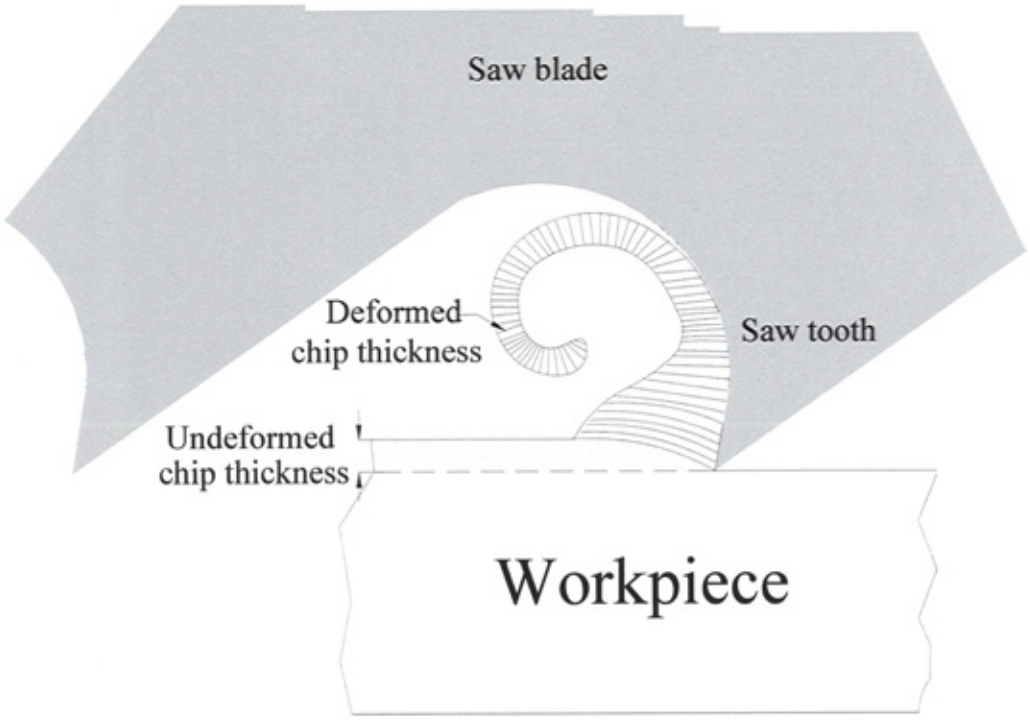

Figure 6 Chip formation in bandsawing [27]

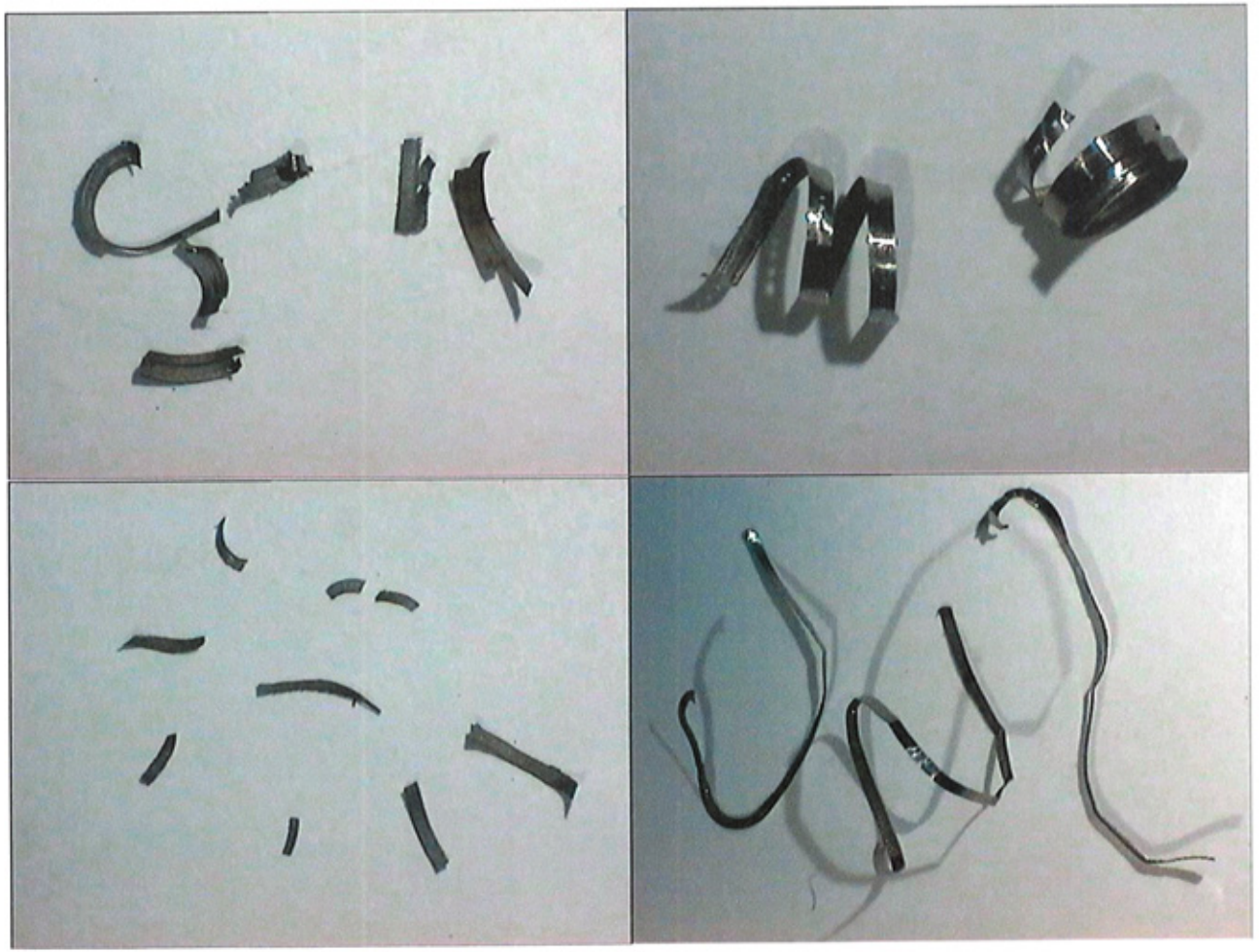

Figure 7 Example of different chip types and sizes found in bandsawing

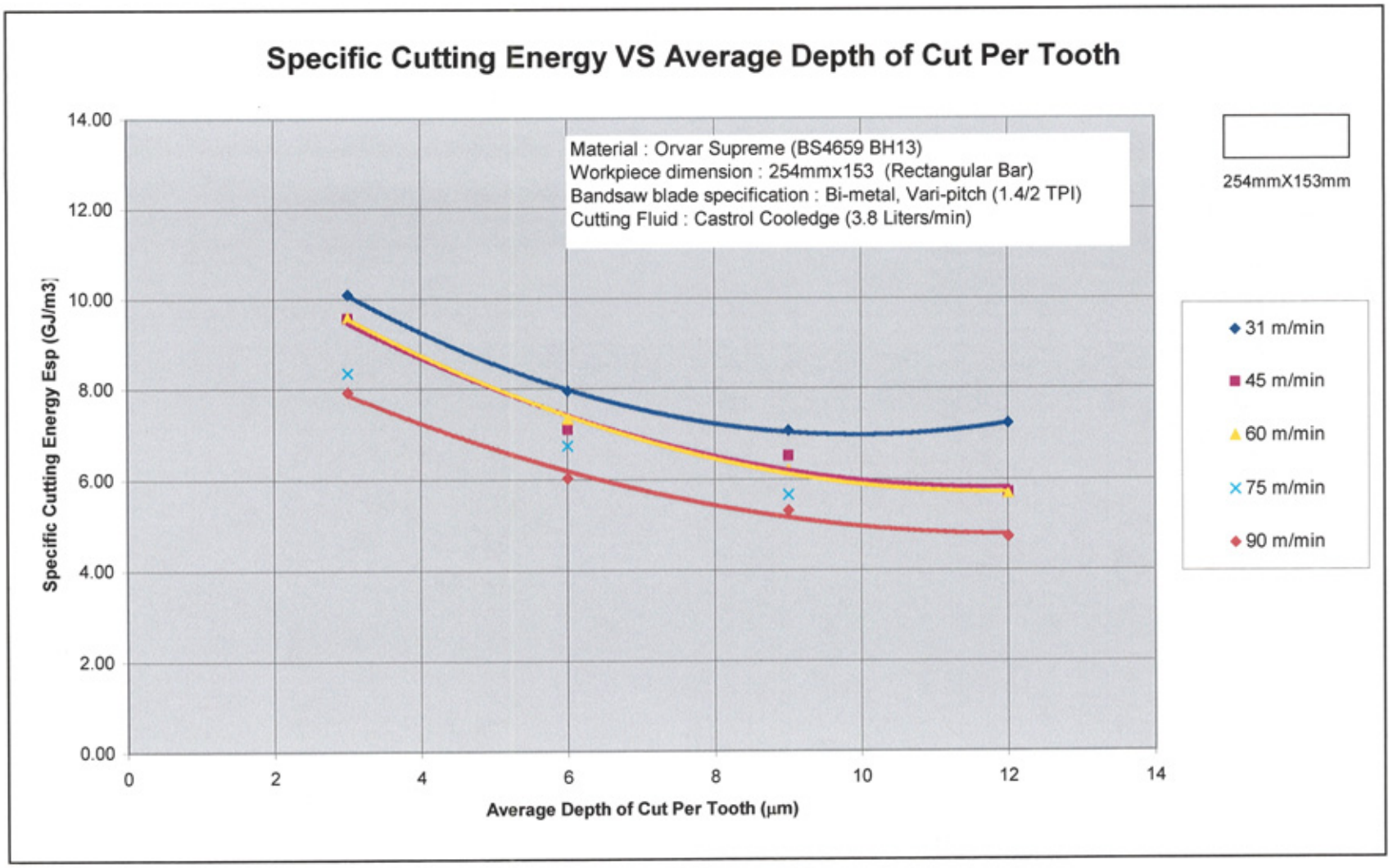

Figure 8 Influence of depth of cut on specific cutting energy

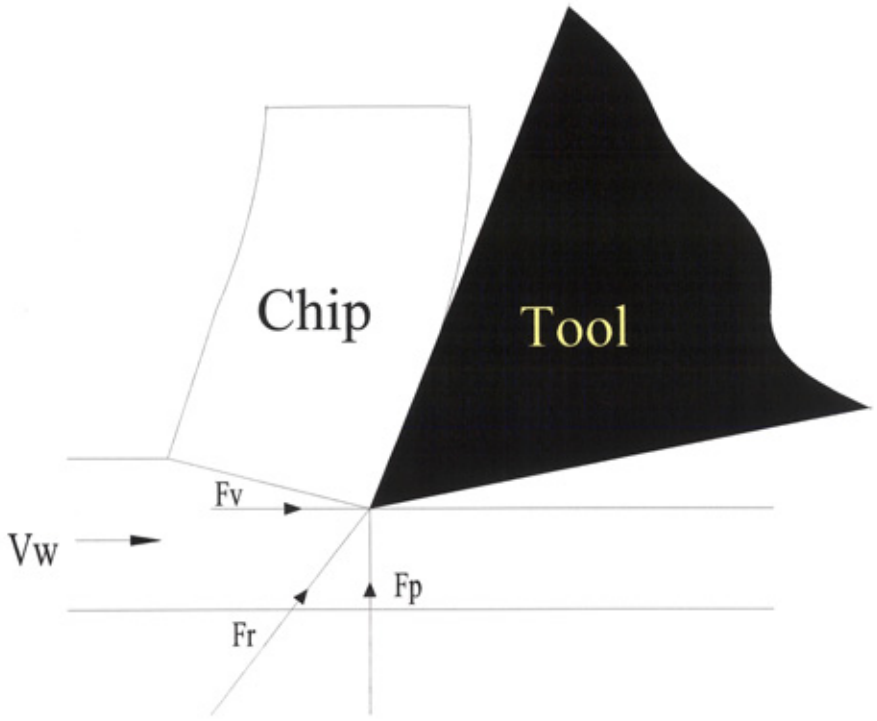

Figure 9 Force diagram for orthogonal cutting

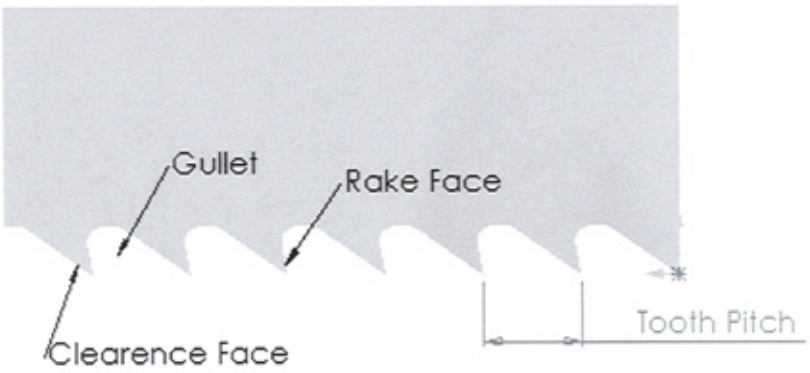

Raker Set Pattern

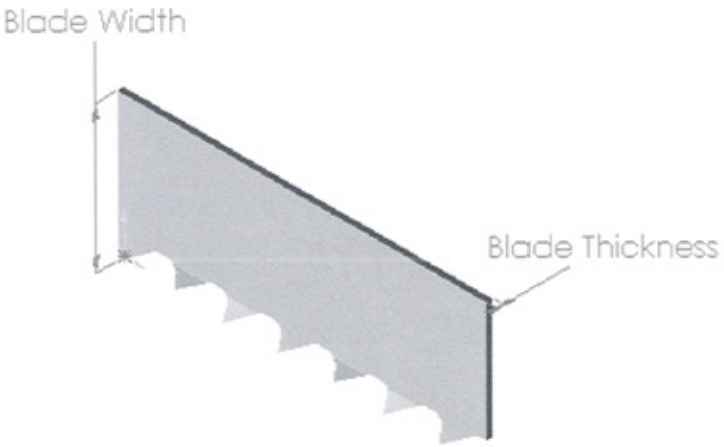

Figure 10 Bandsaw Blade Nomenclature

Figure 11 Behringer Vertical Pillar Bandsaw Machine

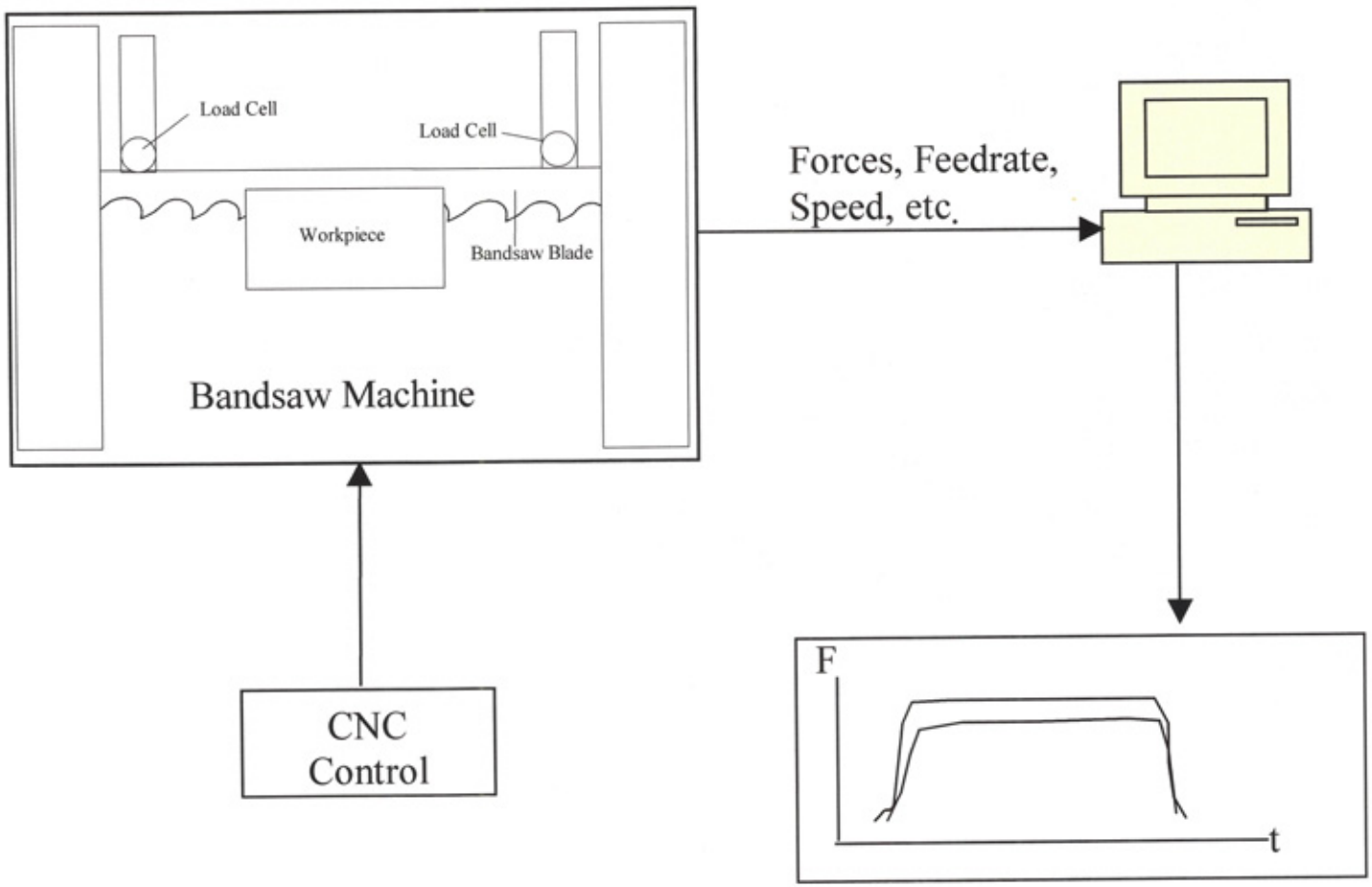

Figure 12 Schematic of experimental set-up

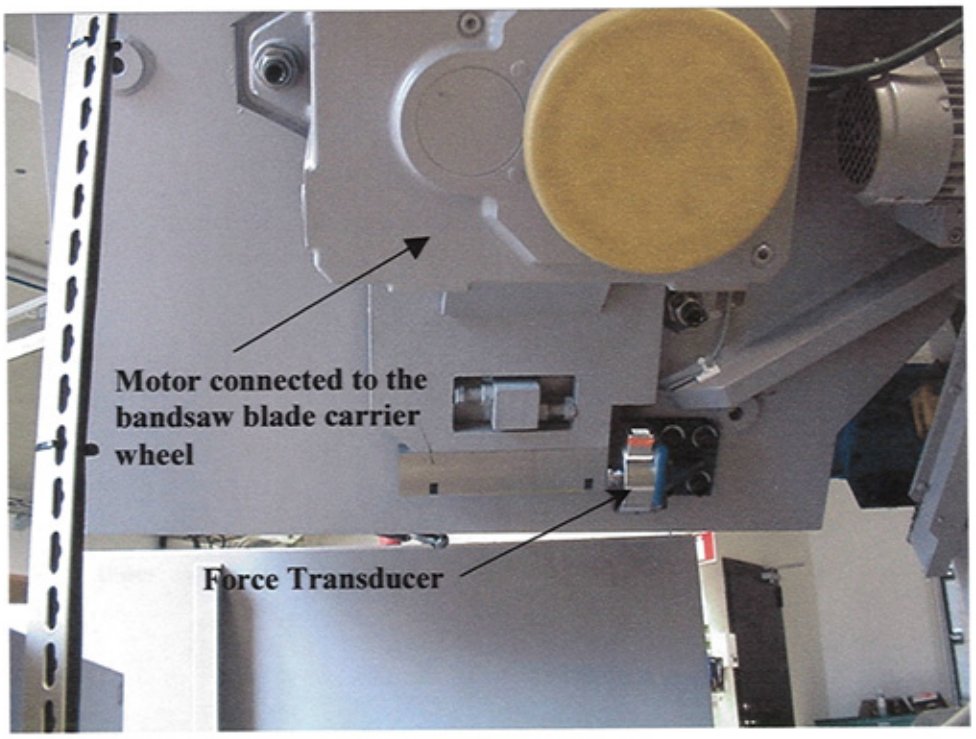

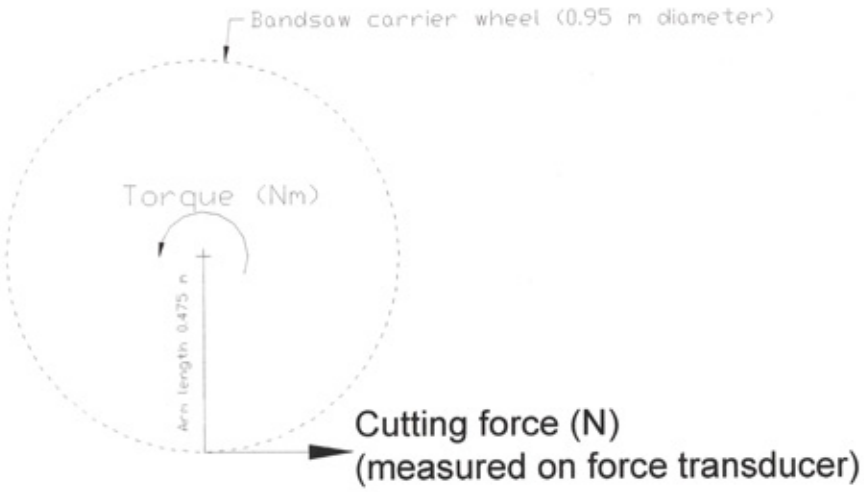

Figure 13 Location of cutting force measuring transducer

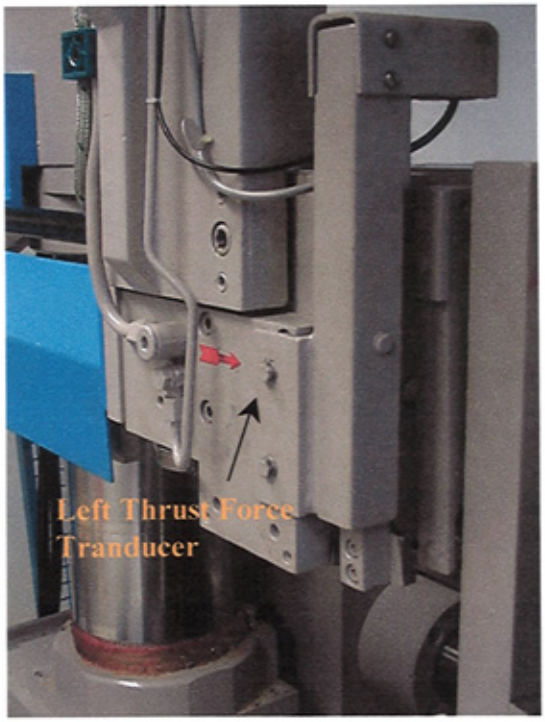

Figure 14 Left band guide thrust force transducer

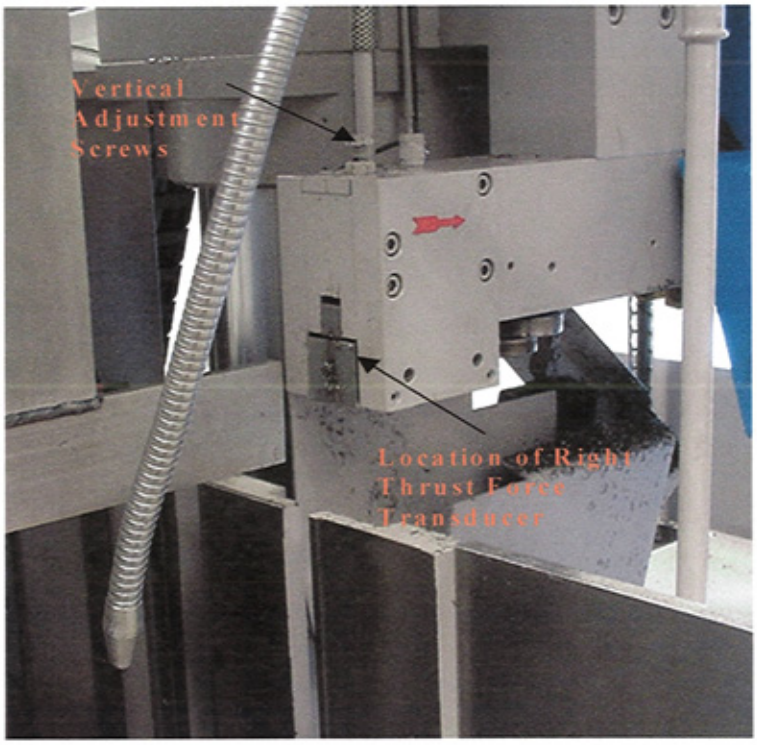

Figure 15 Right band guide thrust force transducer

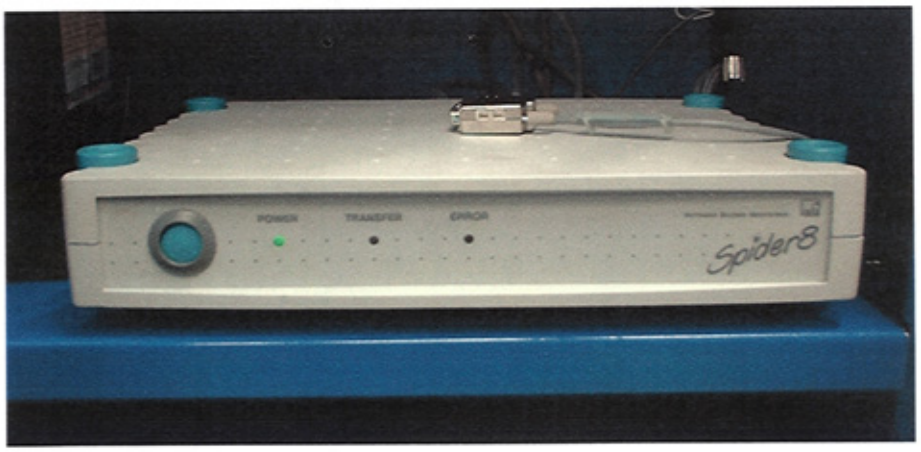

Figure 16 Data logging device, HBM Spider 8.

Figure 17 Data processing console

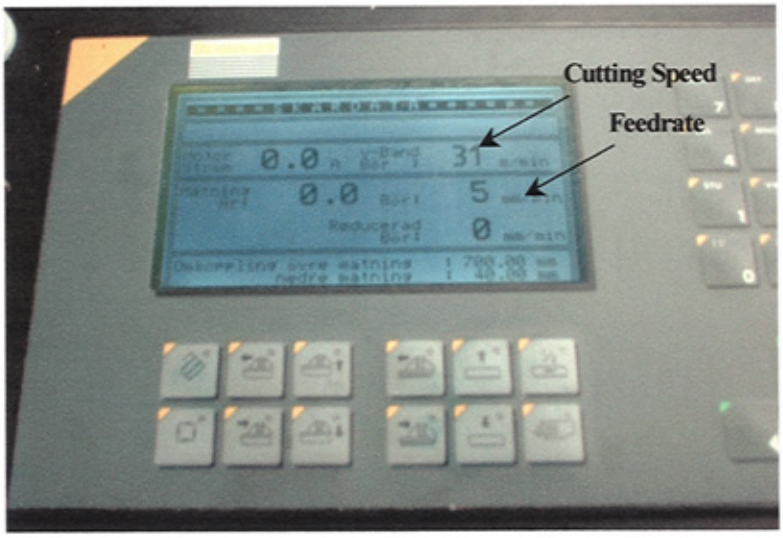

Figure 18 CNC control

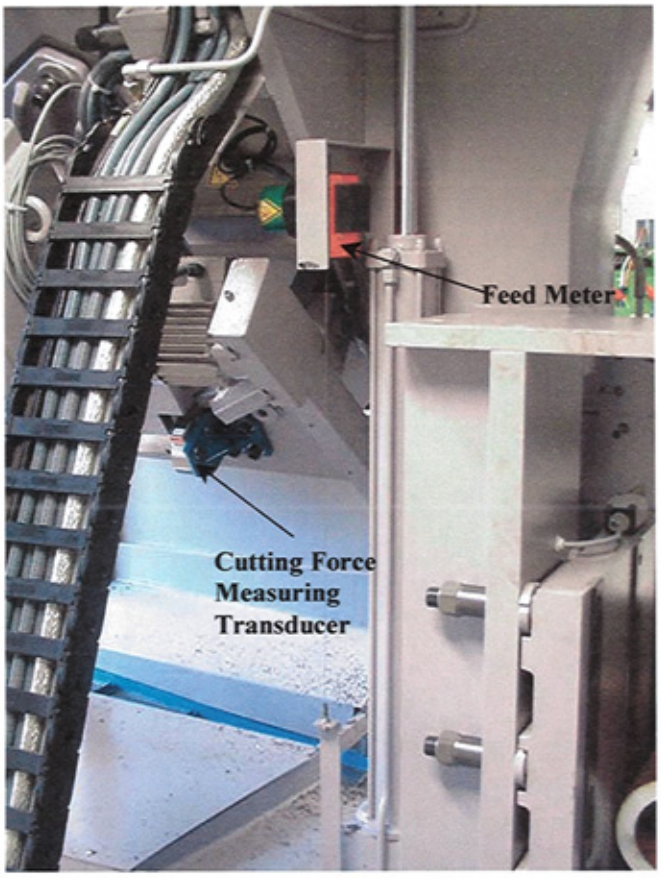

Figure 19 Feed meter location

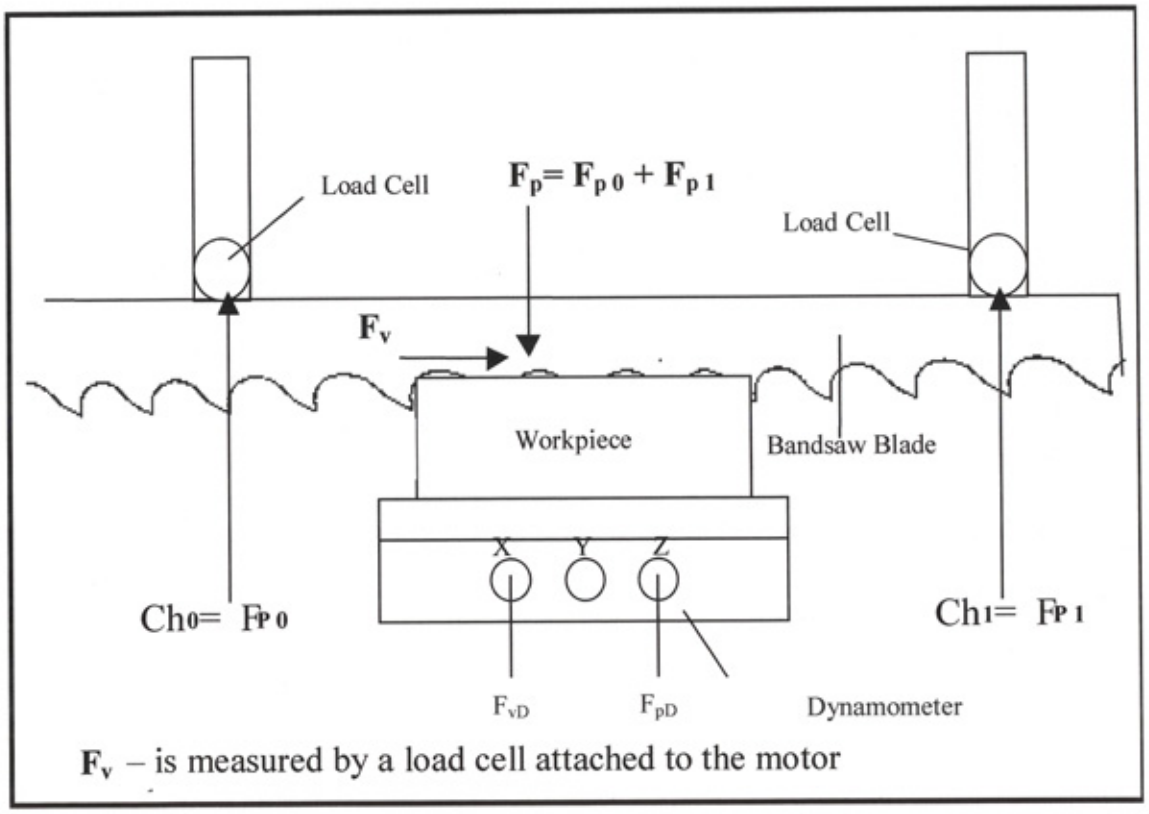

Figure 20 Experiment set-up for assessing the accuracy of force transducers located on the bandsaw machine using Kistler Dynamometer.

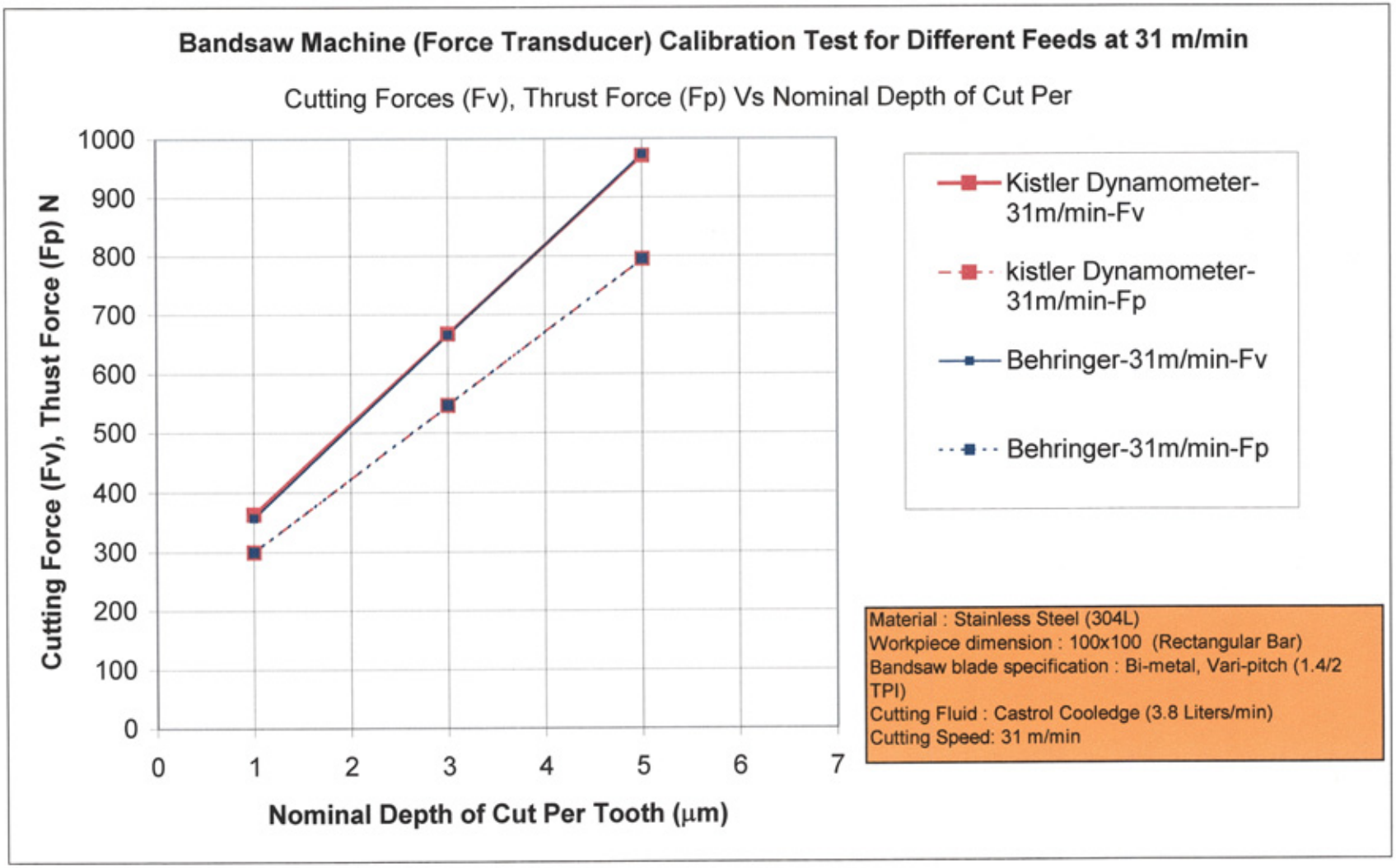

Figure 21 Dynamometer test result at 31 m/min bandspeed

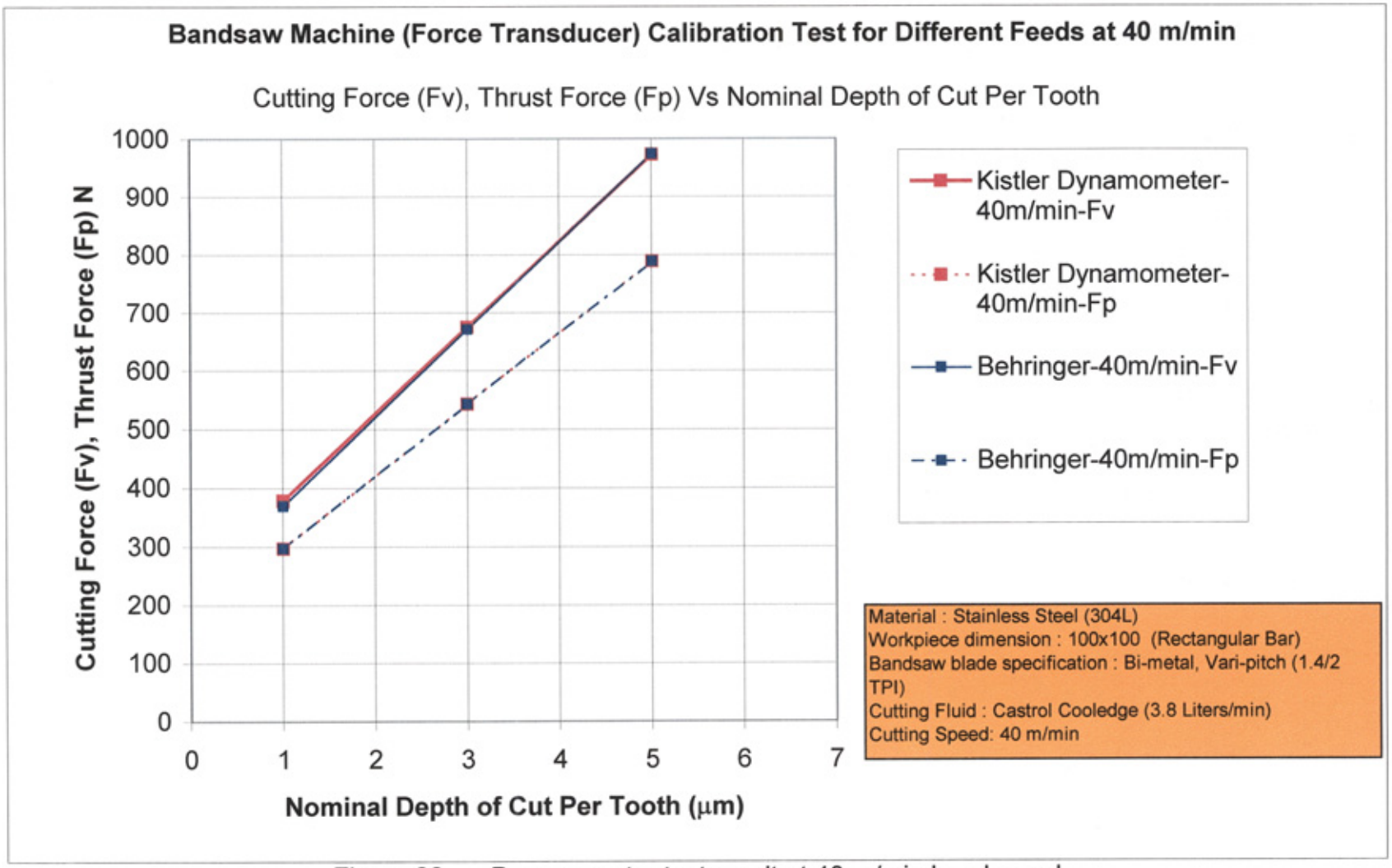

Figure 22 Dynamometer test result at 40 m/min bandspeed

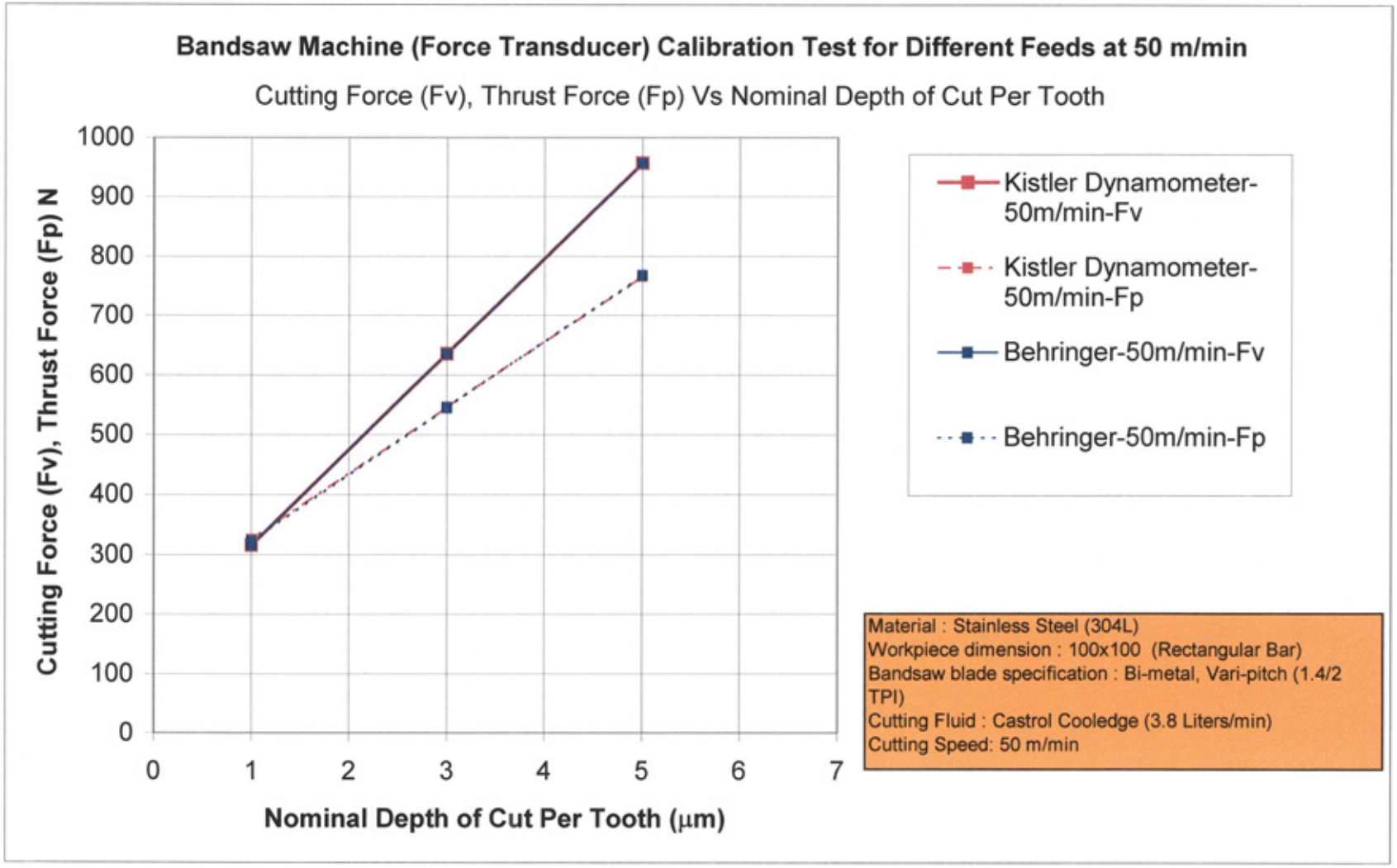

Figure 23 Dynamometer test result at 50 m/min bandspeed

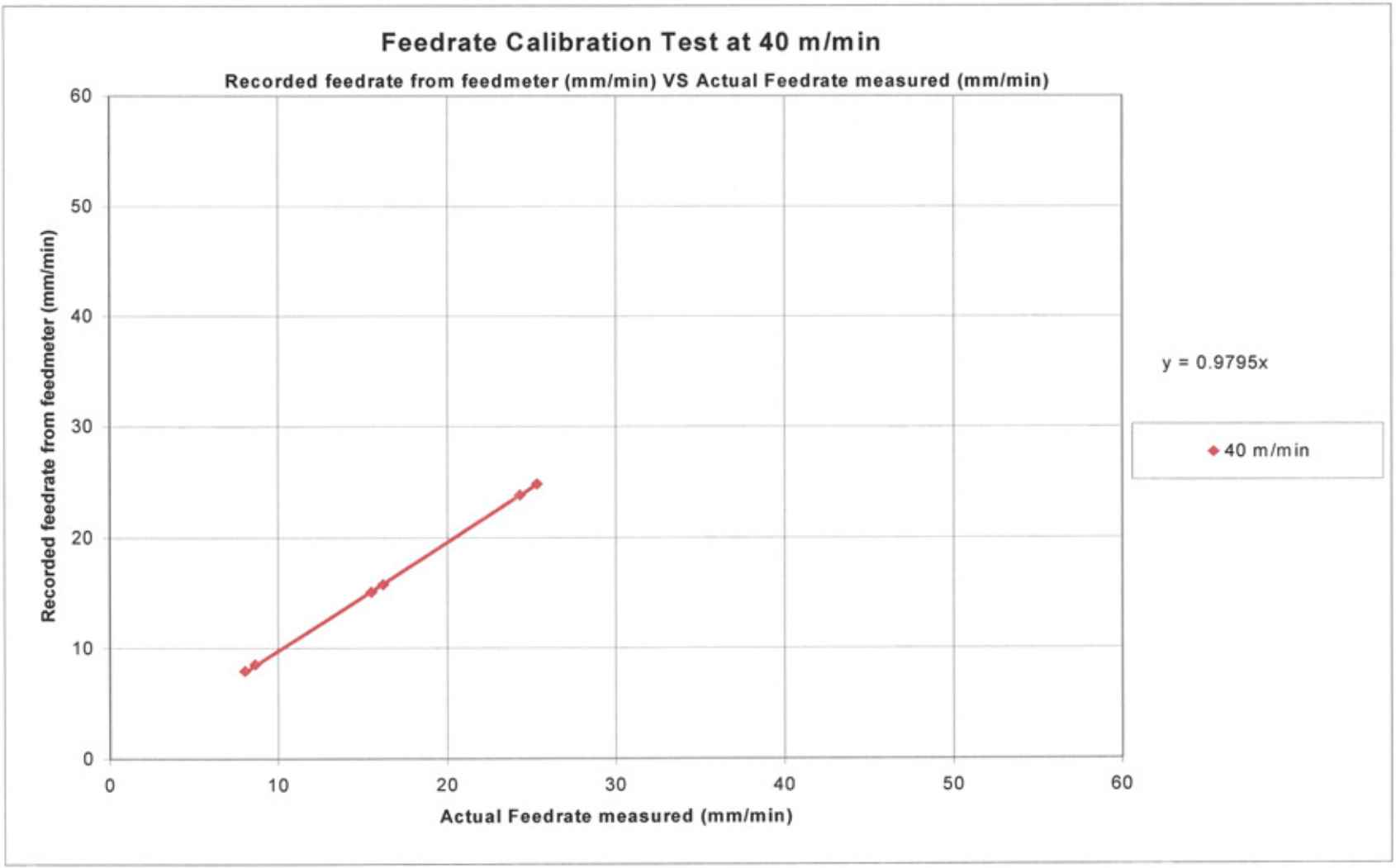

Figure 24 Feedrate Calibration test at 40 m/min

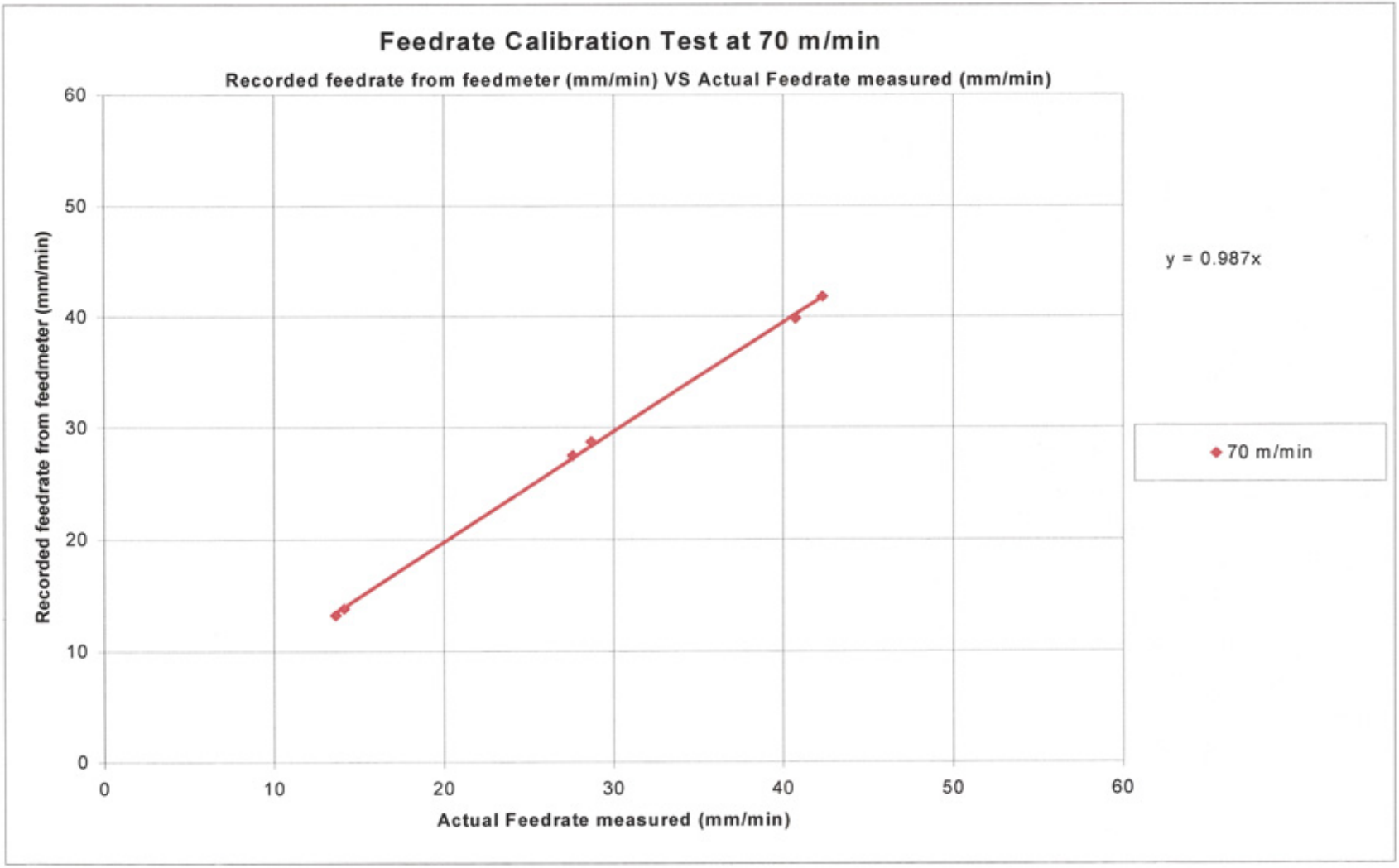

Figure 25 Feedrate Calibration test at 70 m/min

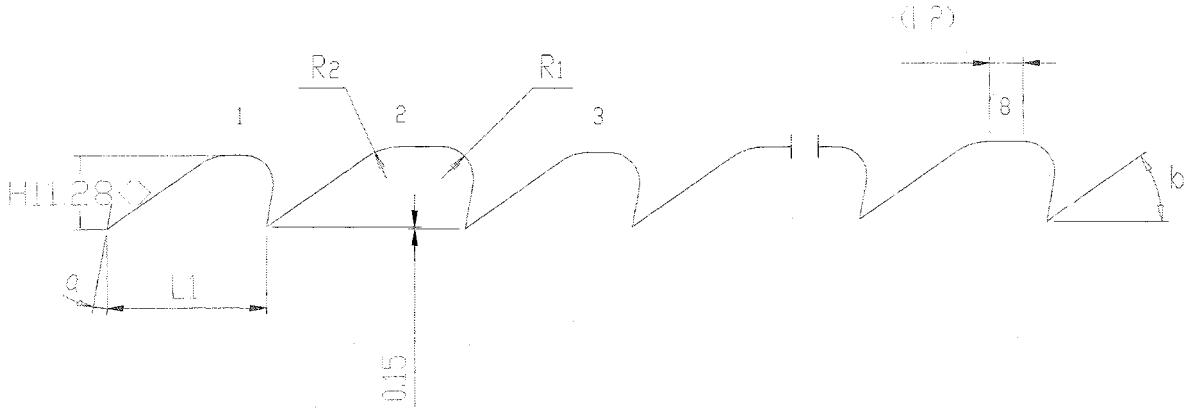

Gullet	L	(L_2)	H	R_1	R_2	a	b
1	12.1	(1.3)	5.6	2.2	3.3	10	35
2	15.2	(3.0)	6.2	2.5	5.0	10	35
3	13.0	(1.7)	5.8	2.3	3.7	10	35
4	15.0	(2.9)	6.1	2.5	4.9	10	35
5	13.6	(2.0)	6.0	2.3	4.0	10	35
6	15.7	(3.3)	6.3	2.5	5.2	10	35
7	12.4	(1.5)	5.7	2.2	3.5	10	35
8	14.3	(2.6)	6.0	2.4	4.5	10	35
S	111.1						

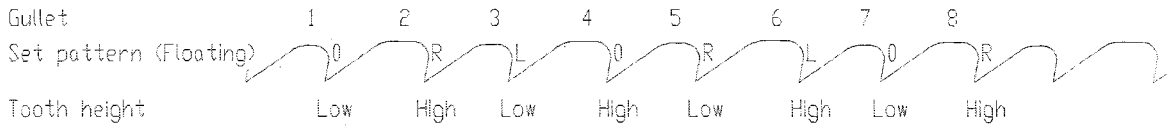

Figure 26 Bandsaw blade specification

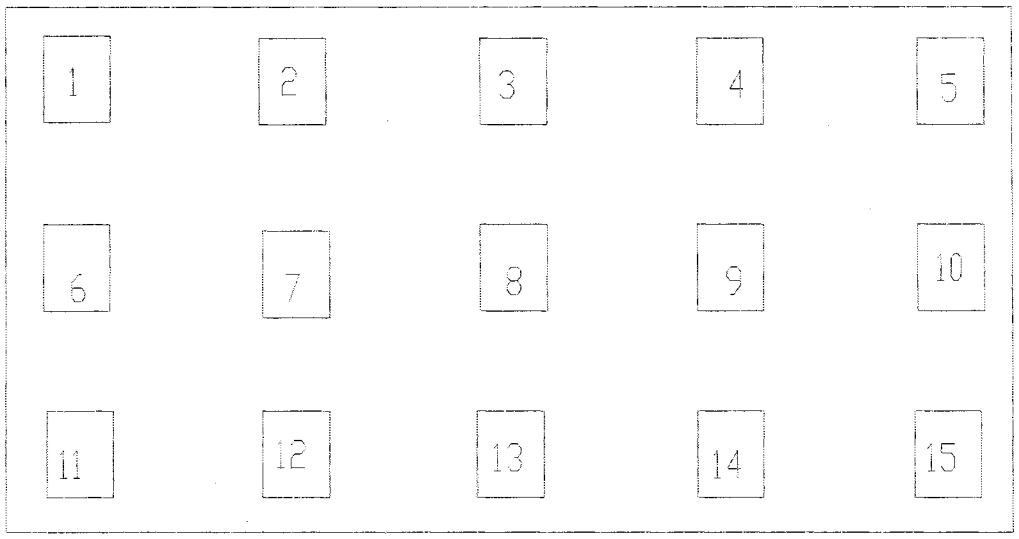

Figure 27 Test sample taken for hardness test from saw section of workpiece material

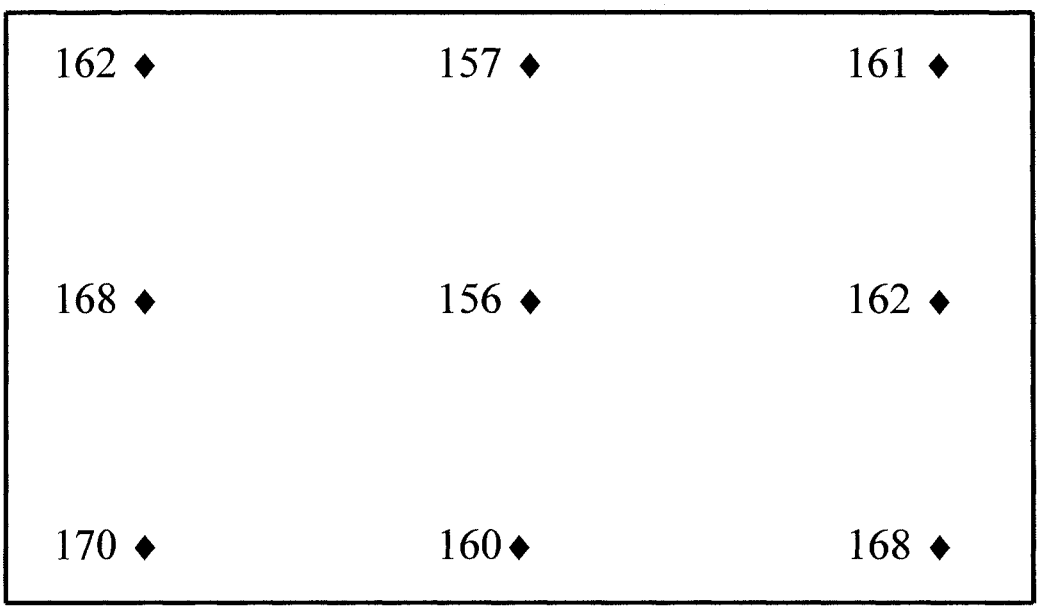

Figure 28 Hardness Measurements for Stainless Steel workpiece material

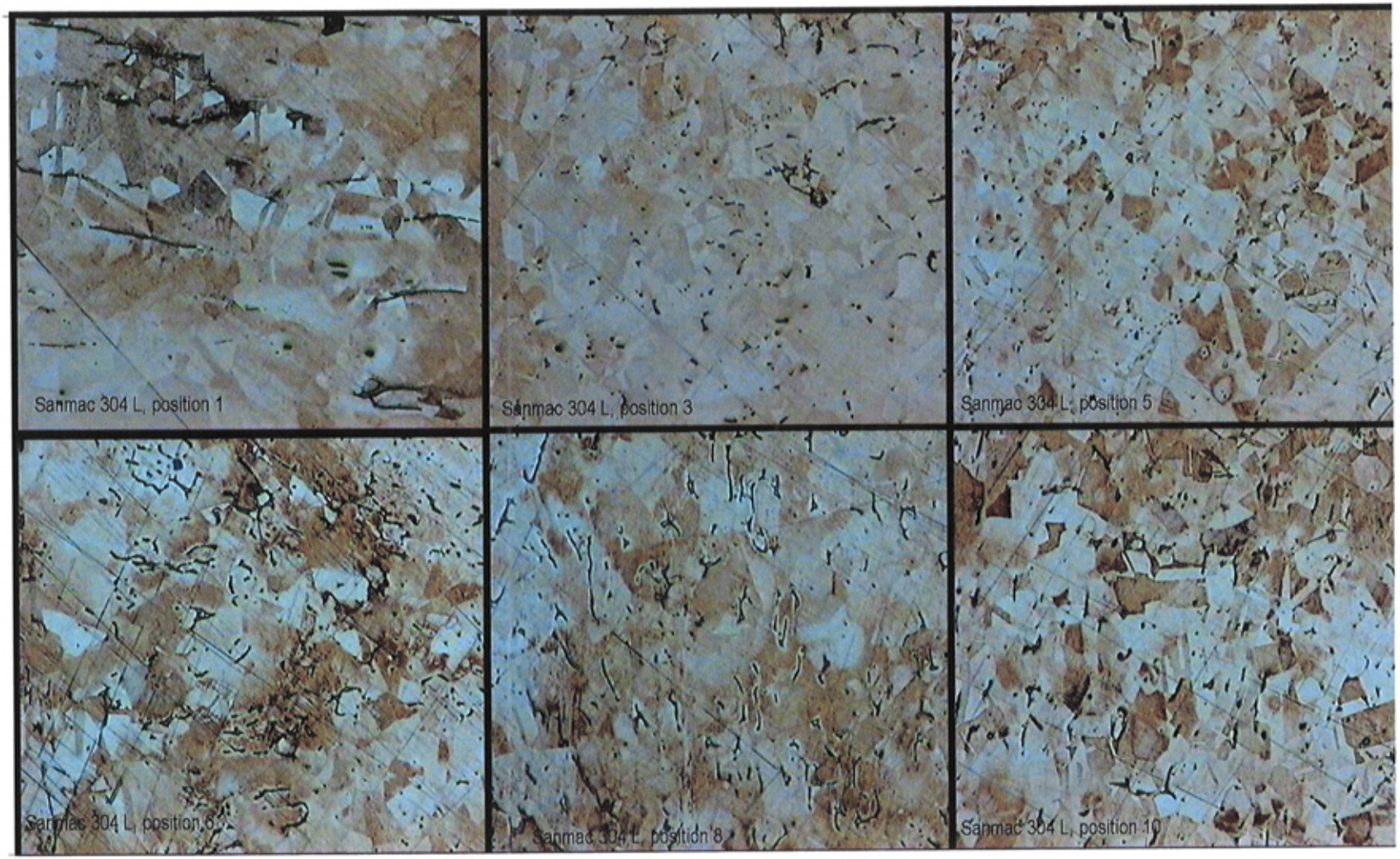

Figure 29 Stainless Steel, Magnification 50X, Etch agent: concentrated hydrochloric acid

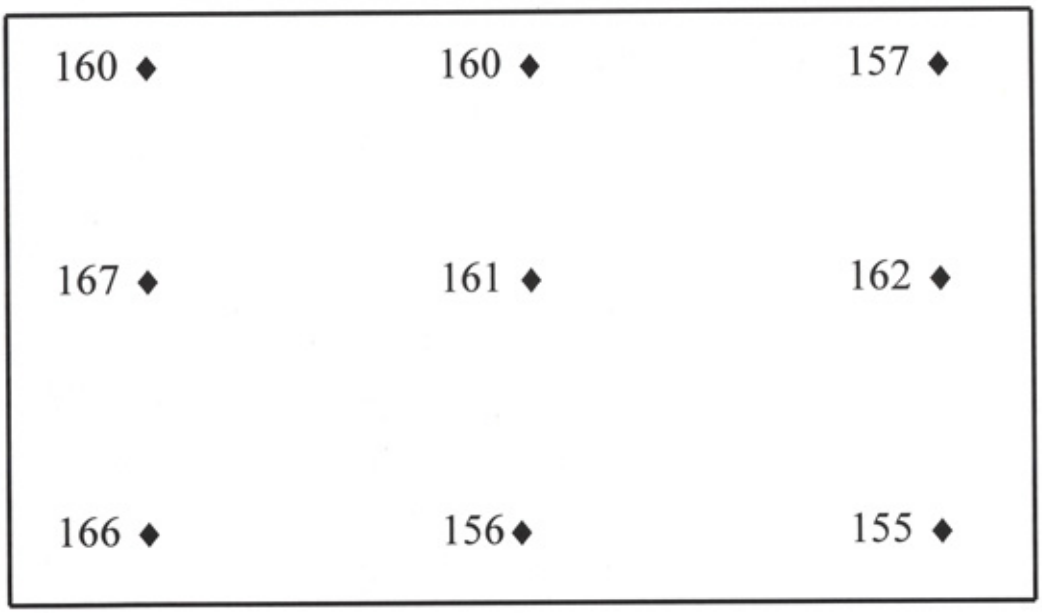

Figure 30 Hardness measurements for Workpiece-X material

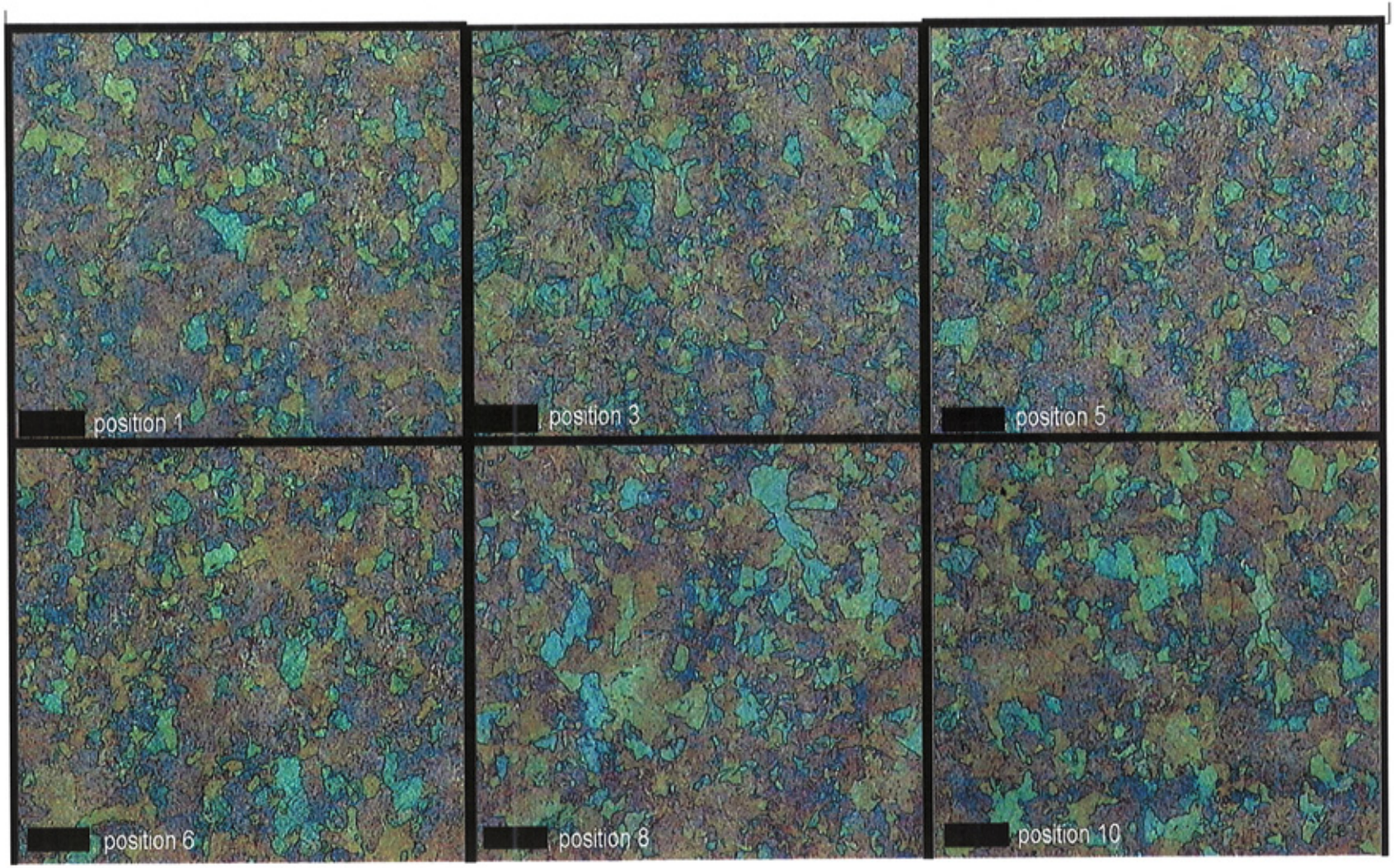

Figure 31 Workpiece-X material, Magnification 200X, Special etch agent

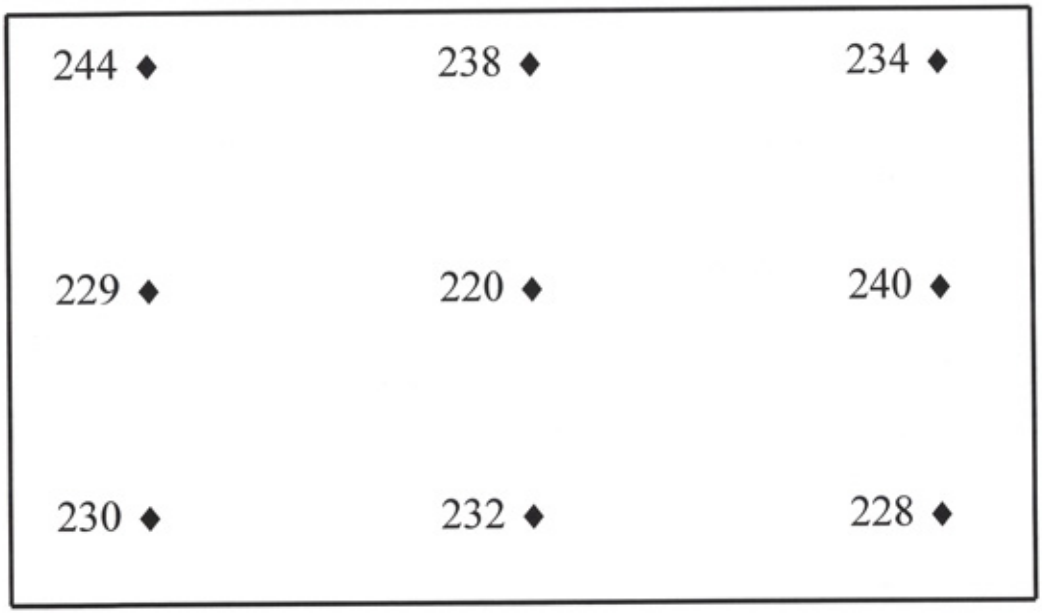

Figure 32 Hardness measurements for Workpiece-Y material

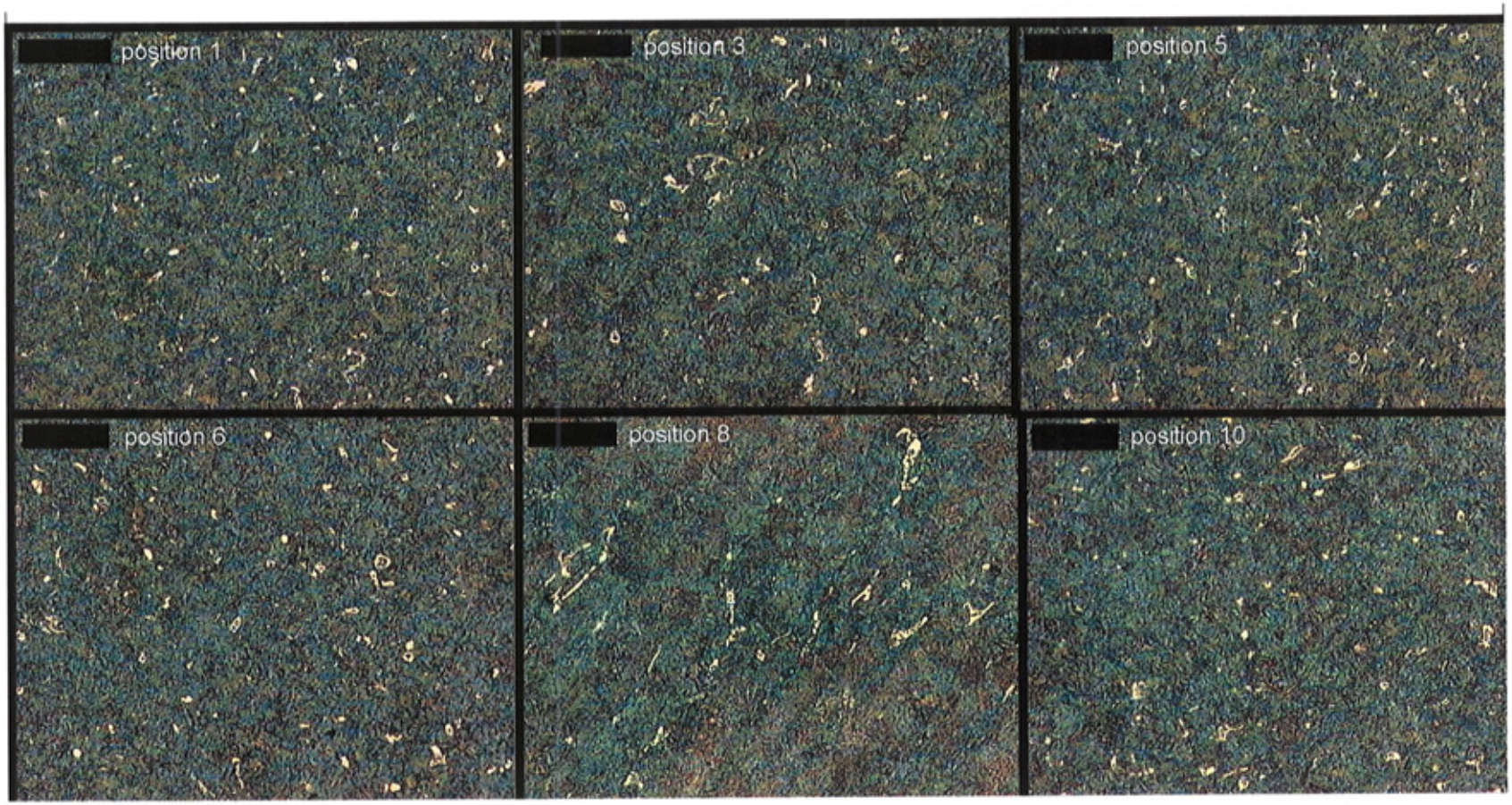

Figure 33 Workpiece-Y material, Magnification 100X, Special etch agent

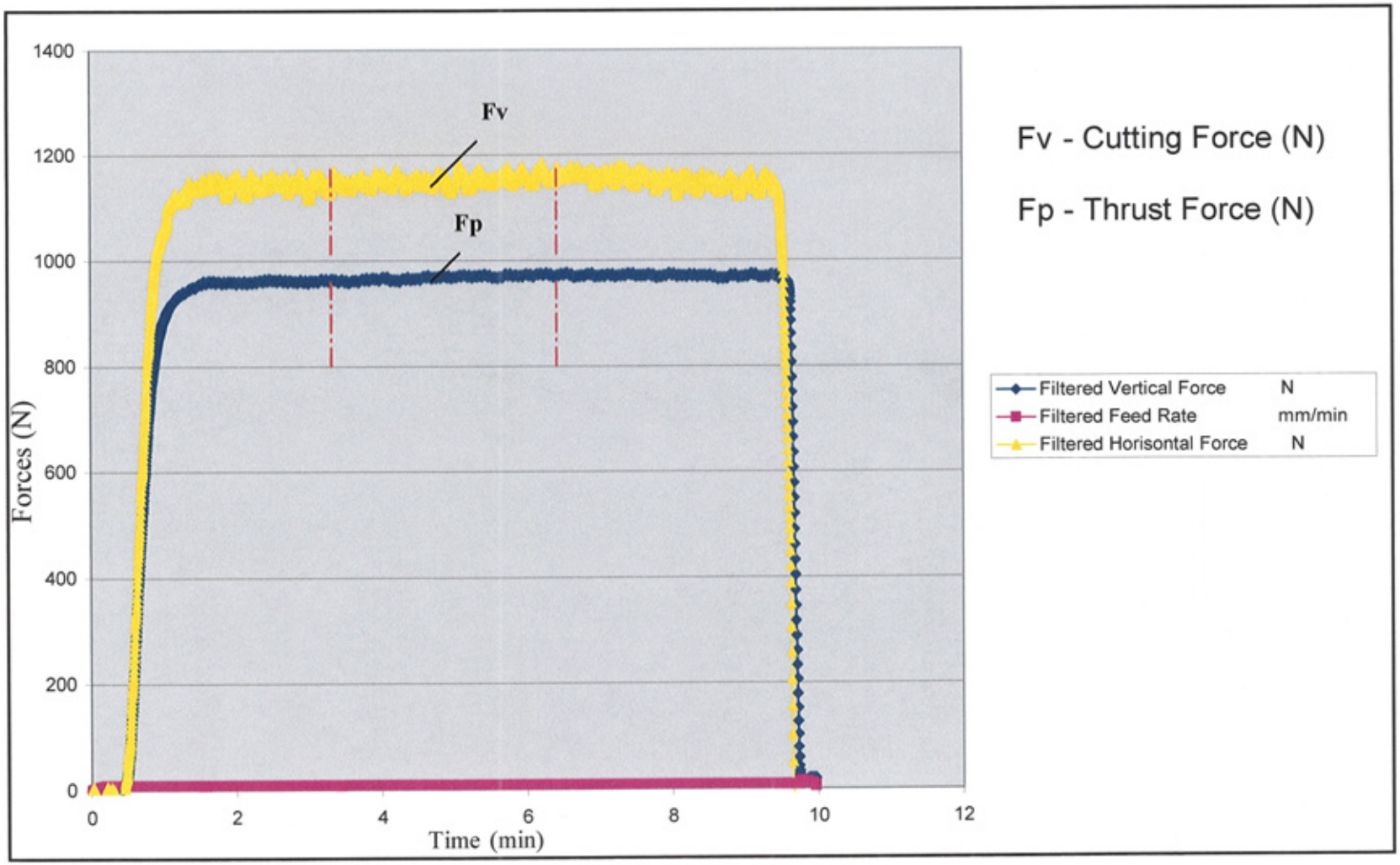

Figure 34 Typical Force against Time measured when sawing a rectangular bar

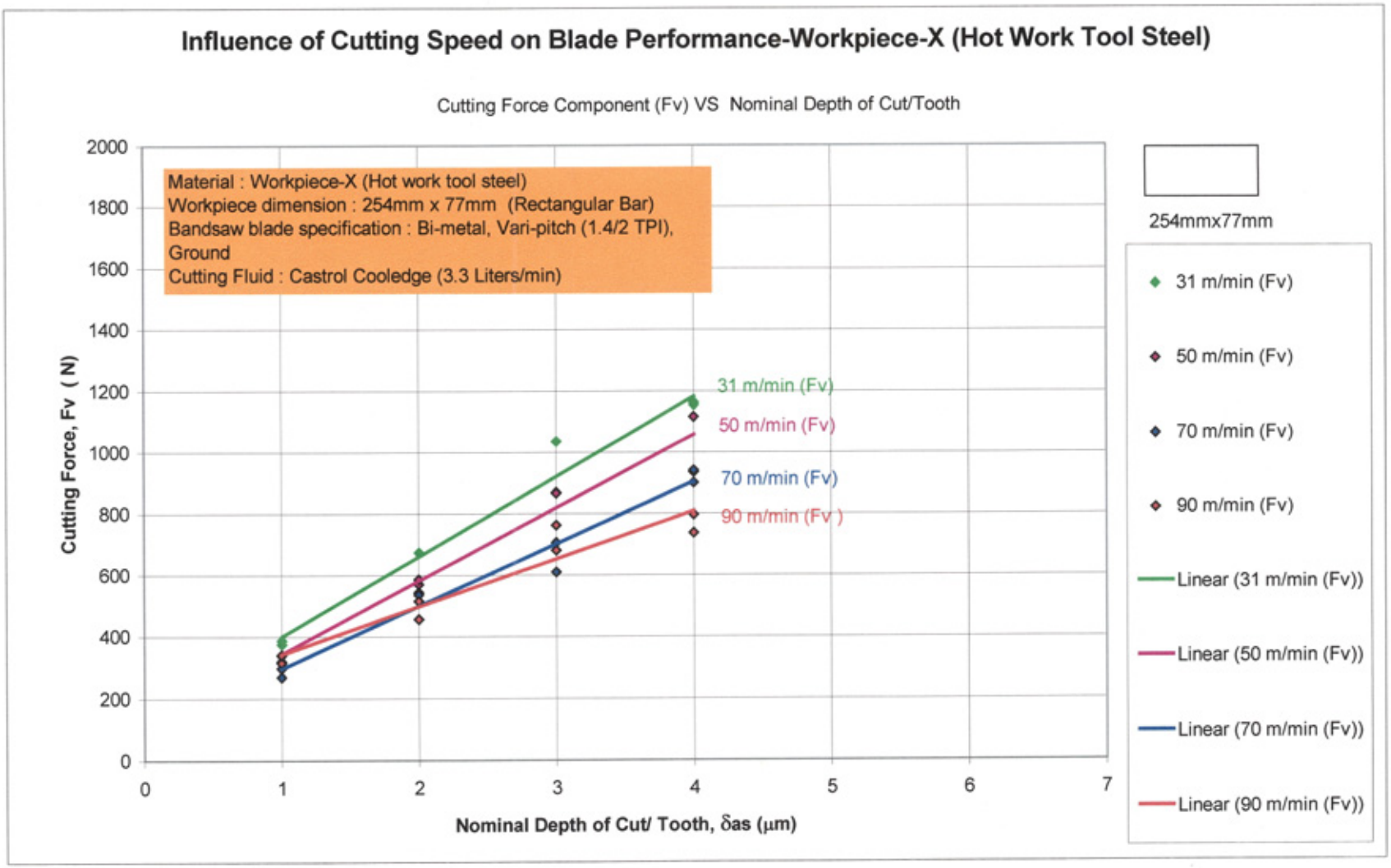

Figure 35 Influence of cutting speed on cutting force for Workpiece-X material

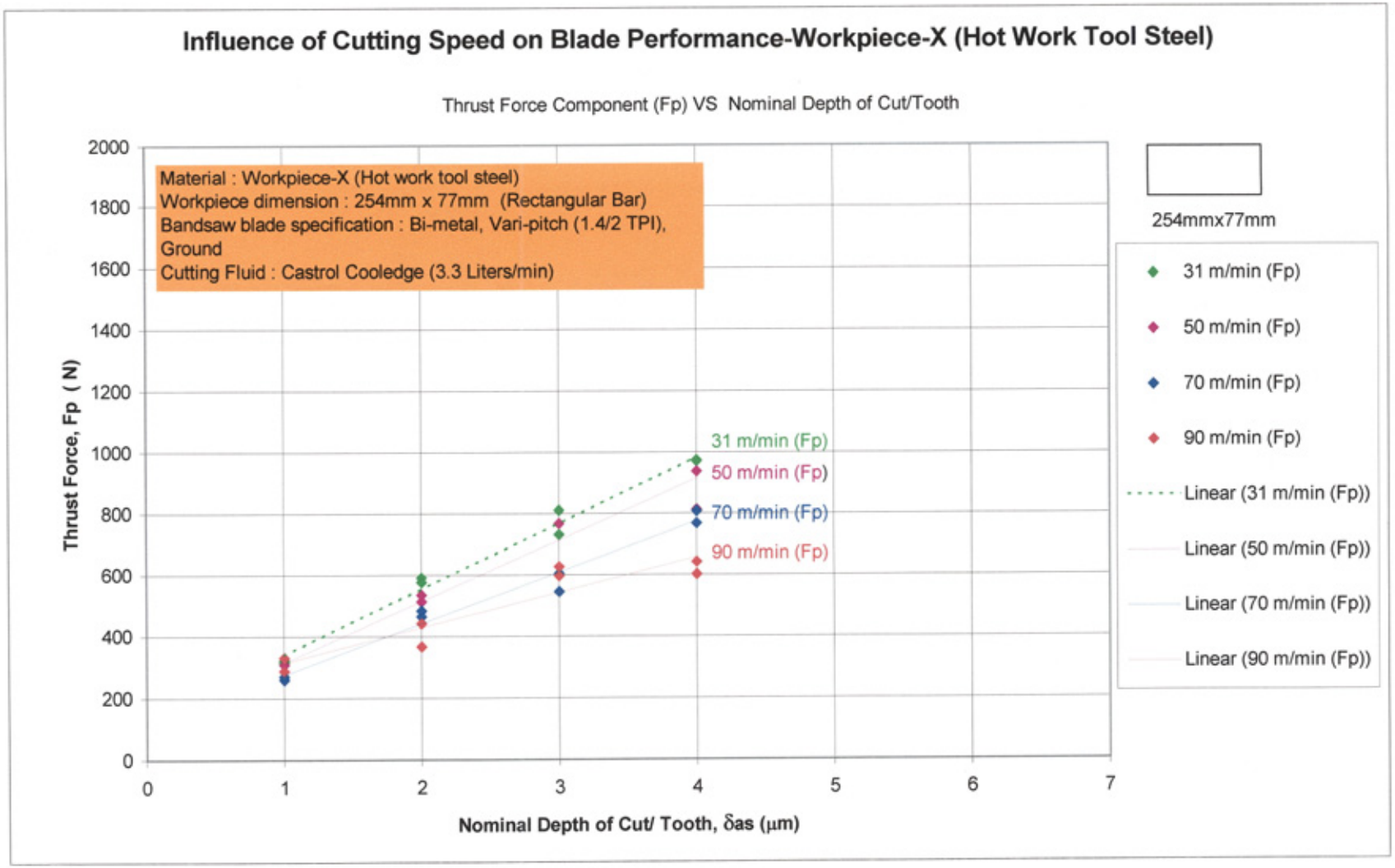

Figure 36 Influence of cutting speed on thrust force for Workpiece-X material

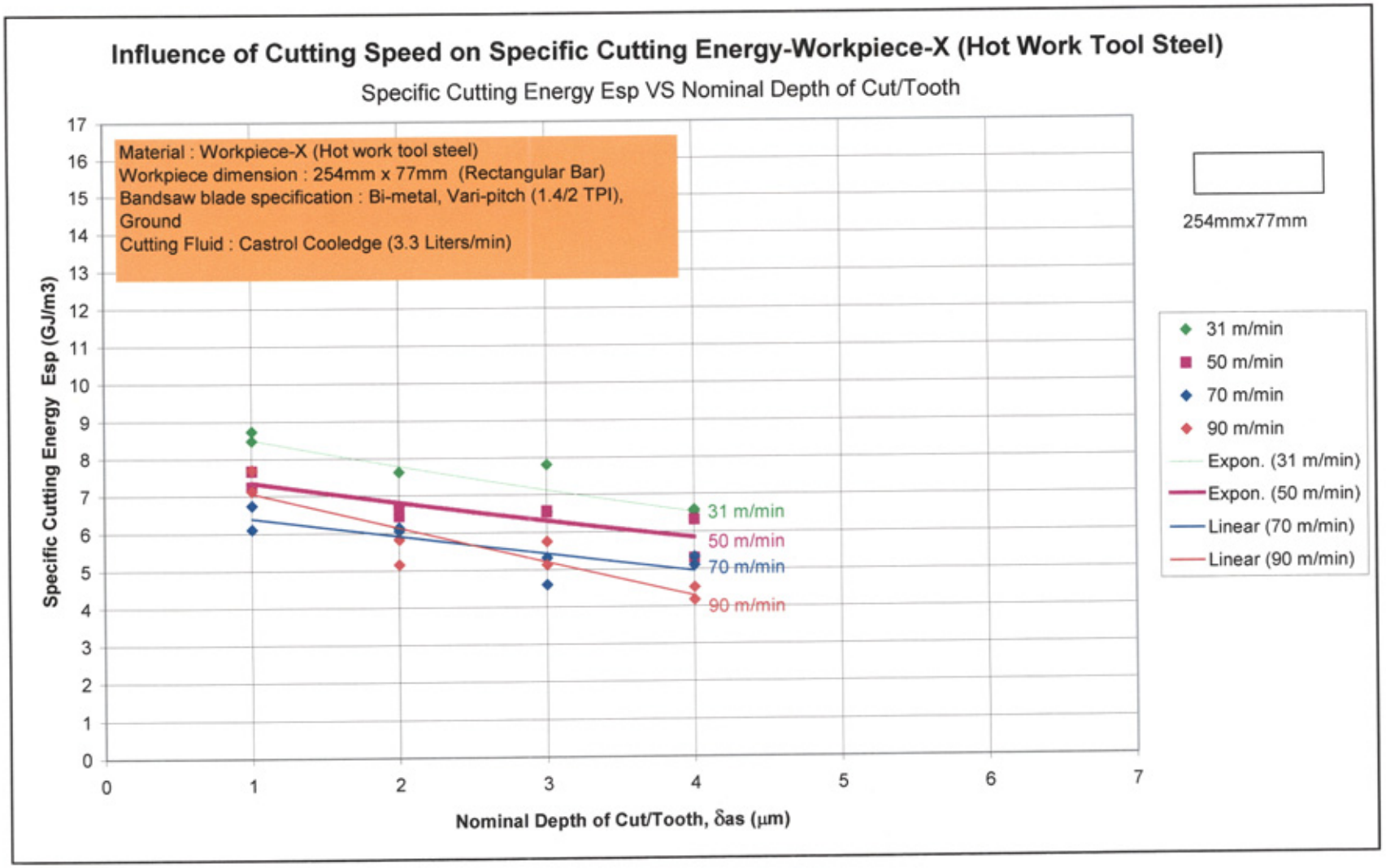

Figure 37 Influence of cutting speed on the performance for Workpiece-X

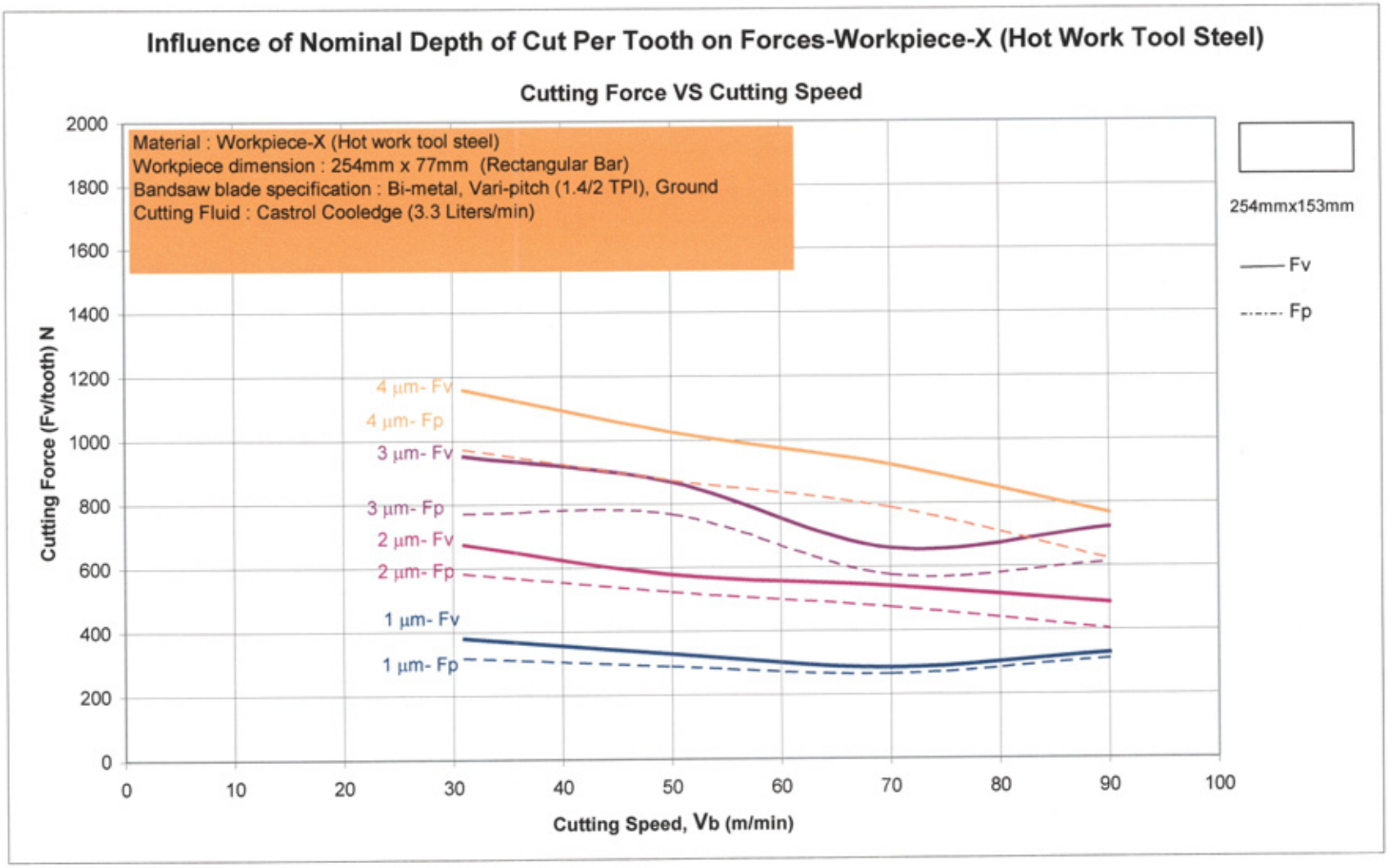

Figure 38 Influence of nominal depth of cut per tooth on forces for Workpiece-X material

Figure 39 Influence of cutting speed on cutting force for Workpiece-Y material

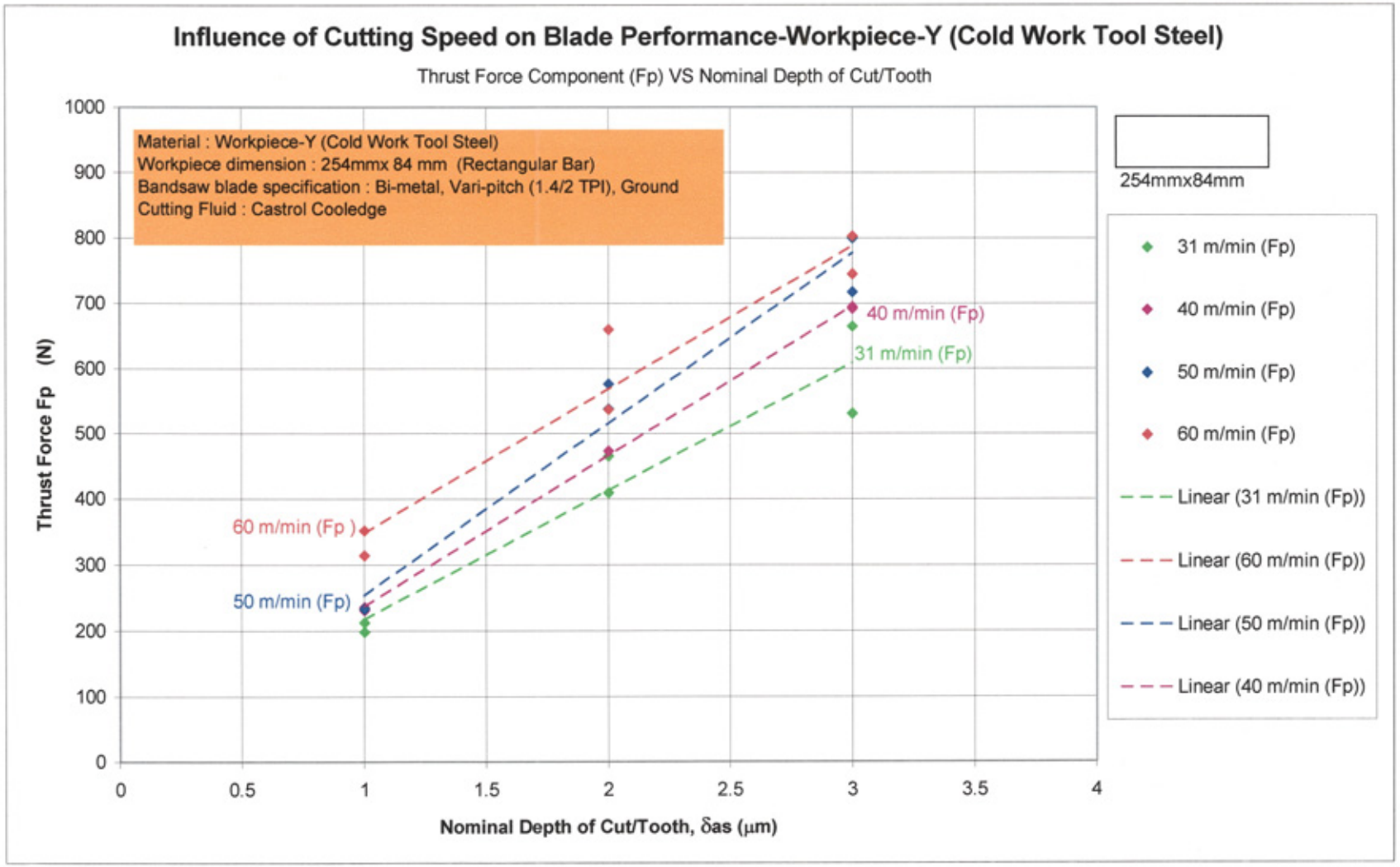

Figure 40 Influence of cutting speed on thrust force Workpiece-Y material

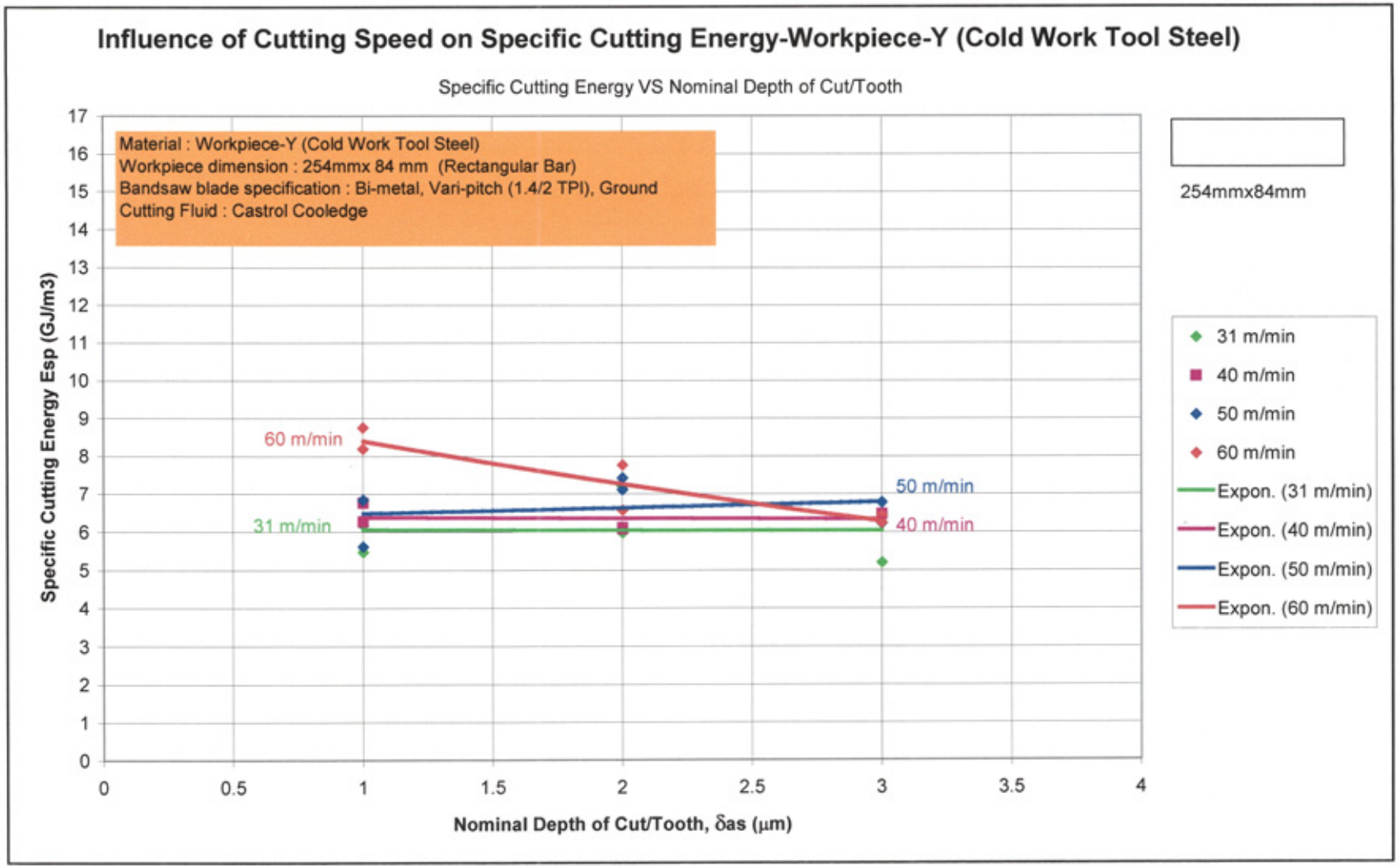

Figure 41 Influence of cutting speed on the performance for Workpiece-Y material

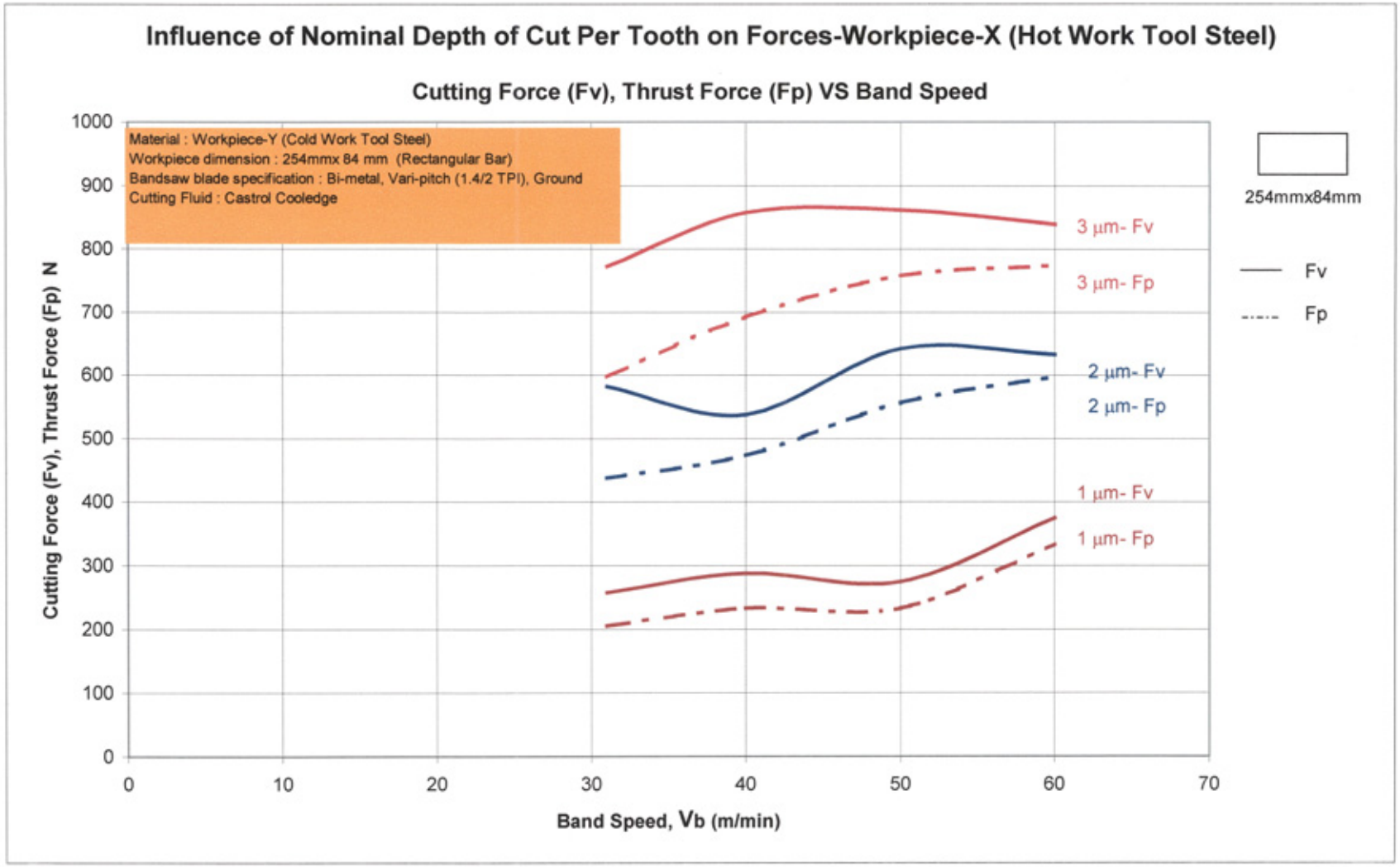

Figure 42 Influence of nominal depth of cut per tooth on forces for Workpiece-Y

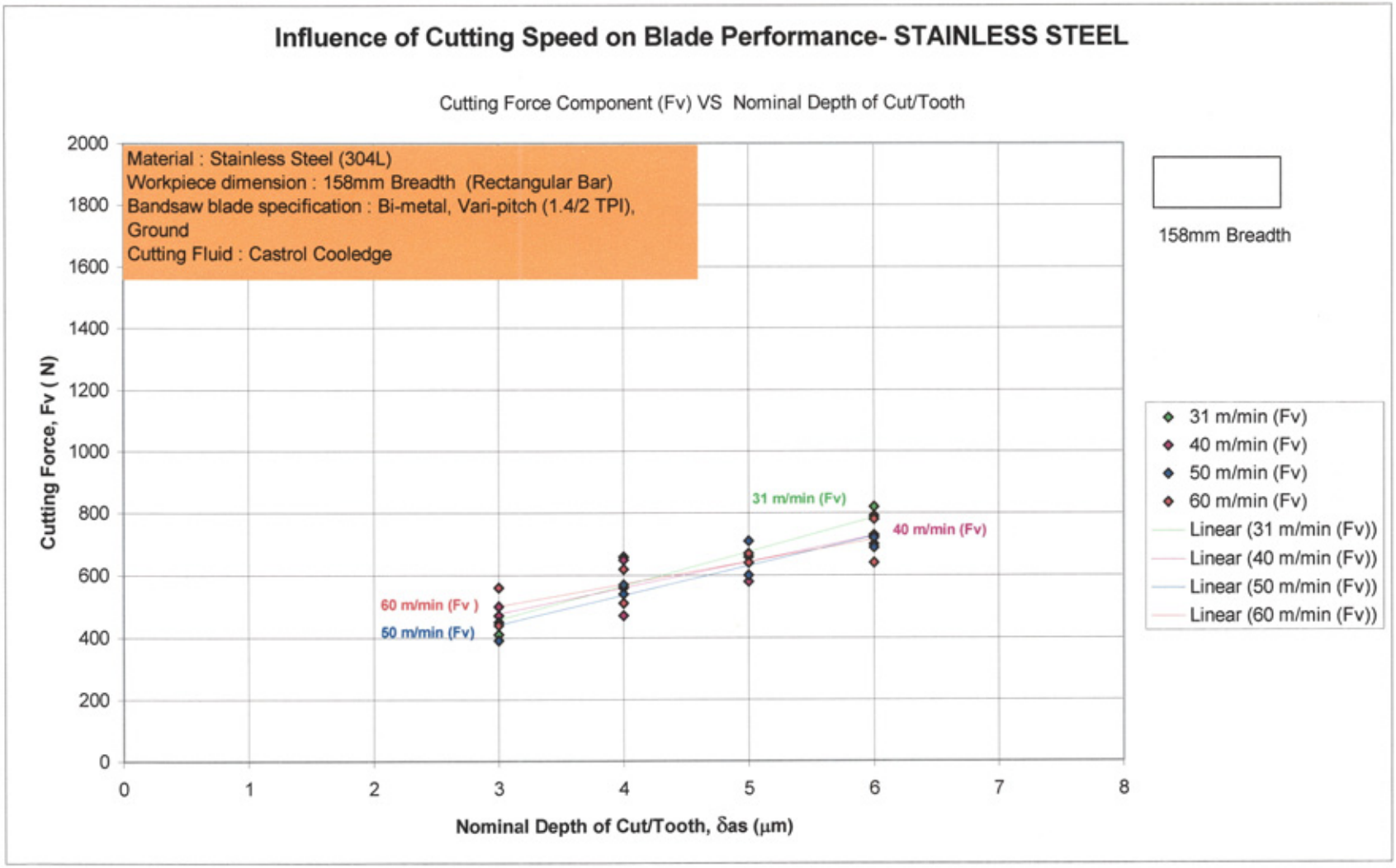

Figure 43 Influence of Cutting Speed on Cutting force for Stainless Steel

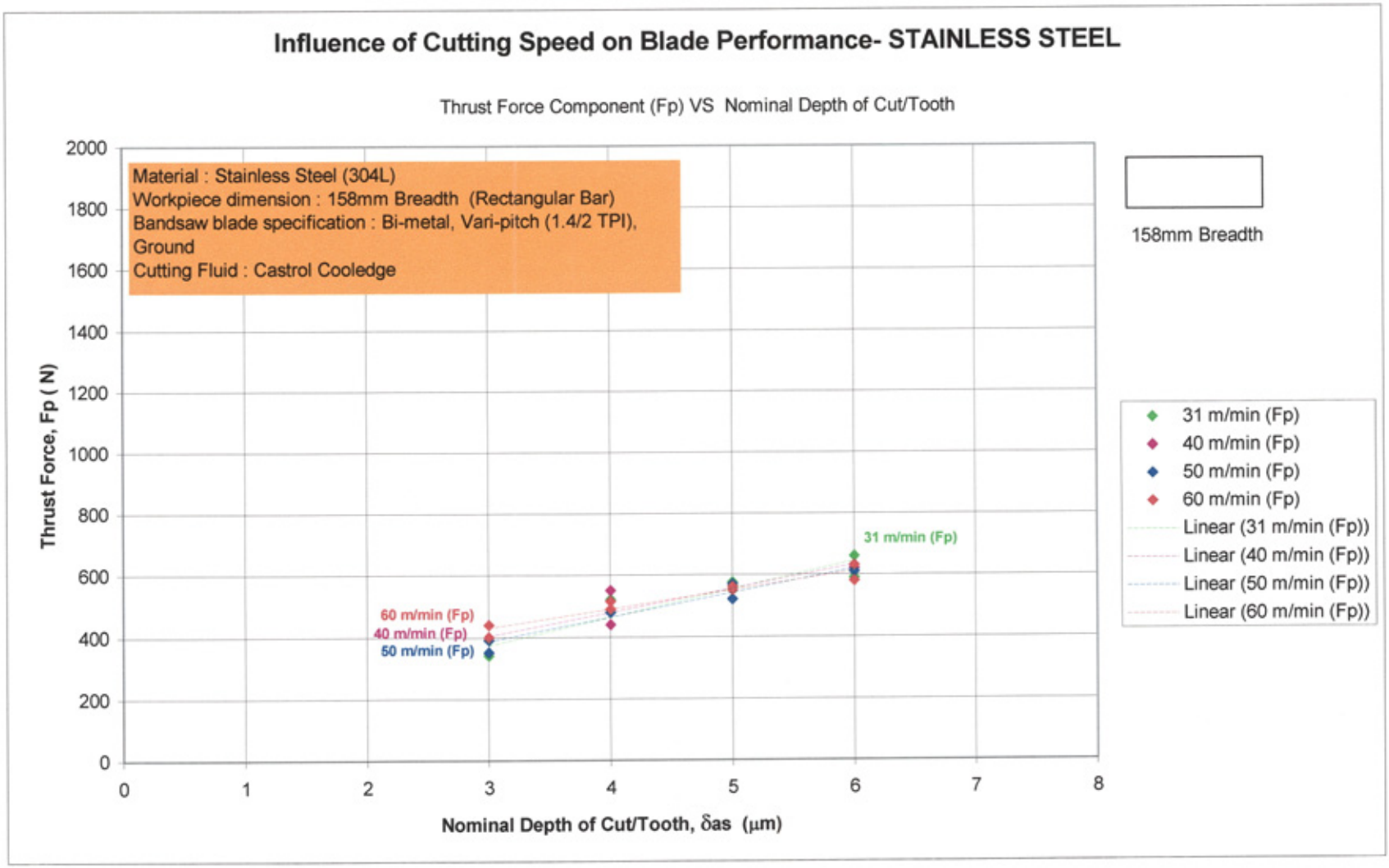

Figure 44 Influence of cutting speed on thrust force for Stainless Steel

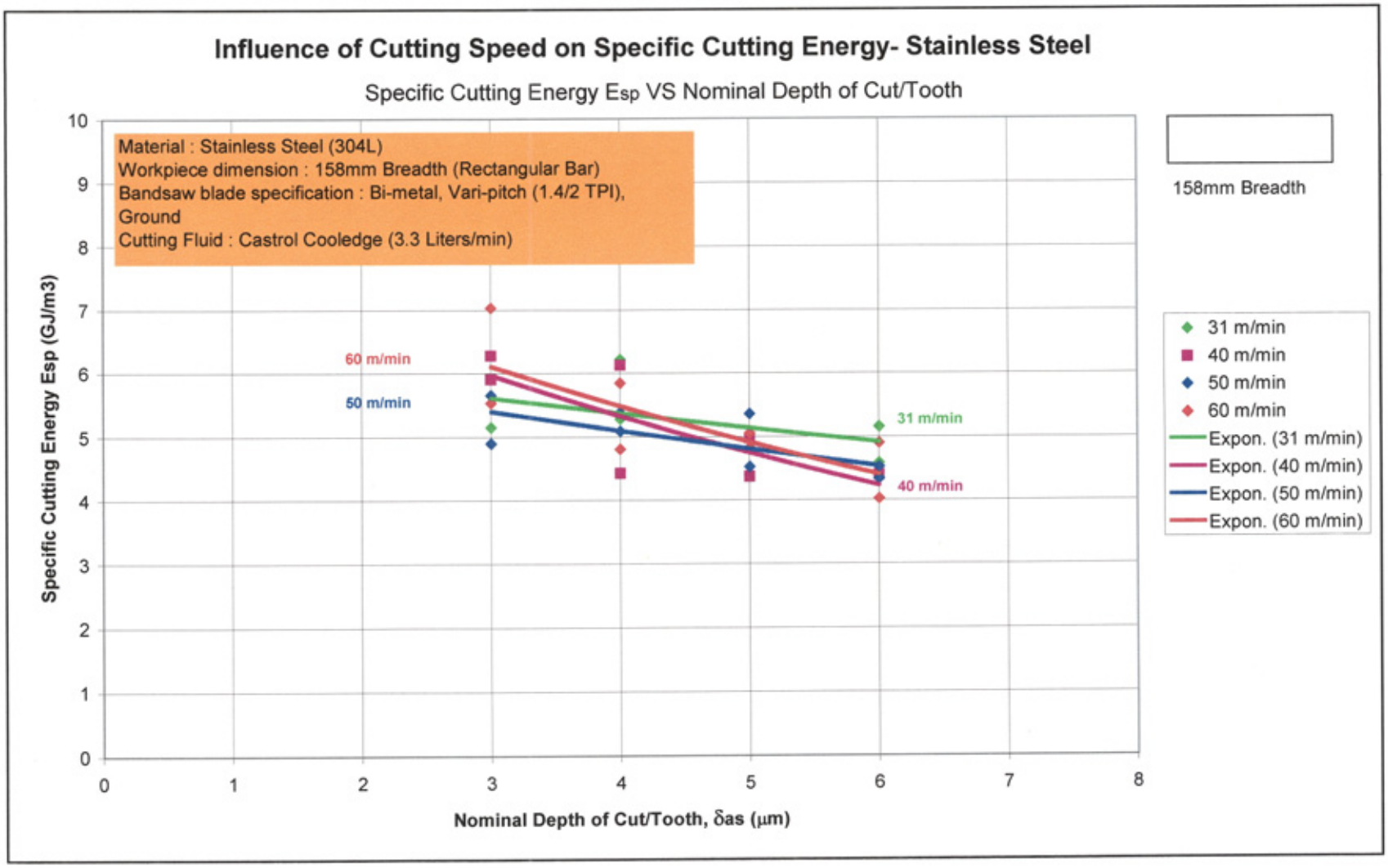

Figure 45 Influence of cutting speed on the performance for Stainless Steel

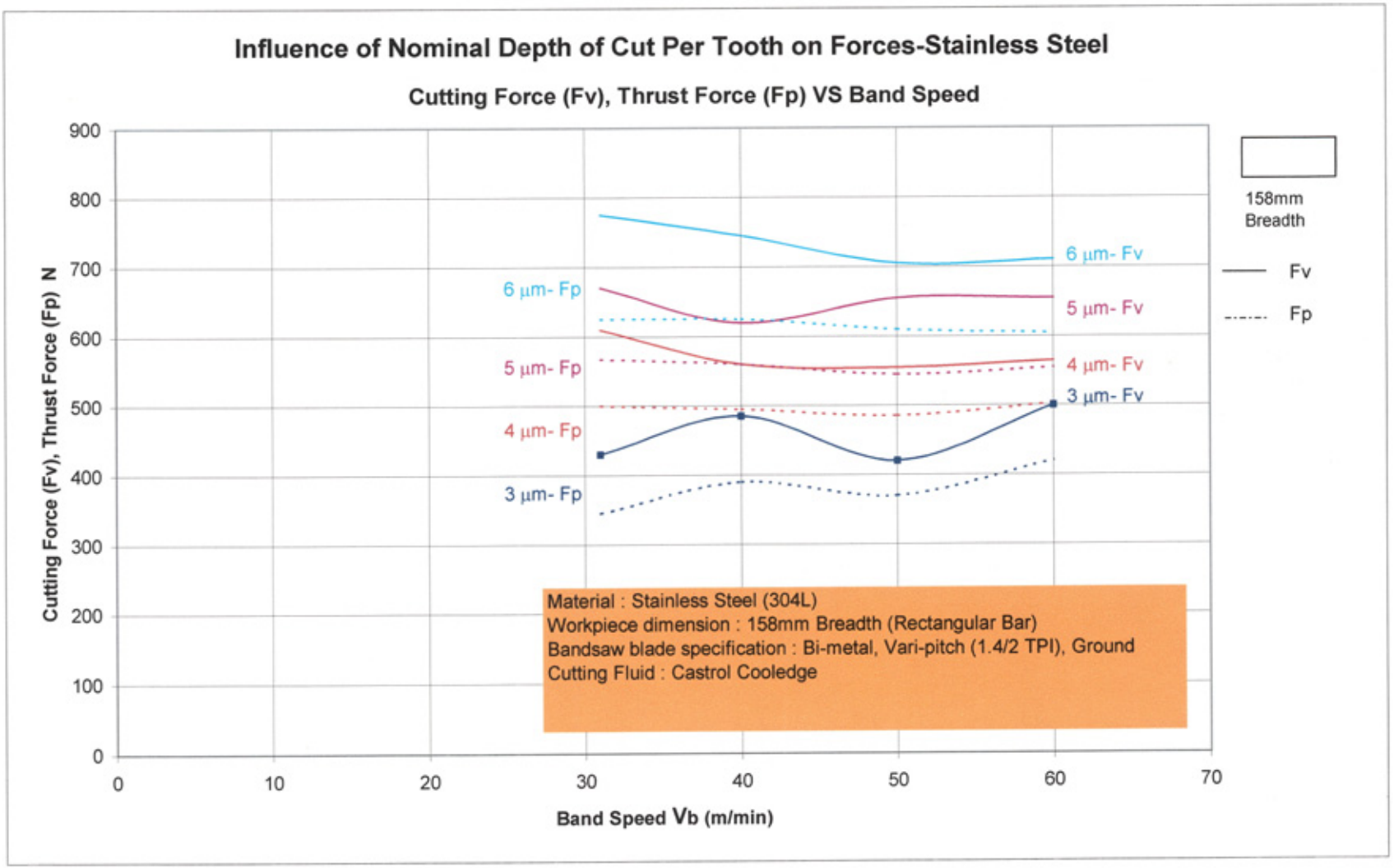

Figure 46 Influence of nominal depth of cut per tooth on cutting forces for Stainless Steel

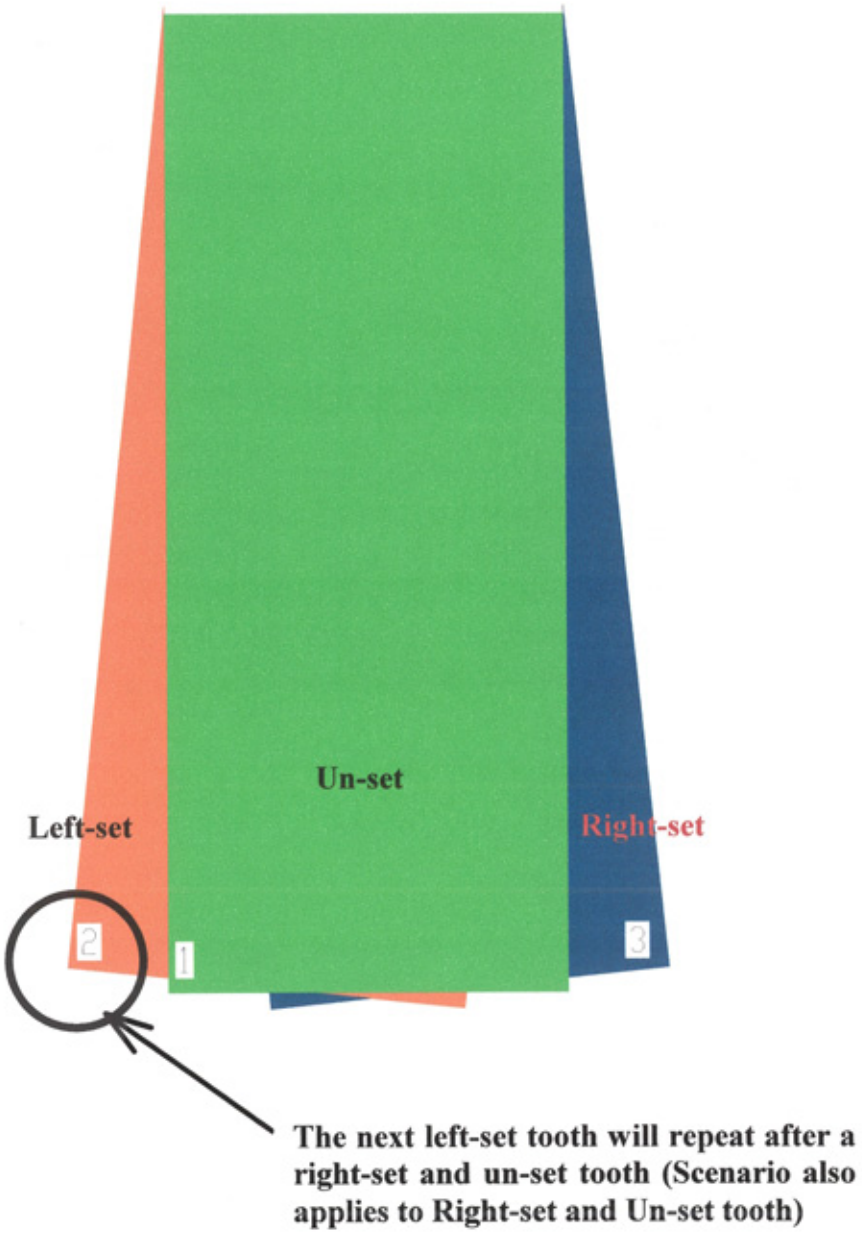

Figure 47 Shadowing effect of tooth setting

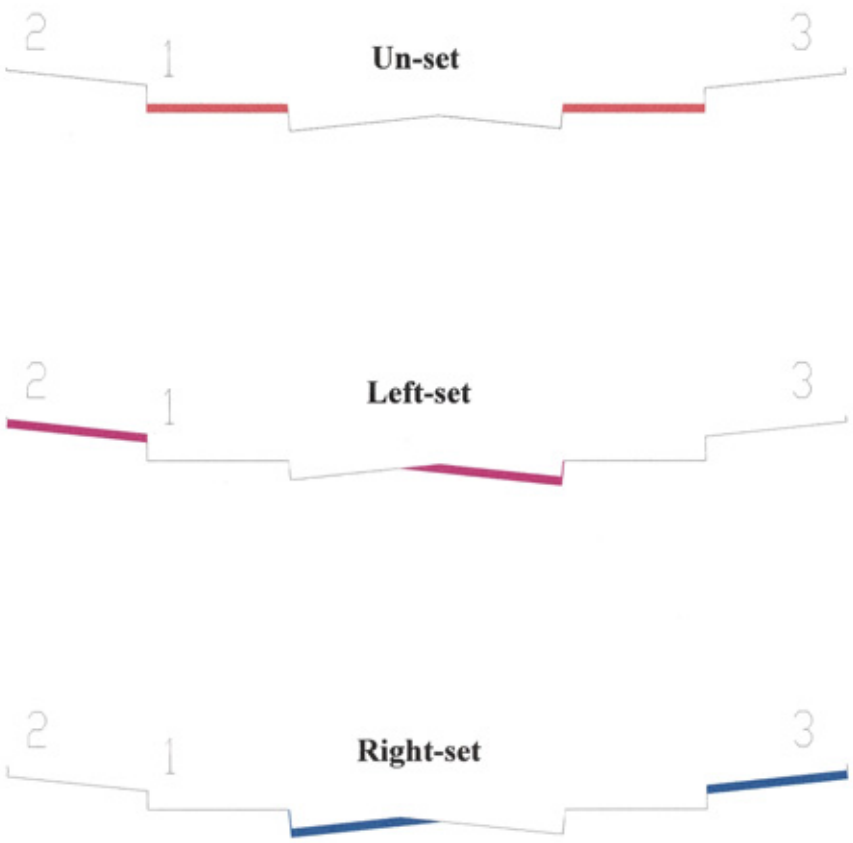

Figure 48 The shadowing effect of teeth setting on the cutting edge area engaged in metal removal (AutoCad drawing)

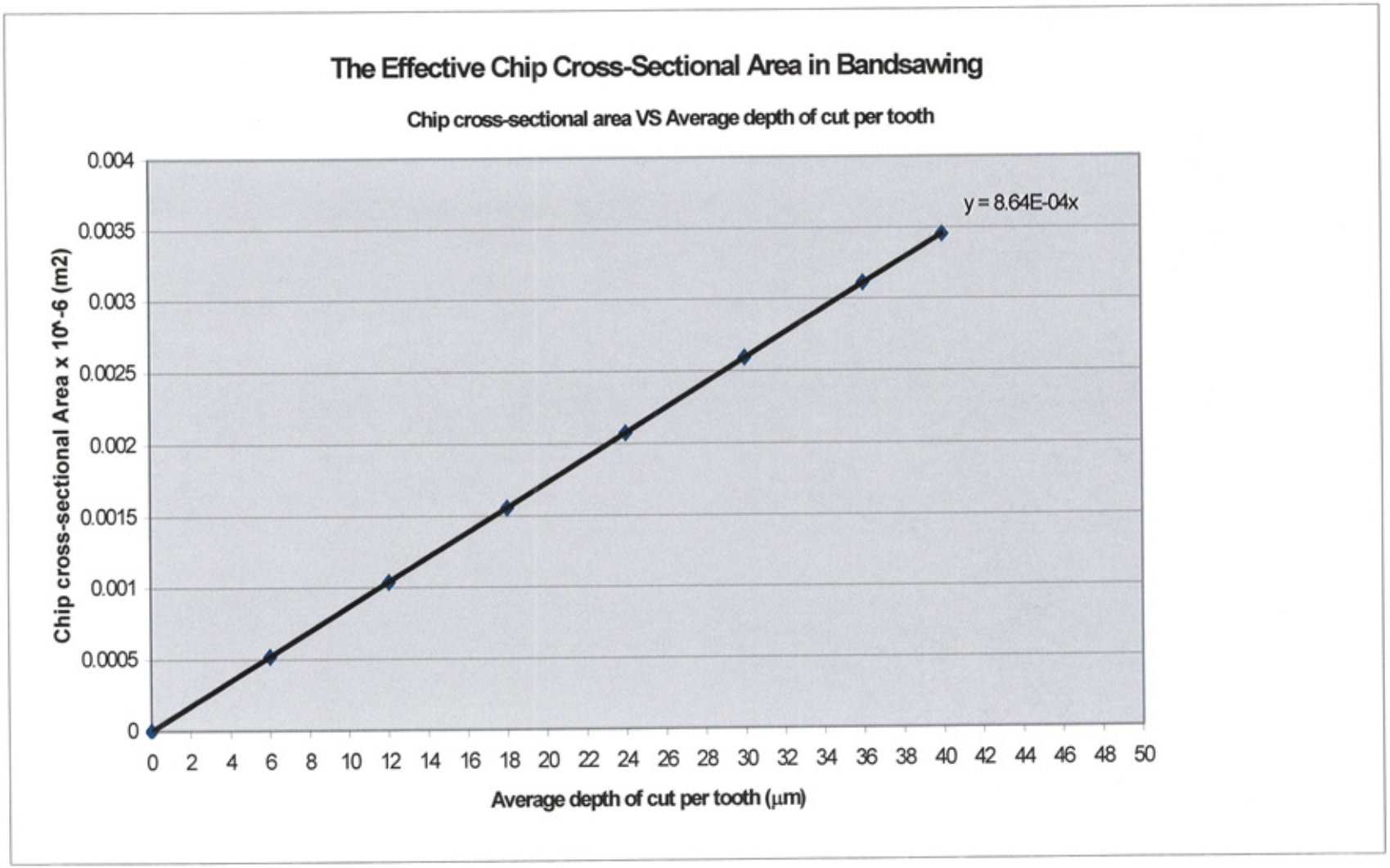

Figure 49 Diagram for determining the chip cross-sectional area from average depth of cut per tooth

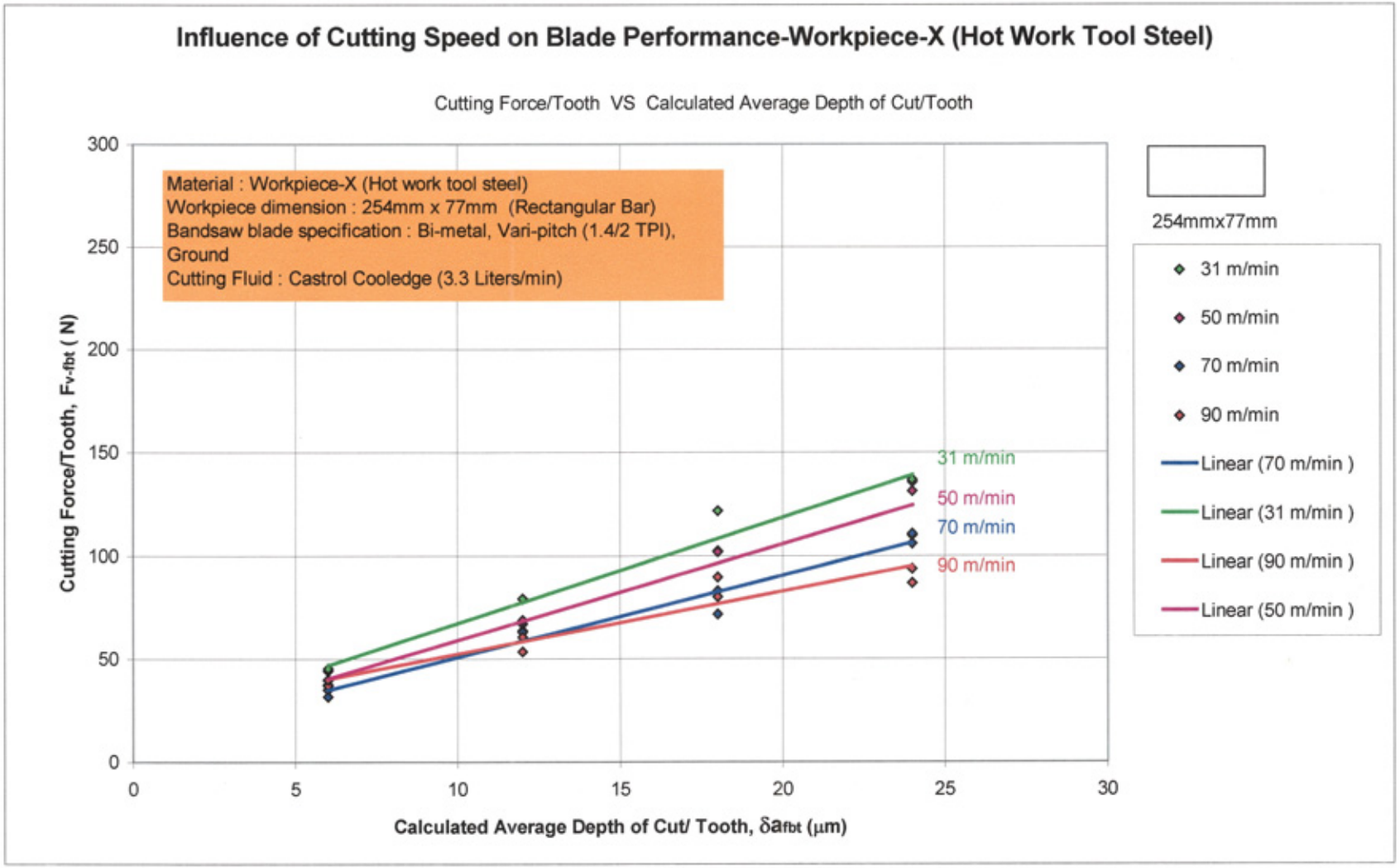

Figure 50 Influence of cutting speed on cutting force per tooth for Workpiece-X material

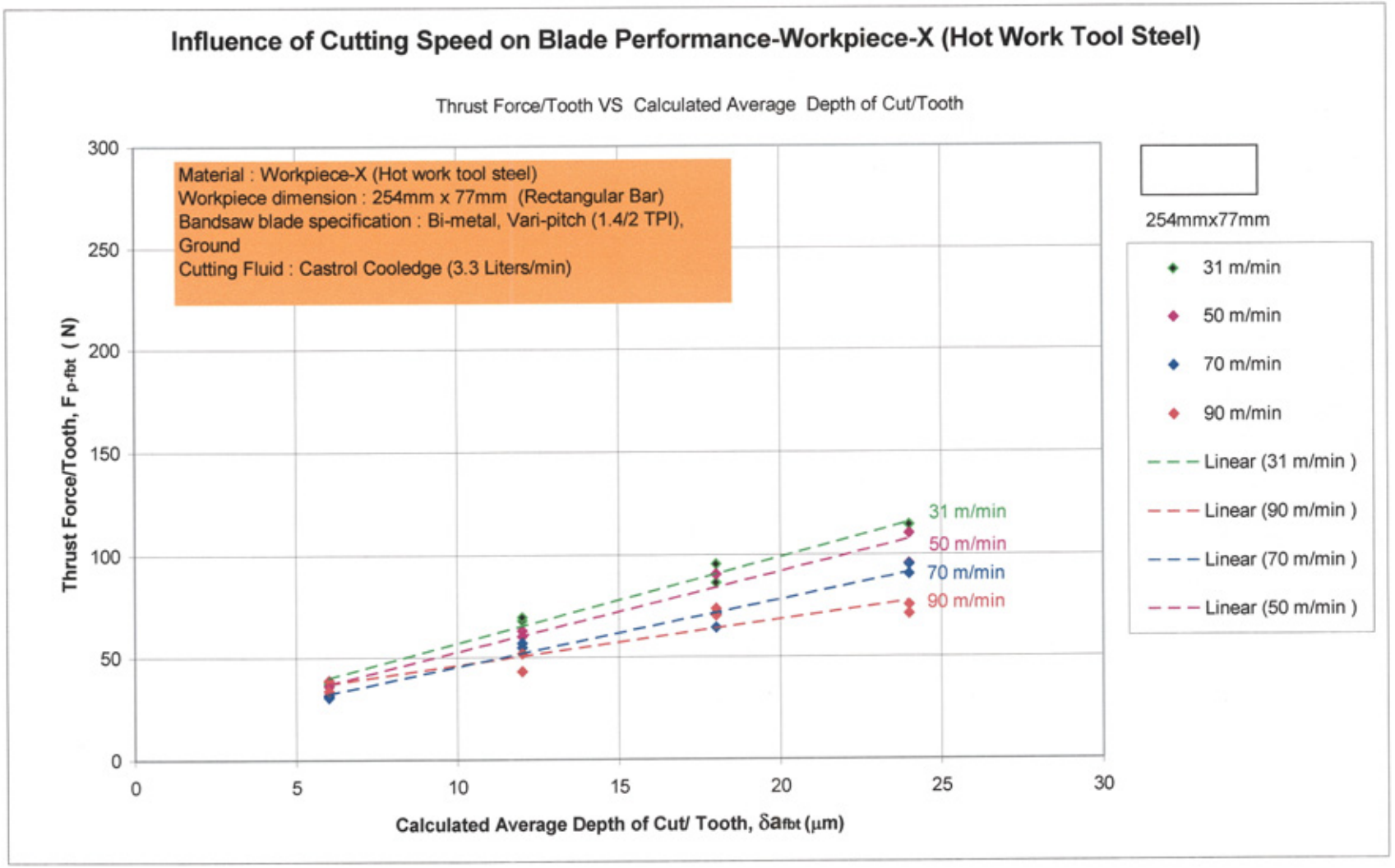

Figure 51 Influence of cutting speed on thrust force per tooth for Workpiece-X material

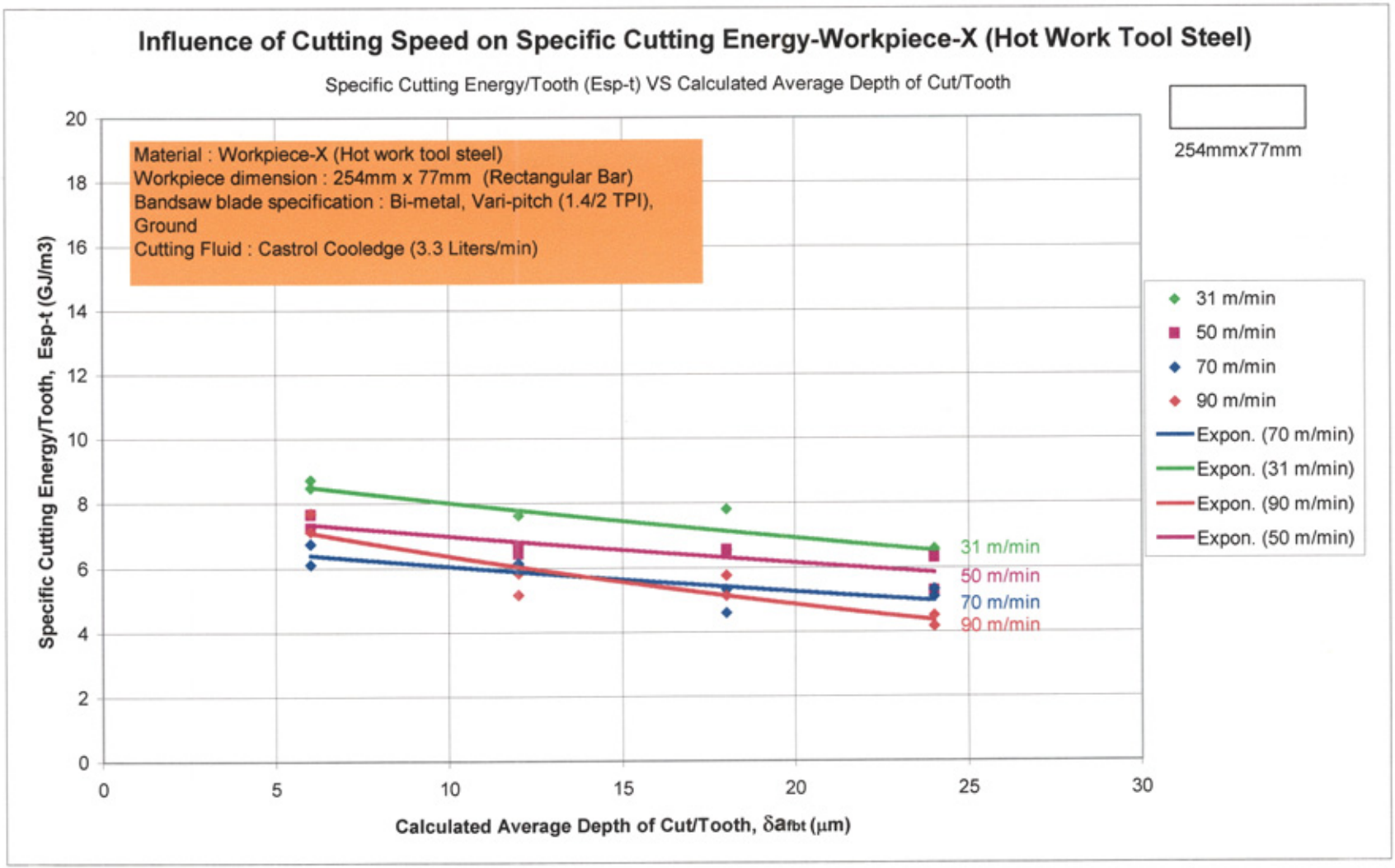

Figure 52 Influence of cutting speed on specific cutting energy per tooth when cutting Workpiece-X material

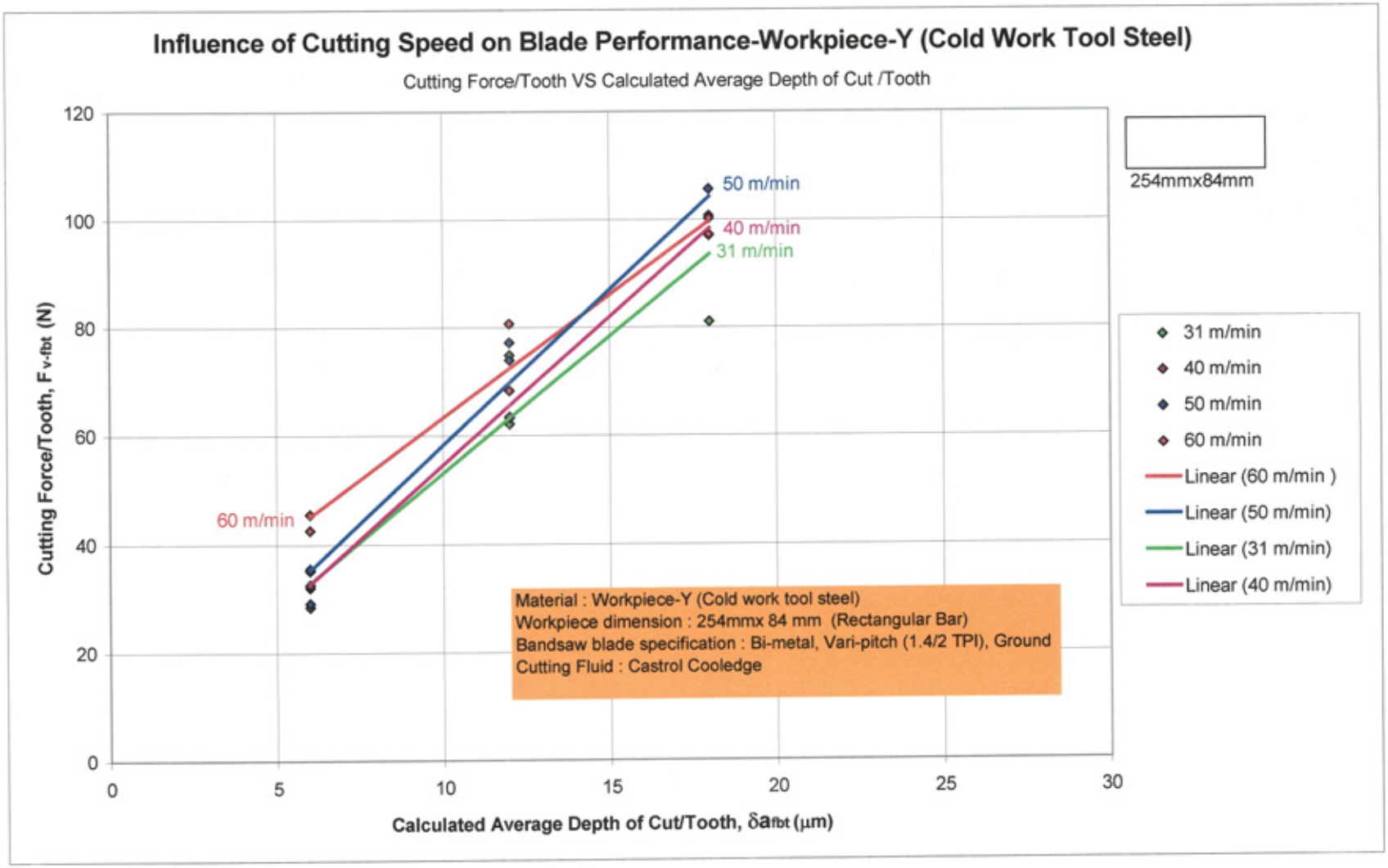

Figure 54 Influence of cutting speed on cutting force per tooth for Workpiece-Y material

Figure 55 Influence of cutting speed on thrust force per tooth for Workpiece-Y material

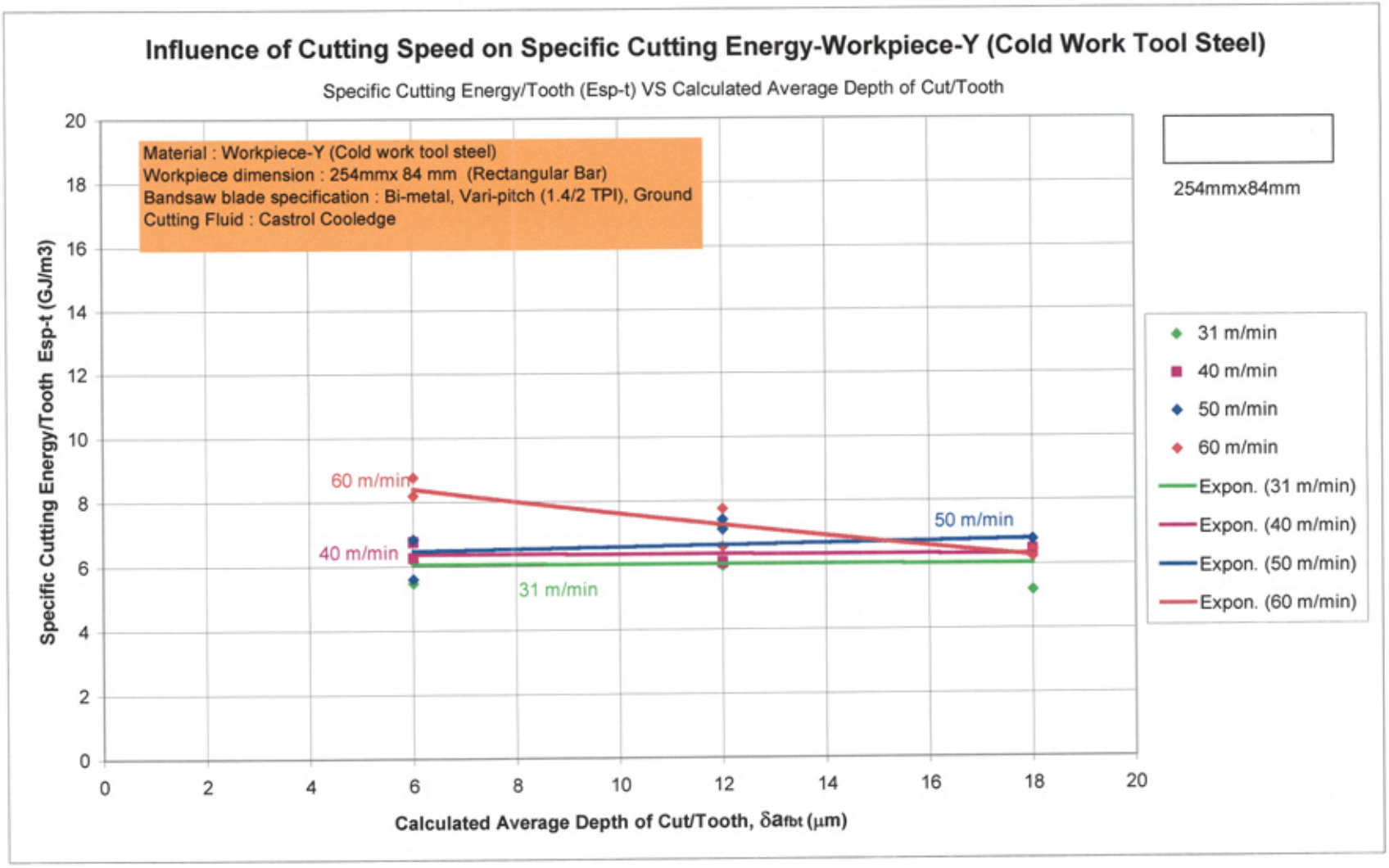

Figure 56 Influence of cutting speed on specific cutting energy per tooth for Workpiece-Y material

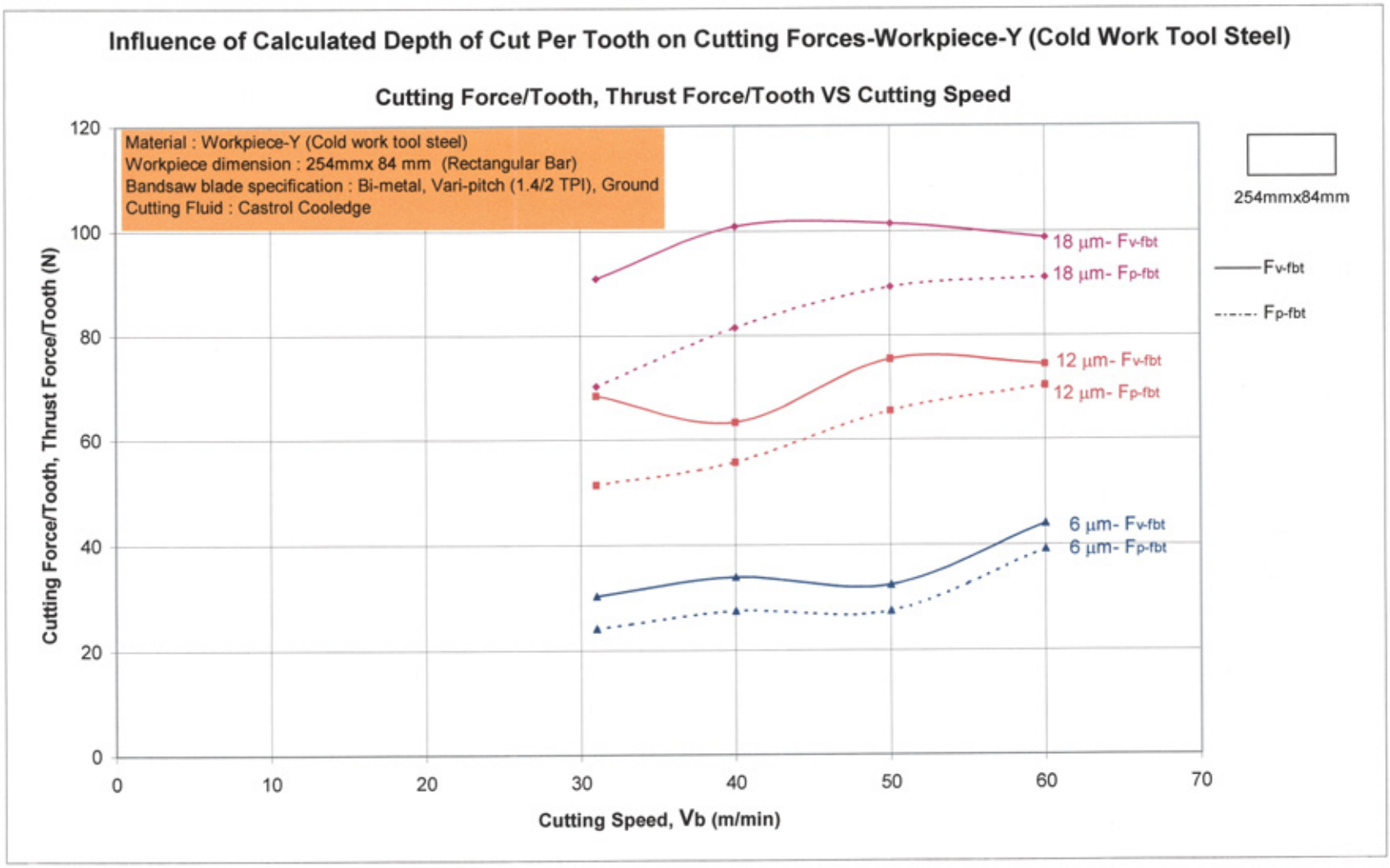

Figure 57 Influence of calculated average depth of cut per tooth on forces per tooth for Workpiece-Y

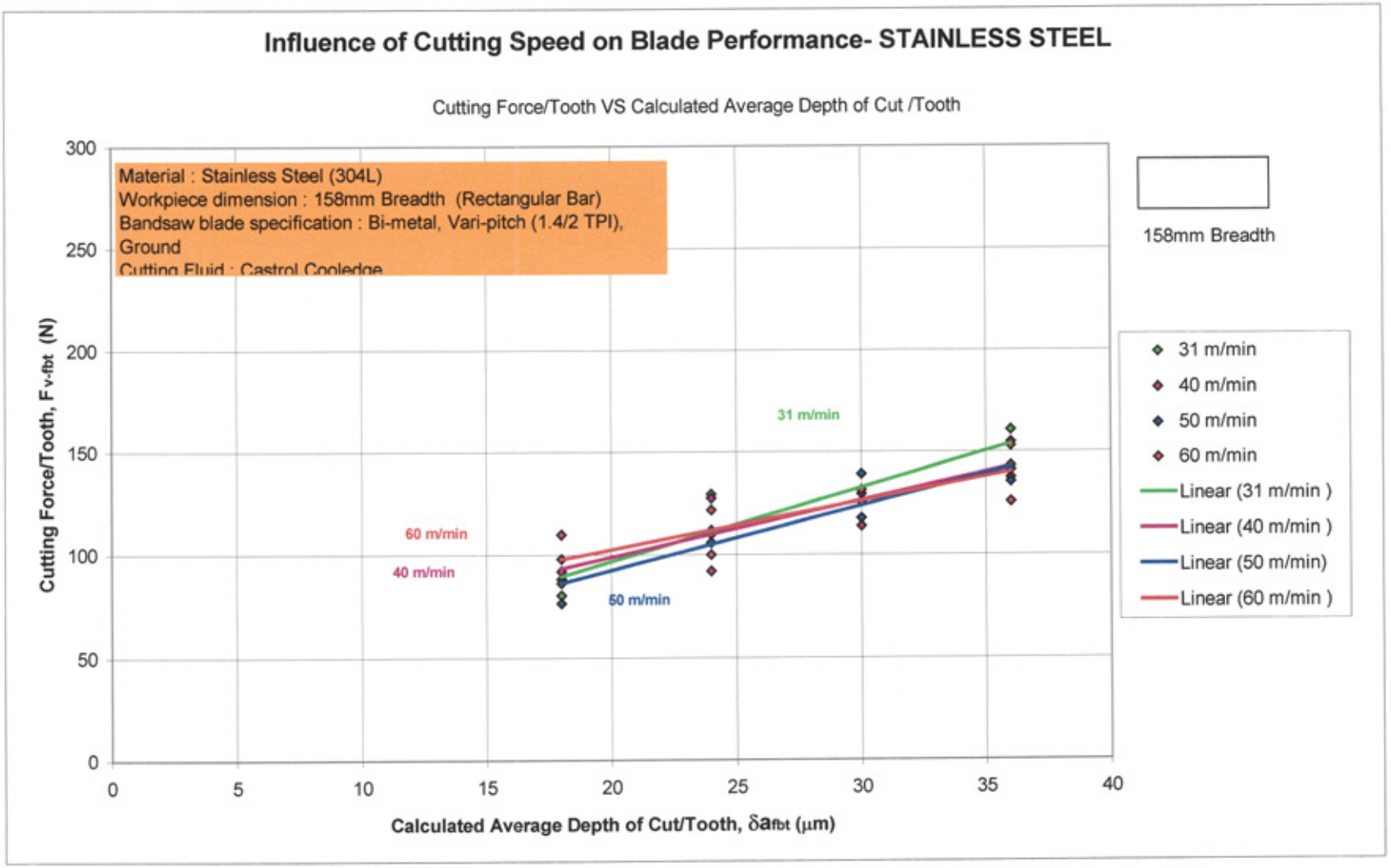

Figure 58 Influence of cutting speed on cutting force per tooth for Stainless Steel

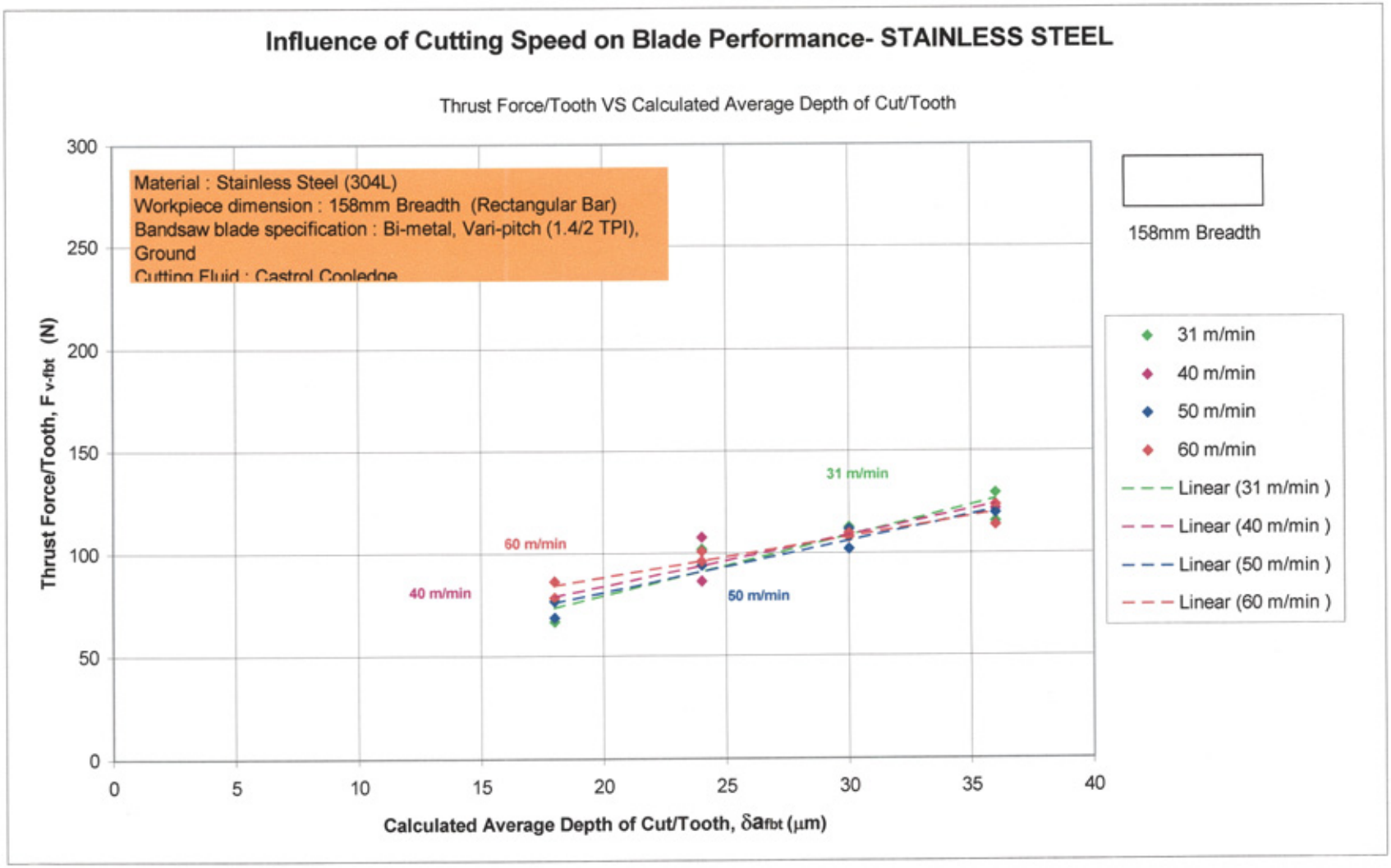

Figure 59 Influence of cutting speed on thrust force per tooth for Stainless Steel

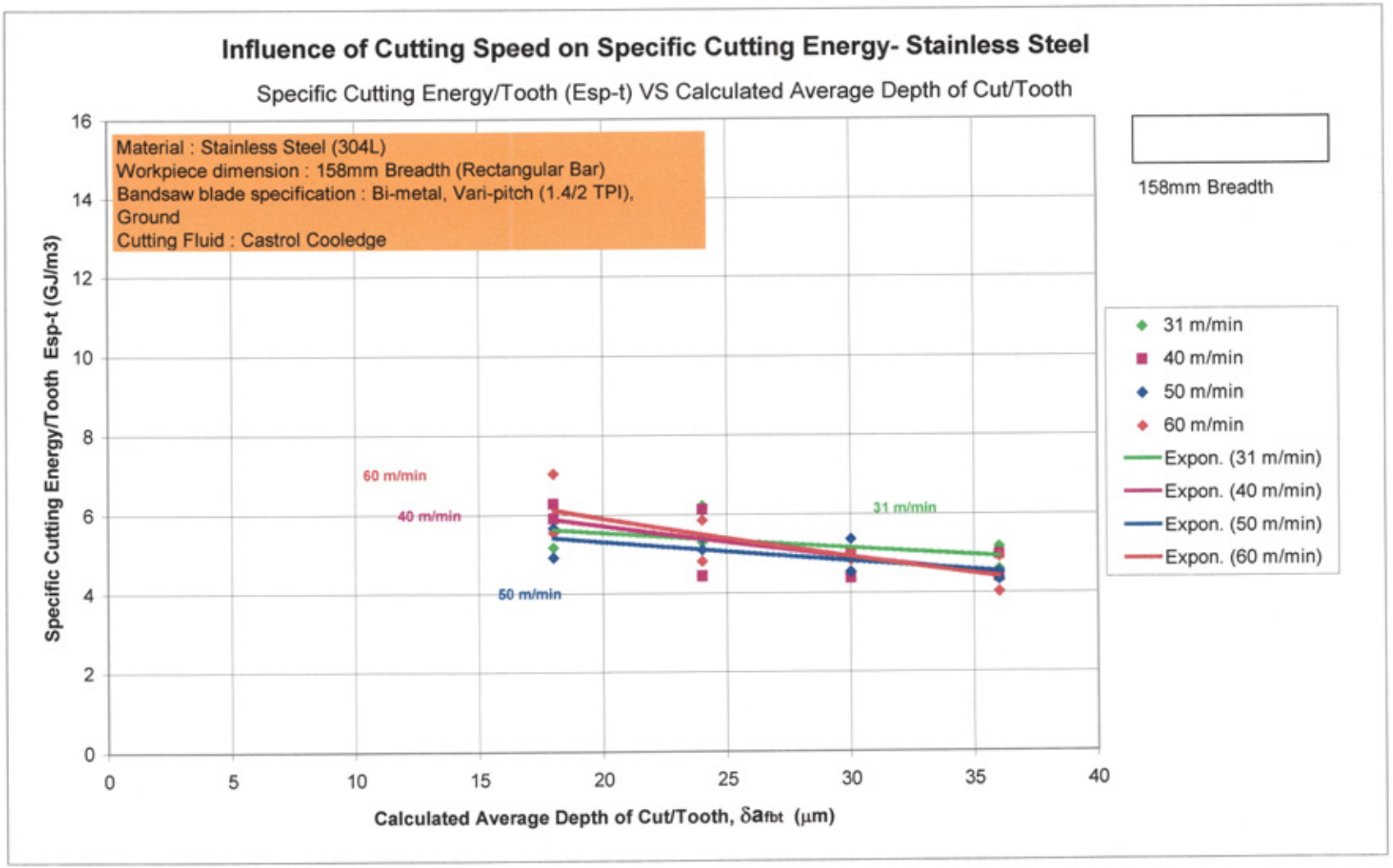

Figure 60 Influence of cutting speed on specific cutting energy per tooth for Stainless Steel

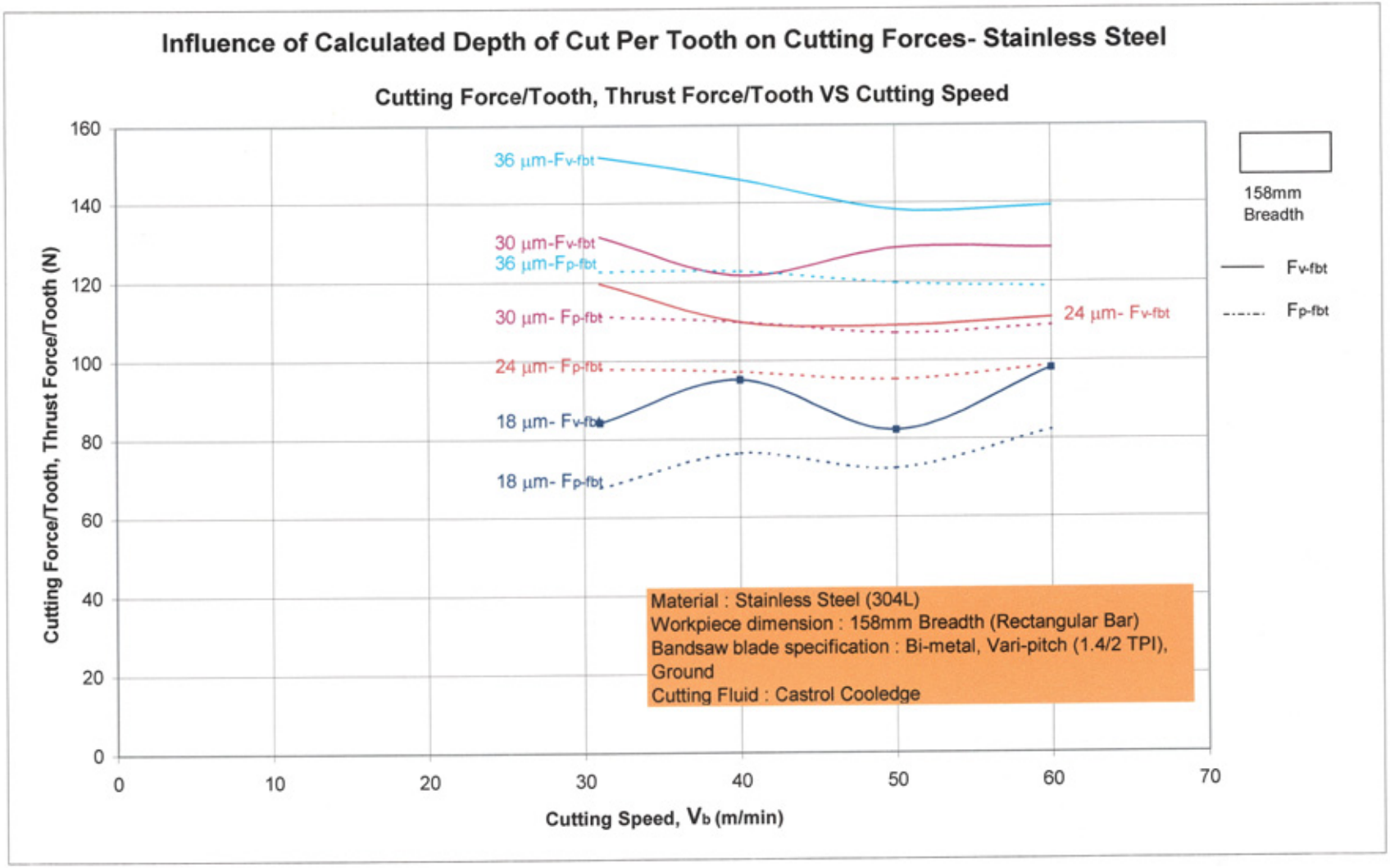

Figure 61 Influence of calculated average depth of cut per tooth on forces per tooth for Stainless Steel

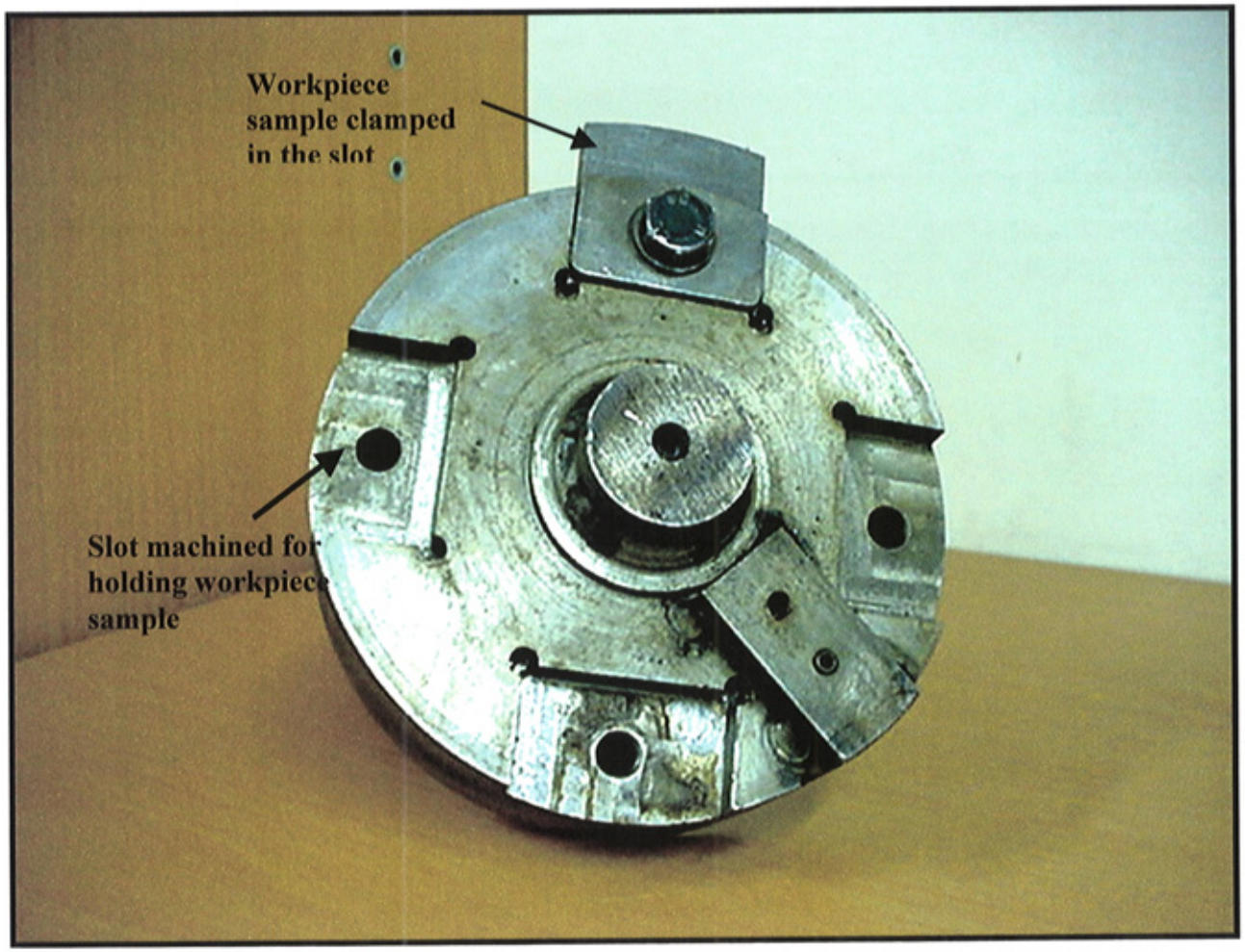

Figure 62 Workpiece holder used in the single tooth test

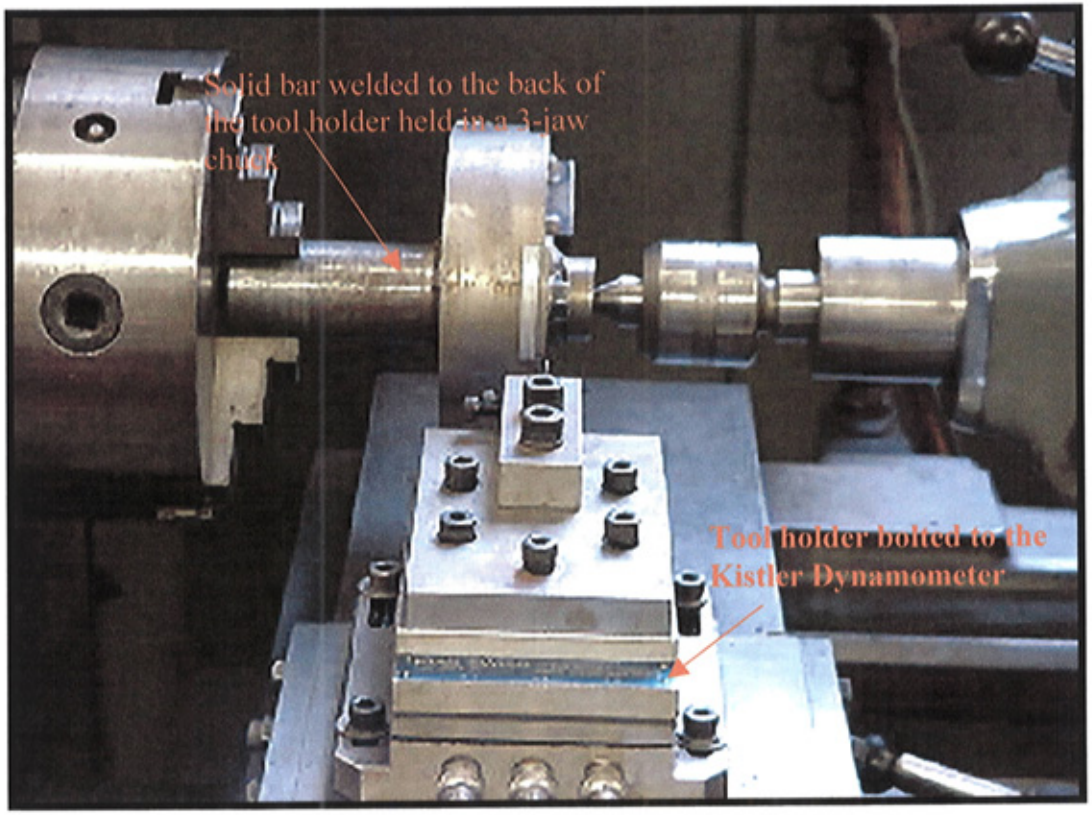

Figure 63 Workpiece holder inserted into a 3-jaw chuck

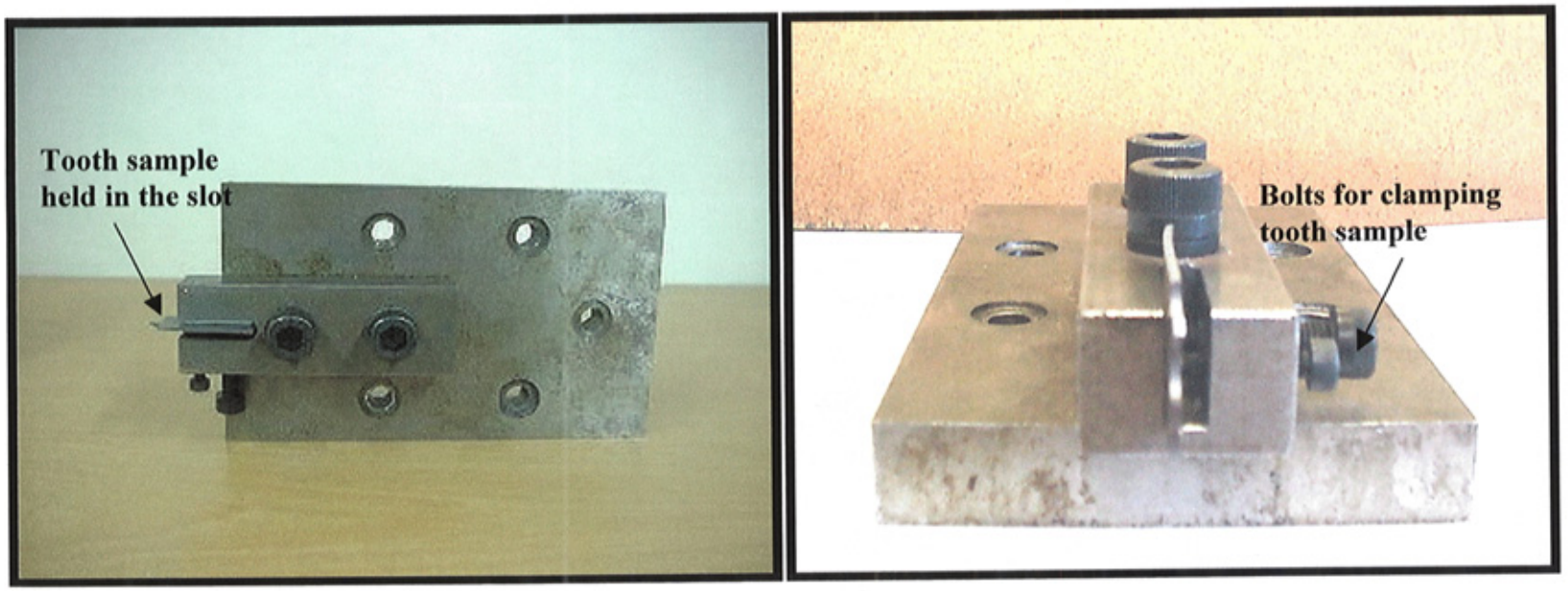

Figure 64 Single tooth sample holder (Test rig STT-1)

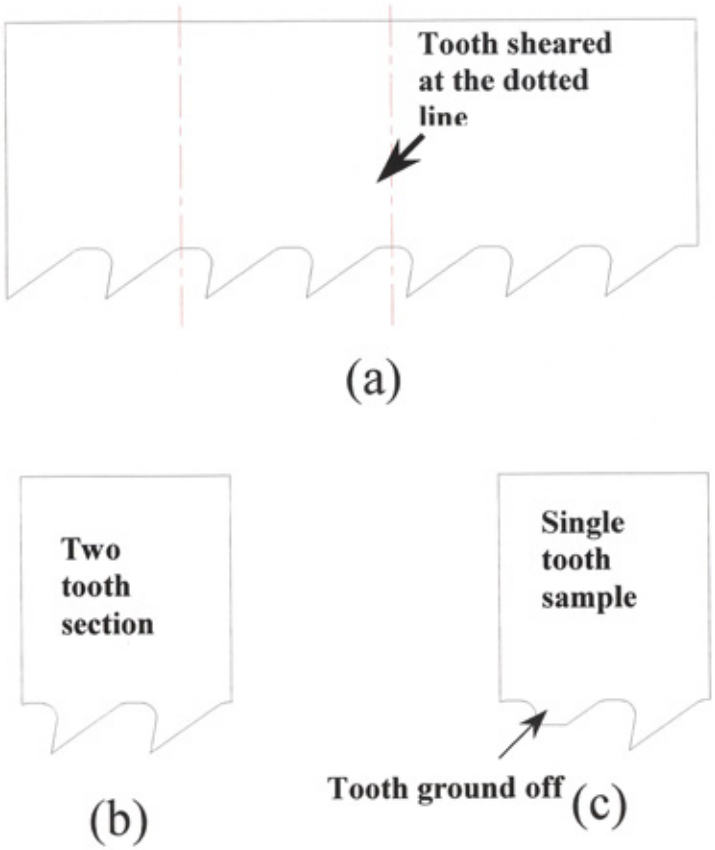

Figure 65 Preparation of single tooth sample

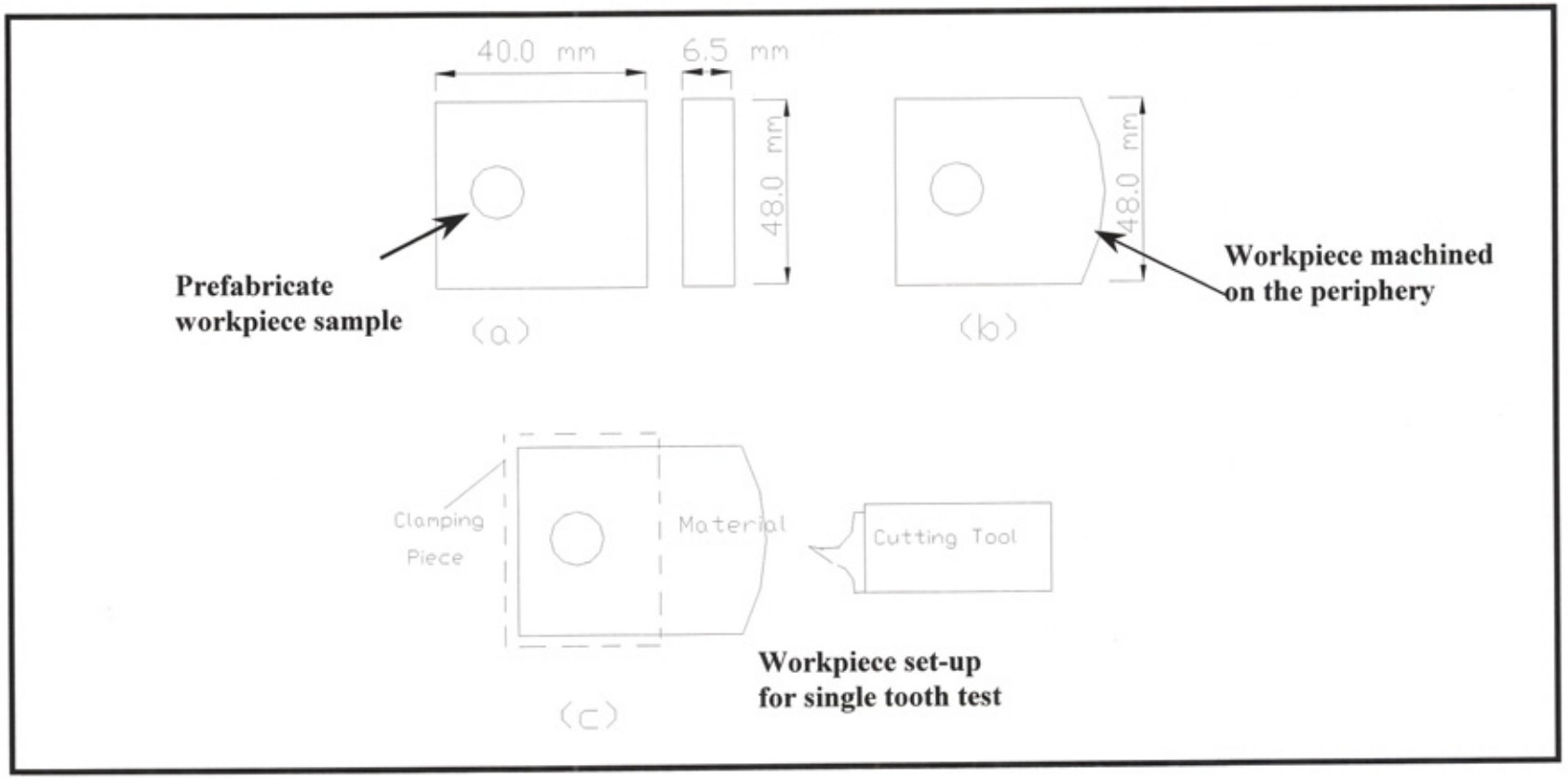

Figure 66 Preparation of workpiece material for single tooth test

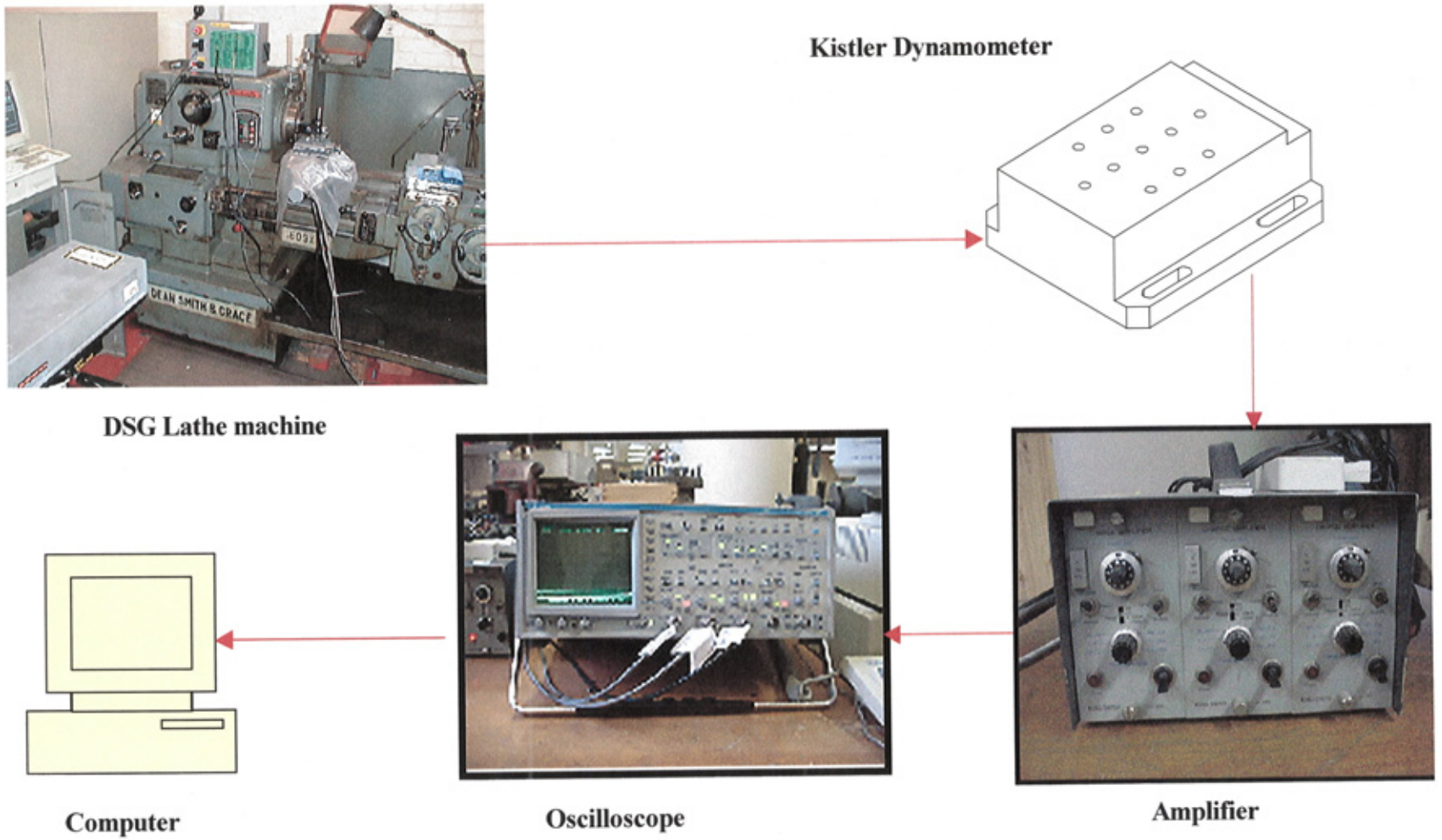

Figure 67 Single tooth test instrumentation set-up (STT-1 test rig)

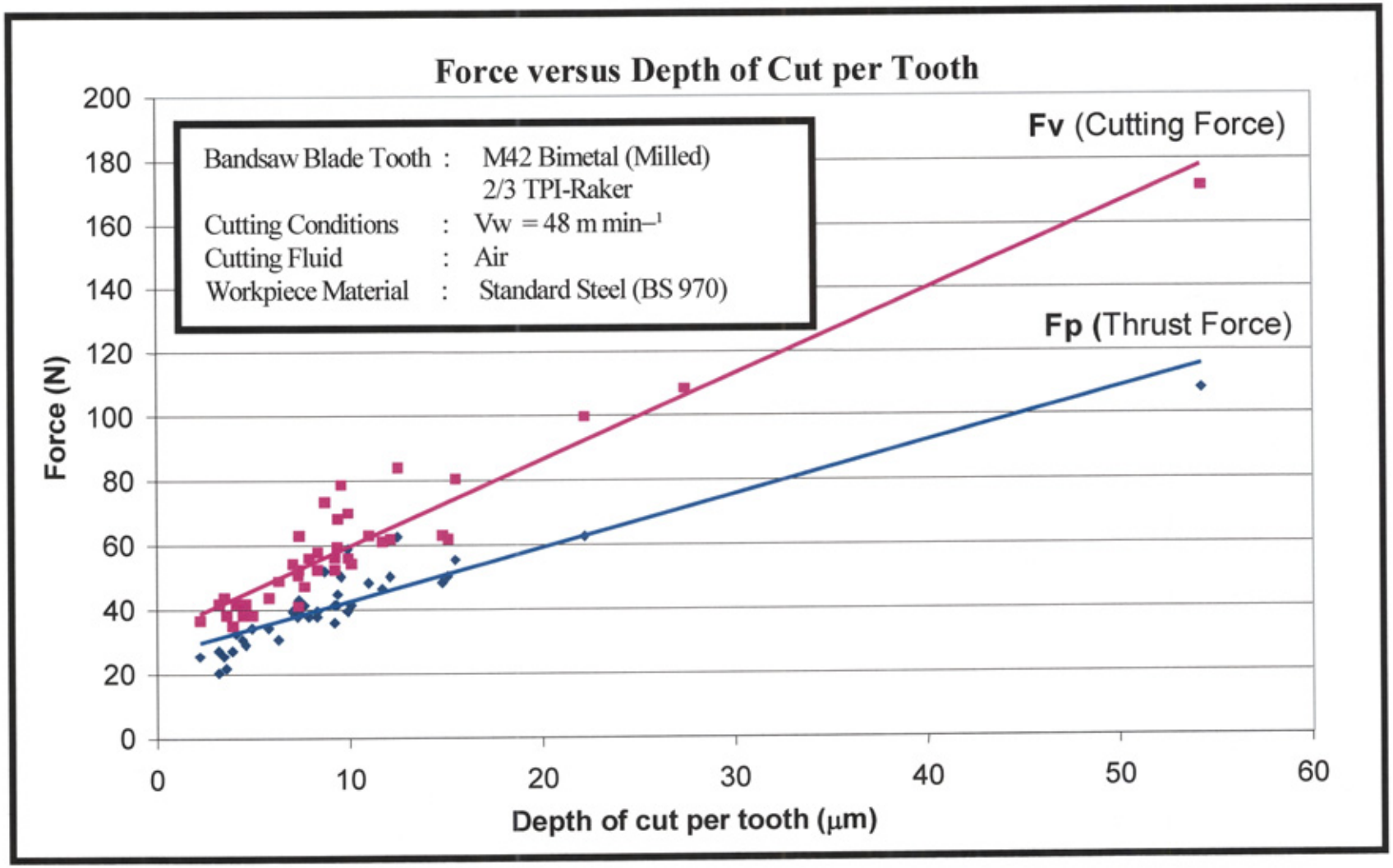

Figure 68 Influence of depth of cut per tooth on cutting force and thrust force for single tooth simulation test (STT-1)

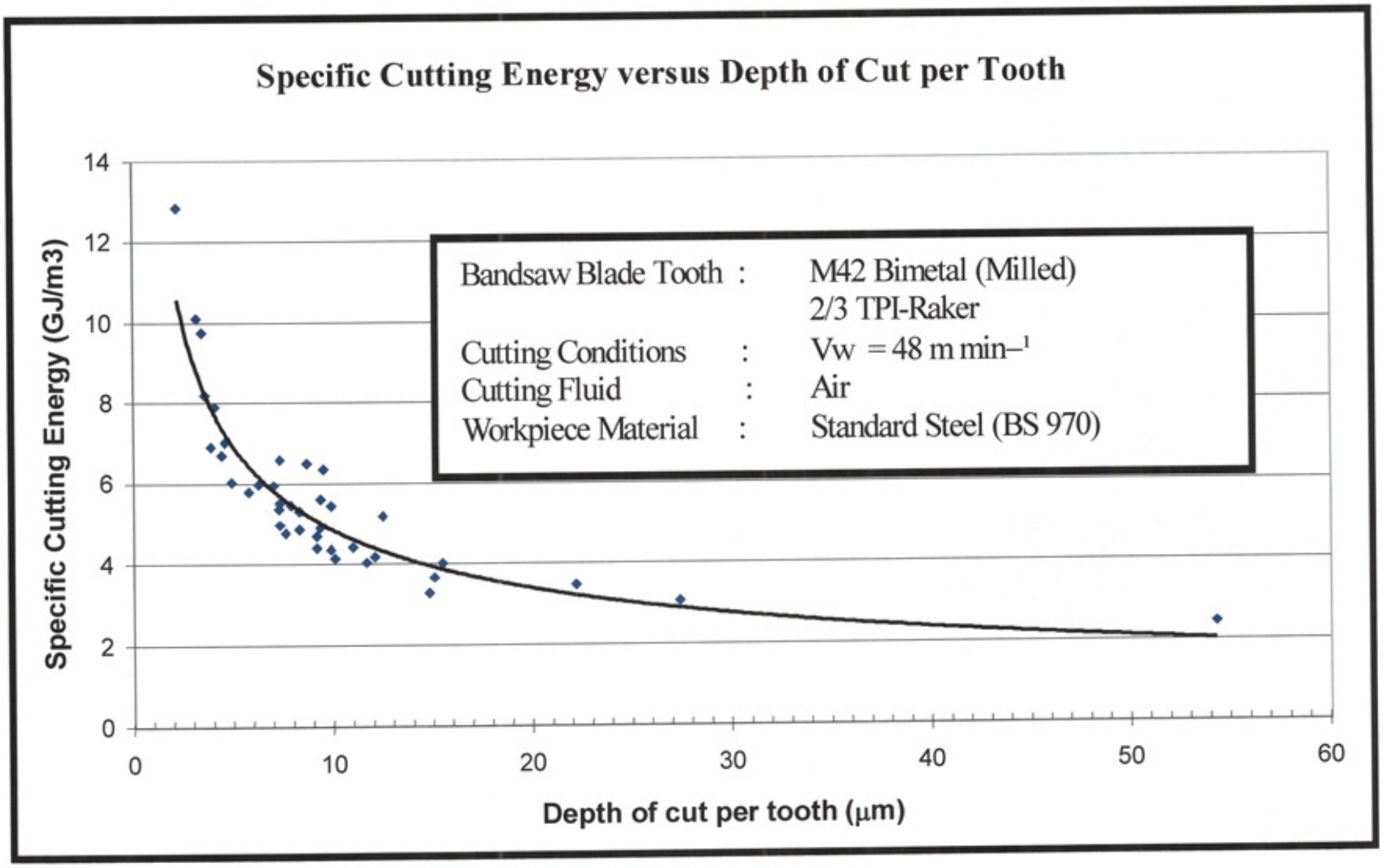

Figure 69 Influence of depth of cut per tooth on specific cutting energy for single tooth simulation test (STT-1)

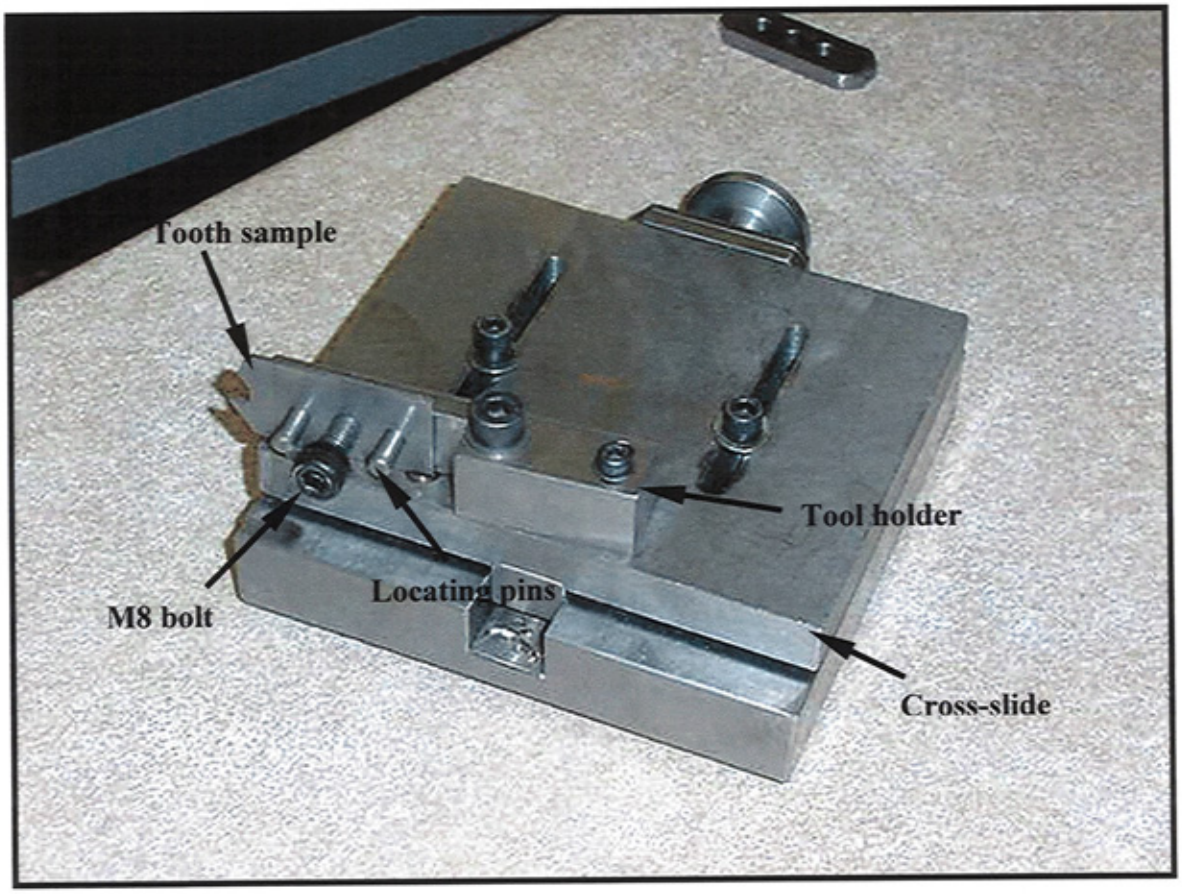

Figure 70 Tool holder cross-slide

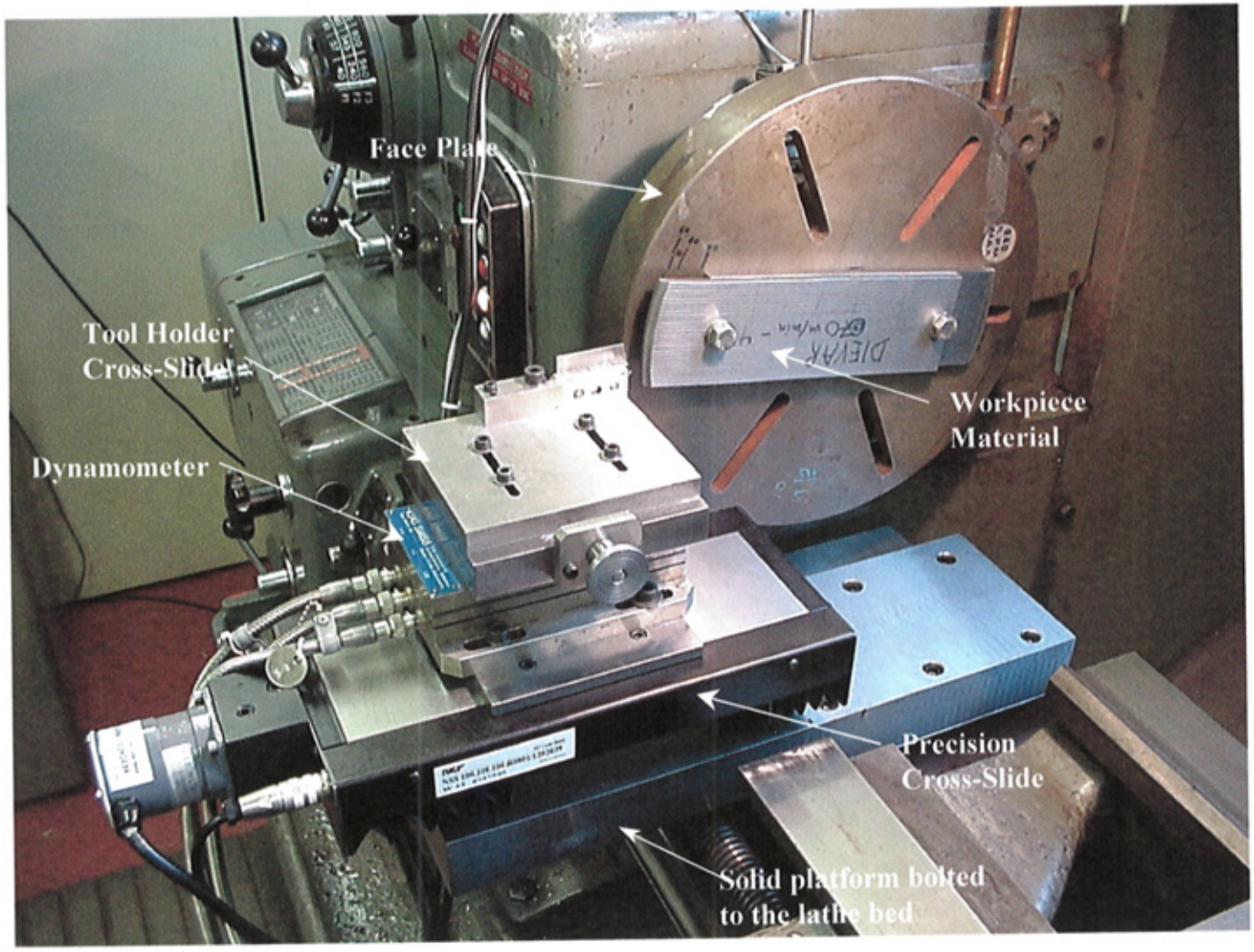

Figure 71 Test rig construction

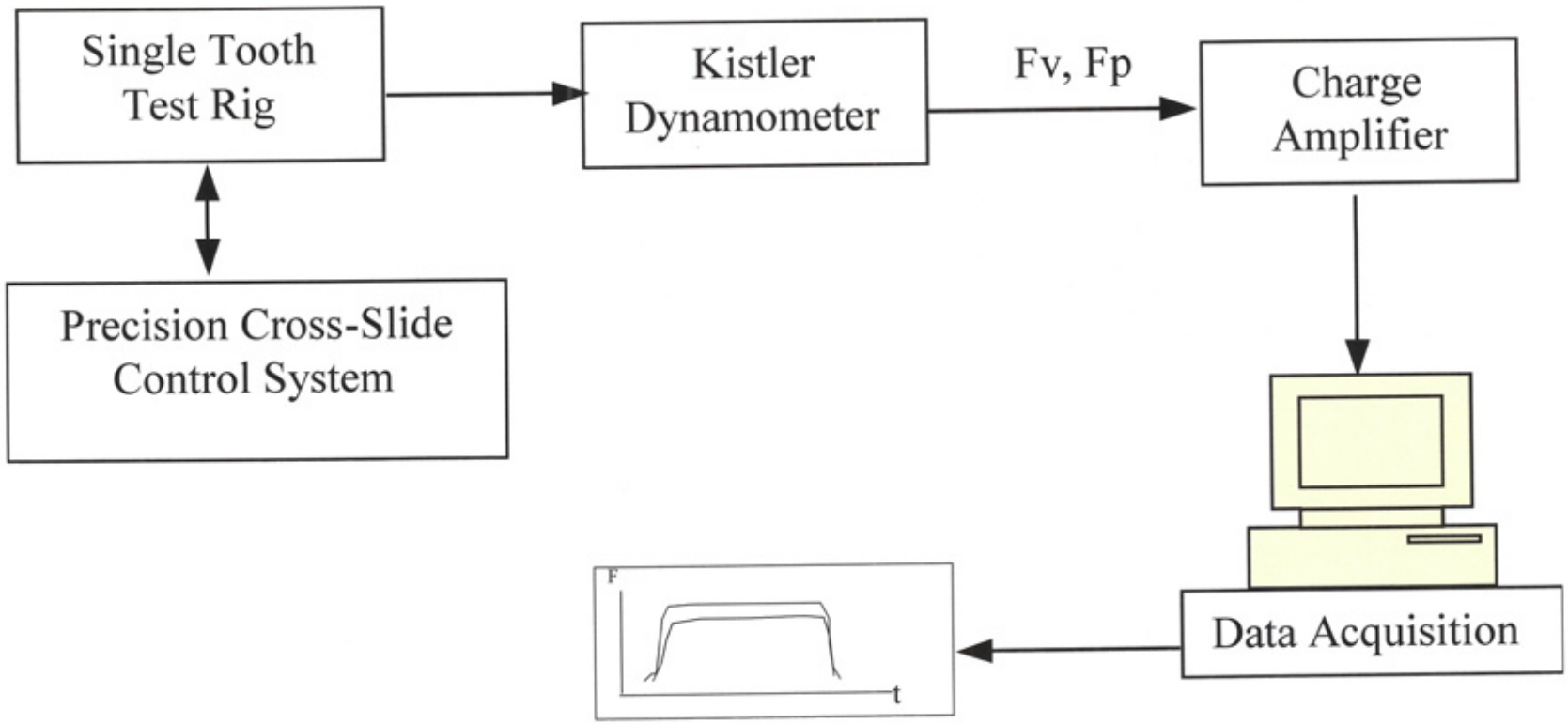

Figure 72 Schematic drawing of single tooth simulation experimental set-up

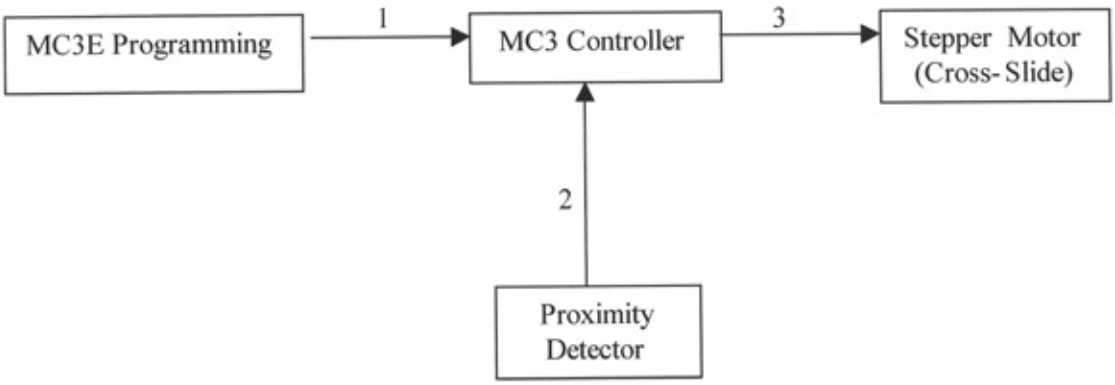

Figure 73 Schematic diagram for the precision cross-slide control system

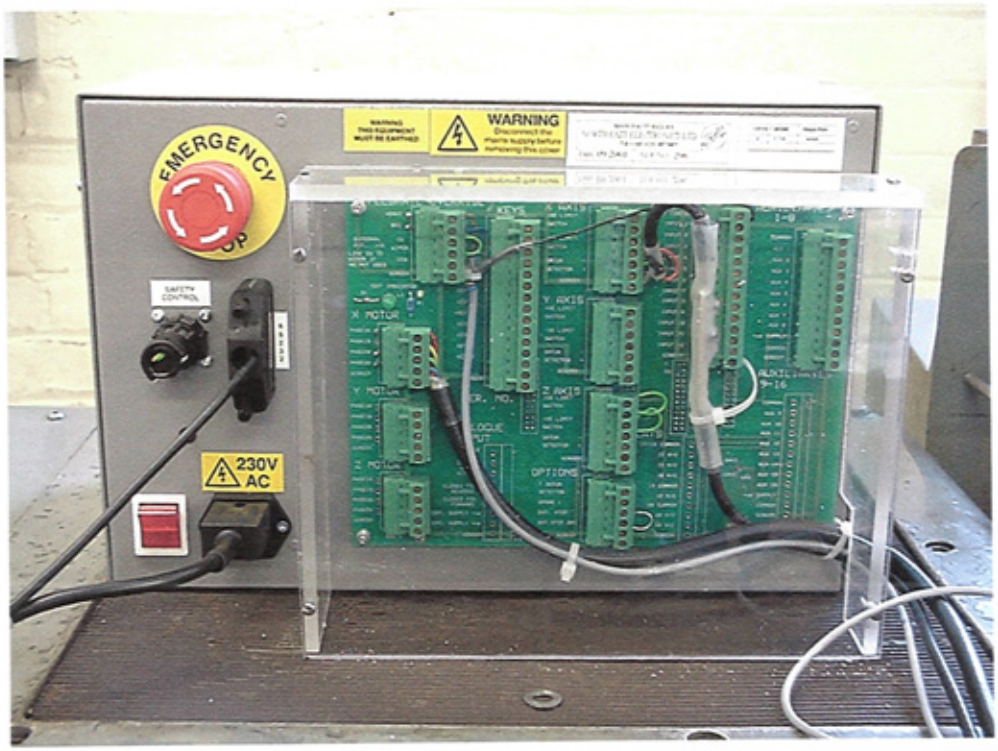

Figure 74 MC3E Controller

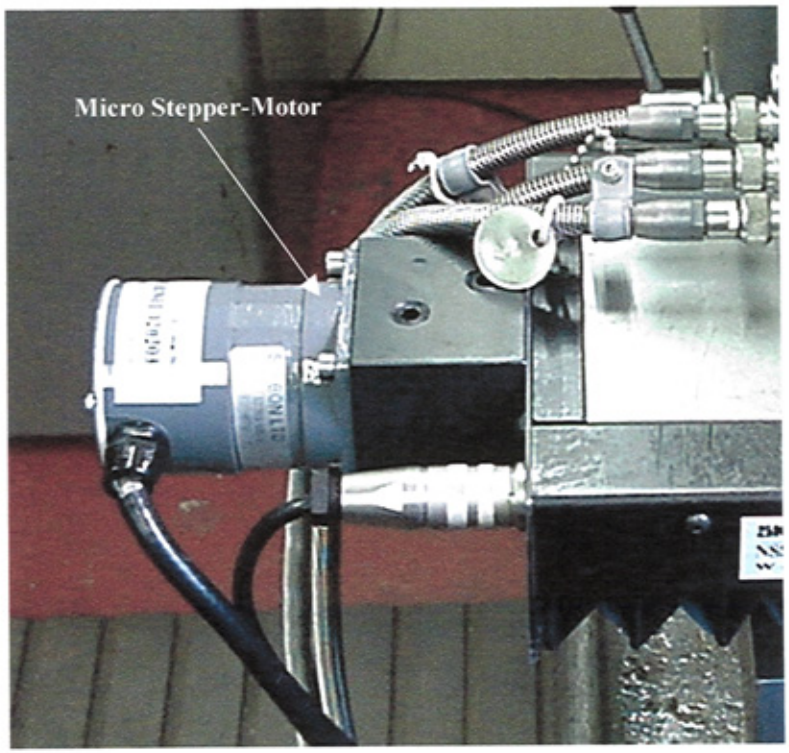

Figure 75 Stepper-motor

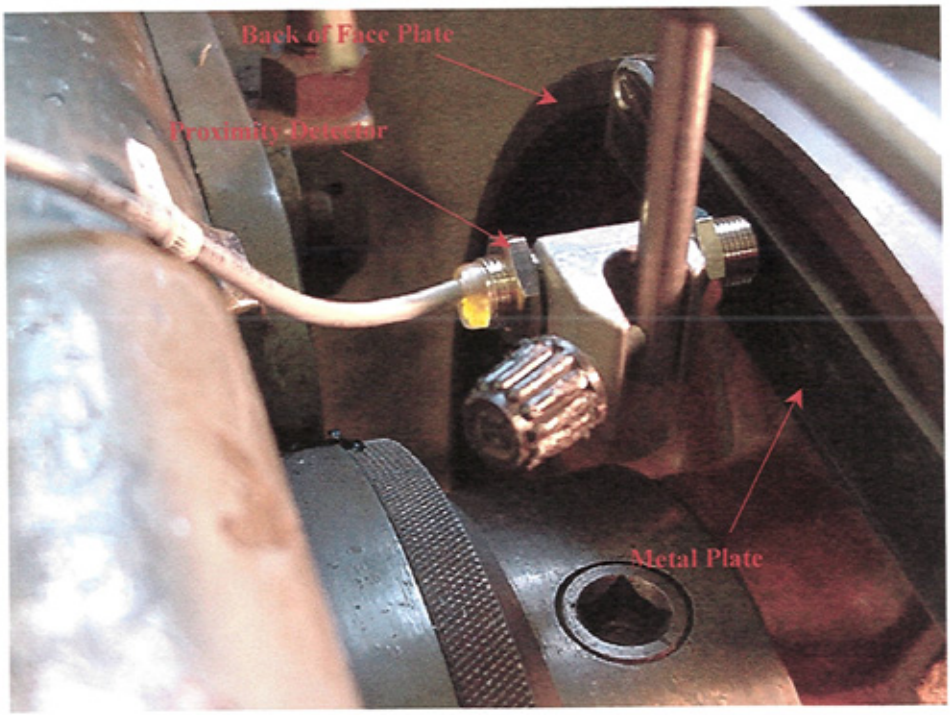

Figure 76 Location of the proximity detector

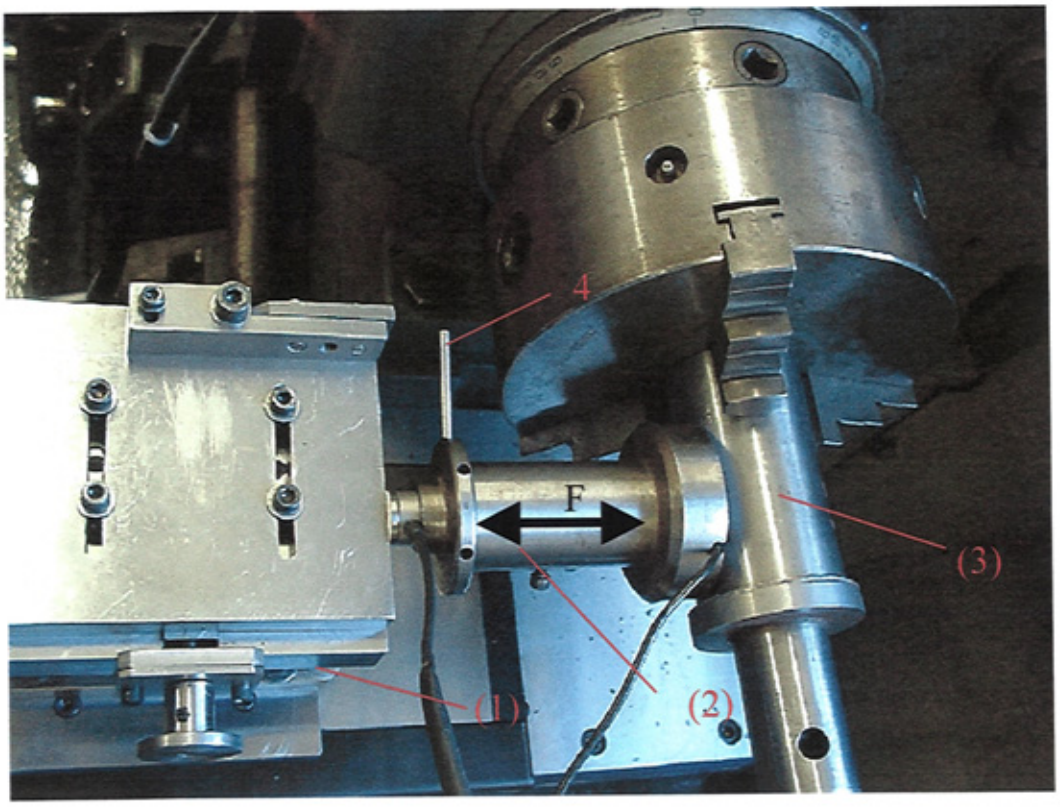

Figure 77 Experimental set-up. 1) Cross-slide 2) Jack 3) 100 mm circular bar in a 3-jaw chuck 4) Screw

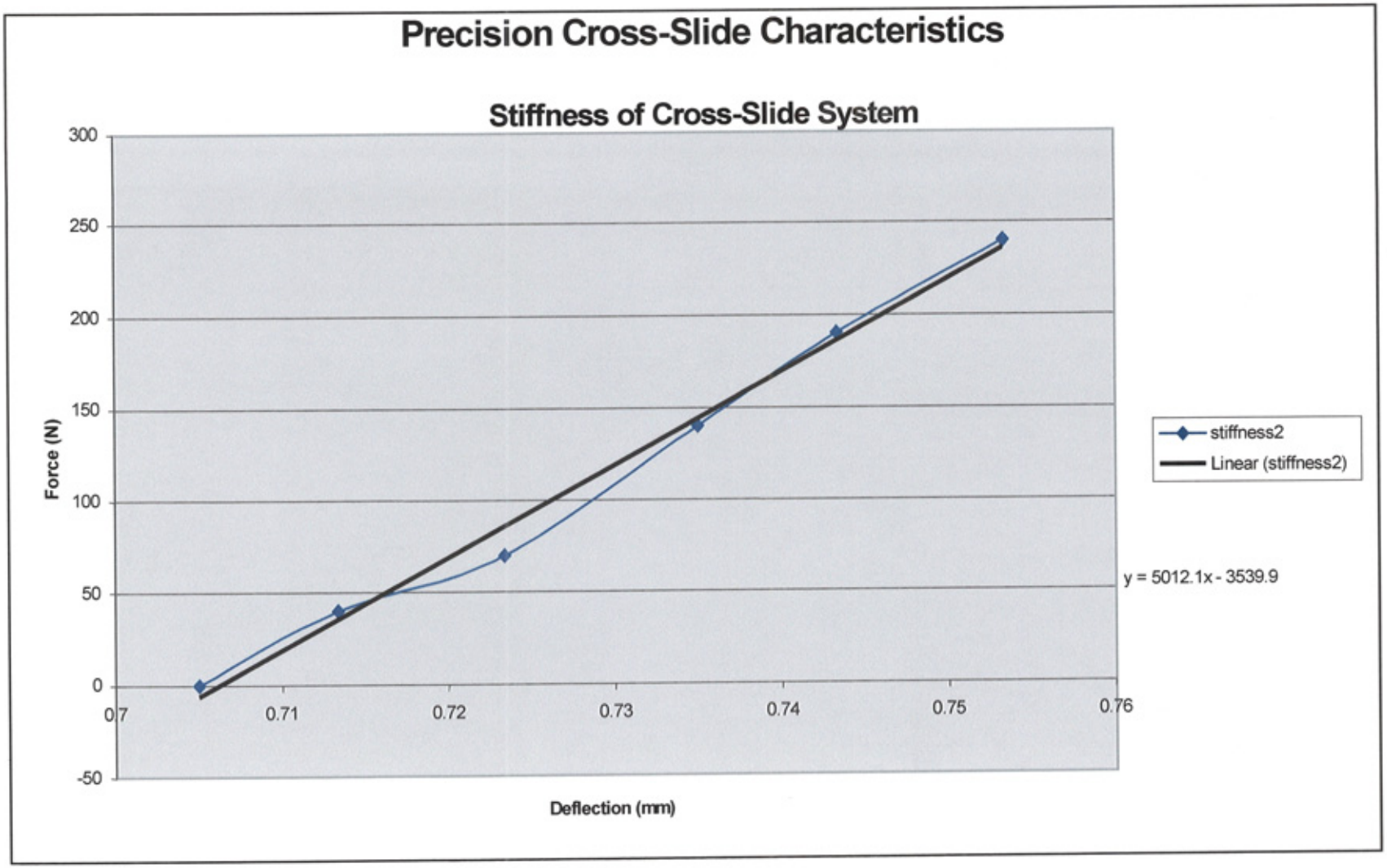

Figure 78 Graph of Force VS Deflection

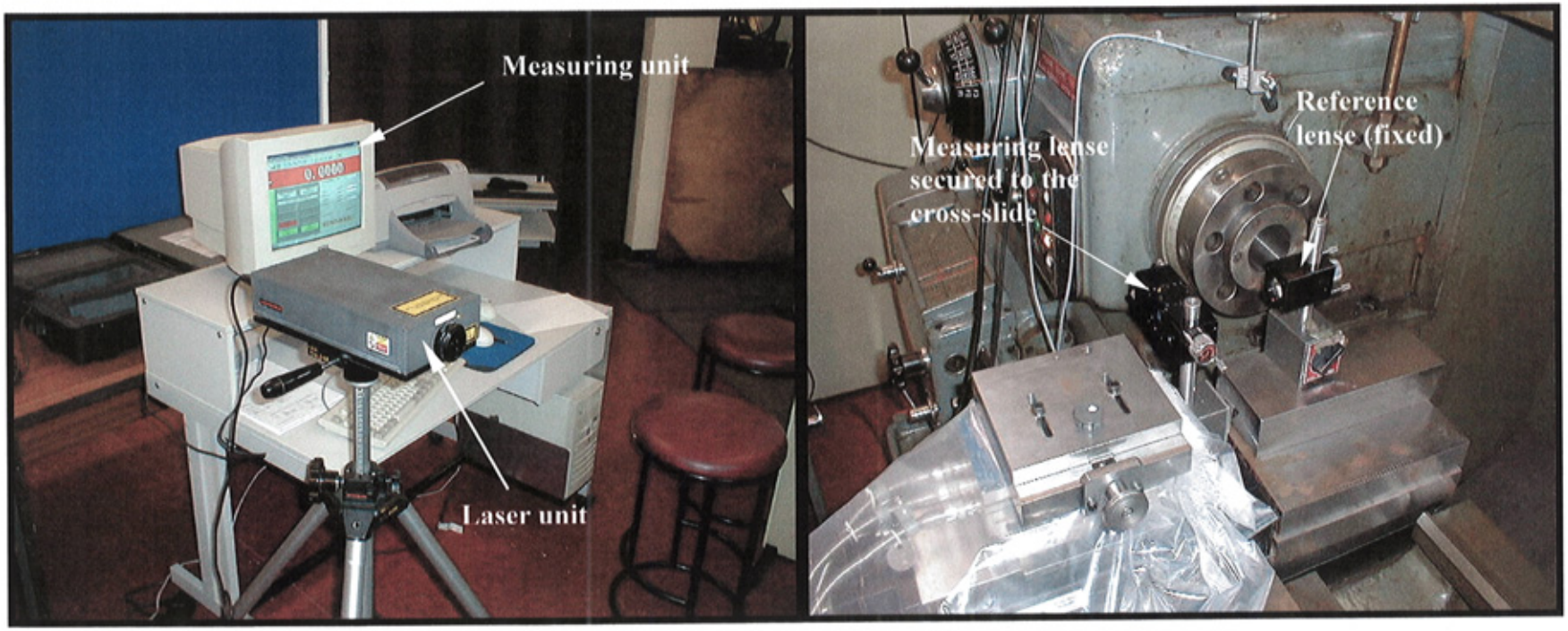

Figure 79 Laser interferometer apparatus used to measure the accuracy of the precision cross-slide

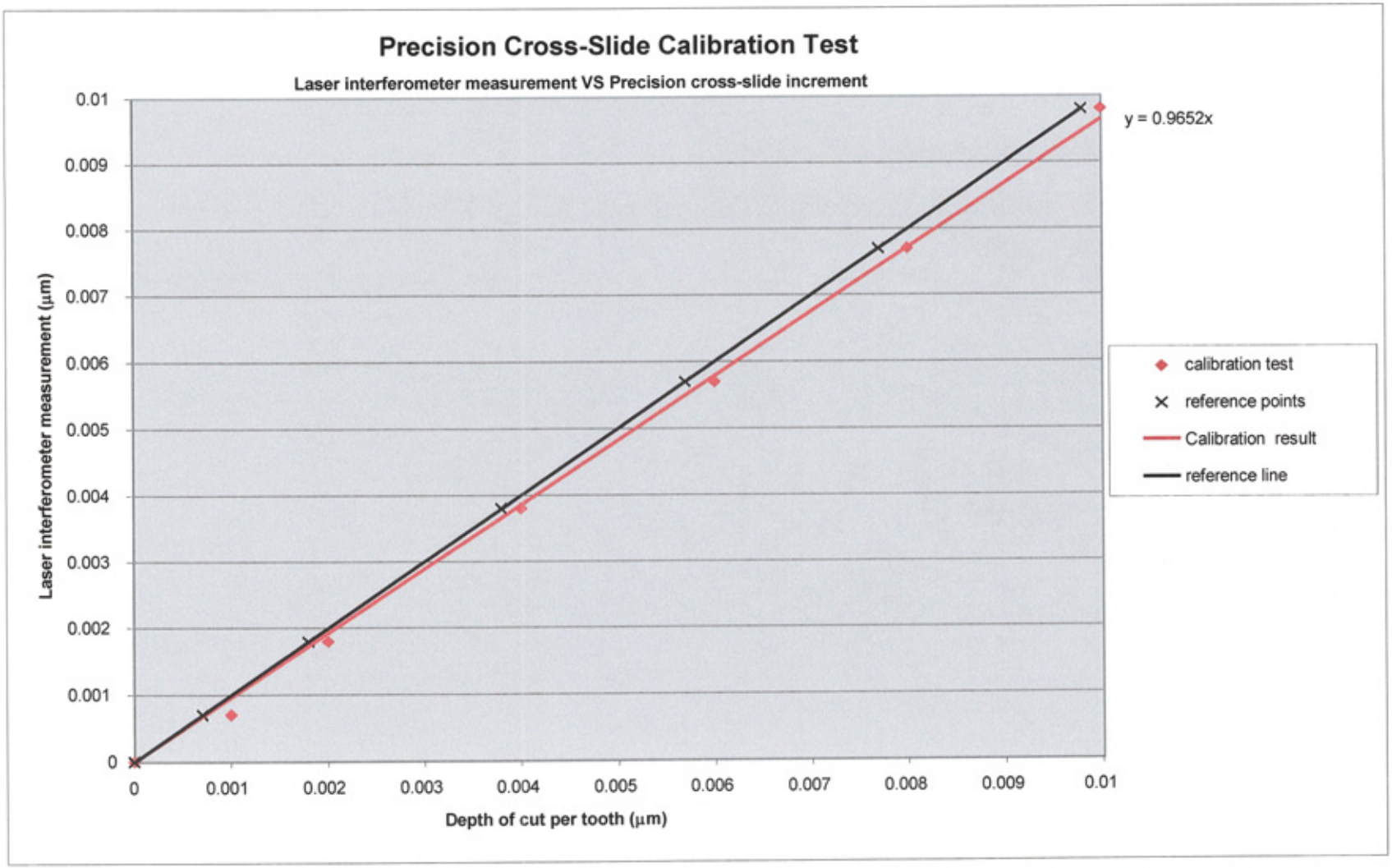

Figure 80 Accuracy of the precision cross-slide feed system

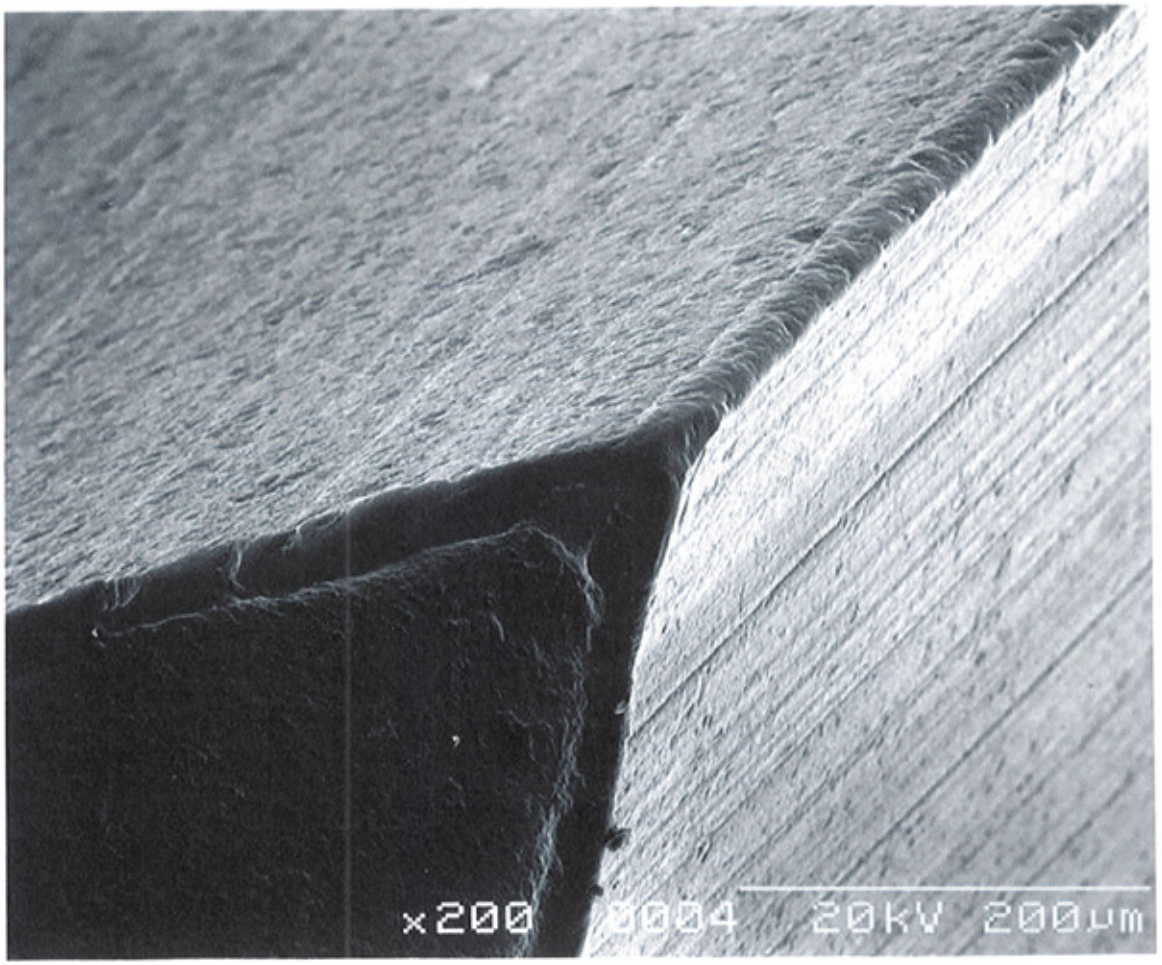

Figure 81 Cutting edge of saw tooth samples used in single tooth tests

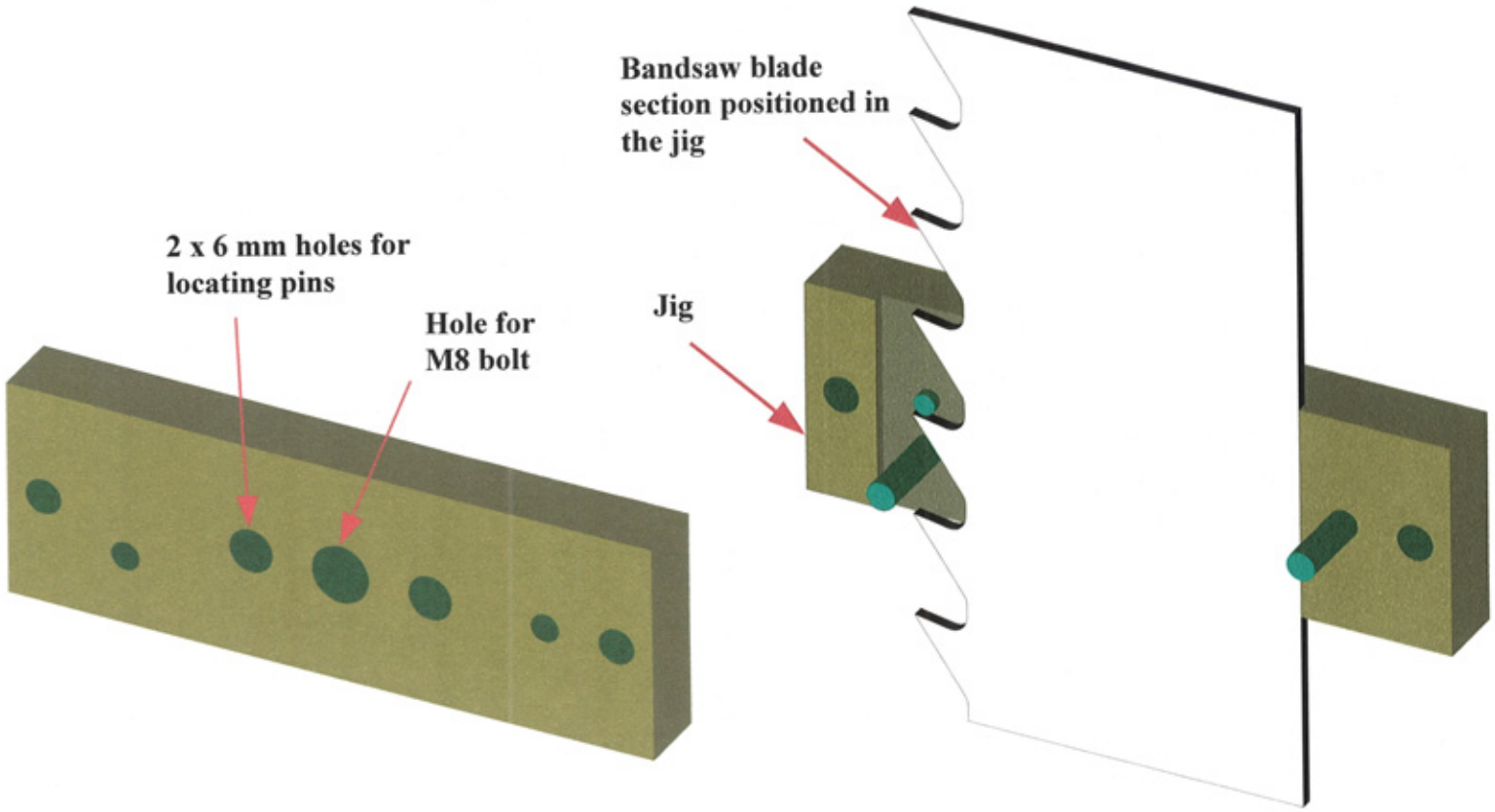

Figure 82 Jig for drilling holes through the single tooth sample to enable mounting of sample to the tool holder

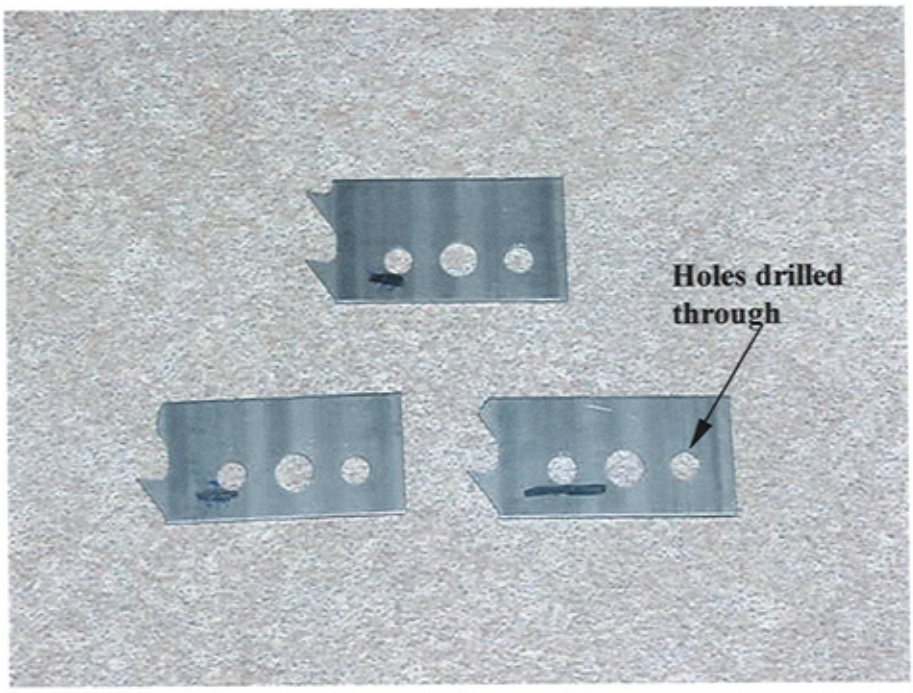

Figure 83 Single tooth samples

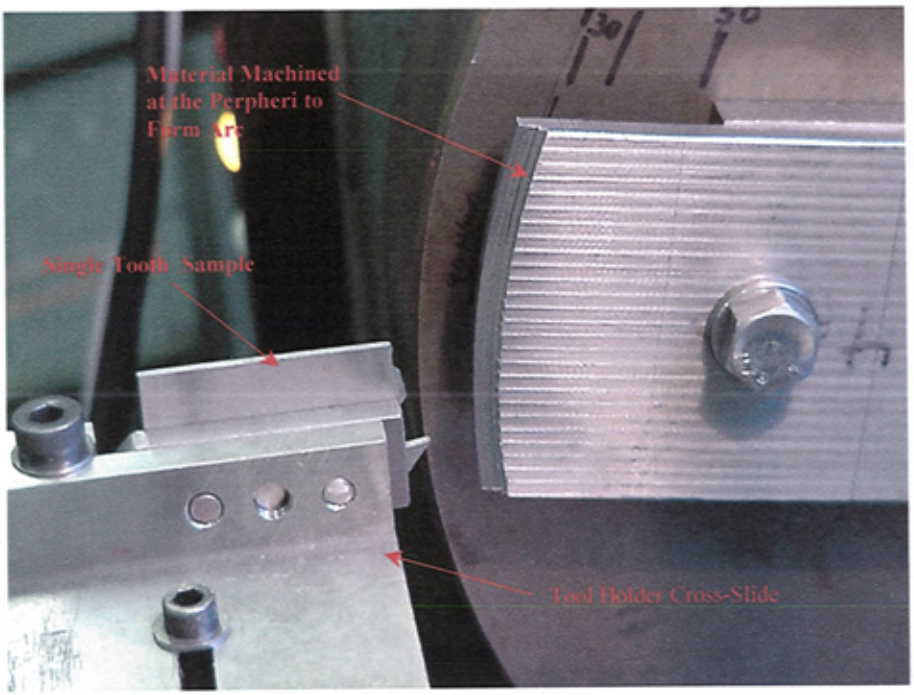

Figure 84 Workpiece material pre-machined on the periphery using a single tooth sample

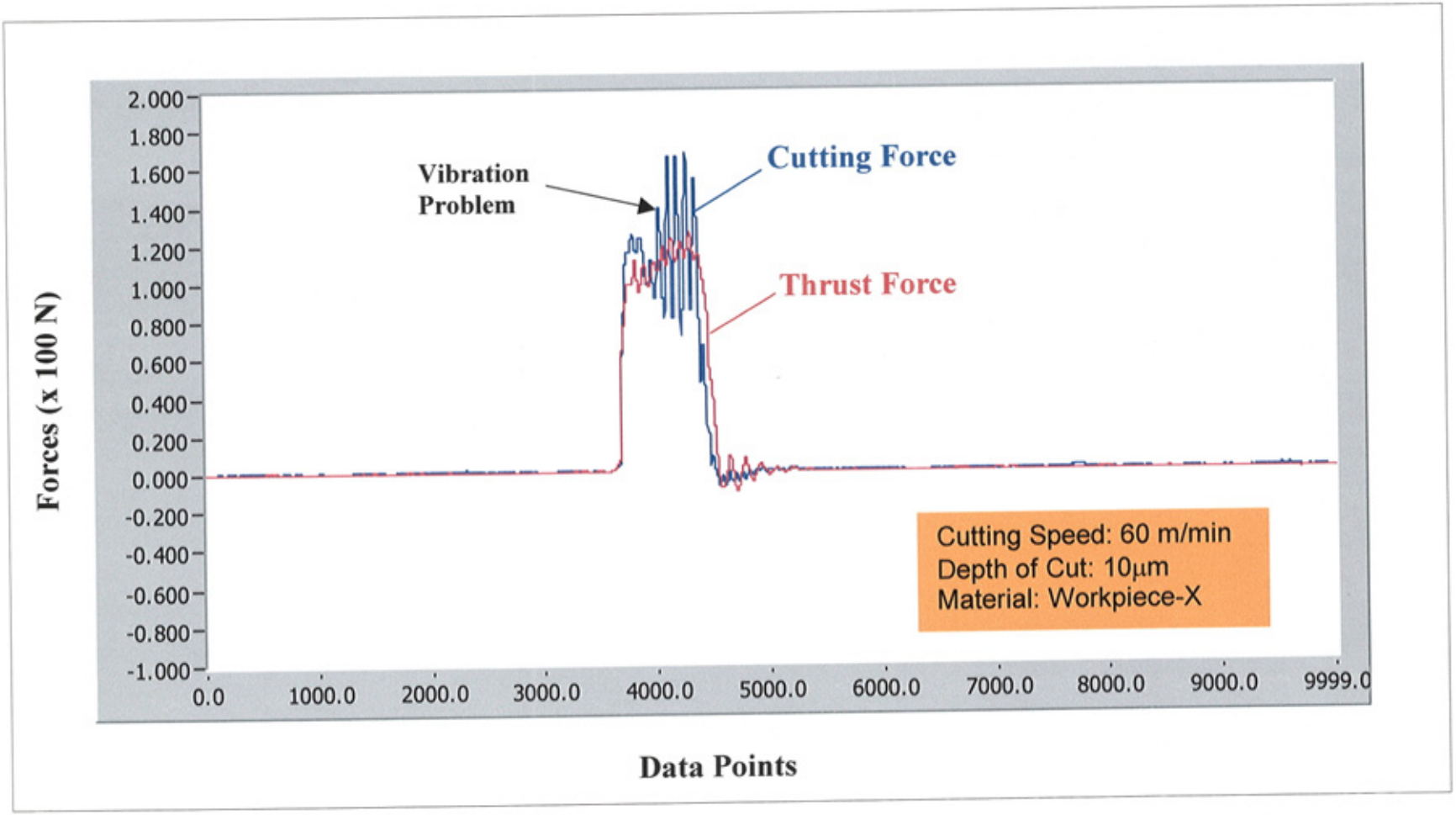

Figure 85 Force signal obtained without 20 kg solid metal block fastened on top of tool holder cross-slide

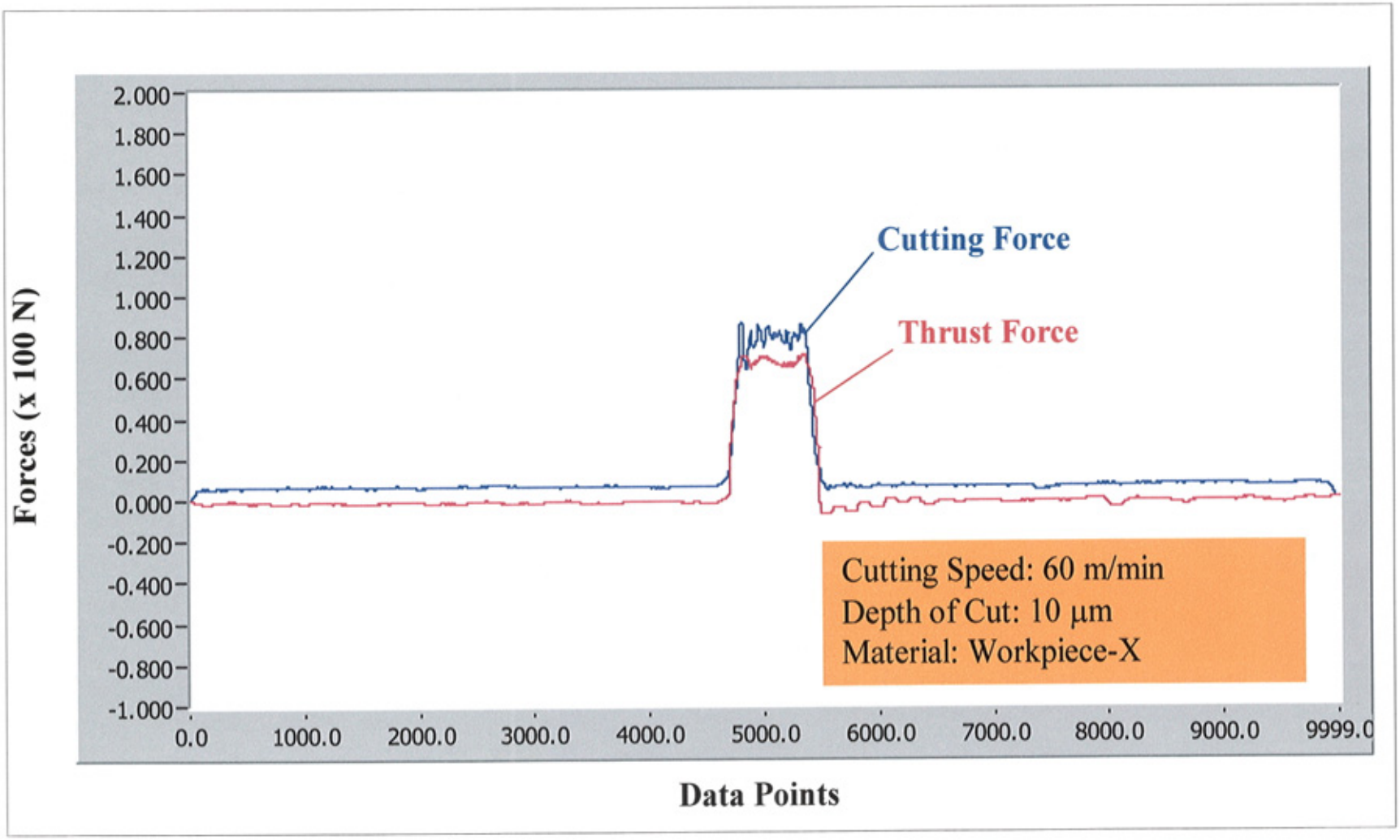

Figure 86 Force signal obtained with 20 kg solid metal block fastened on top of tool holder cross-slide

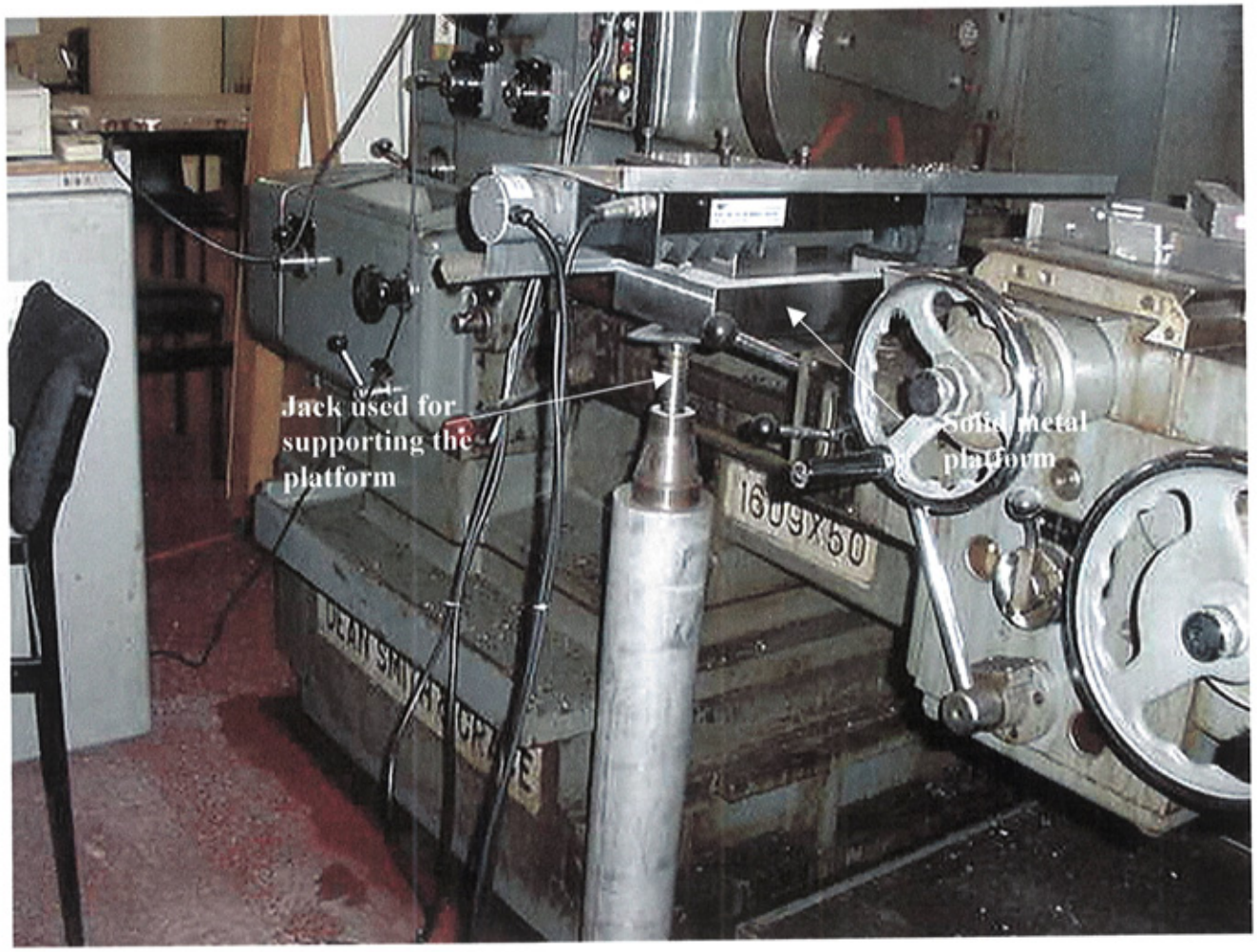

Figure 87 Modification to test rig design to reduce the effect of vibration

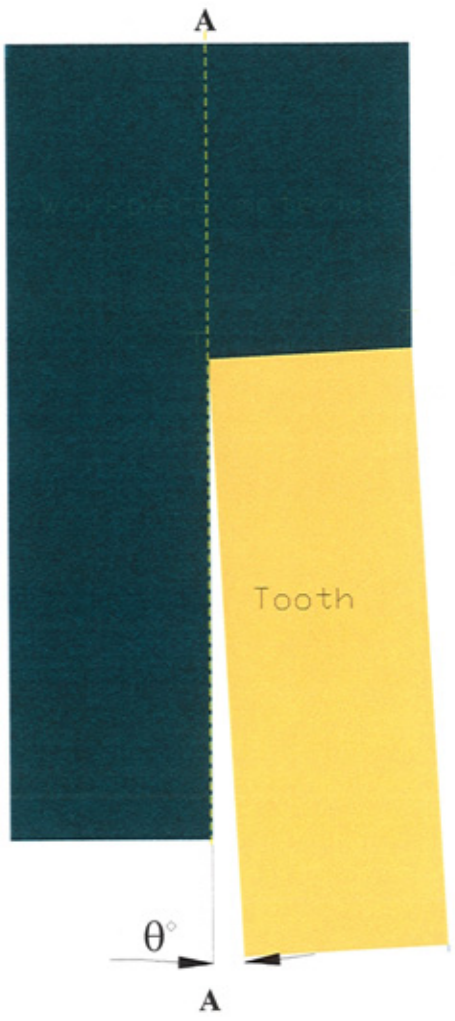

Figure 88 Single tooth setting to provide side clearance during cutting

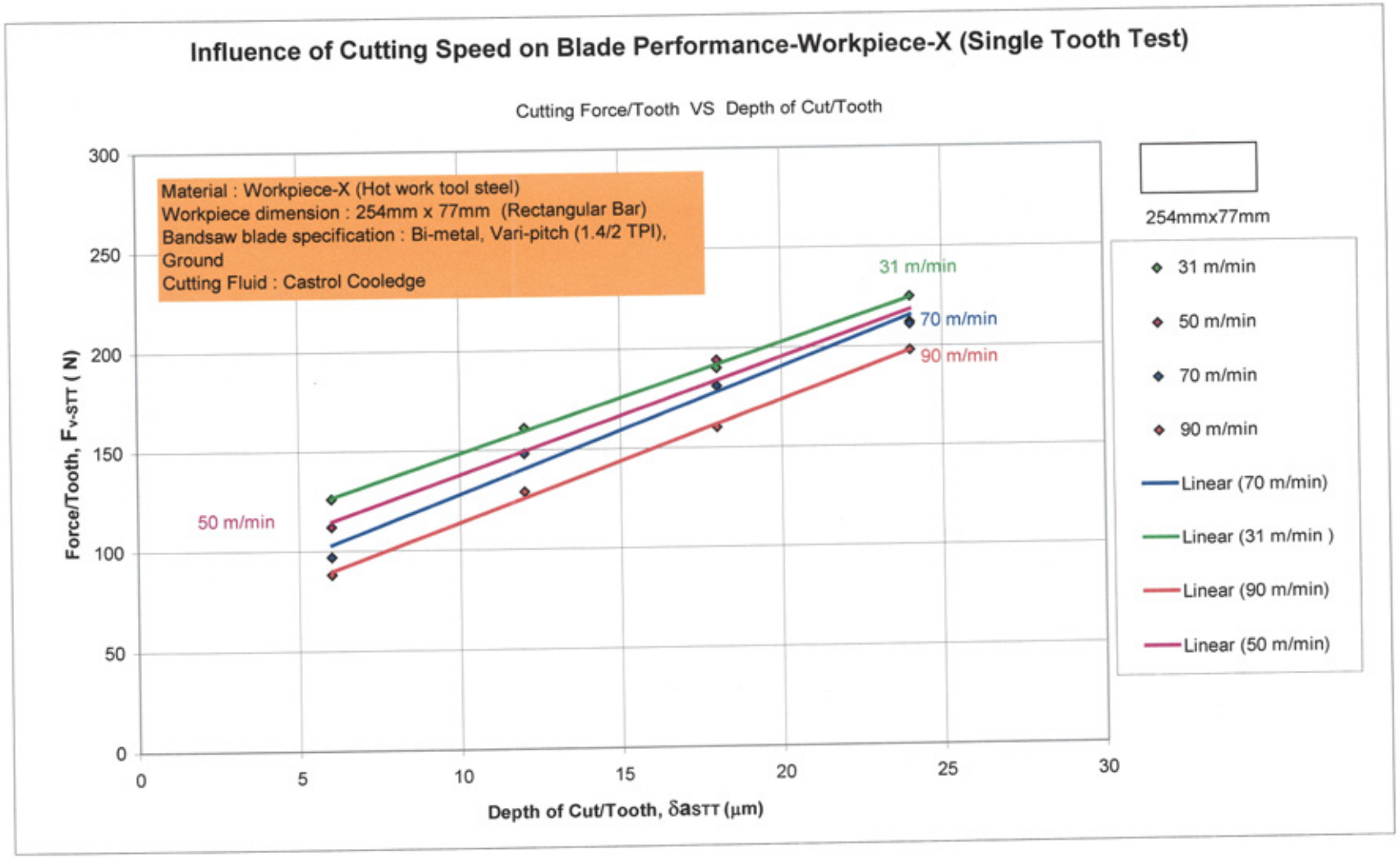

Figure 89 Influence of the cutting speed on the cutting force at different depth of cut per tooth (Single tooth test)

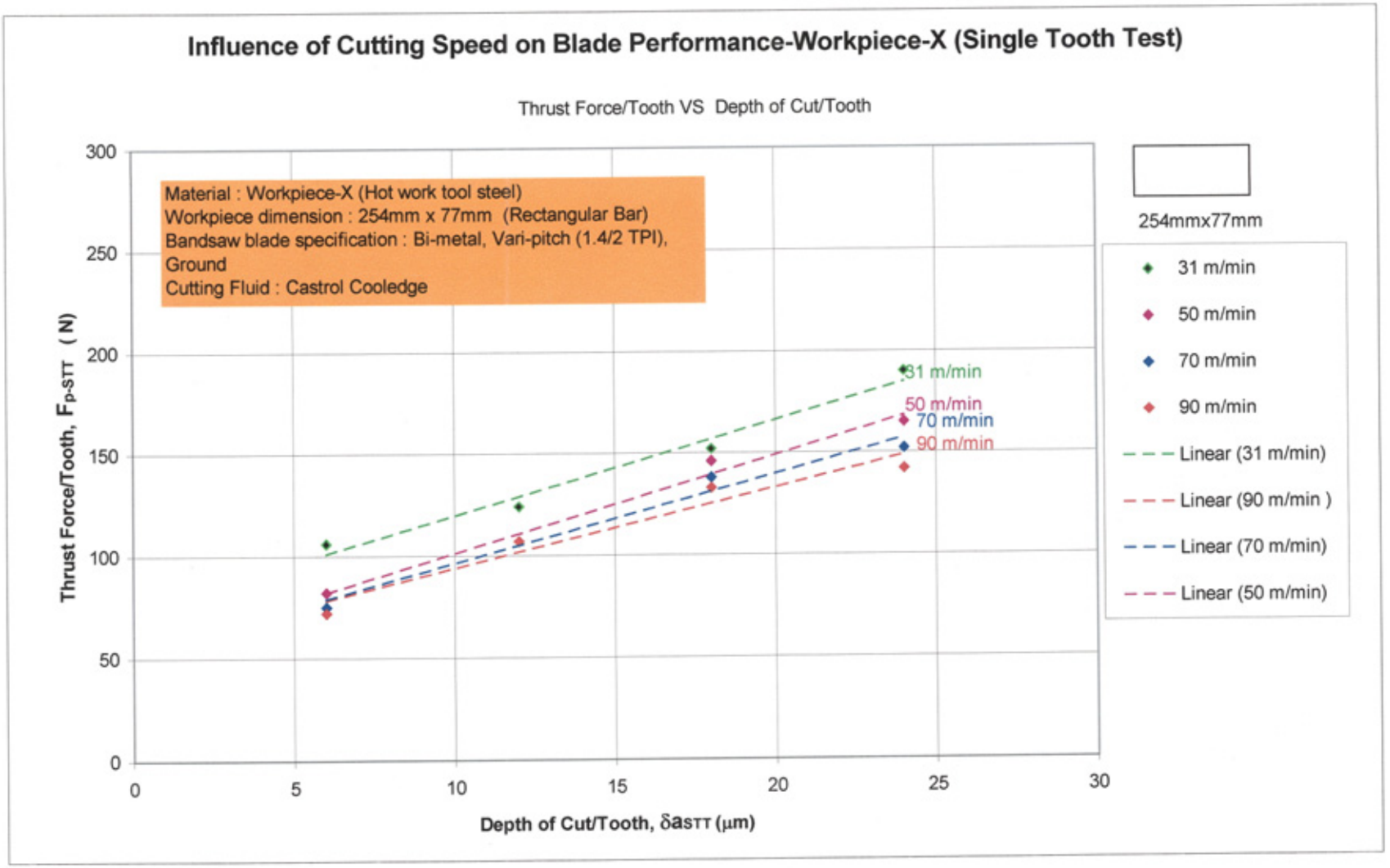

Figure 90 Influence of the cutting speed on the thrust force at different depth of cut per tooth (Single tooth test)

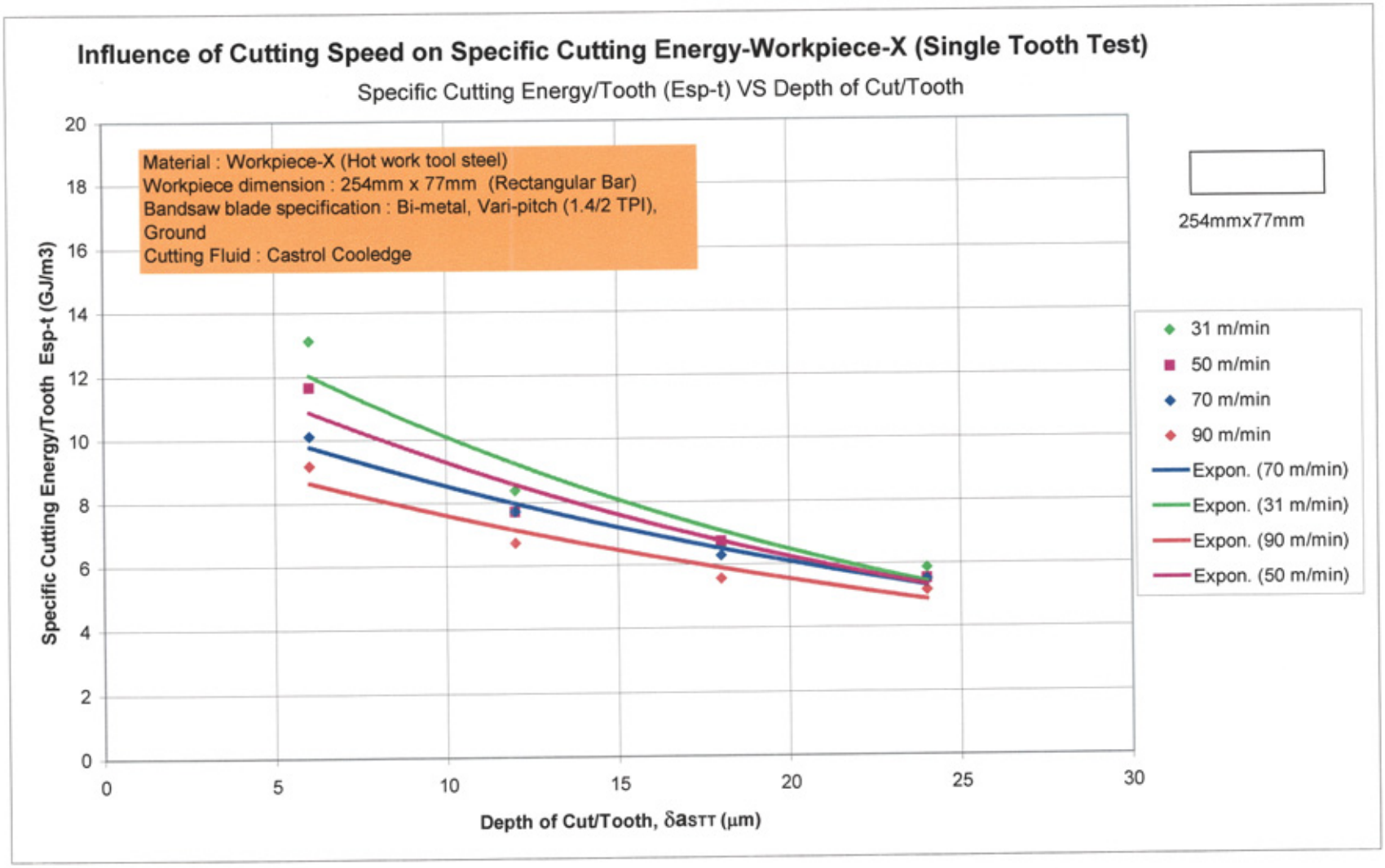

Figure 91 The influence of cutting speed on specific cutting energy (Single tooth test)

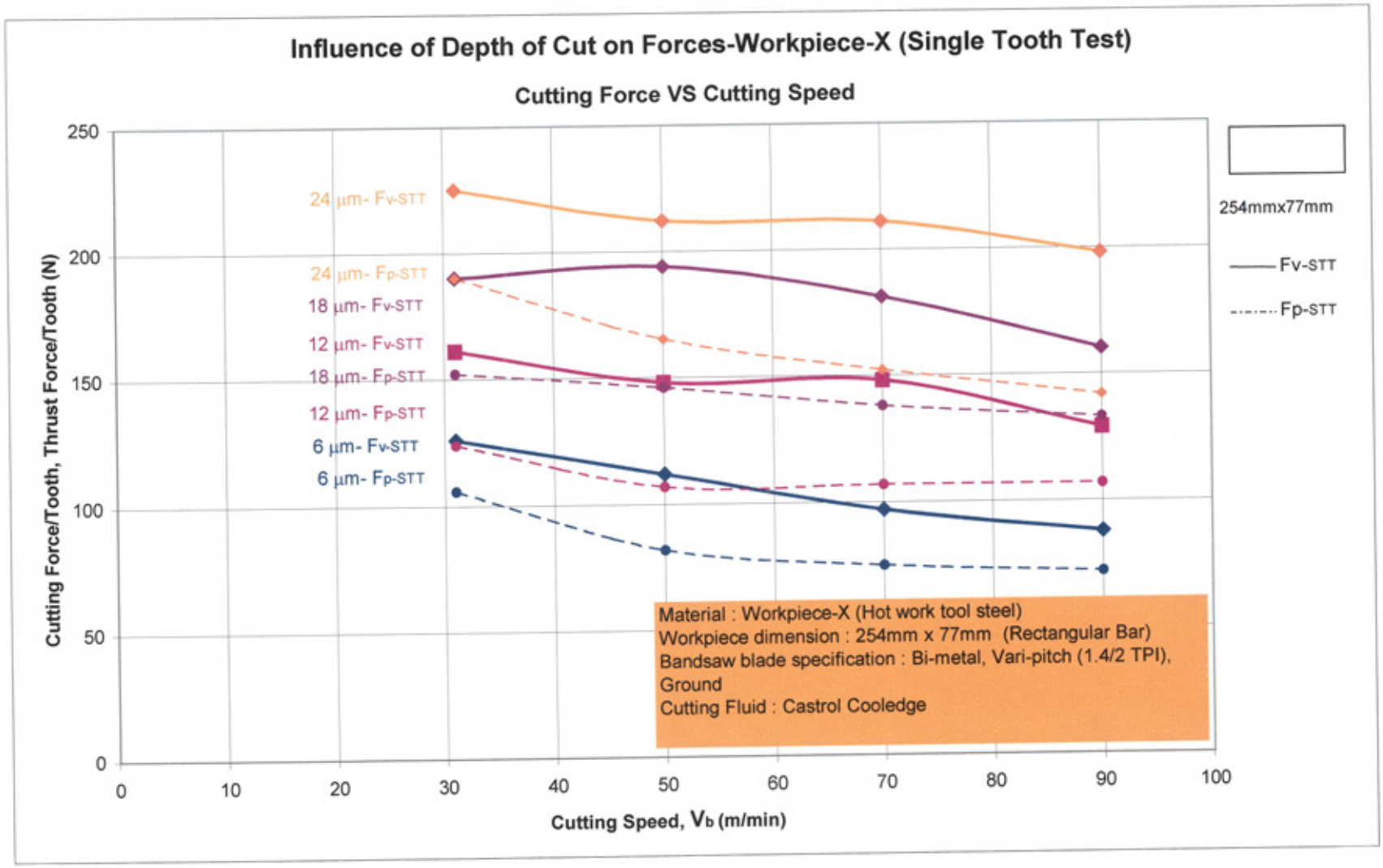

Figure 92 The influence of the depth of cut per tooth on forces for different cutting speeds (Single tooth test)

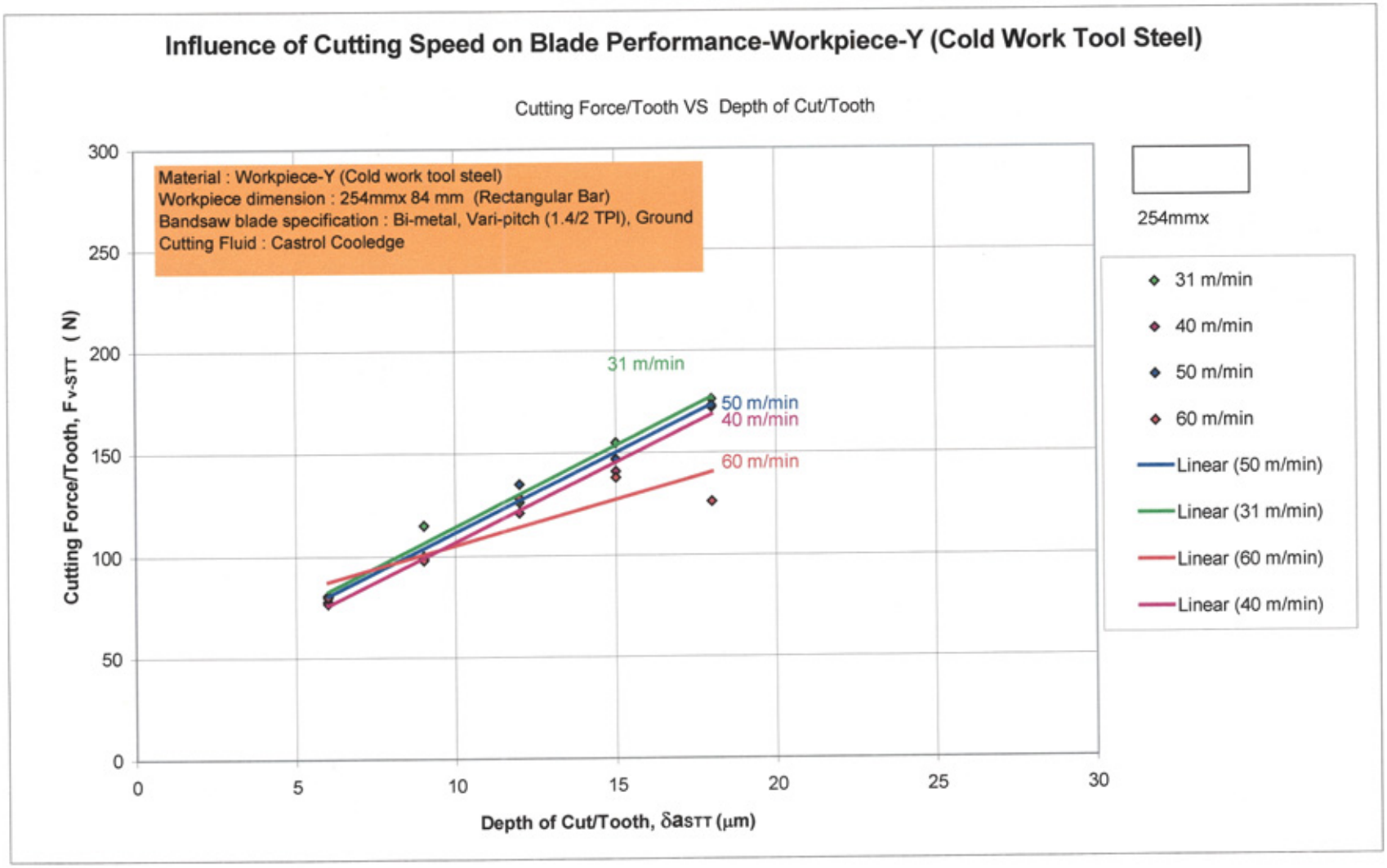

Figure 93 Influence of the cutting speed on the cutting force at different depth of cut per tooth (Single tooth test)

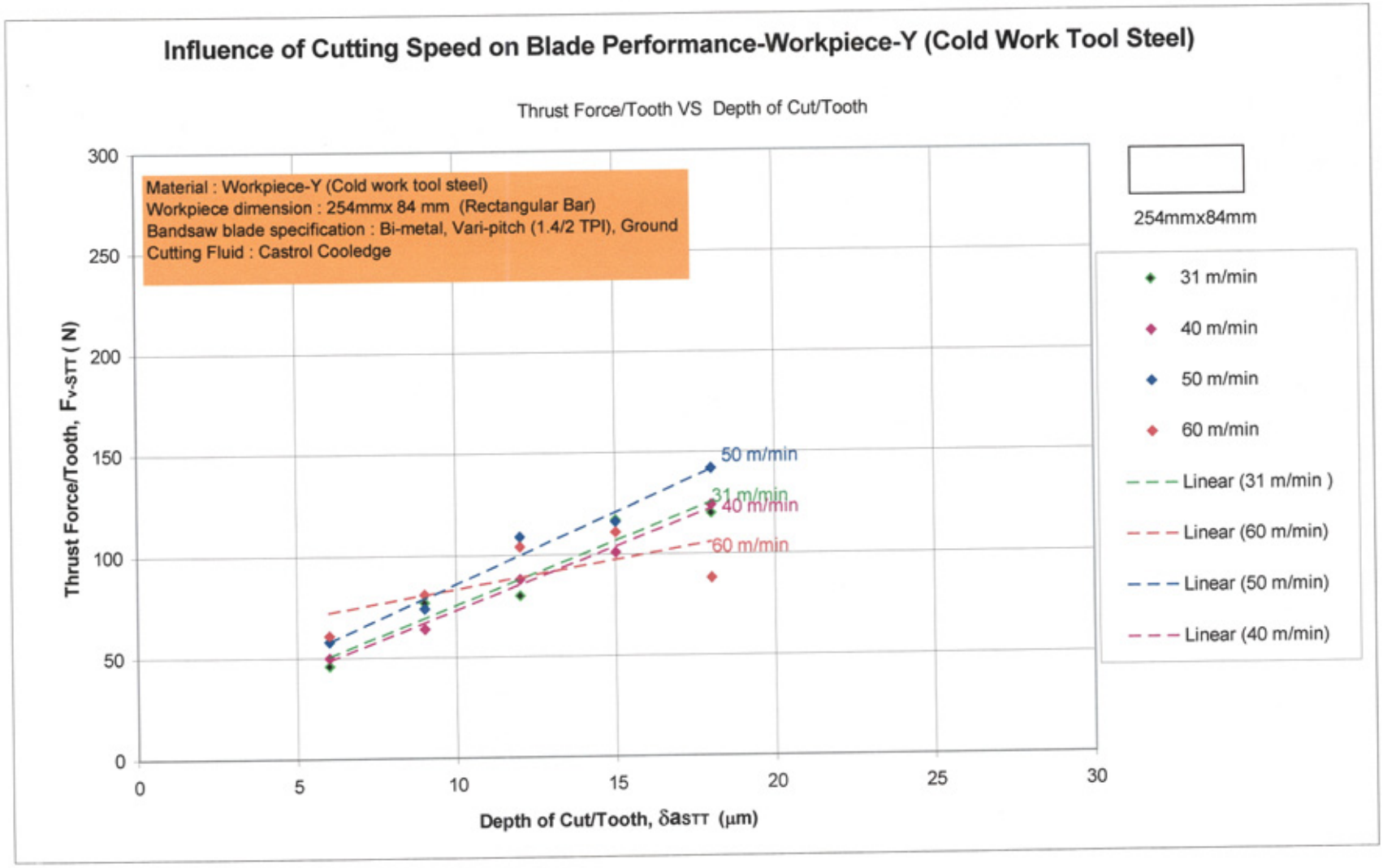

Figure 94 Influence of the cutting speed on the thrust force at different depth of cut per tooth (Single tooth test)

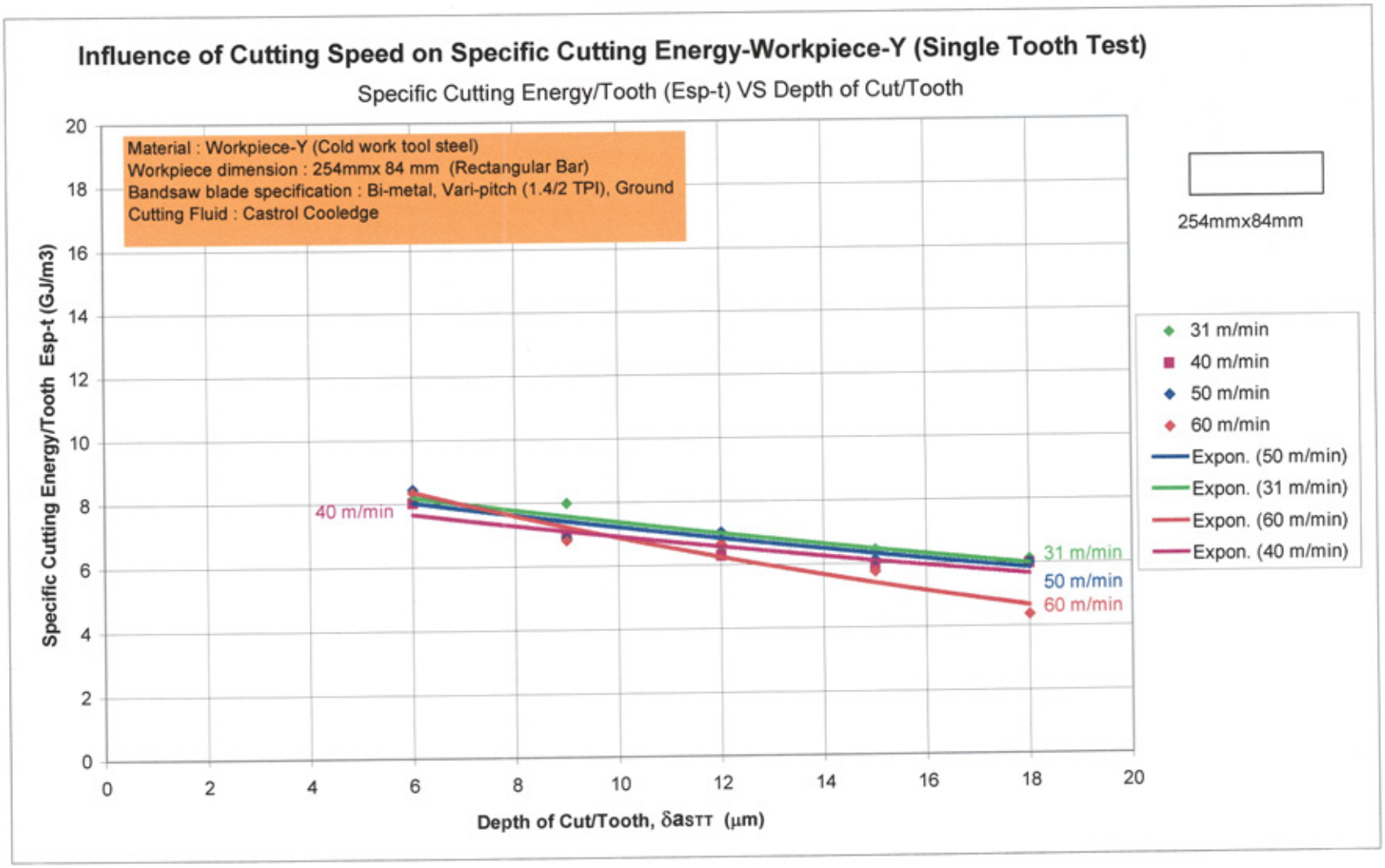

Figure 95 The influence of cutting speed on specific cutting energy (Single tooth test)

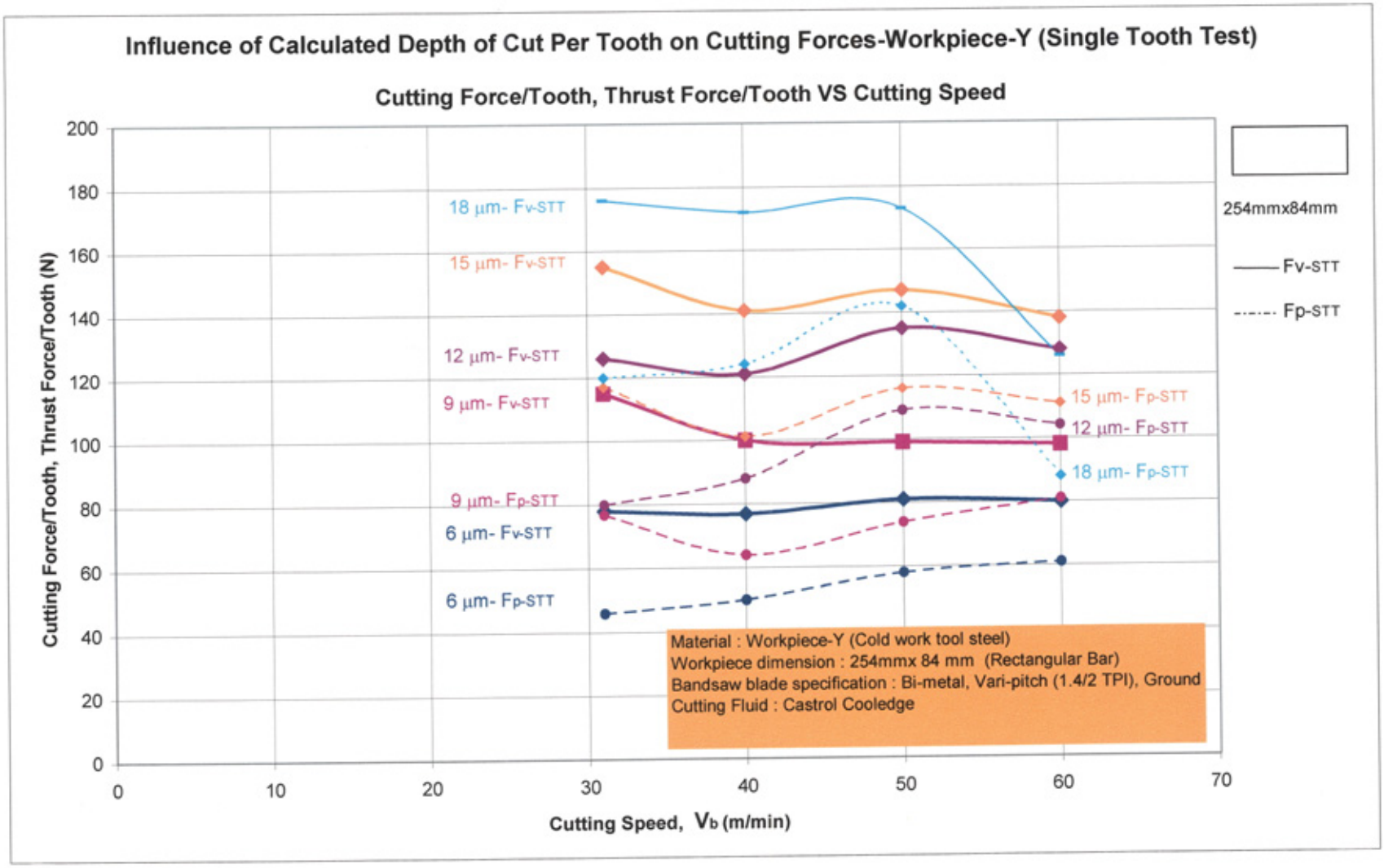

Figure 96 The influence of the depth of cut per tooth on forces for different cutting speeds (Single tooth test)

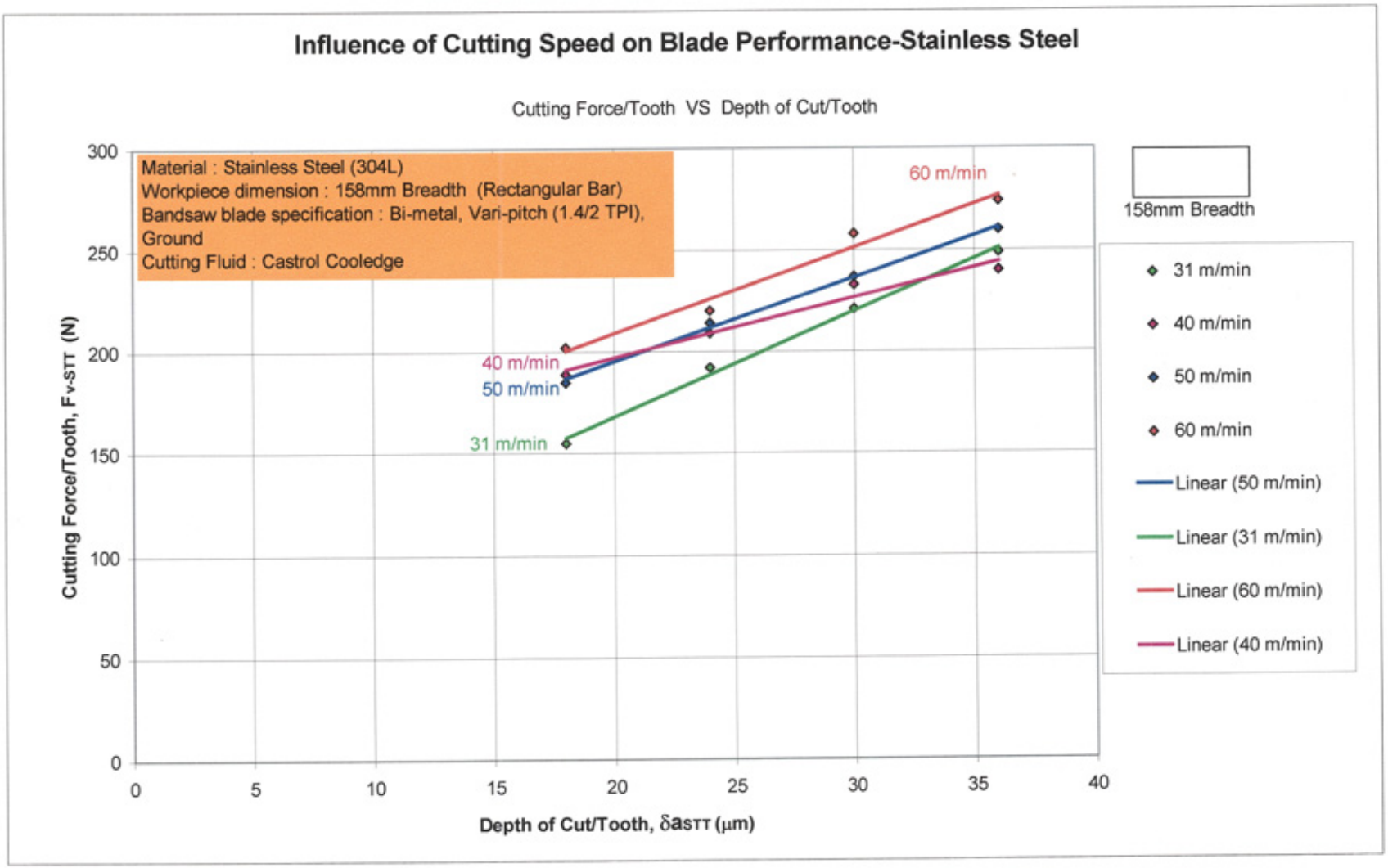

Figure 97 Influence of the cutting speed on the cutting force at different depth of cut per tooth (Single tooth test)

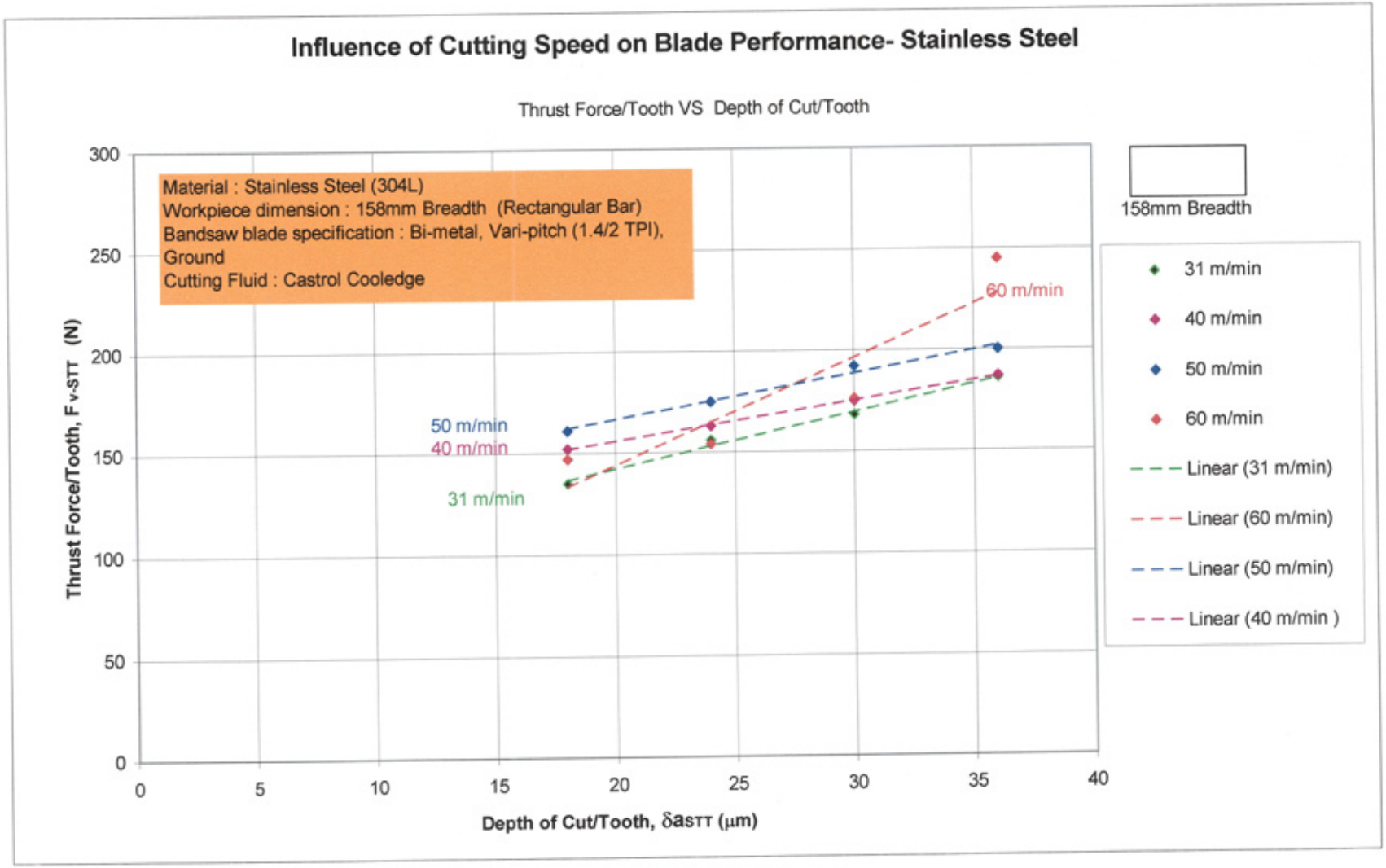

Figure 98 Influence of the cutting speed on the thrust force at different depth of cut per tooth (Single tooth test)

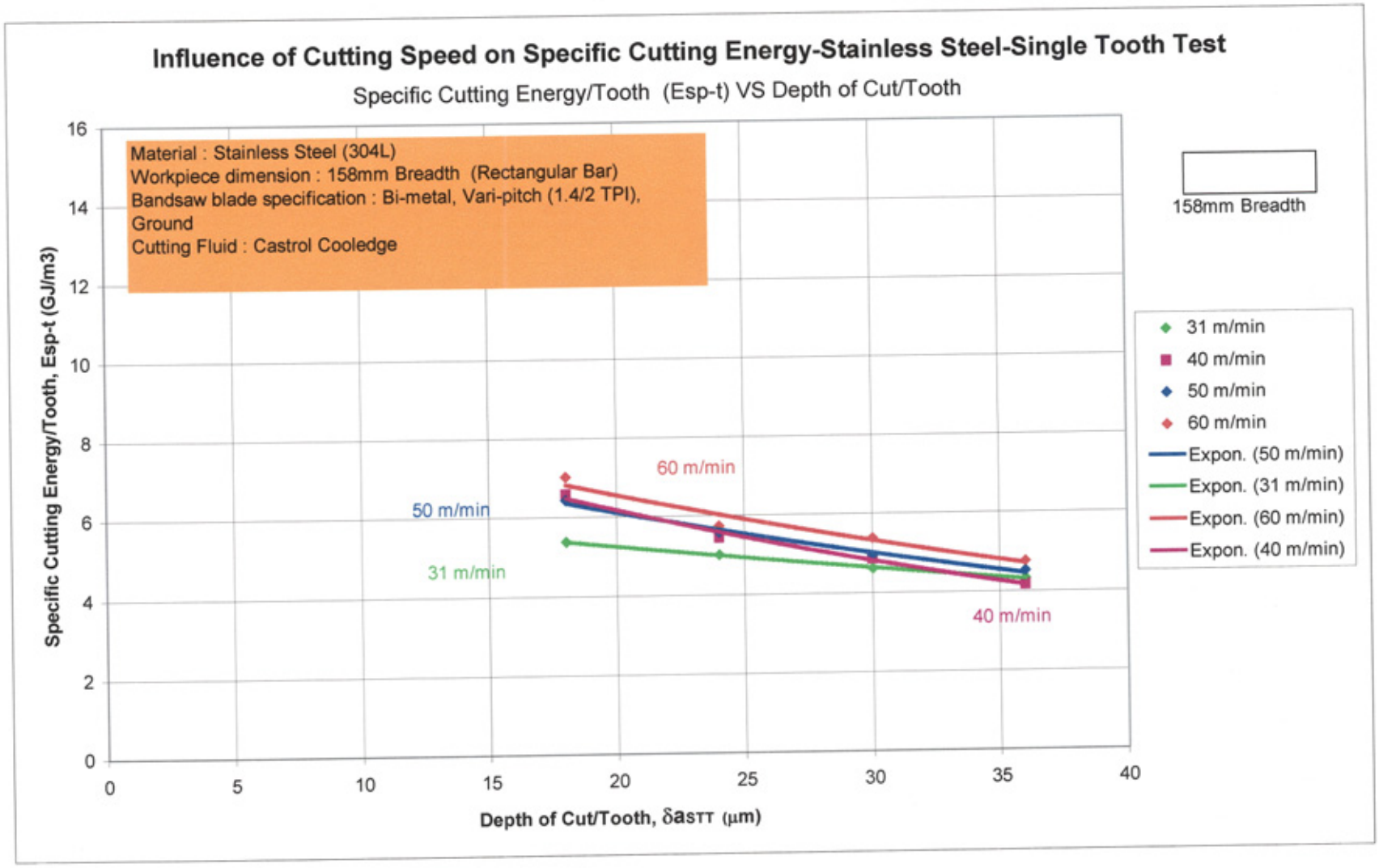

Figure 99 Influence of cutting speed on specific cutting energy (Single tooth test)

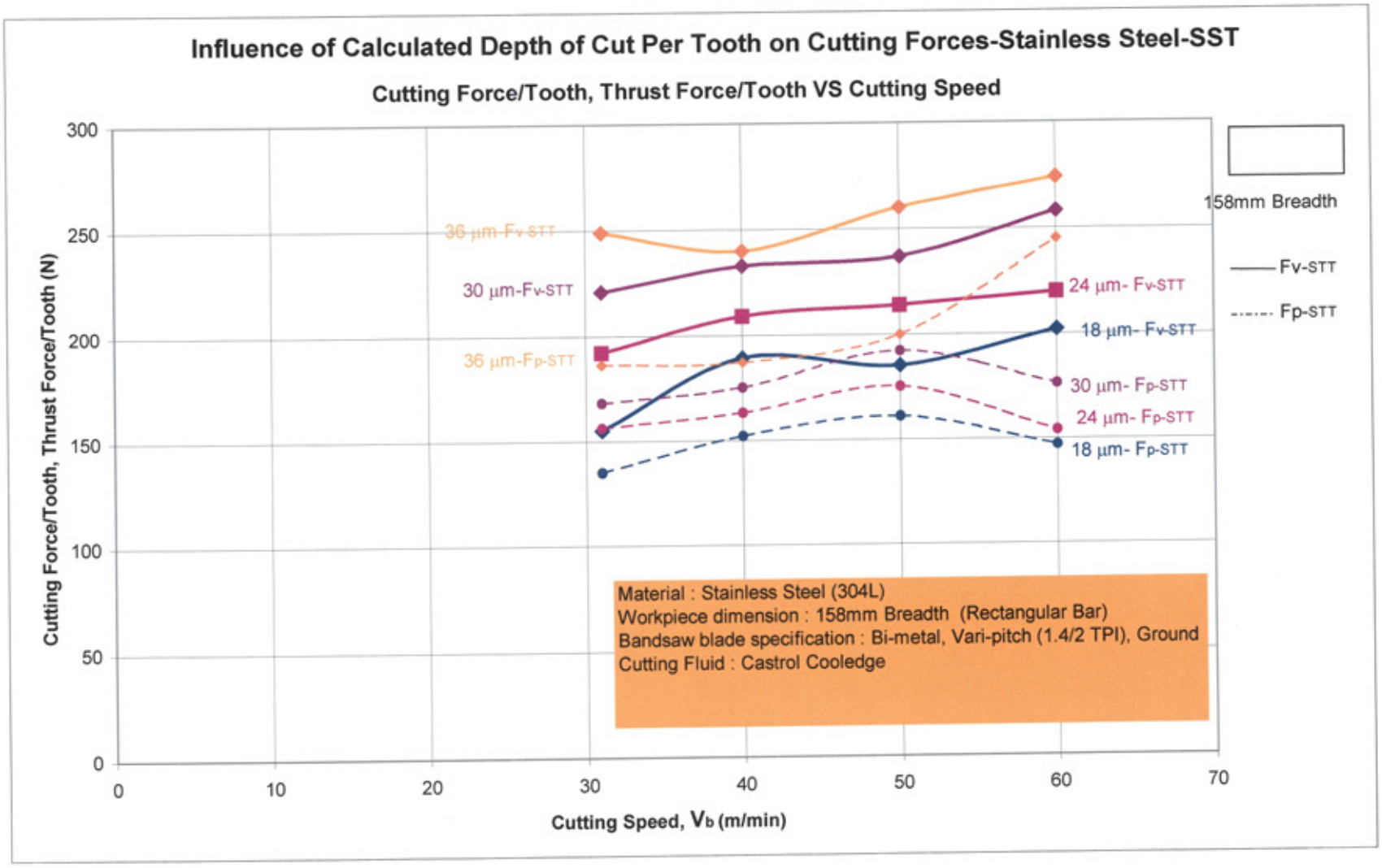

Figure 100 Influence of the depth of cut per tooth on forces for different cutting speeds (Single tooth test)

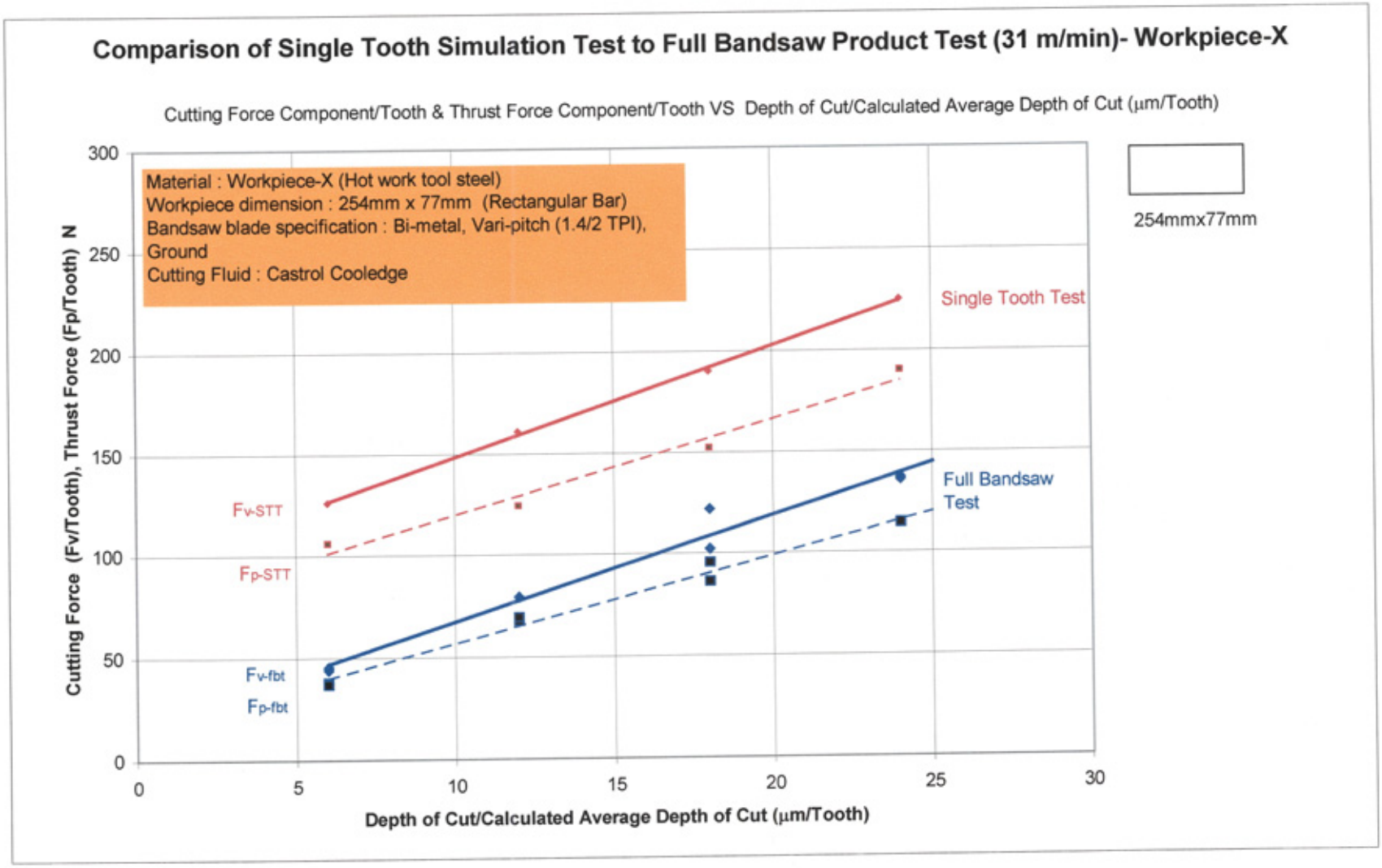

Figure 101 Comparison of single tooth simulation test to full bandsaw product test (31 m/min)

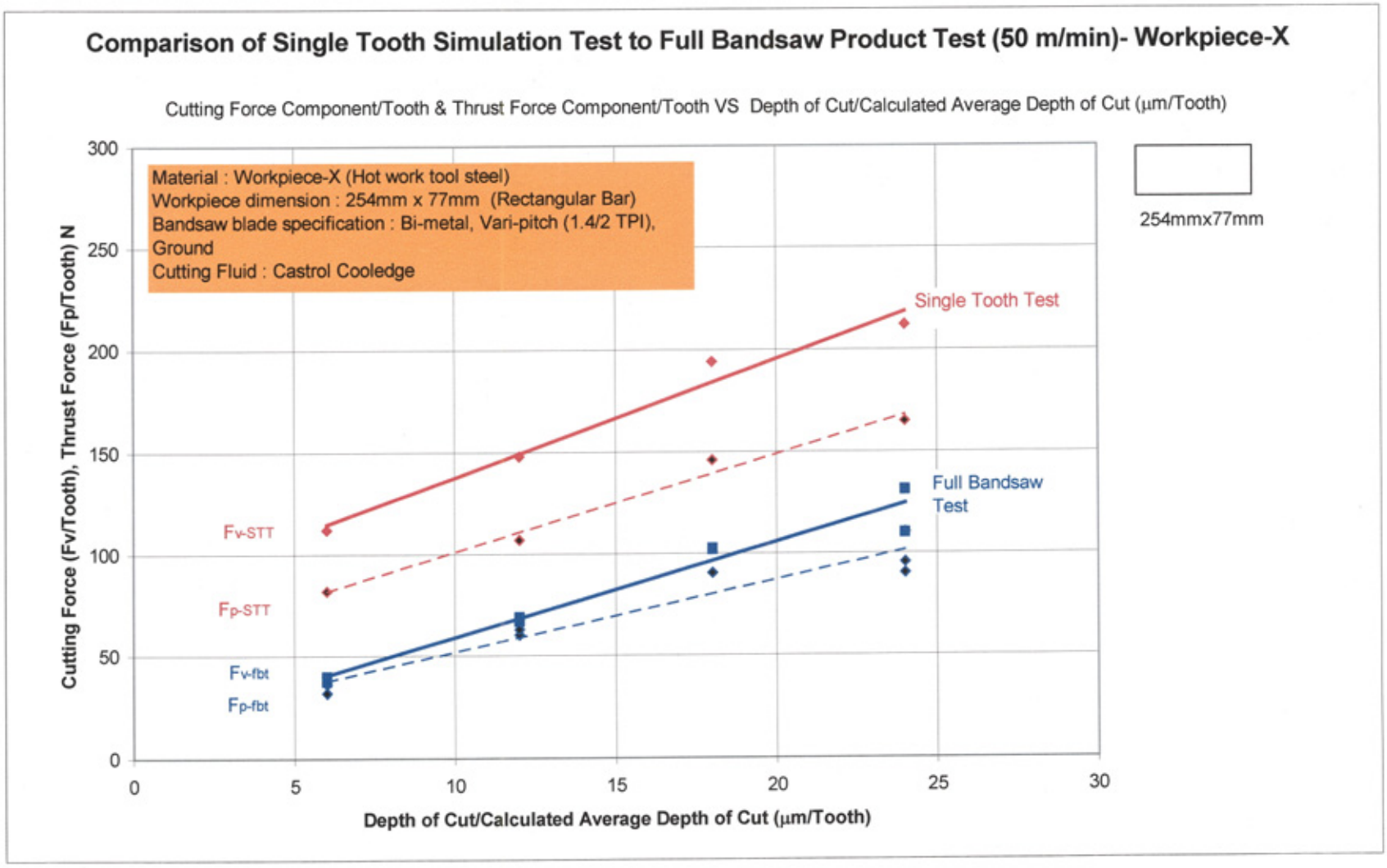

Figure 102 Comparison of single tooth simulation test to full bandsaw product test (50 m/min)

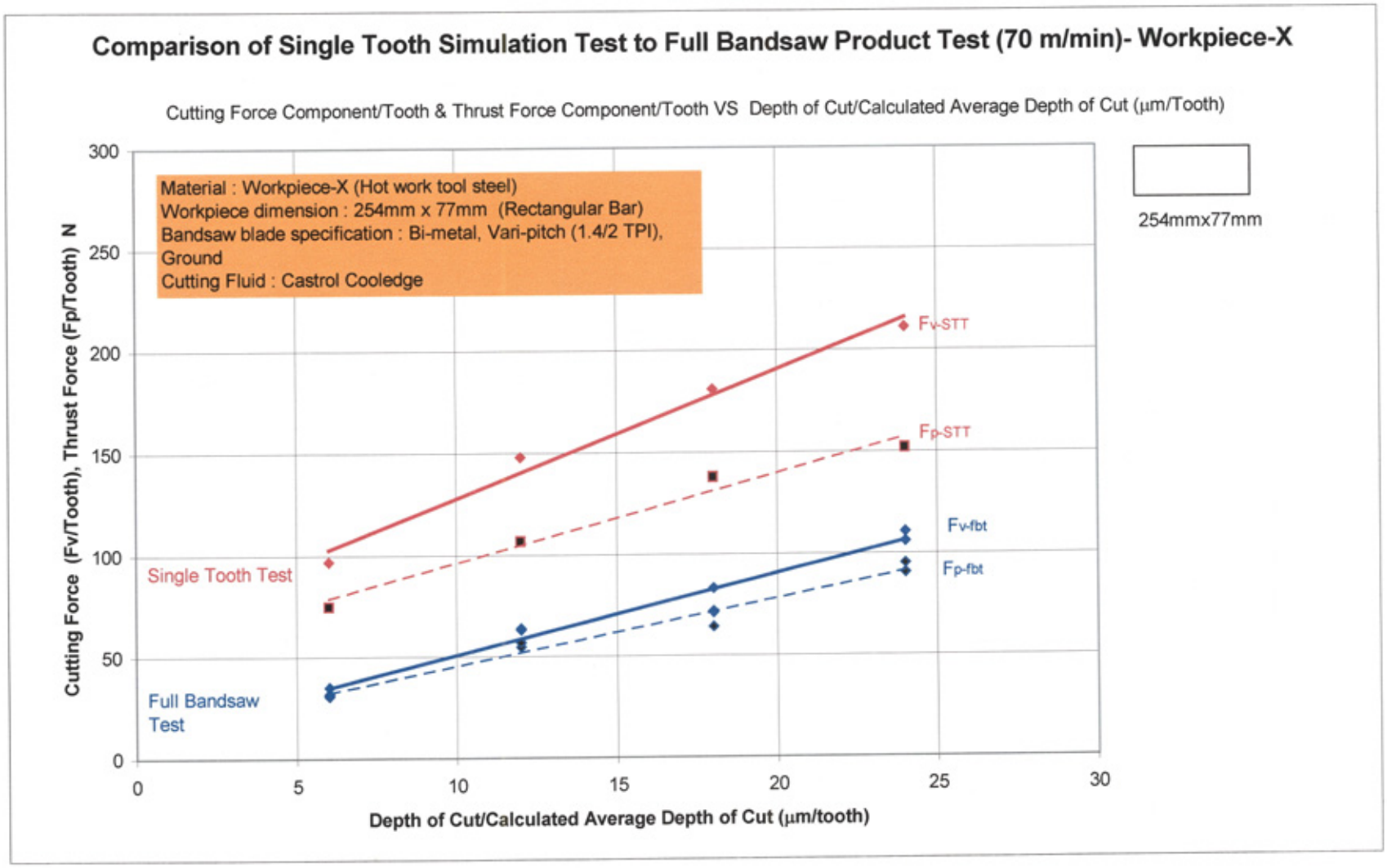

Figure 103 Comparison of single tooth simulation test to full bandsaw product test (70 m/min)

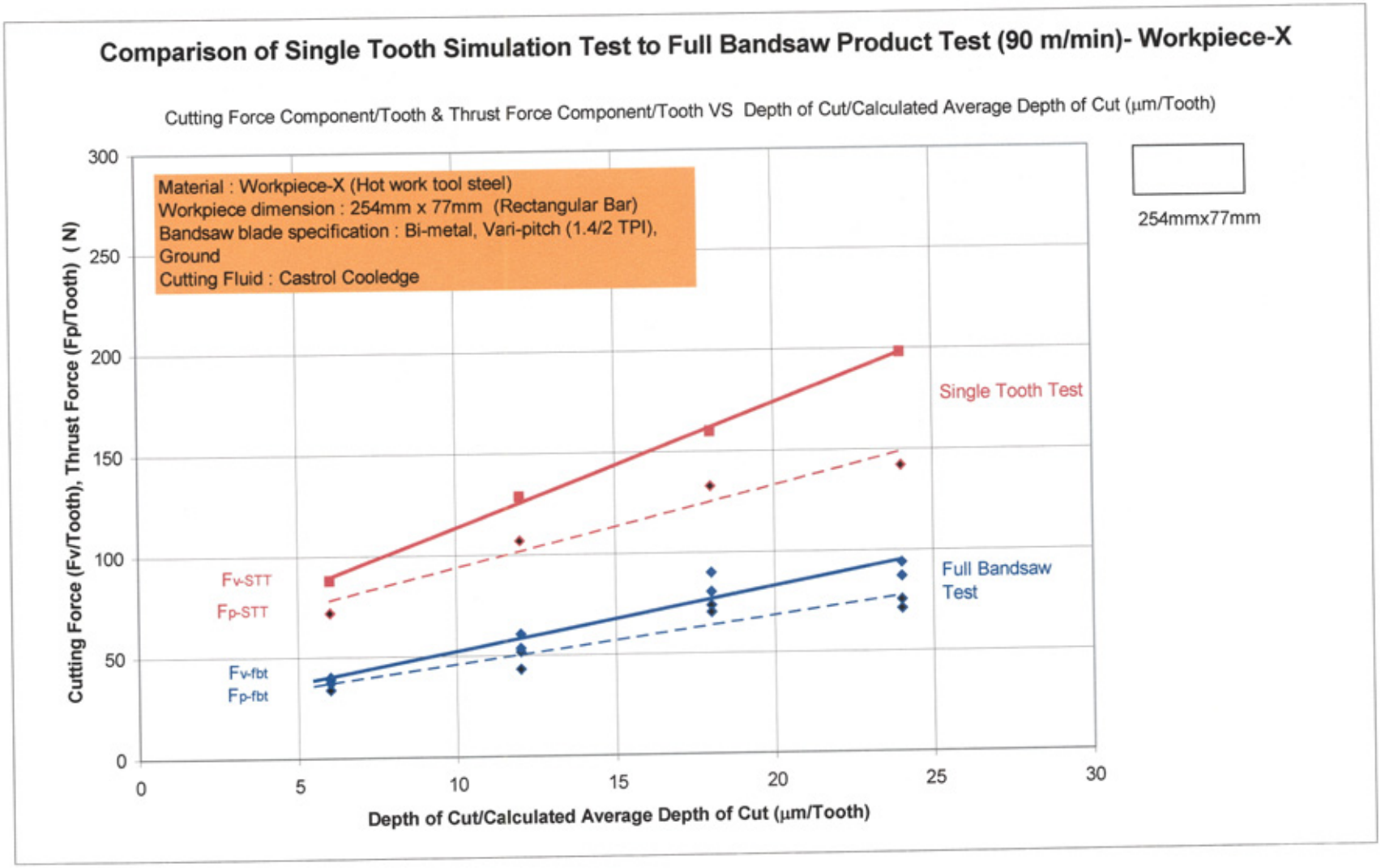

Figure 104 Comparison of single tooth simulation test to full bandsaw product test (90 m/min)

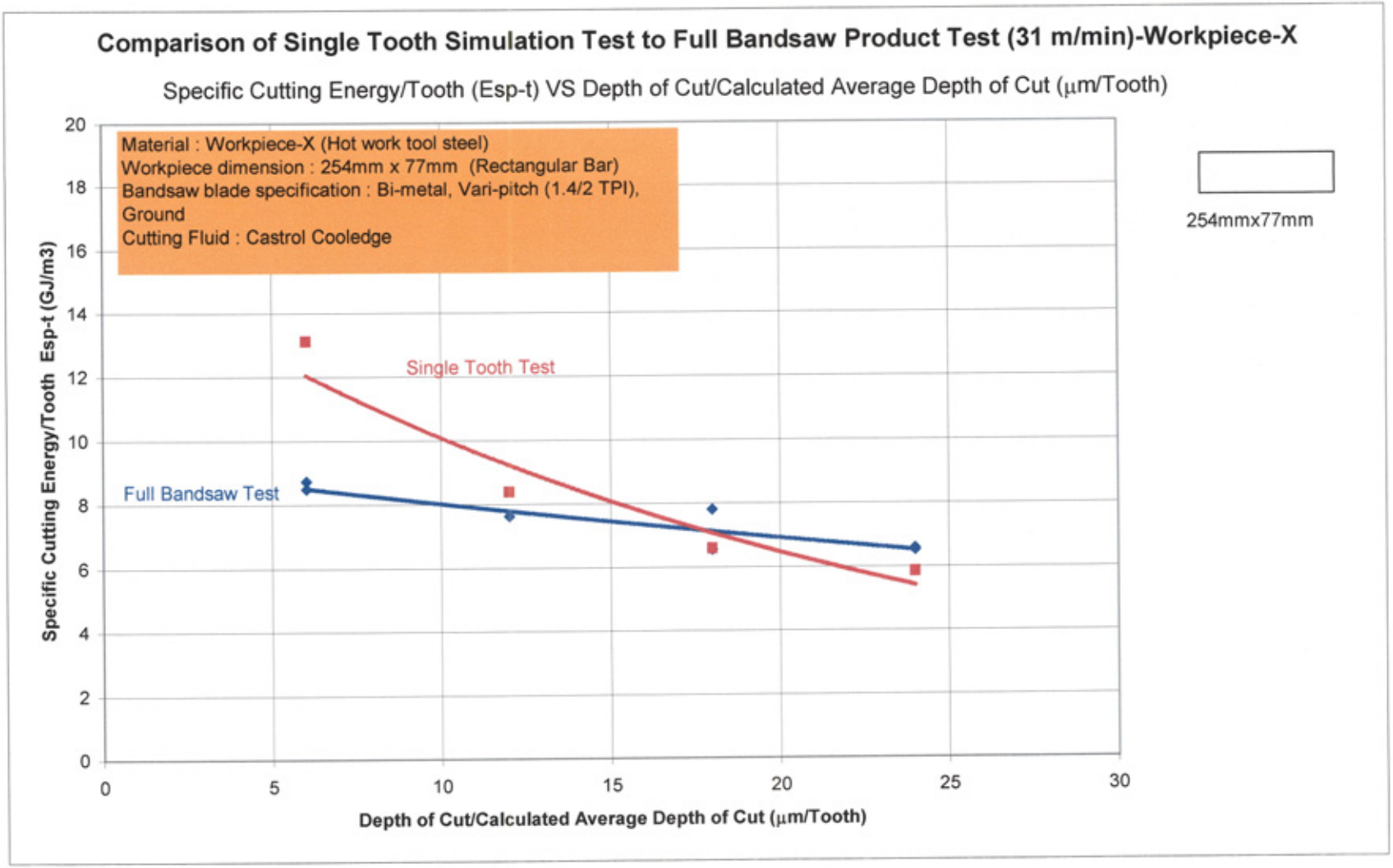

Figure 105 Comparison of E_{sp} values obtained from simulation test to full bandsaw product test at 31 m/min

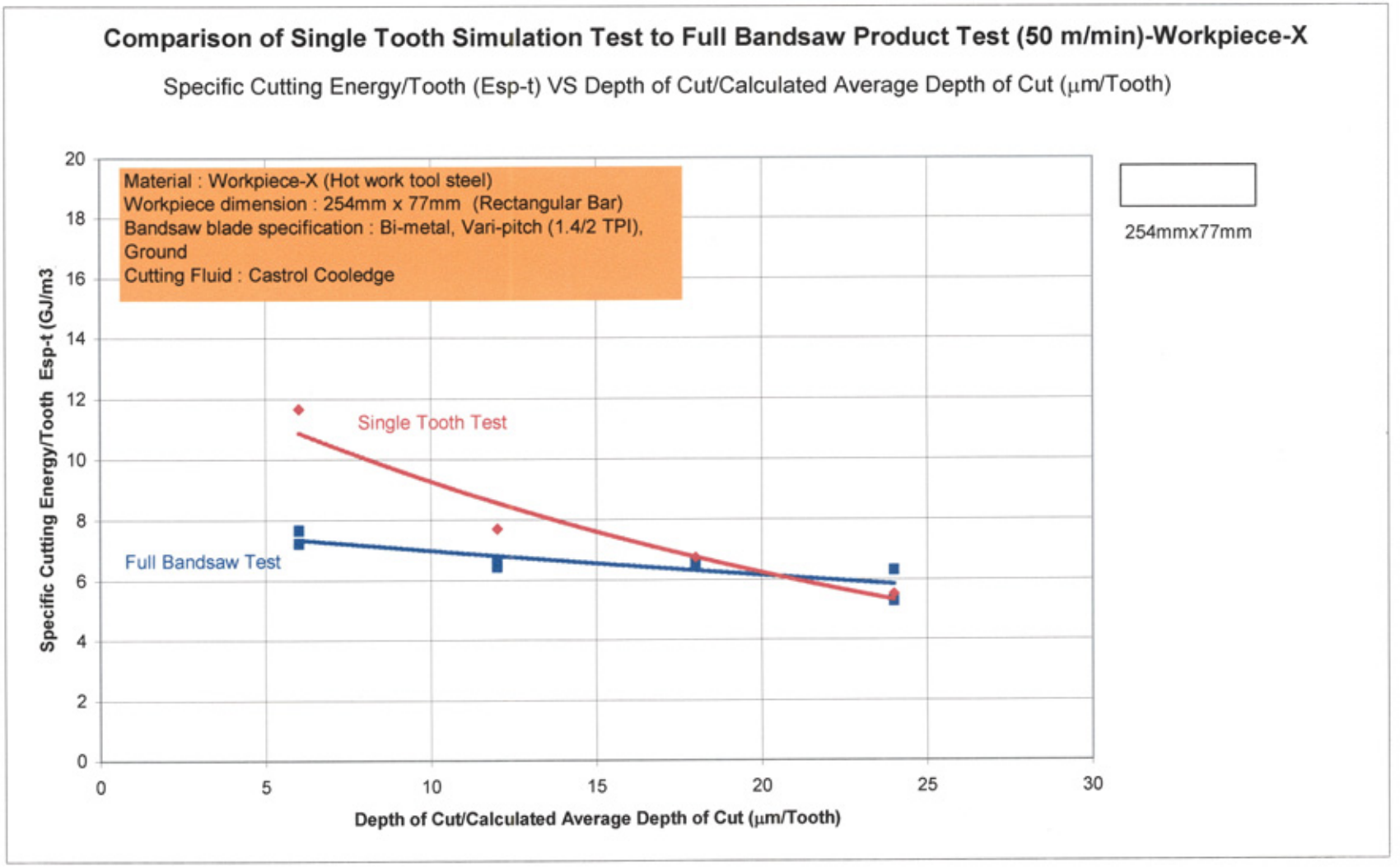

Figure 106 Comparison of E_{sp} values obtained from simulation test to full bandsaw product test at 31 m/min

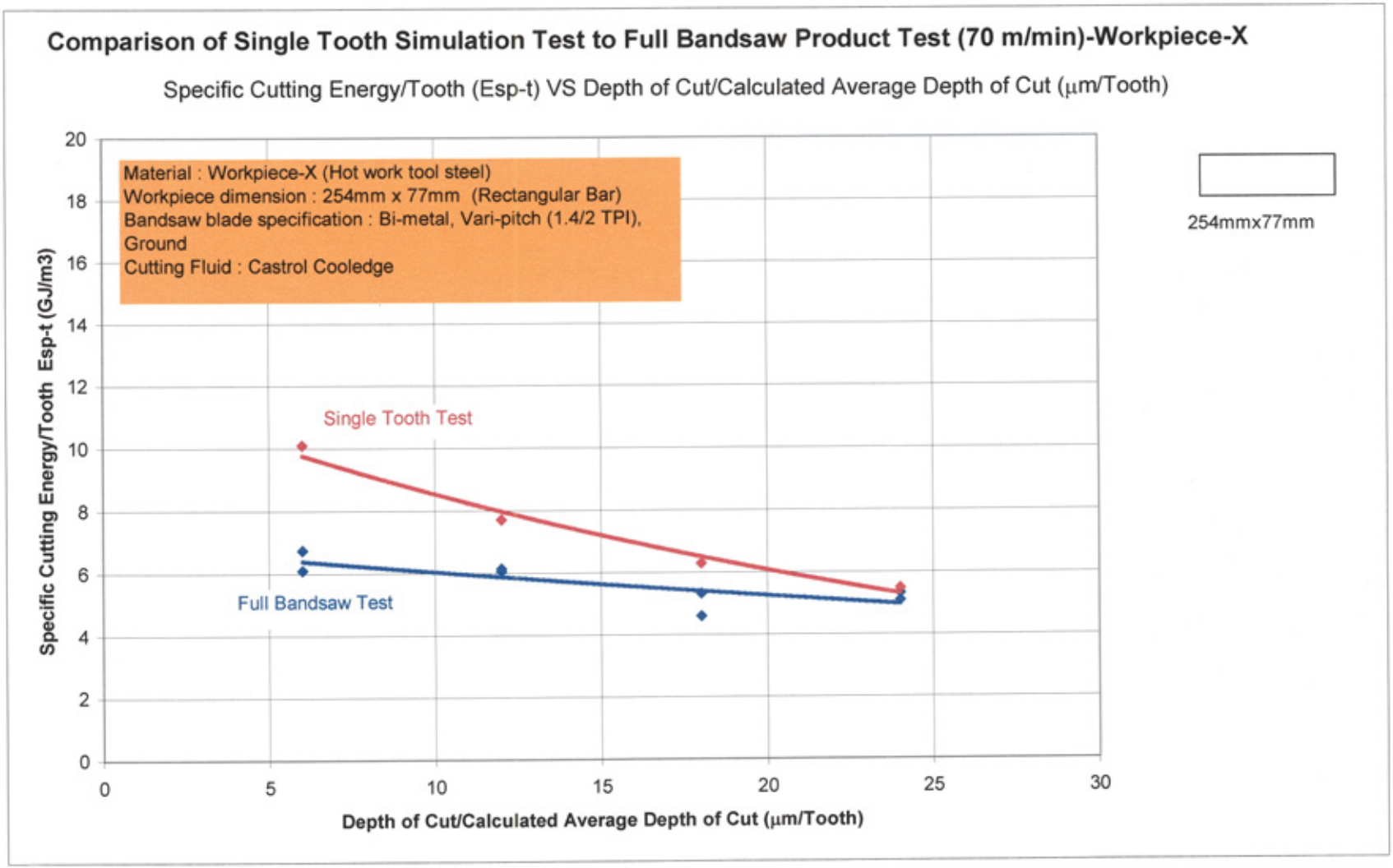

Figure 107 Comparison of E_{sp} values obtained from simulation test to full bandsaw product test at 70

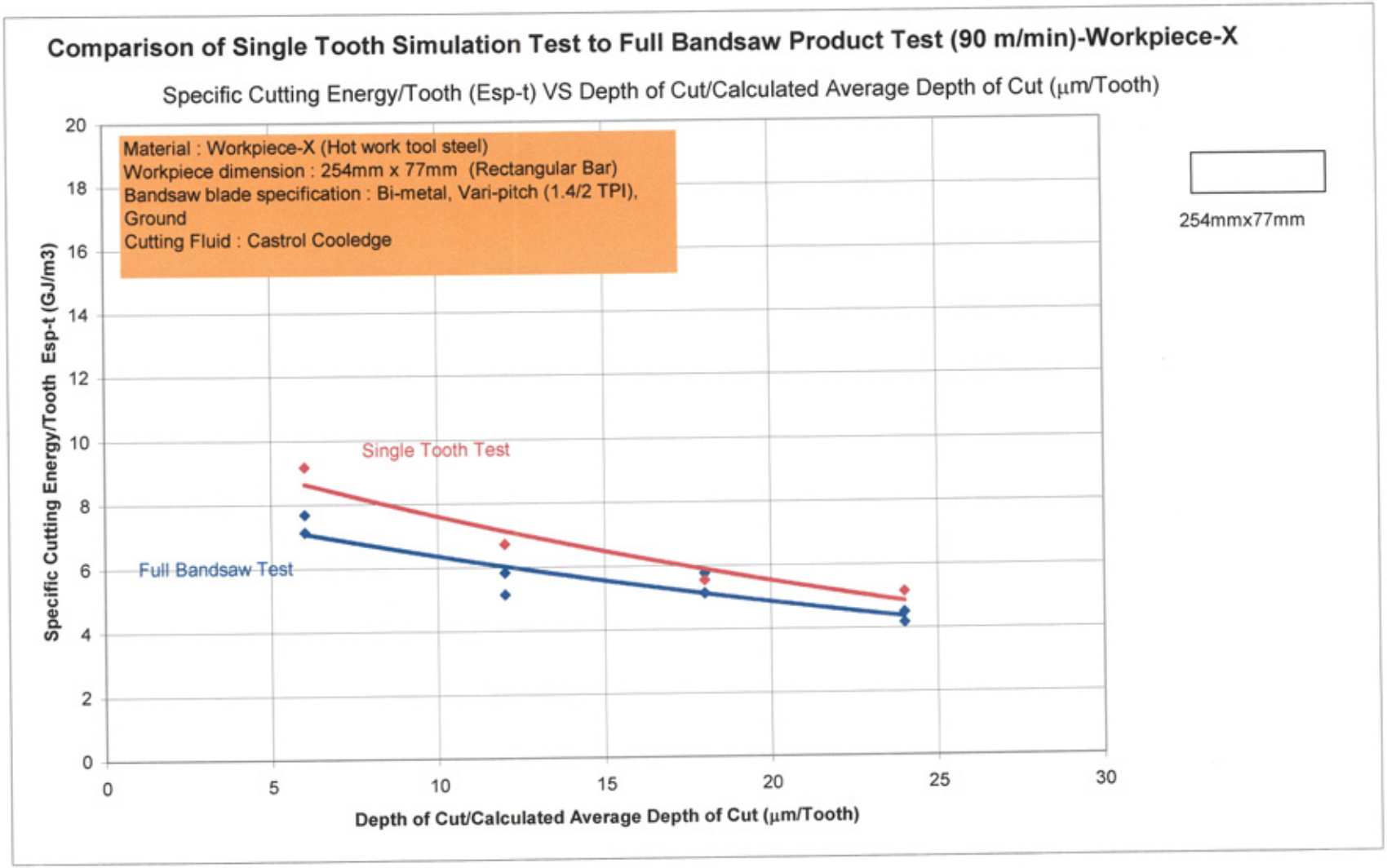

Figure 108 Comparison of E_{sp} values obtained from simulation test to full bandsaw product test at 90 m/min

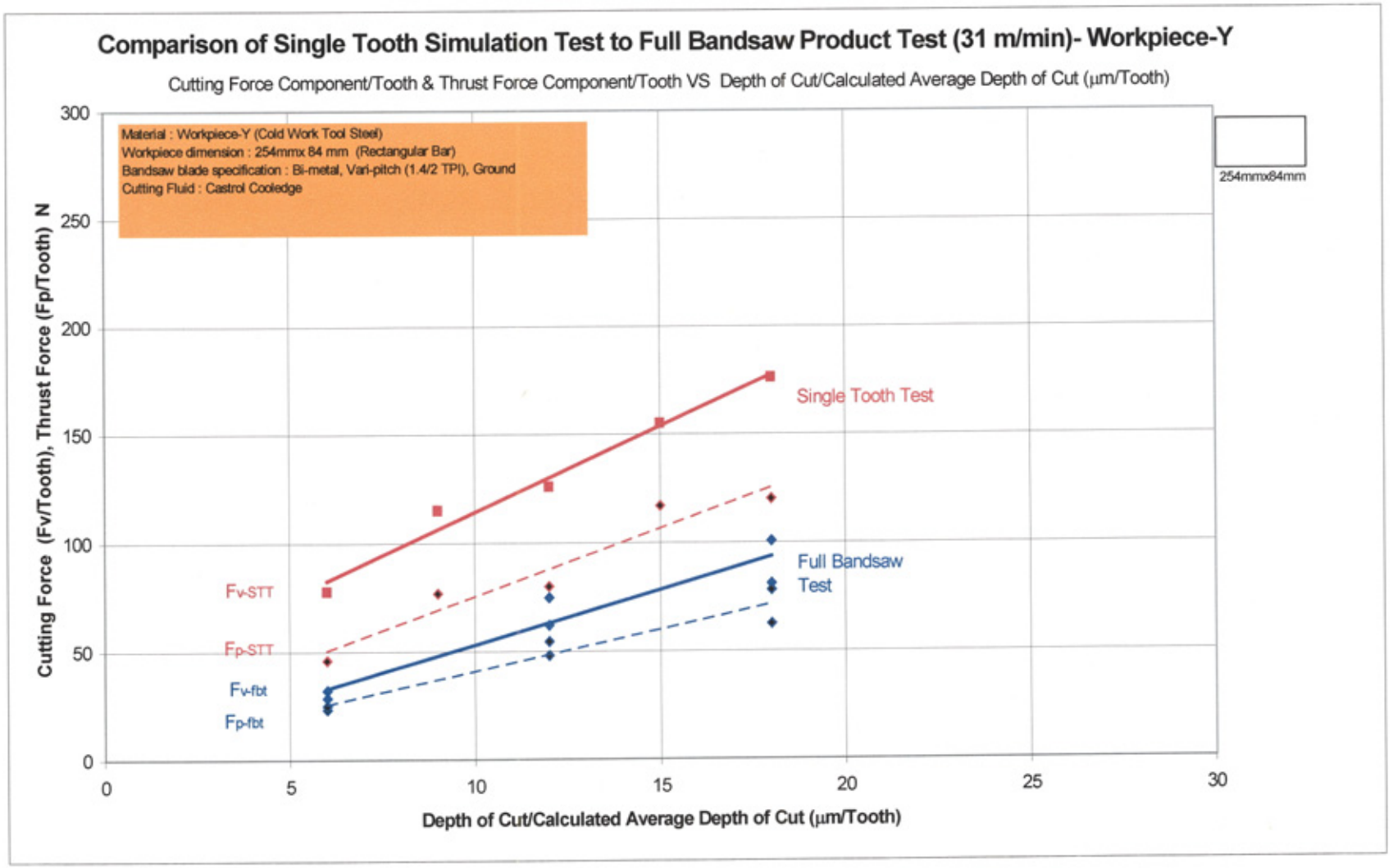

Figure 109 Comparison of single tooth simulation test to full bandsaw product test (31 m/min)- Workpiece-Y

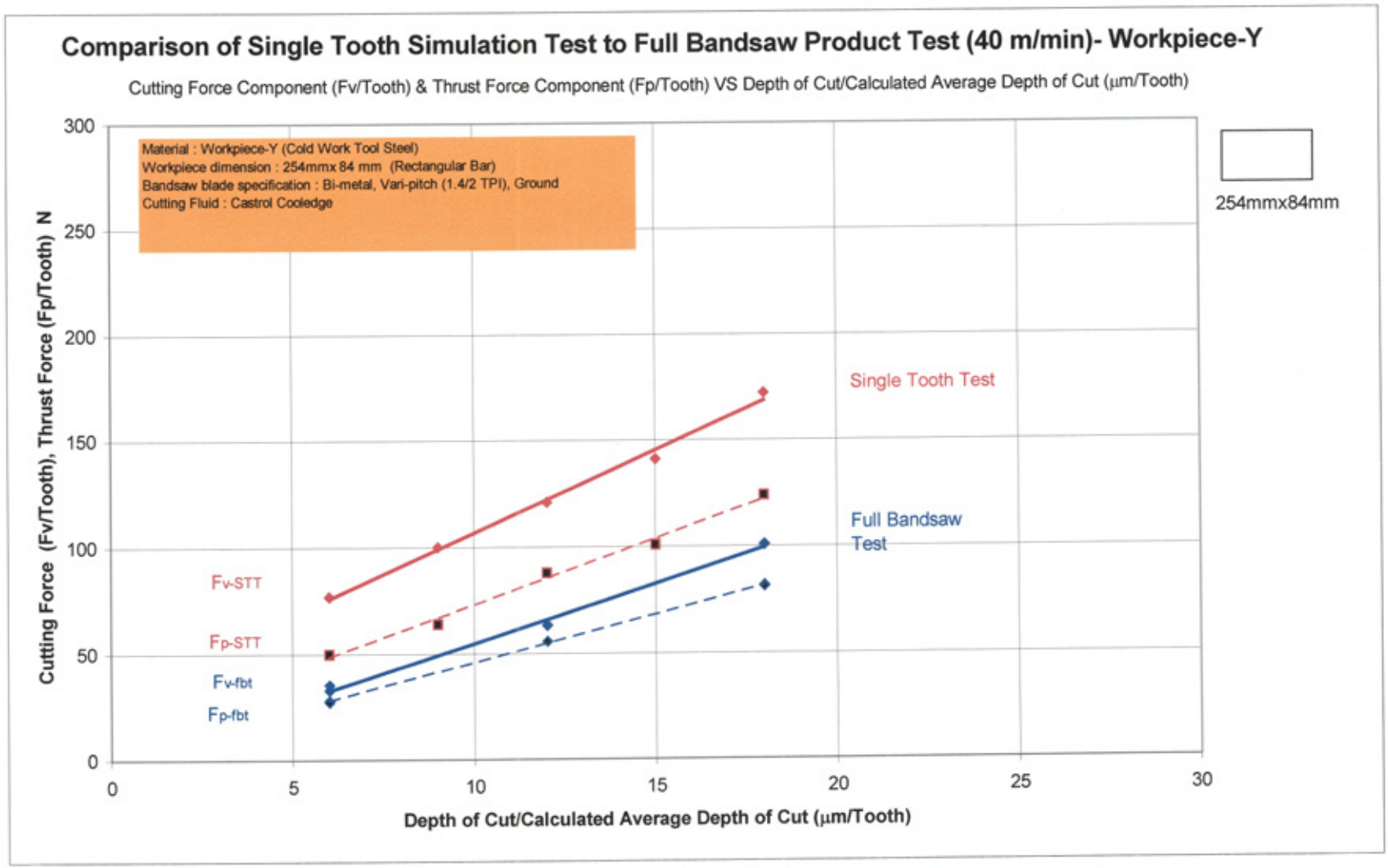

Figure 110 Comparison of single tooth simulation test to full bandsaw product test (40 m/min)- Workpiece-Y

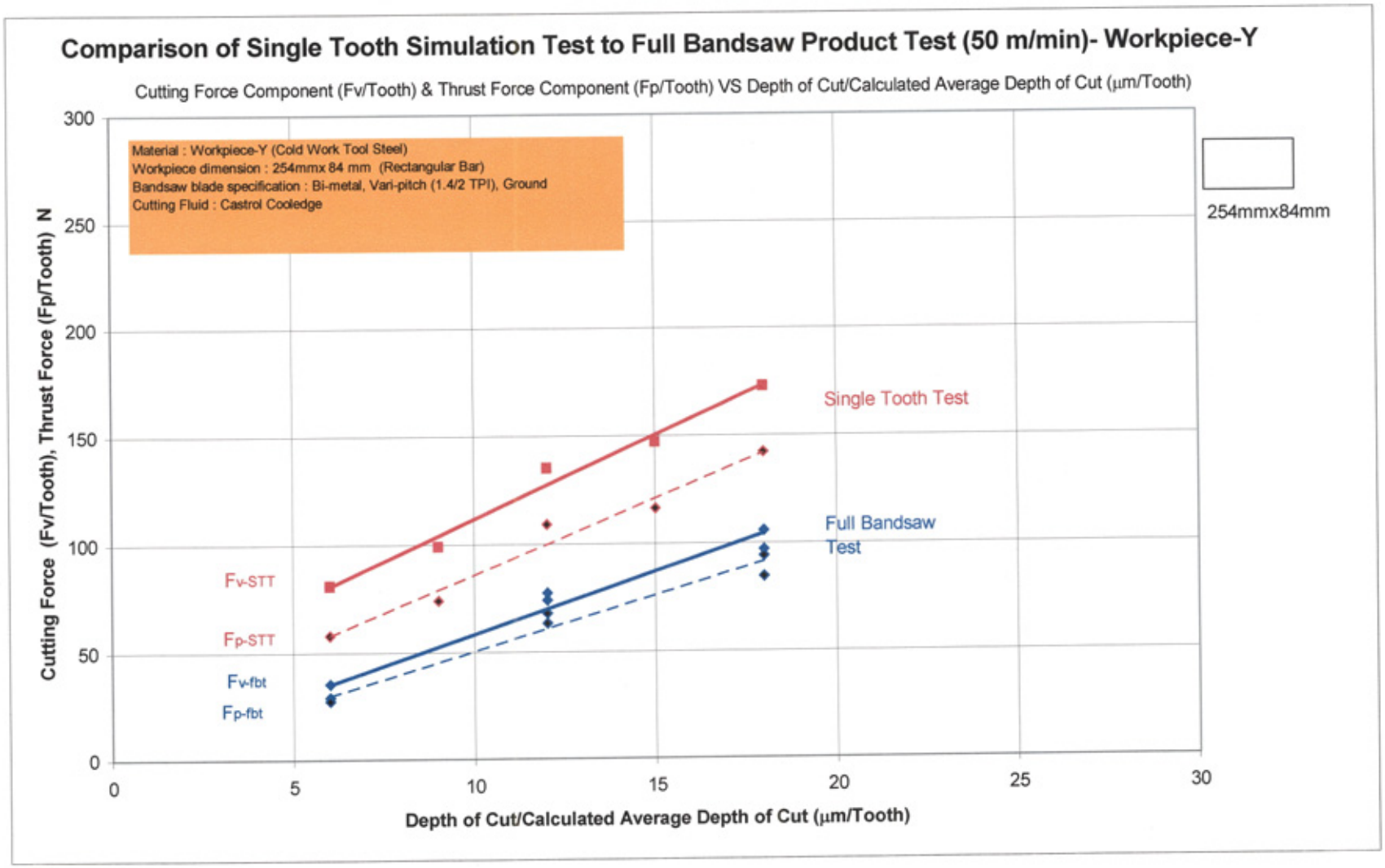

Figure 111 Comparison of single tooth simulation test to full bandsaw product test (50 m/min)- Workpiece-Y

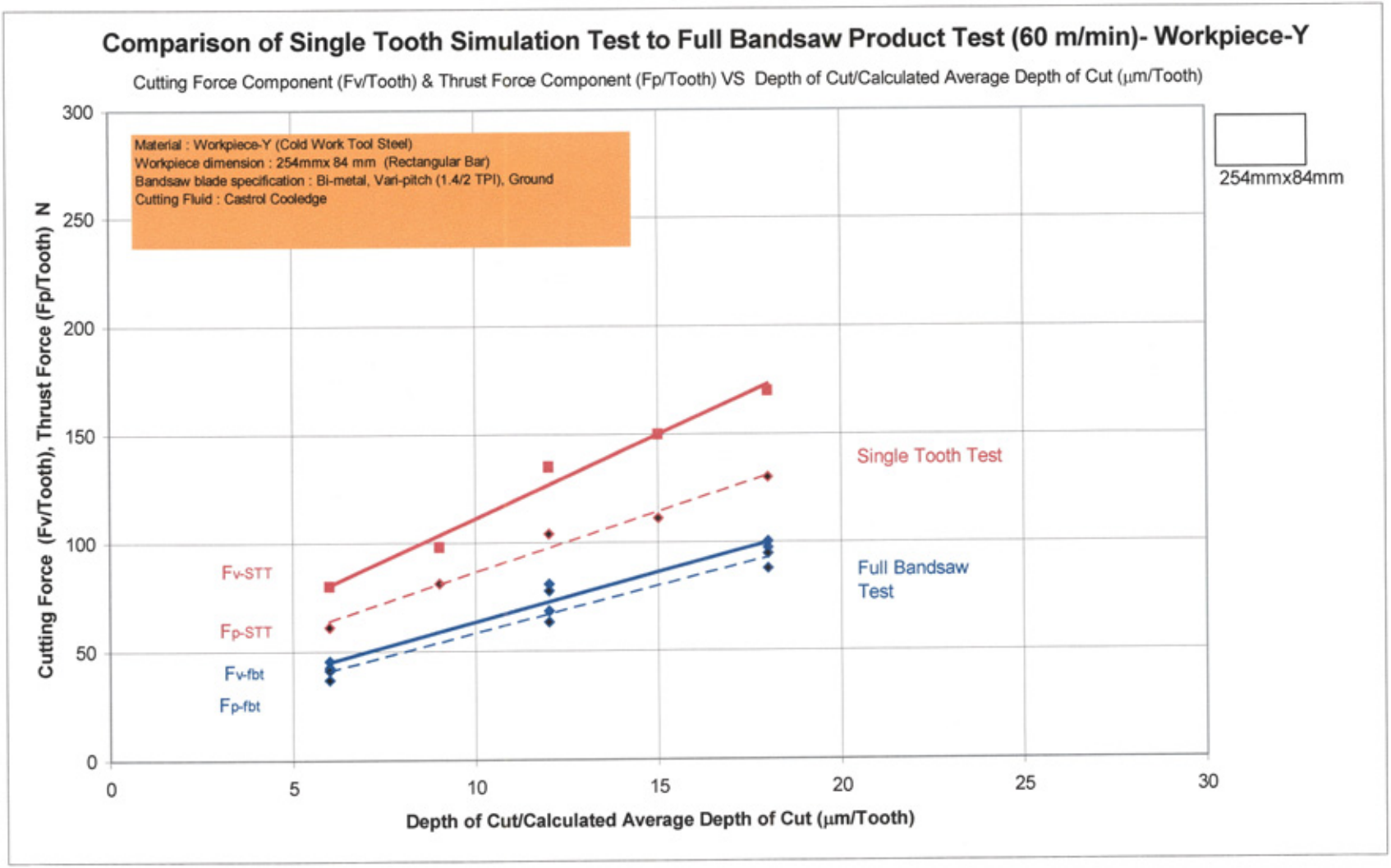

Figure 112 Comparison of single tooth simulation test to full bandsaw product test (60 m/min)- Workpiece-Y

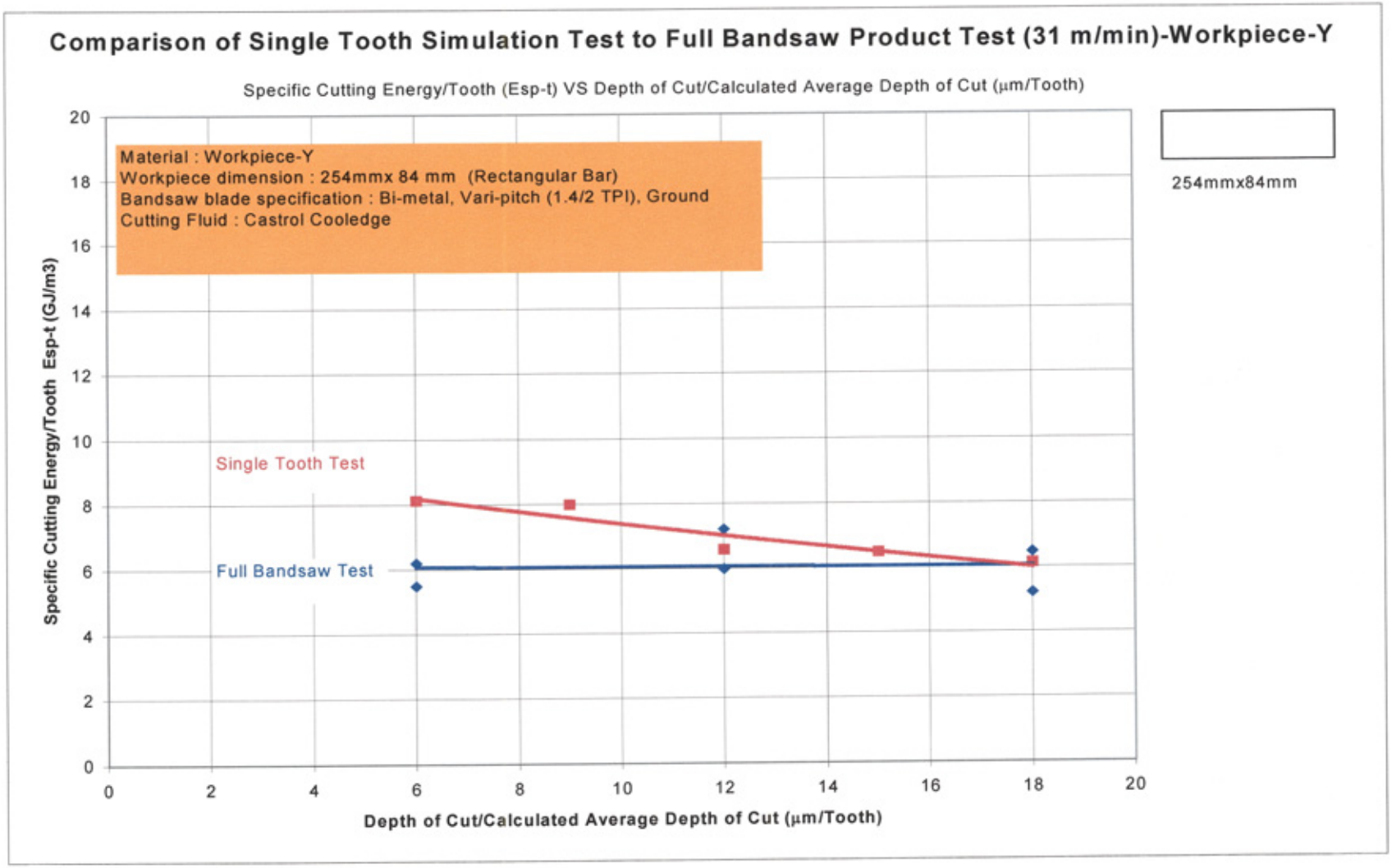

Figure 113 Comparison of E_{sp} values obtained from simulation test to full bandsaw product test at 31 m/min

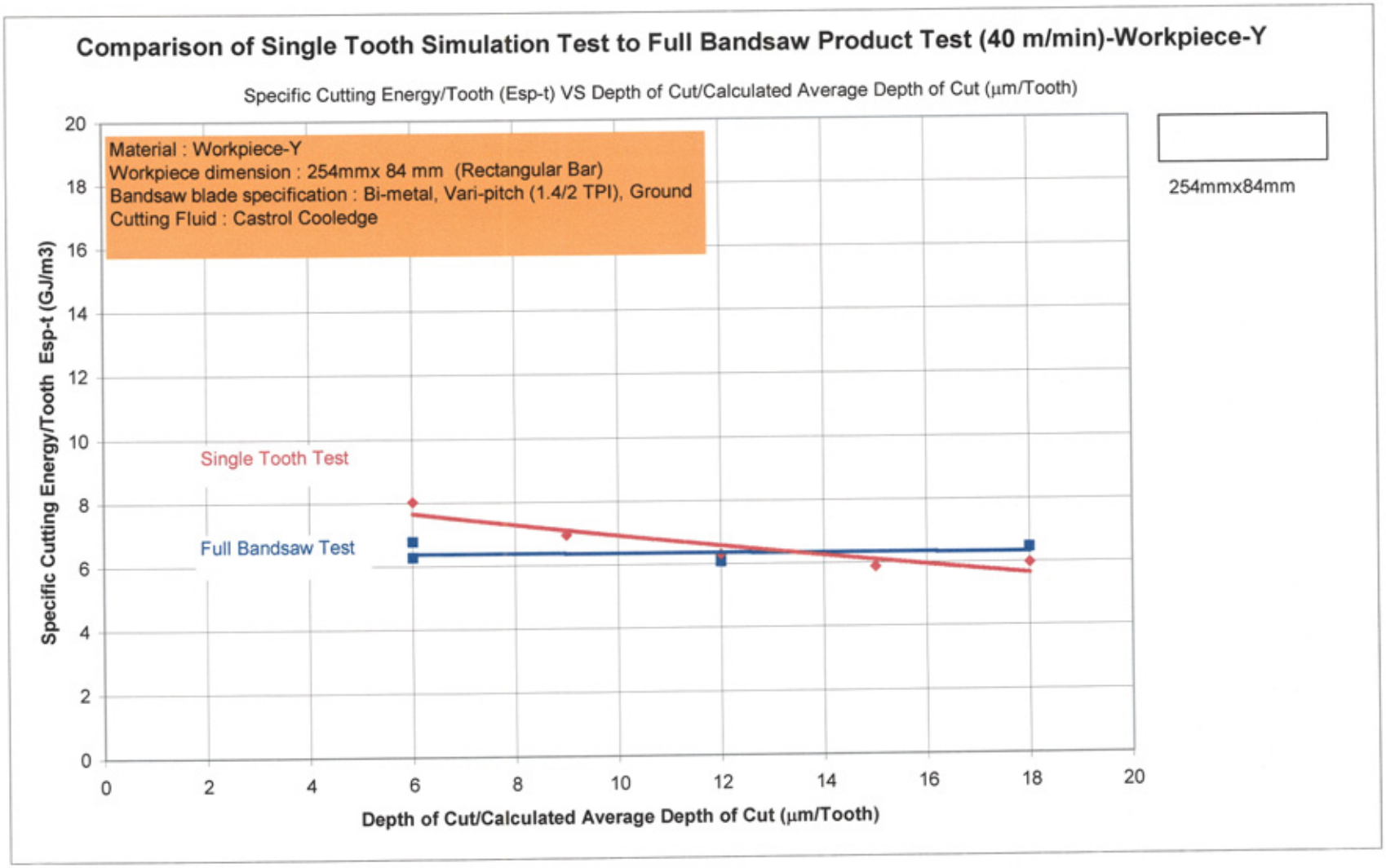

Figure 114 Comparison of E_{sp} values obtained from simulation test to full bandsaw product test at 40 m/min

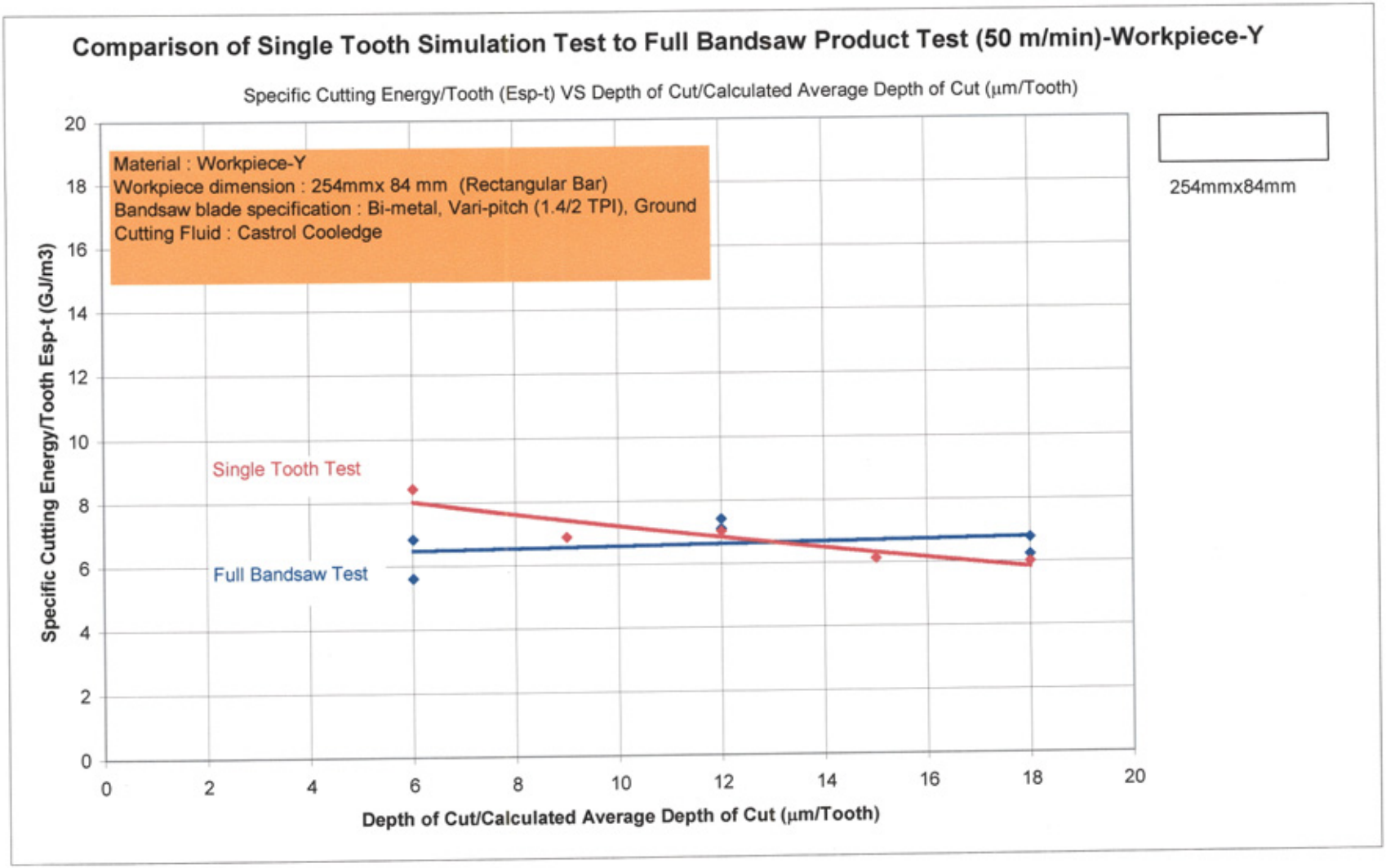

Figure 115 Comparison of E_{sp} values obtained from simulation test to full bandsaw product test at 50 m/min

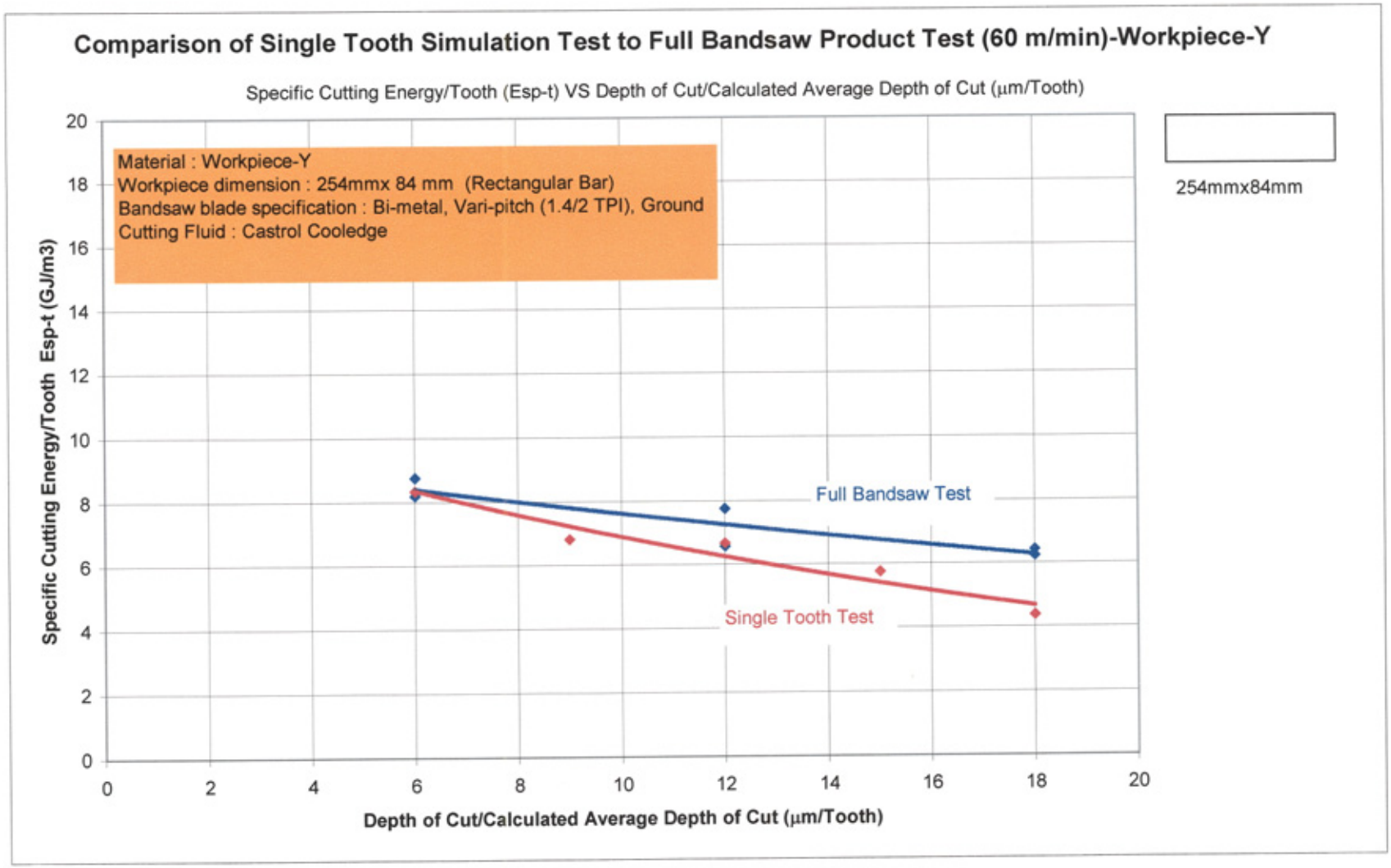

Figure 116 Comparison of E_{sp} values obtained from simulation test to full bandsaw product test at 60 m/min

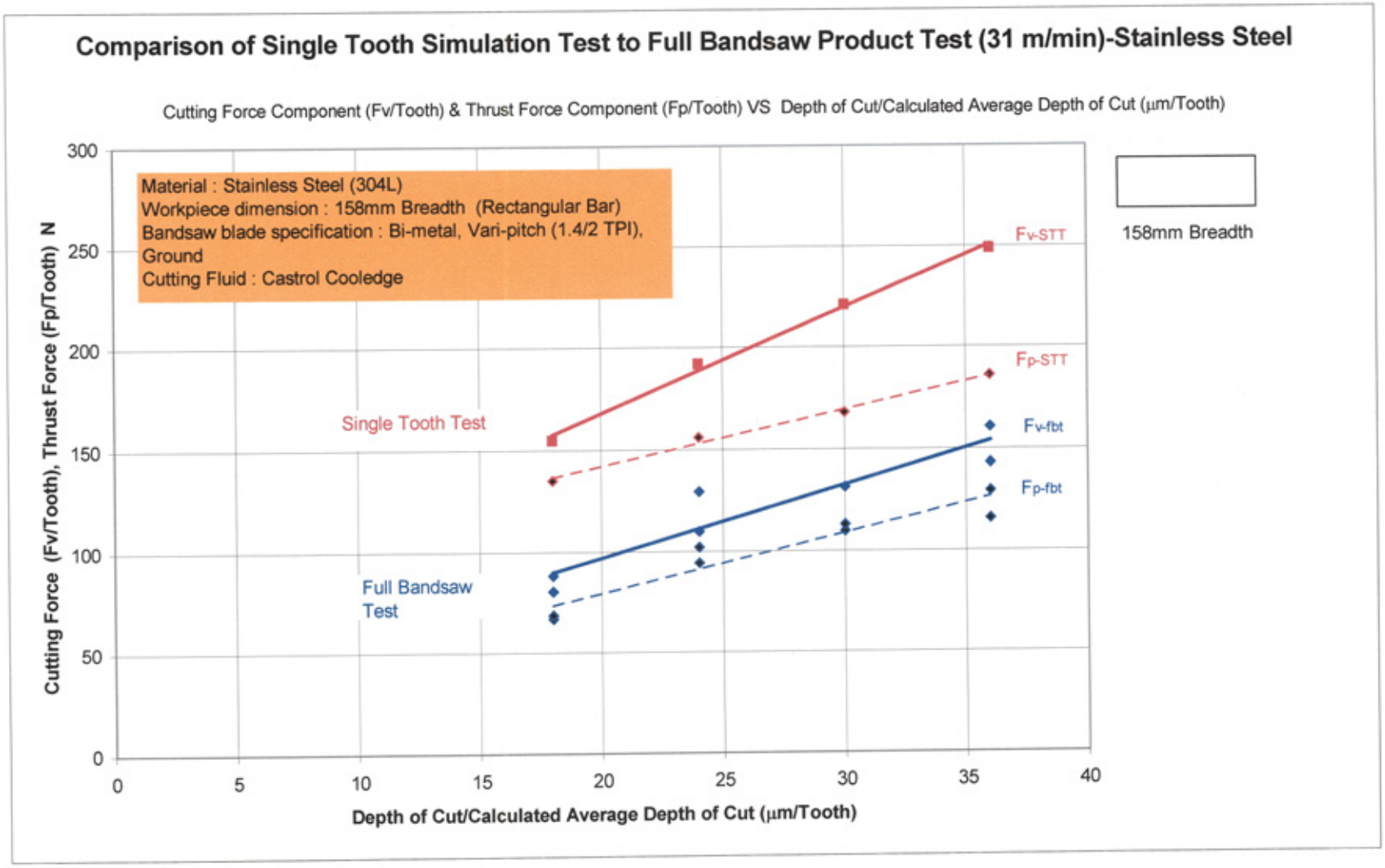

Figure 117 Comparison of single tooth simulation test to full bandsaw product test (31 m/min)-Stainless Steel

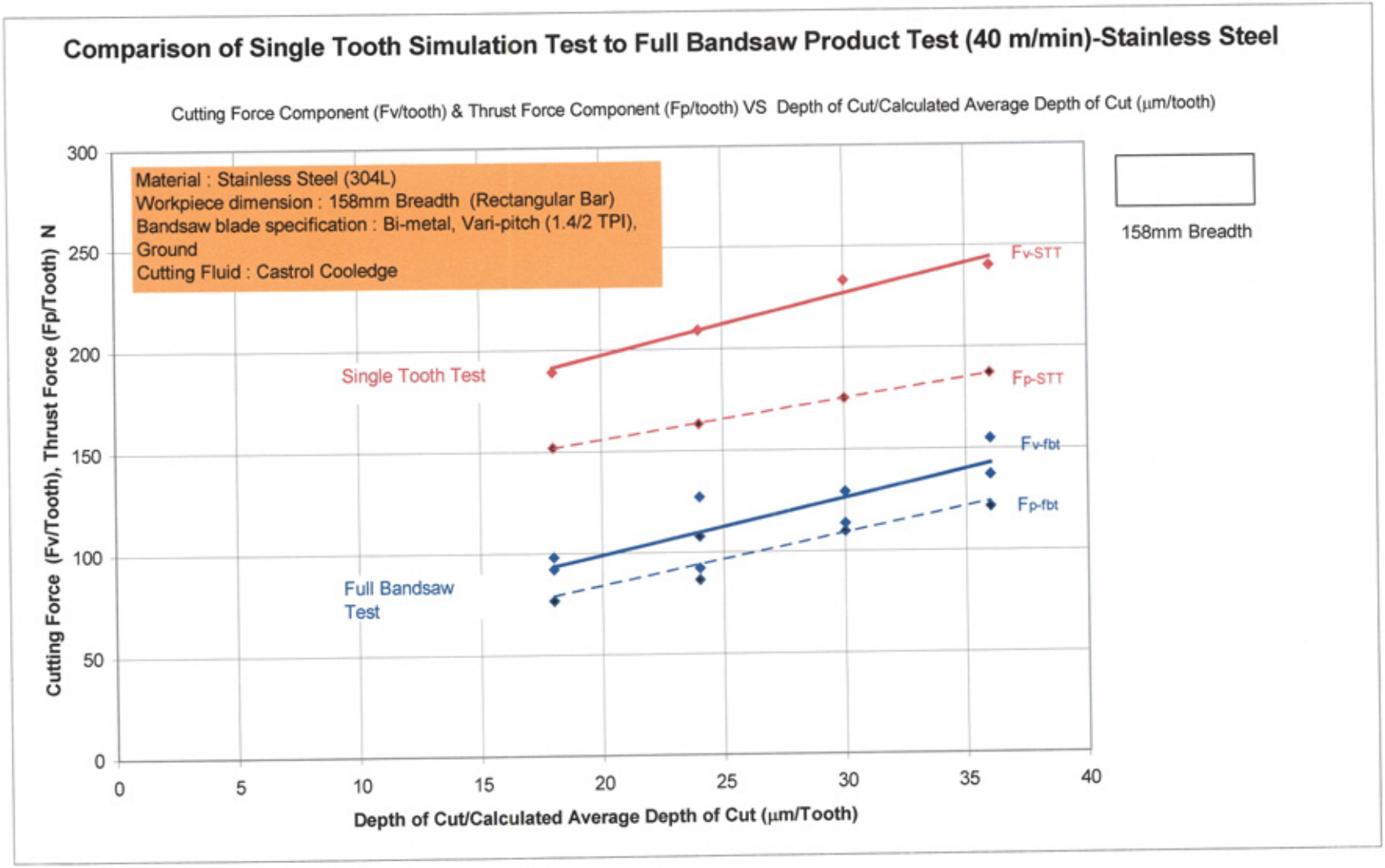

Figure 118 Comparison of single tooth simulation test to full bandsaw product test (40 m/min)-Stainless Steel

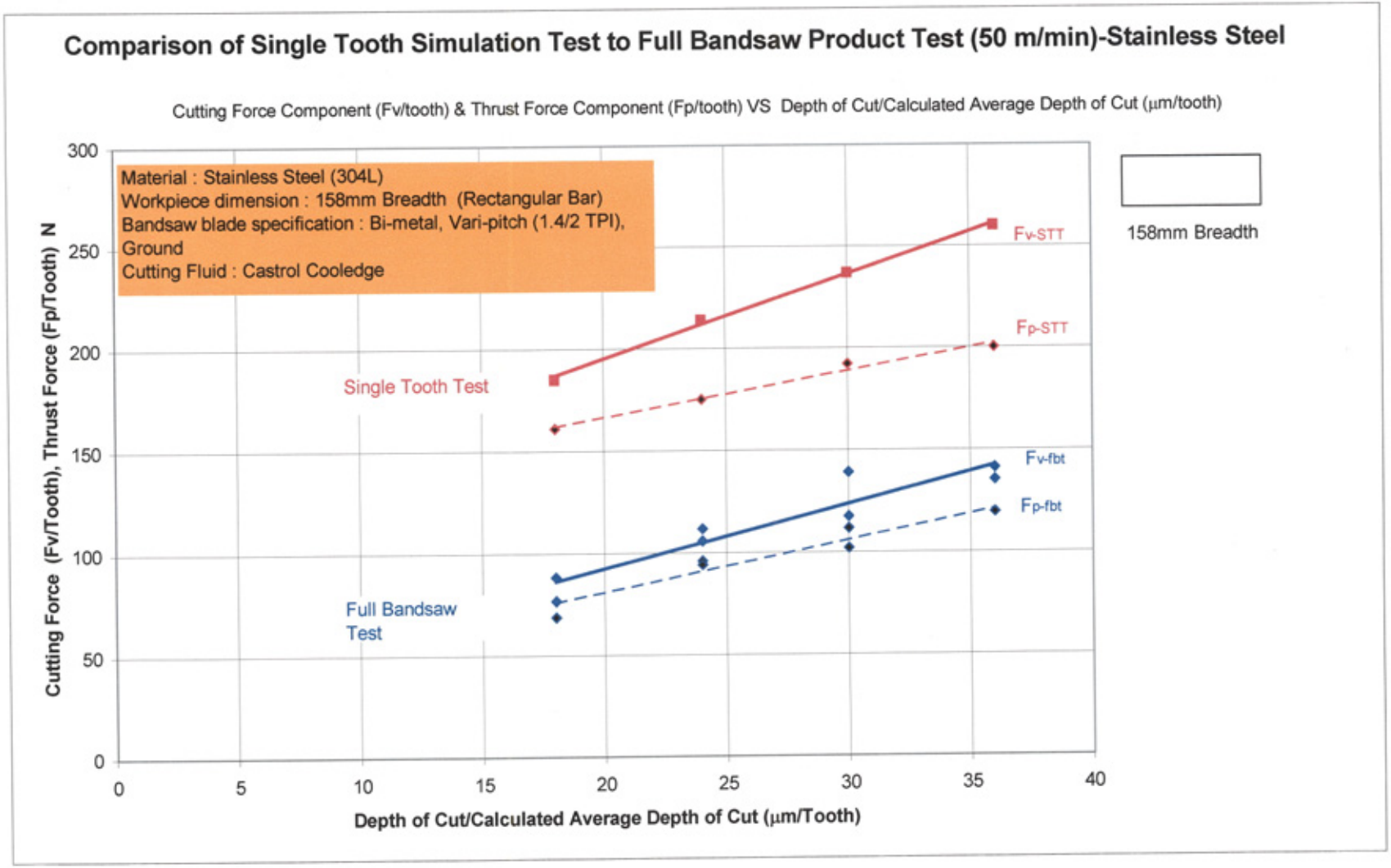

Figure 119 Comparison of single tooth simulation test to full bandsaw product test (50 m/min)-Stainless Steel

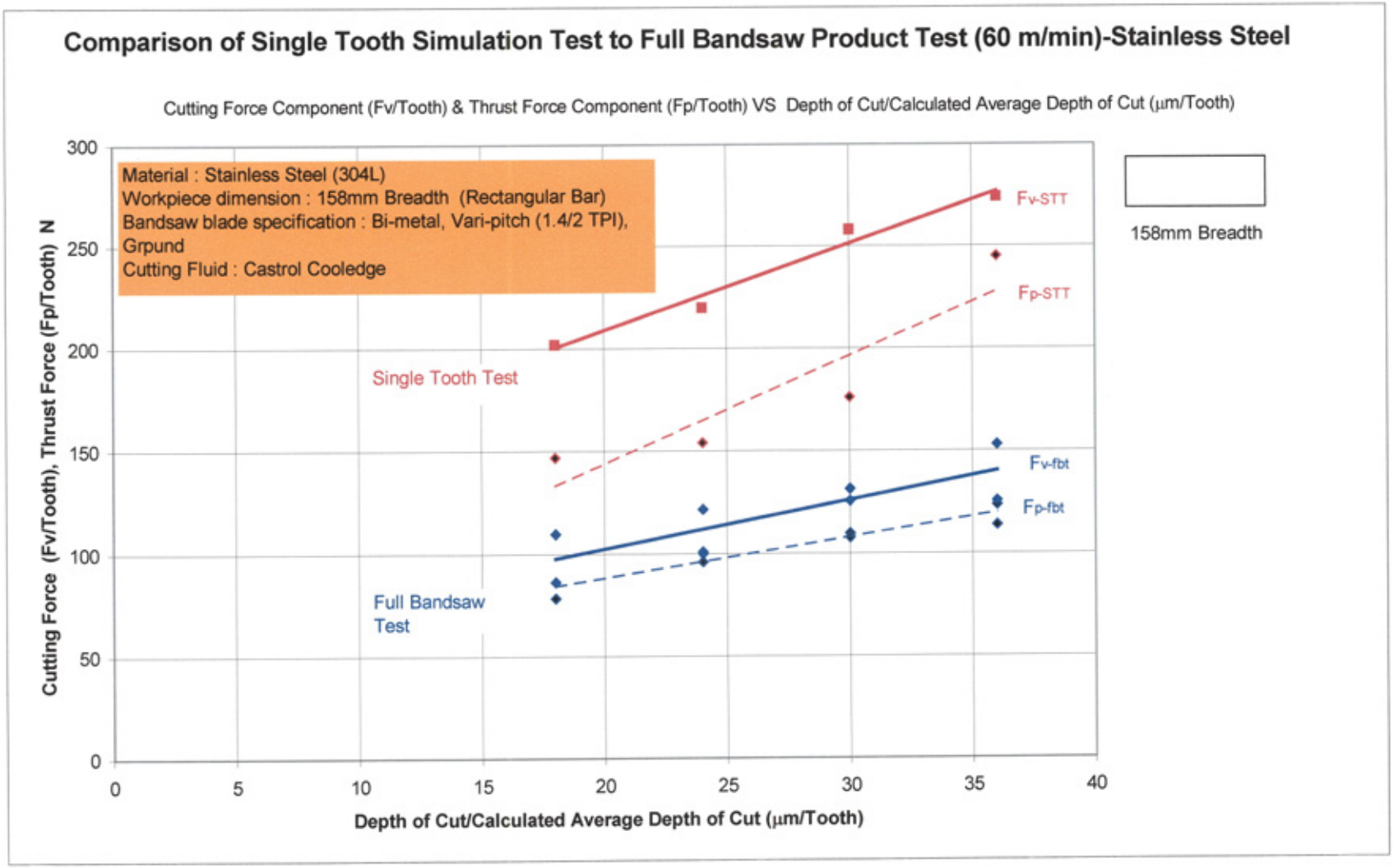

Figure 120 Comparison of single tooth simulation test to full bandsaw product test (60 m/min)-Stainless Steel

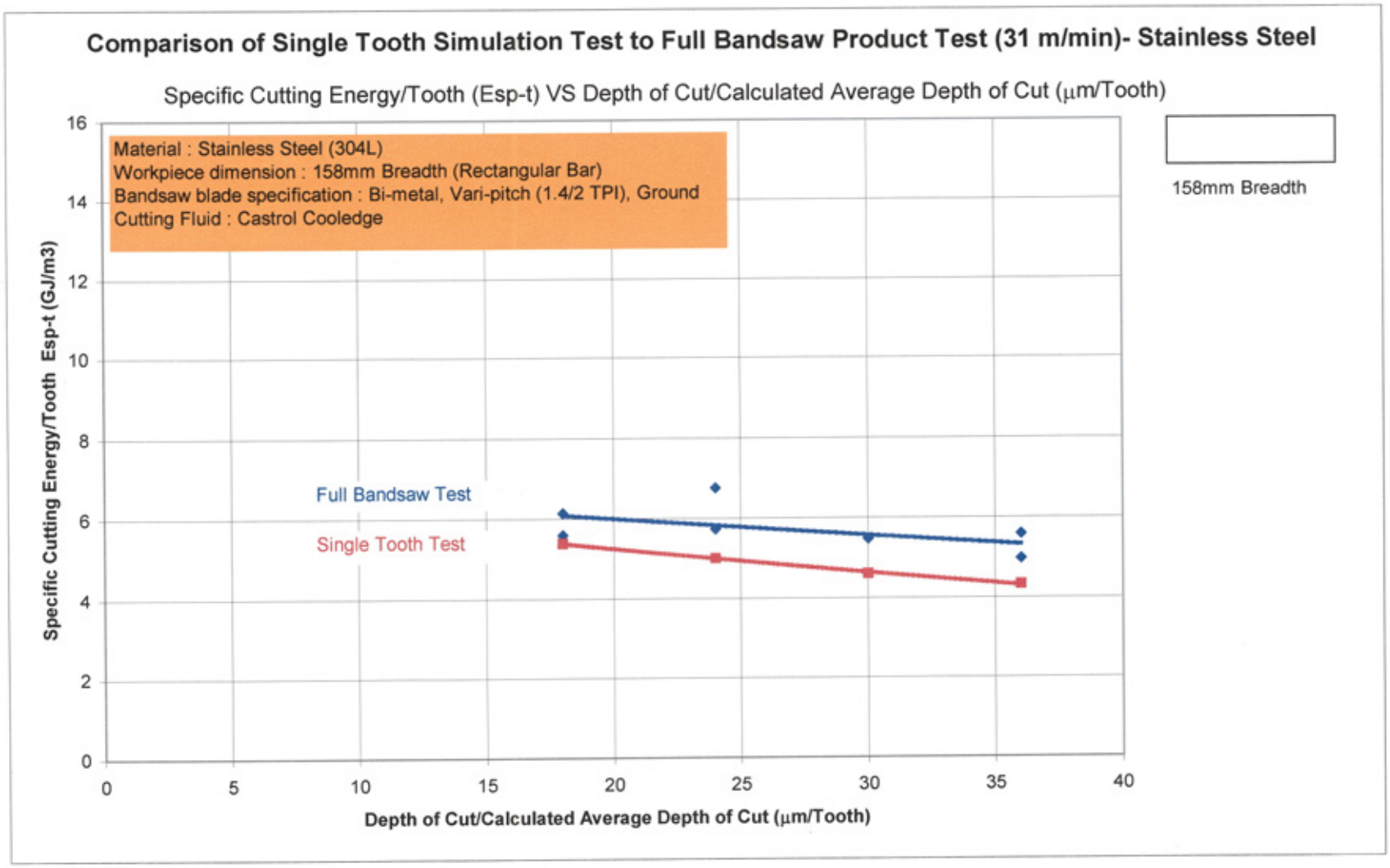

Figure 121 Comparison of E_{sp} values obtained from simulation test to full bandsaw product test at 31 m/min

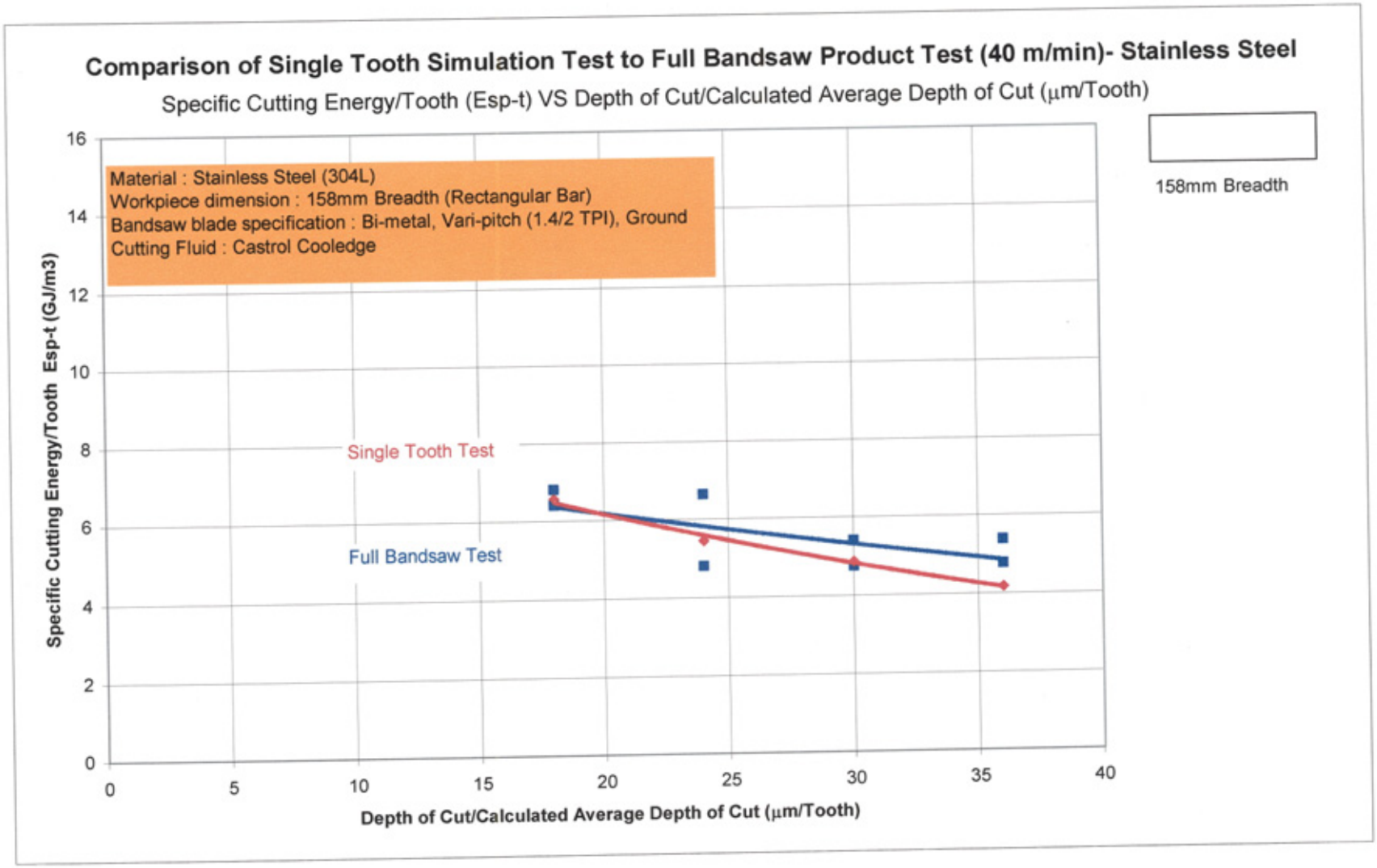

Figure 122 Comparison of E_{sp} values obtained from simulation test to full bandsaw product test at 40 m/min

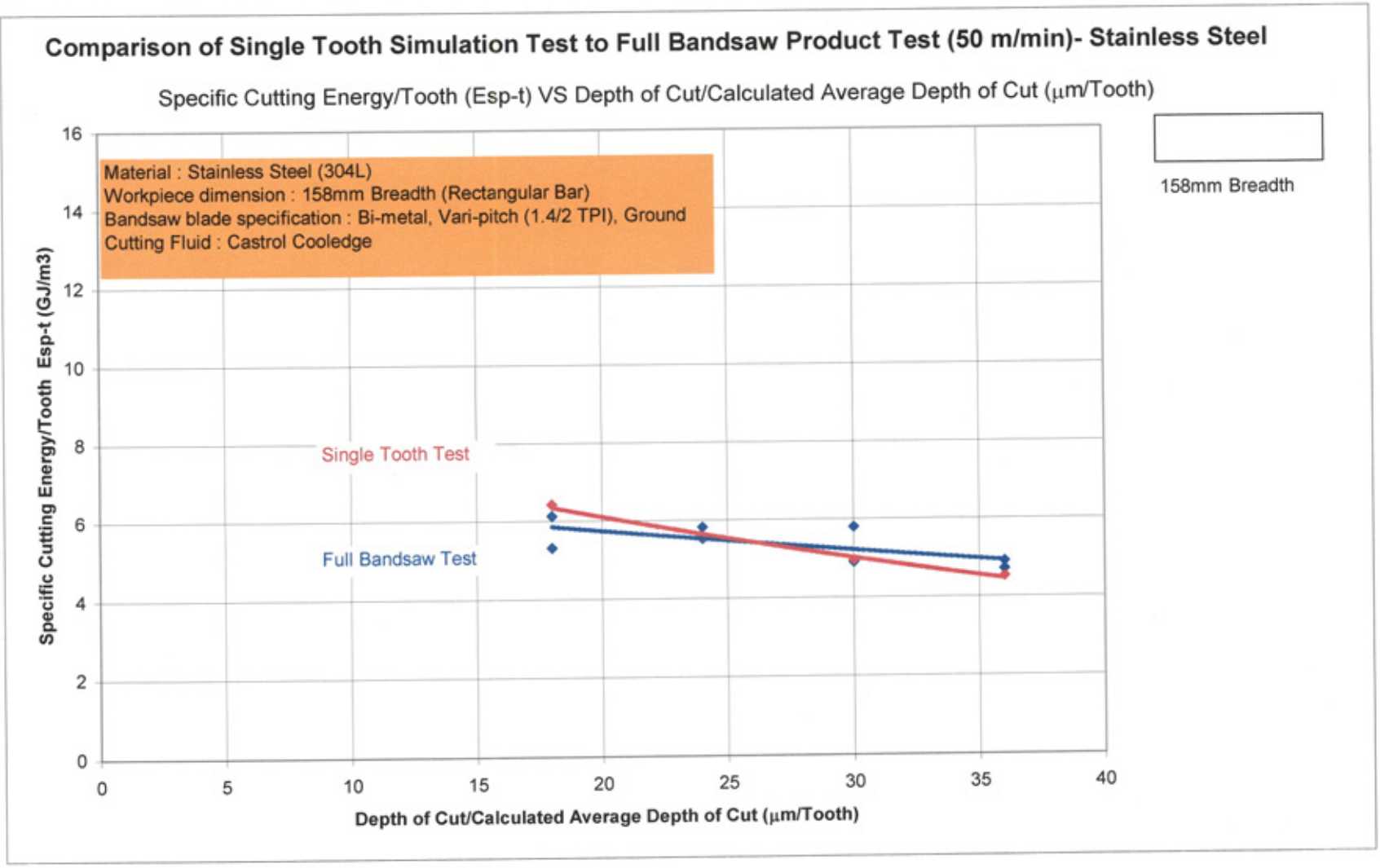

Figure 123 Comparison of E_{sp} values obtained from simulation test to full bandsaw product test at 50 m/min

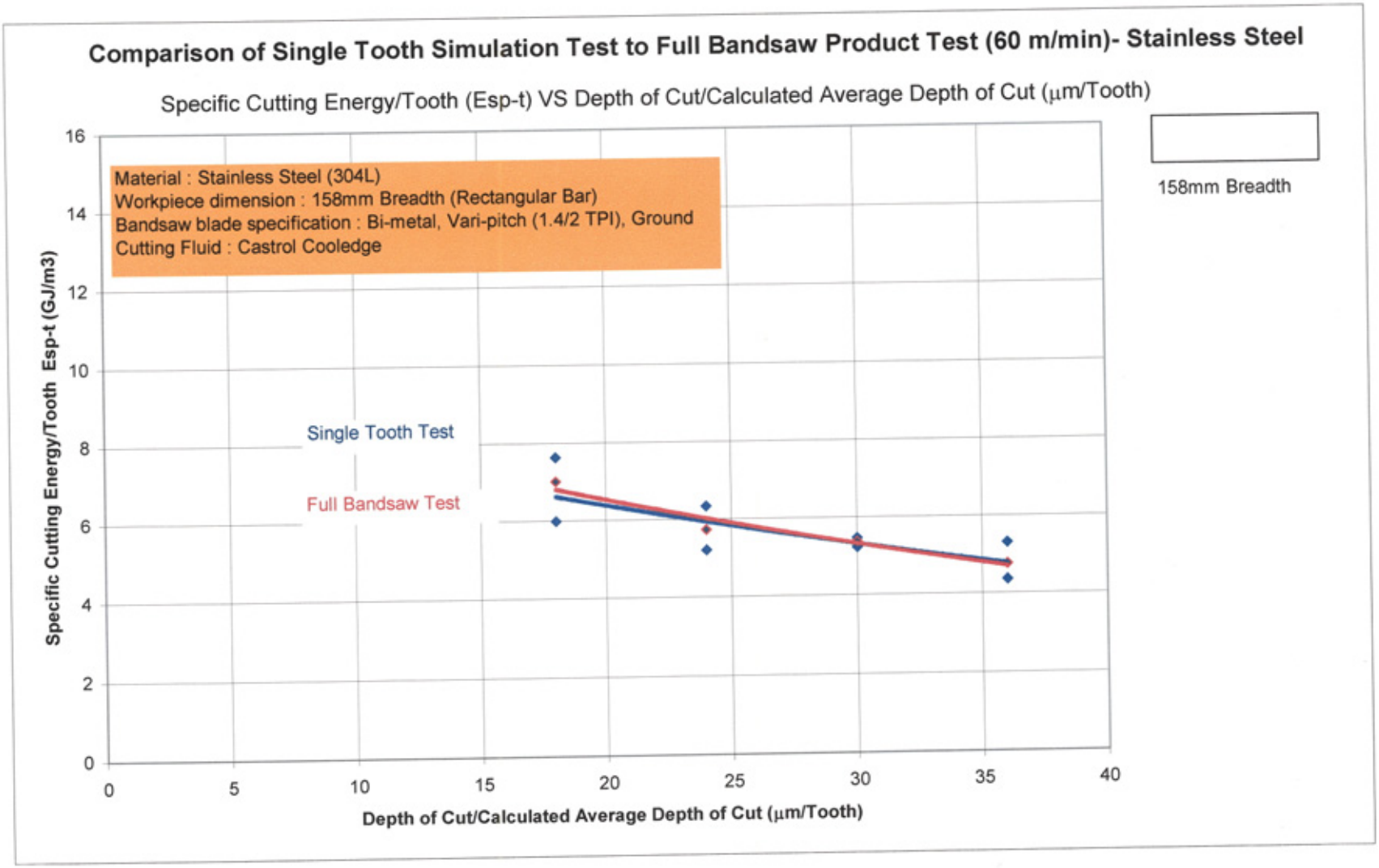

Figure 124 Comparison of E_{sp} values obtained from simulation test to full bandsaw product test at 60 m/min

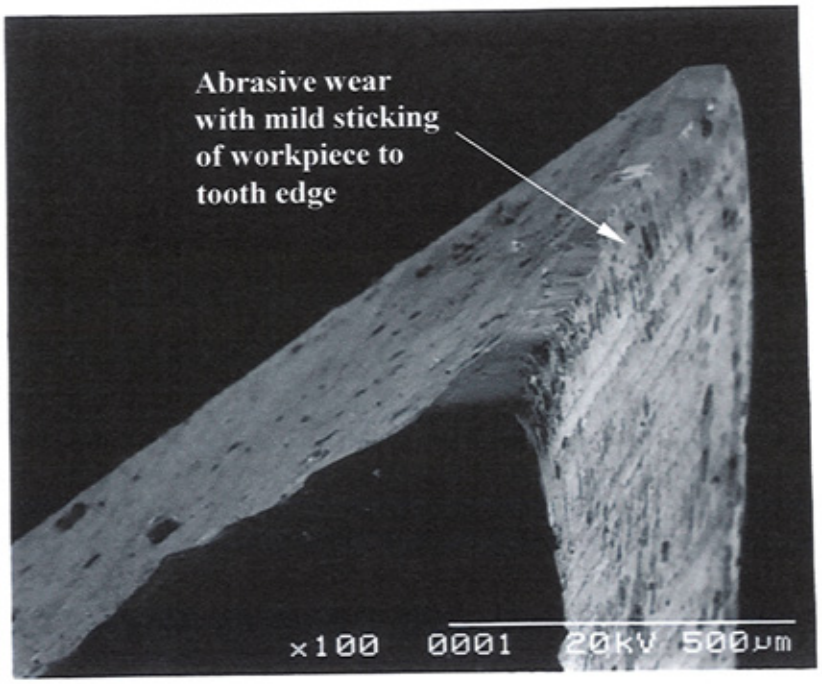

Figure 125 Photomicrograph of single tooth sample used for Stainless Steel

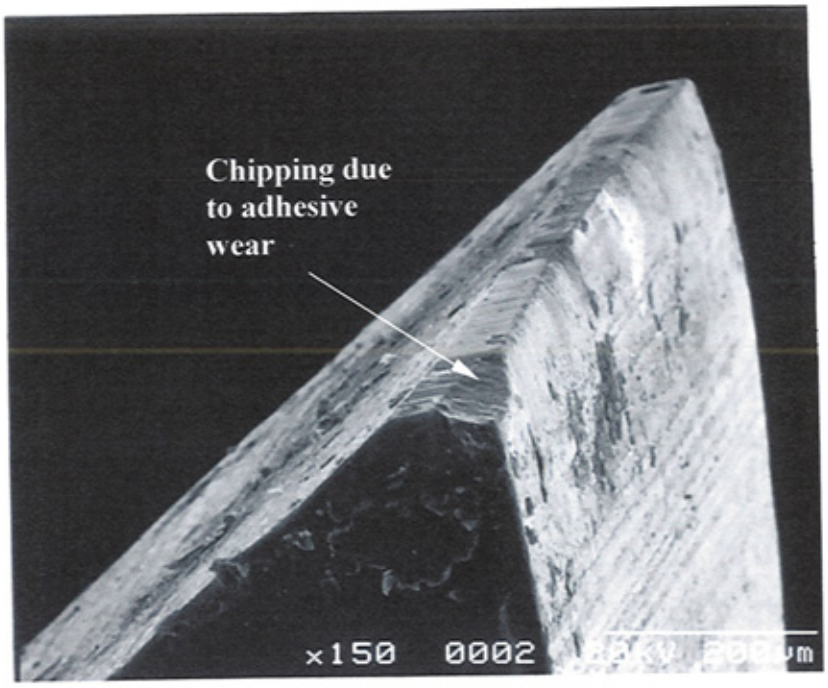

Figure 126 Photomicrograph of single tooth sample used for Workpiece-X

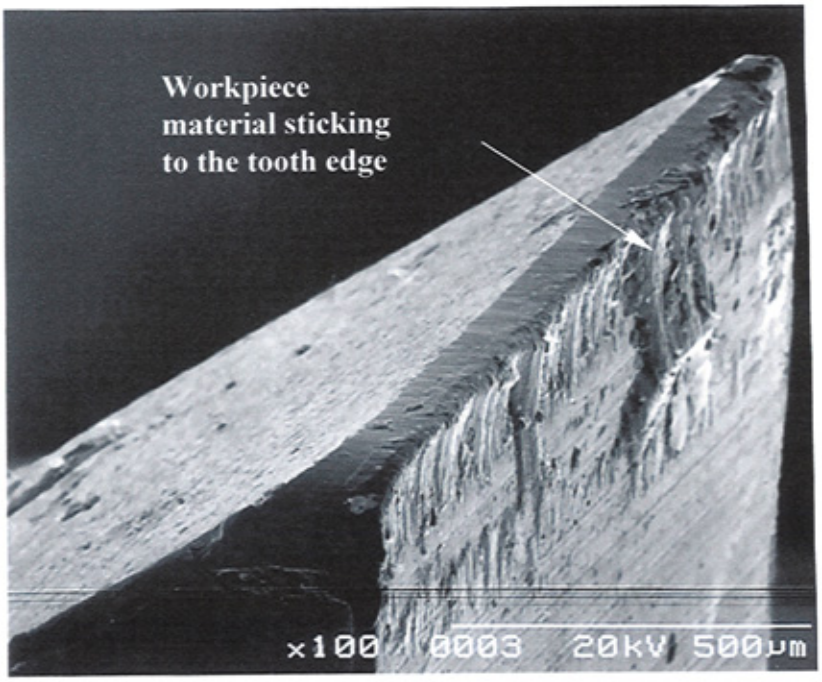

Figure 127 Photomicrograph of single tooth sample used for Workpiece-Y

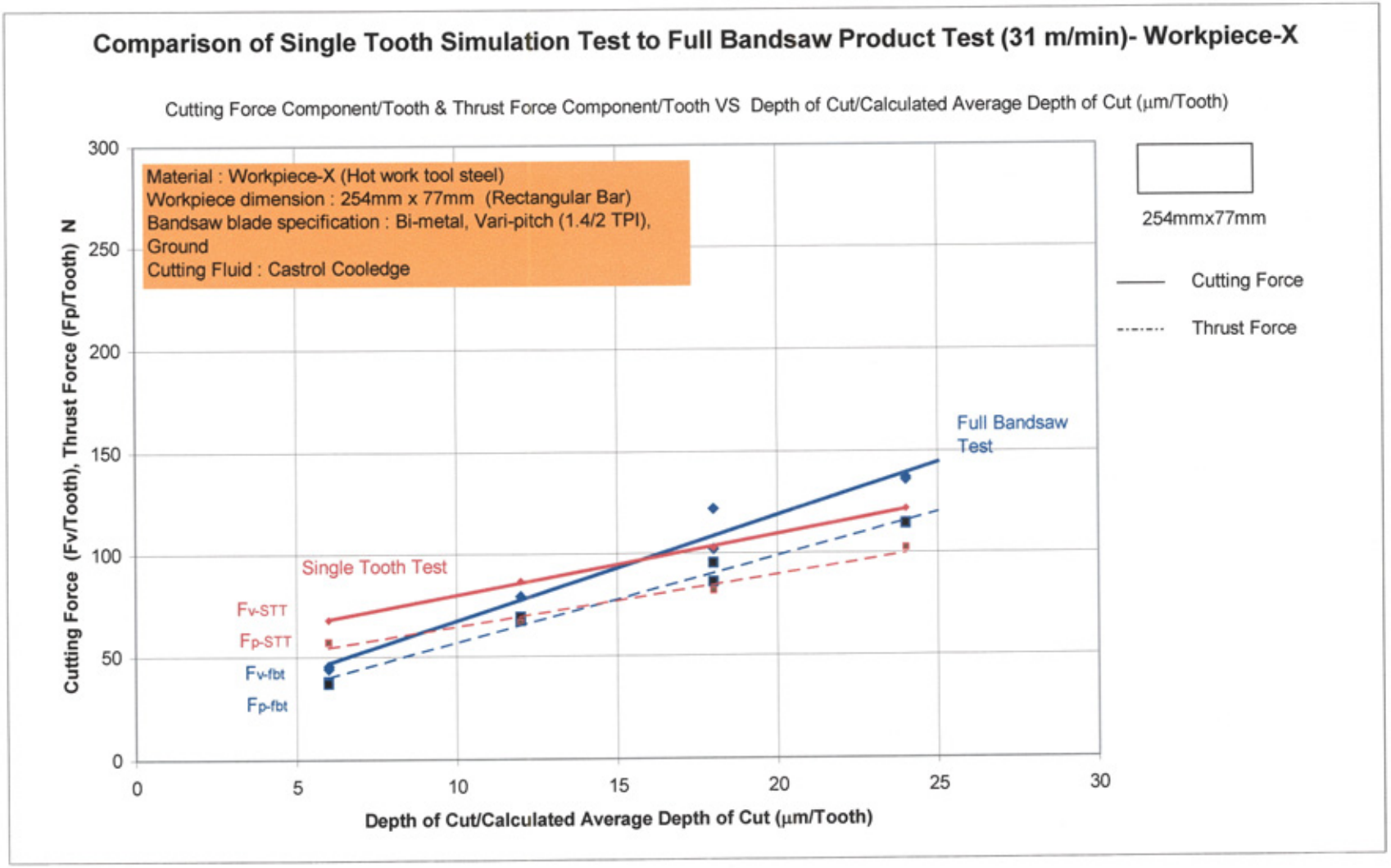

Figure 128 Validation of single tooth test results for Workpiece-X at 31 m/min using correction factor

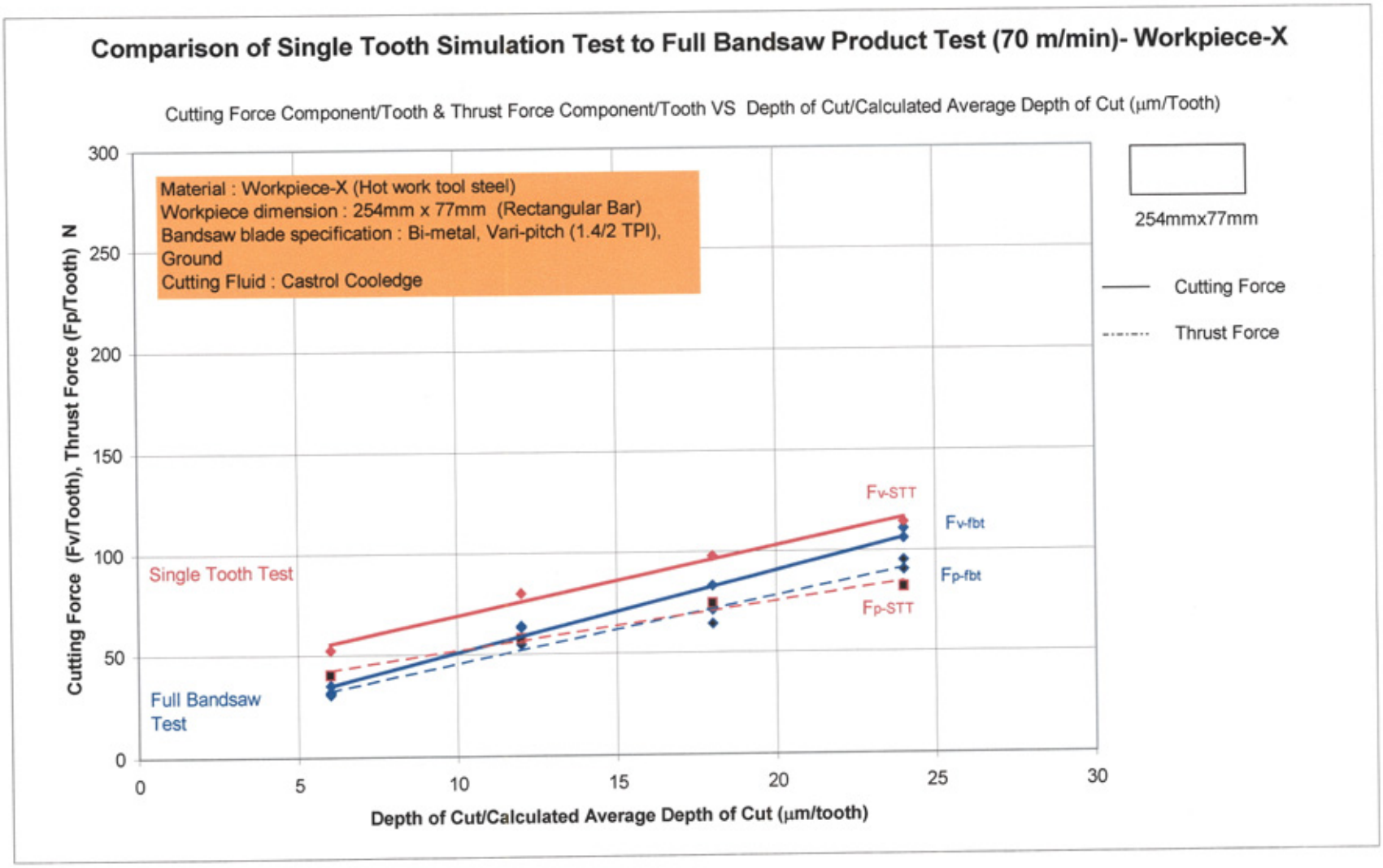

Figure 130 Validation of single tooth test results for Workpiece-X at 70 m/min, using correction factor

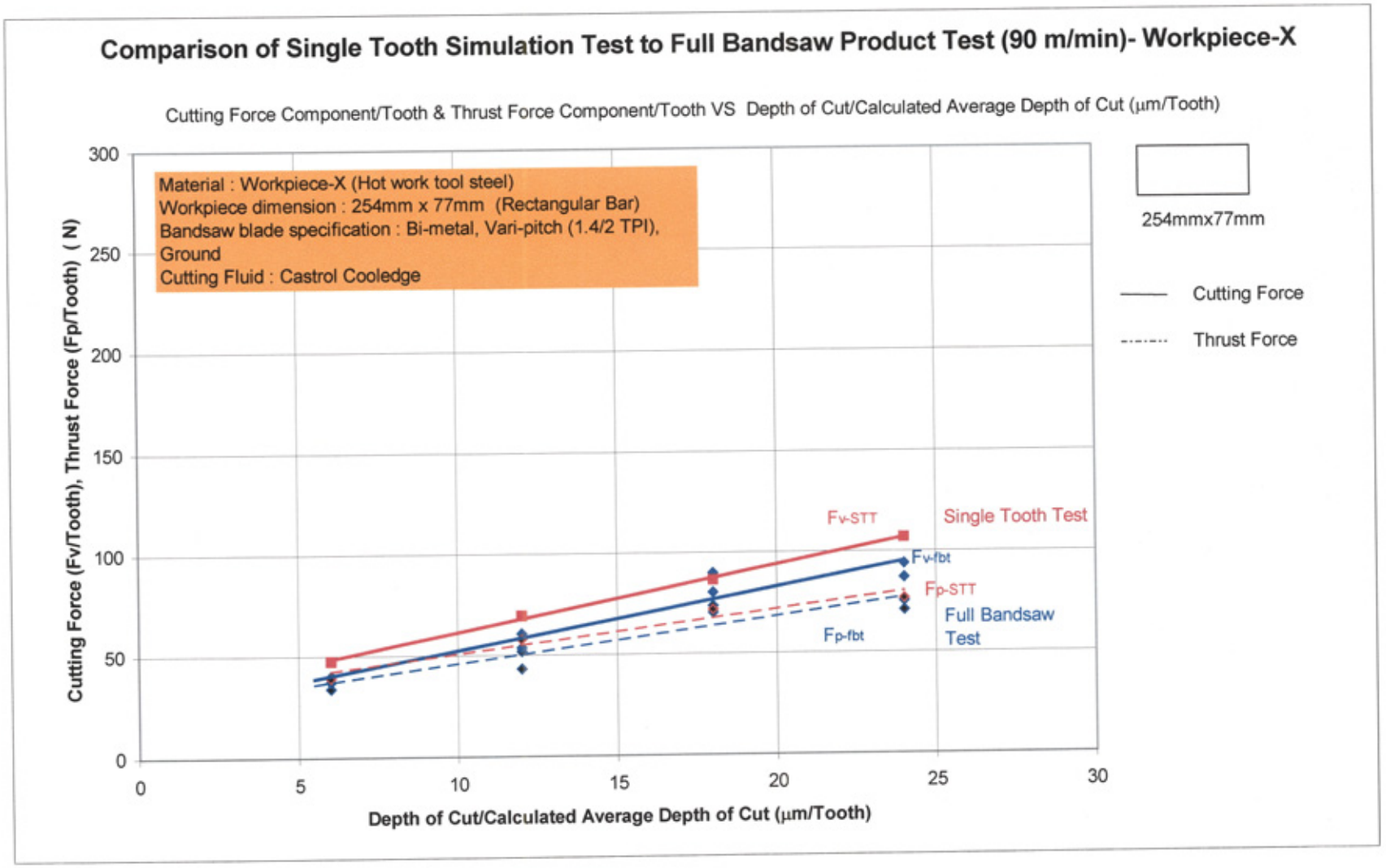

Figure 131 Validation of single tooth test results for Workpiece-X at 90 m/min, using correction factor

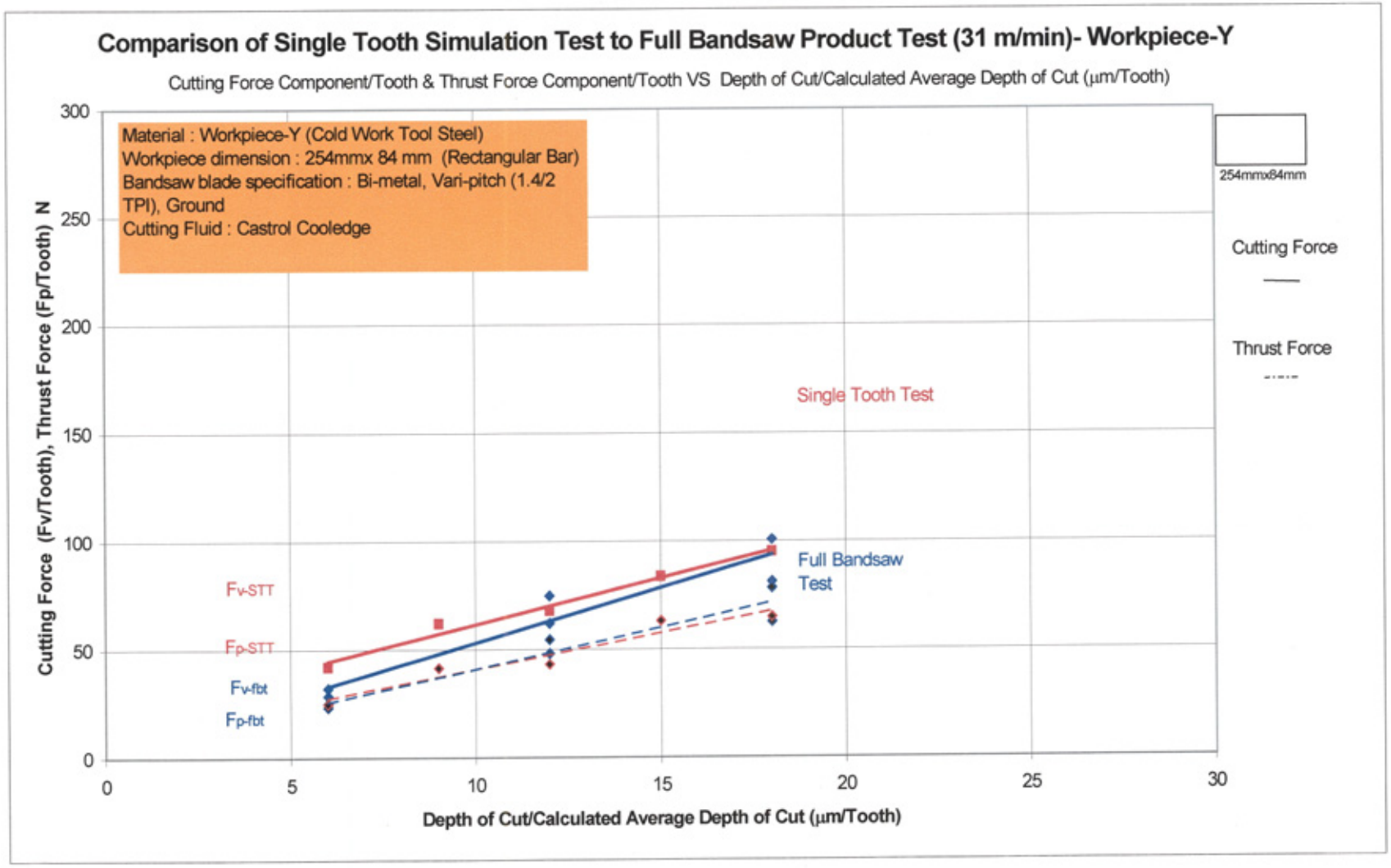

Figure 132 Validation of single tooth test results for Workpiece-Y at 31 m/min, using correction factor

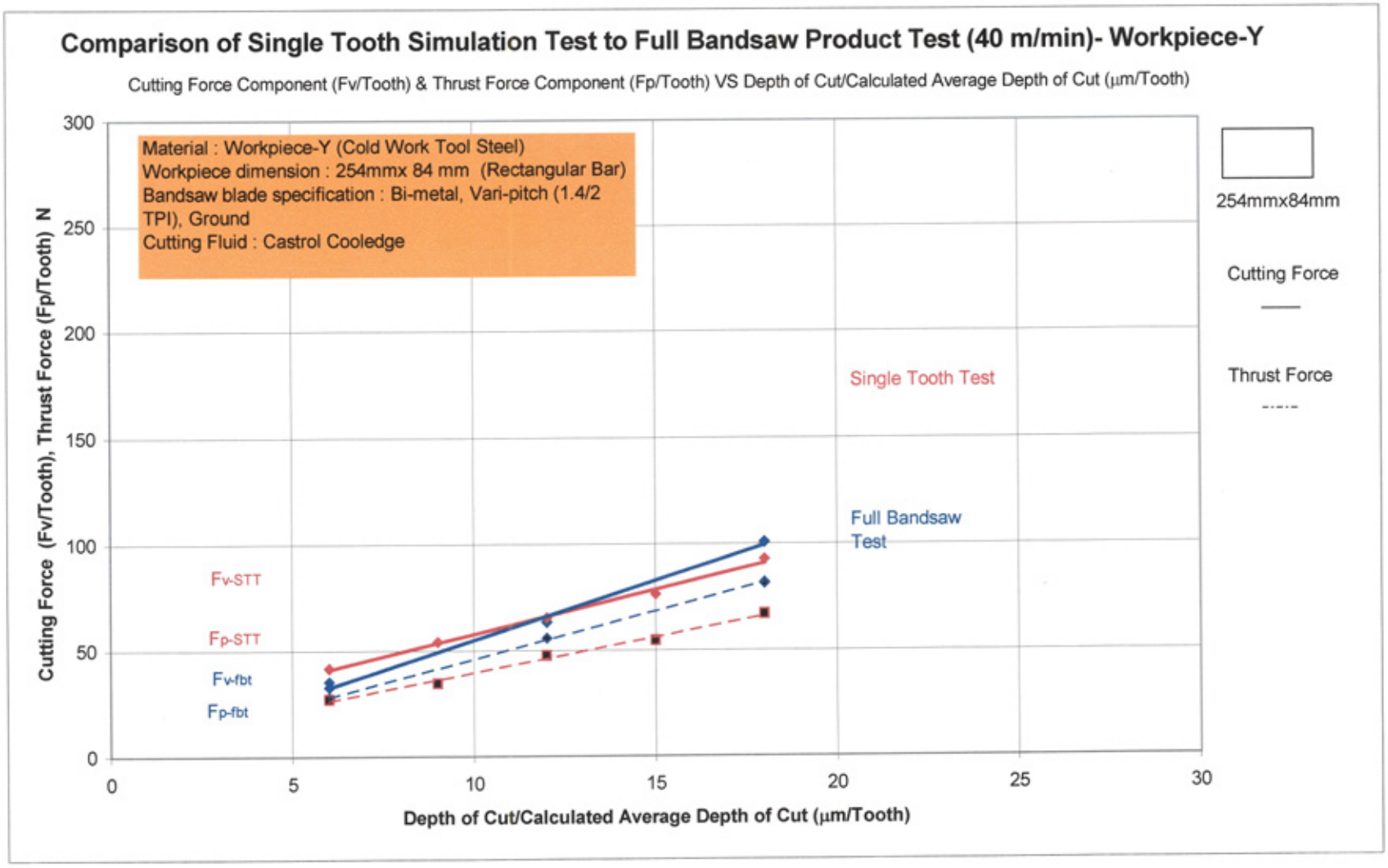

Figure 133 Validation of single tooth test results for Workpiece-Y at 40 m/min, using correction factor

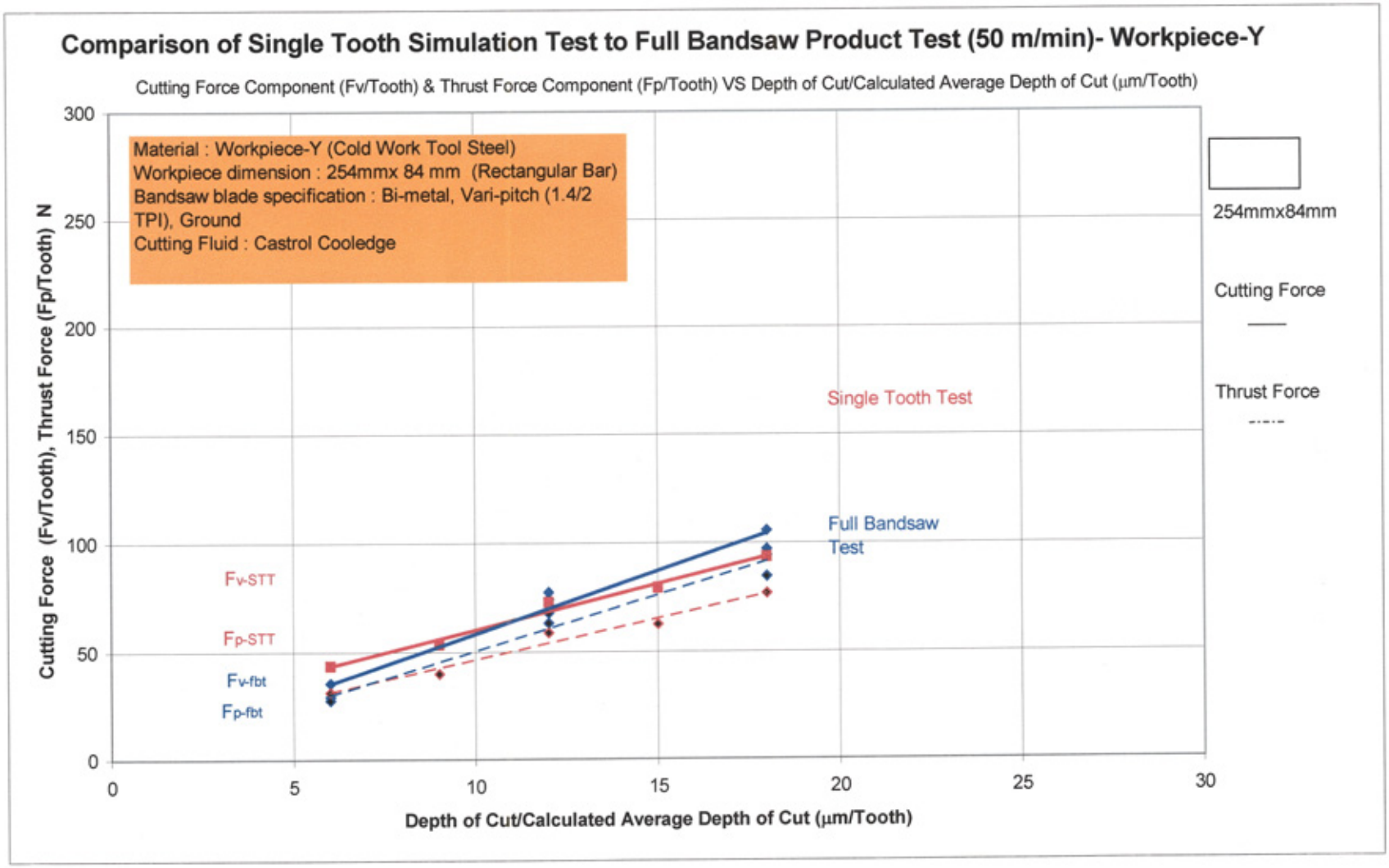

Figure 134 Validation of single tooth test results for Workpiece-Y at 50 m/min, using correction factor

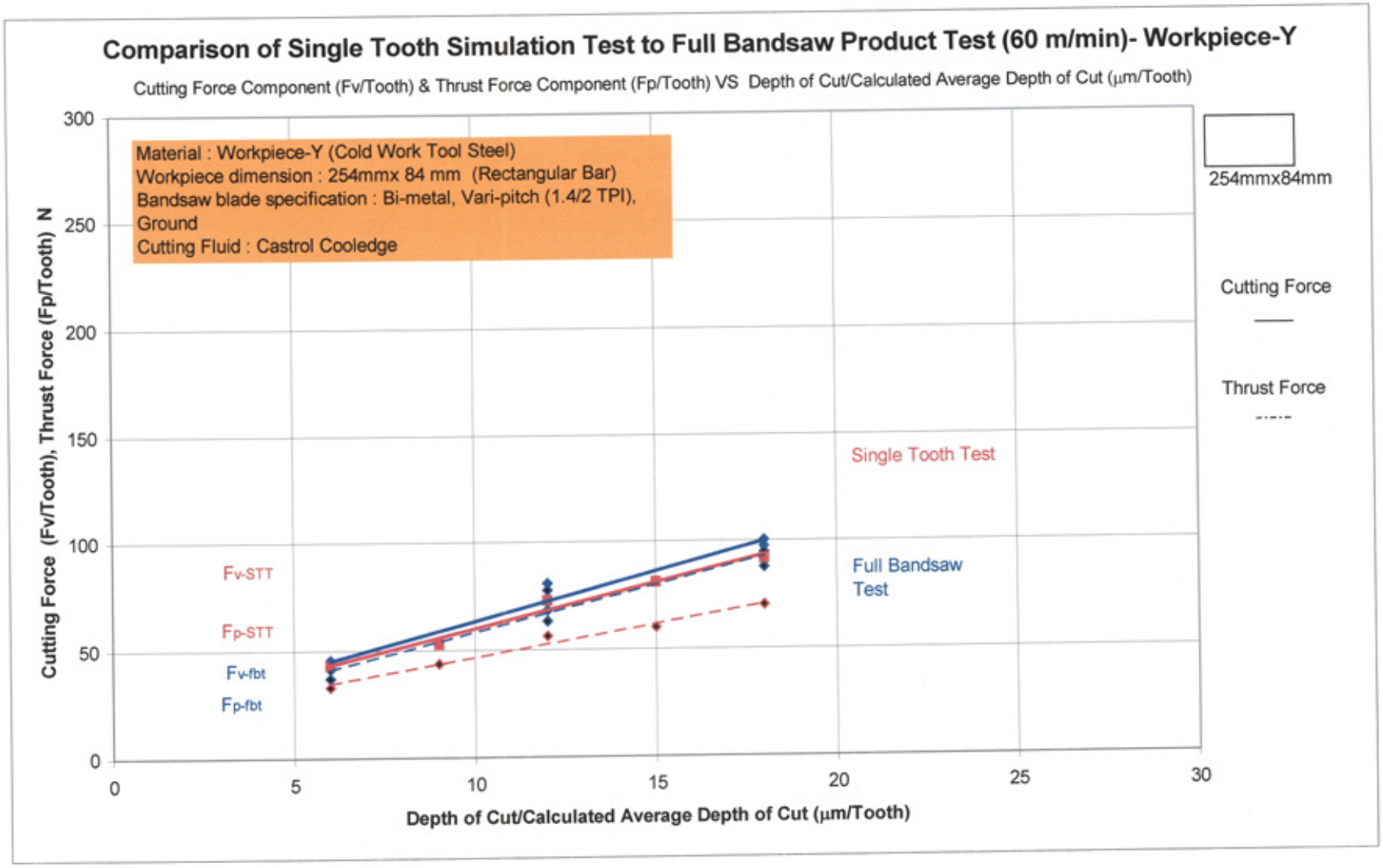

Figure 135 Validation of single tooth test results for Workpiece-Y at 60 m/min, using correction factor

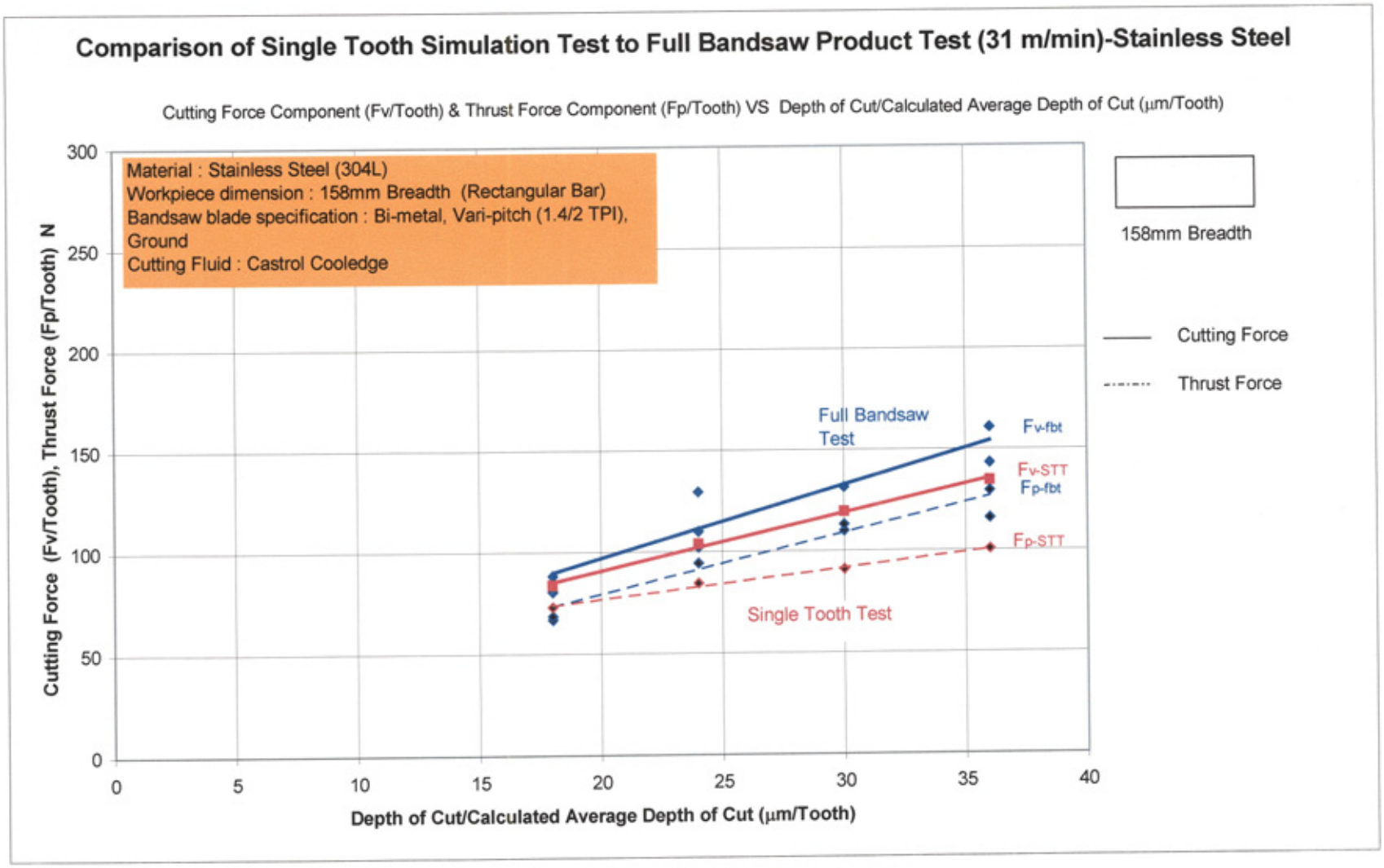

Figure 136 Validation of single tooth test results for Stainless Steel at 31 m/min, using correction factor

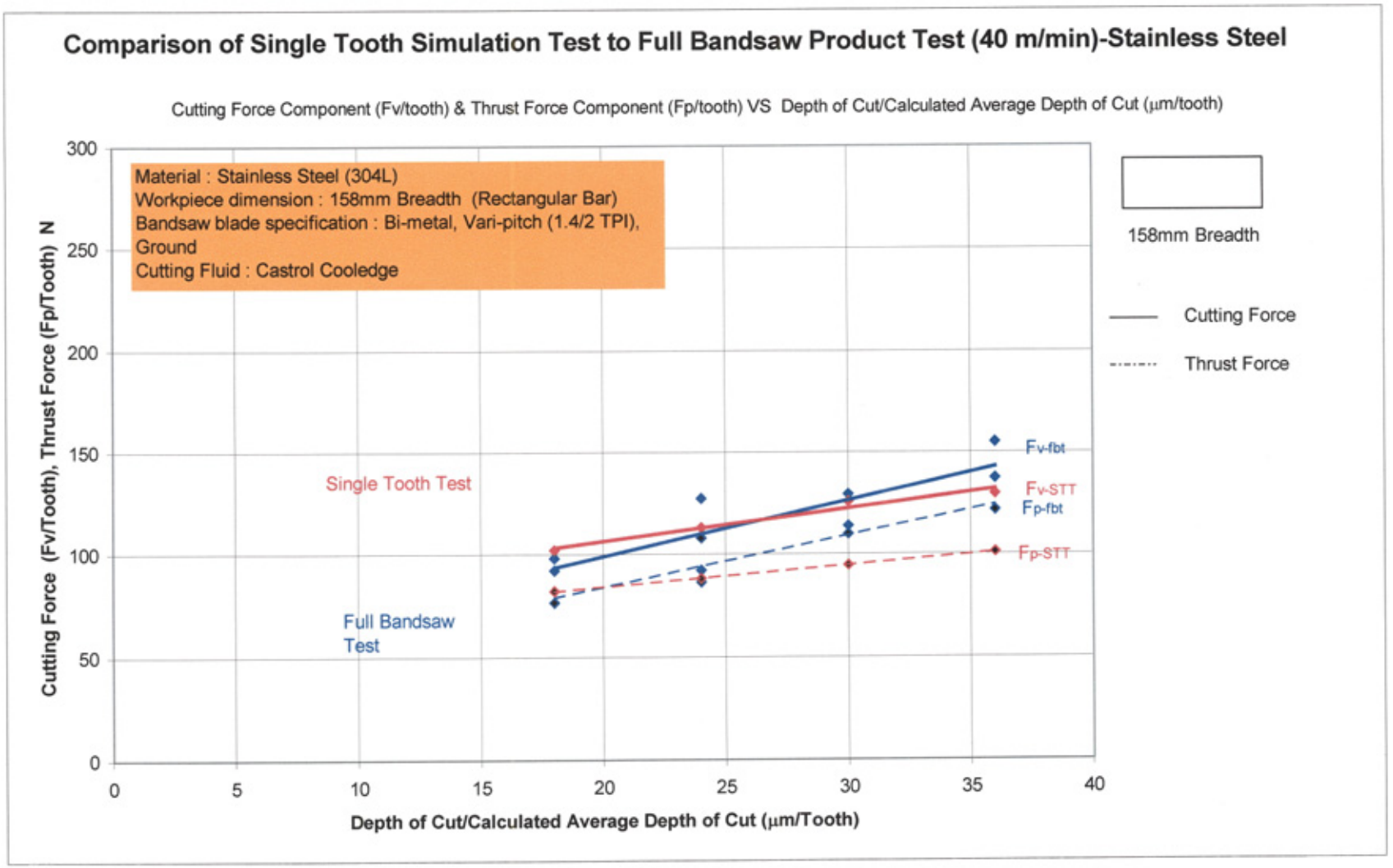

Figure 137 Validation of single tooth test results for Stainless Steel at 40 m/min, using correction factor

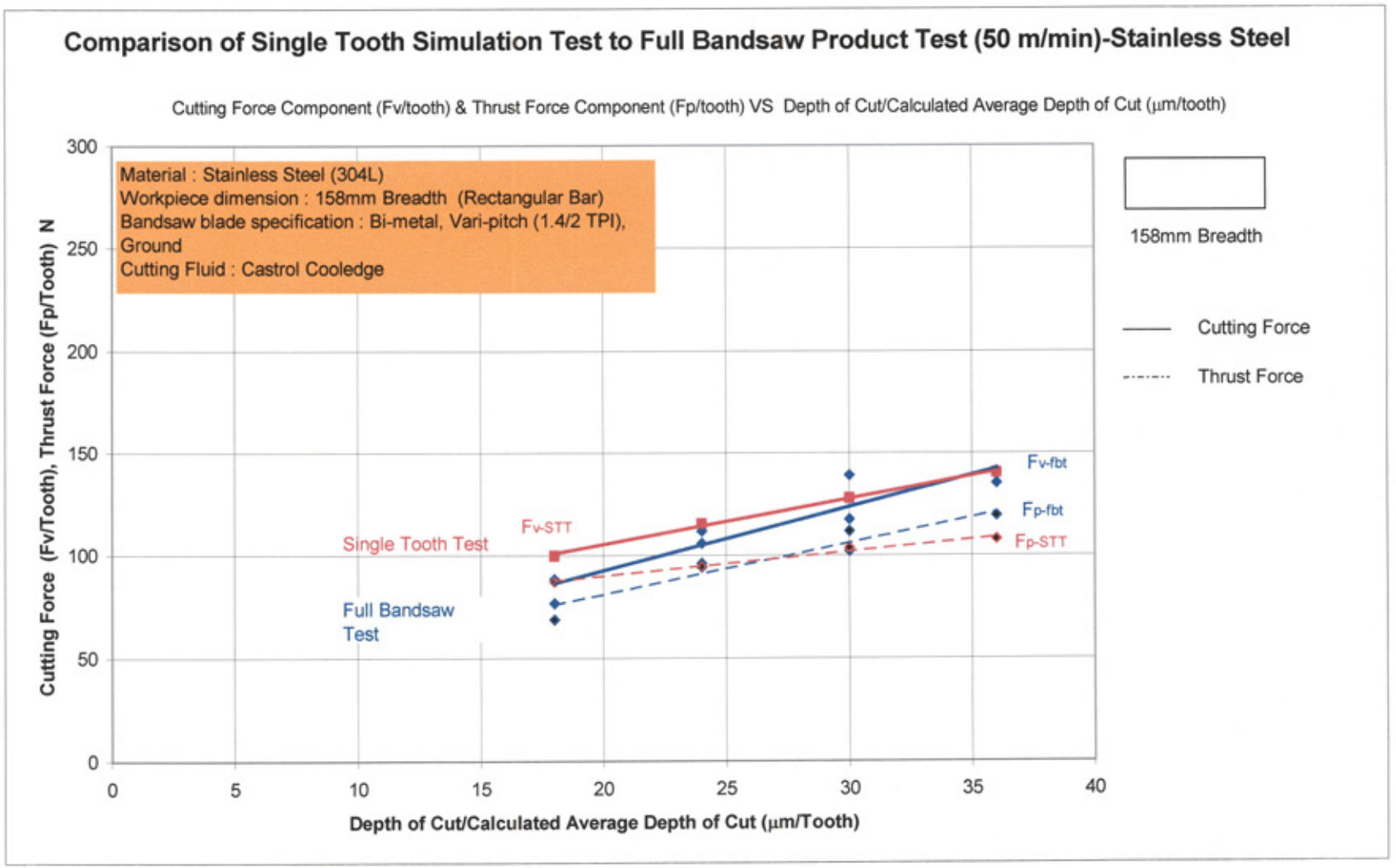

Figure 138 Validation of single tooth test results for Stainless Steel at 50 m/min, using correction factor

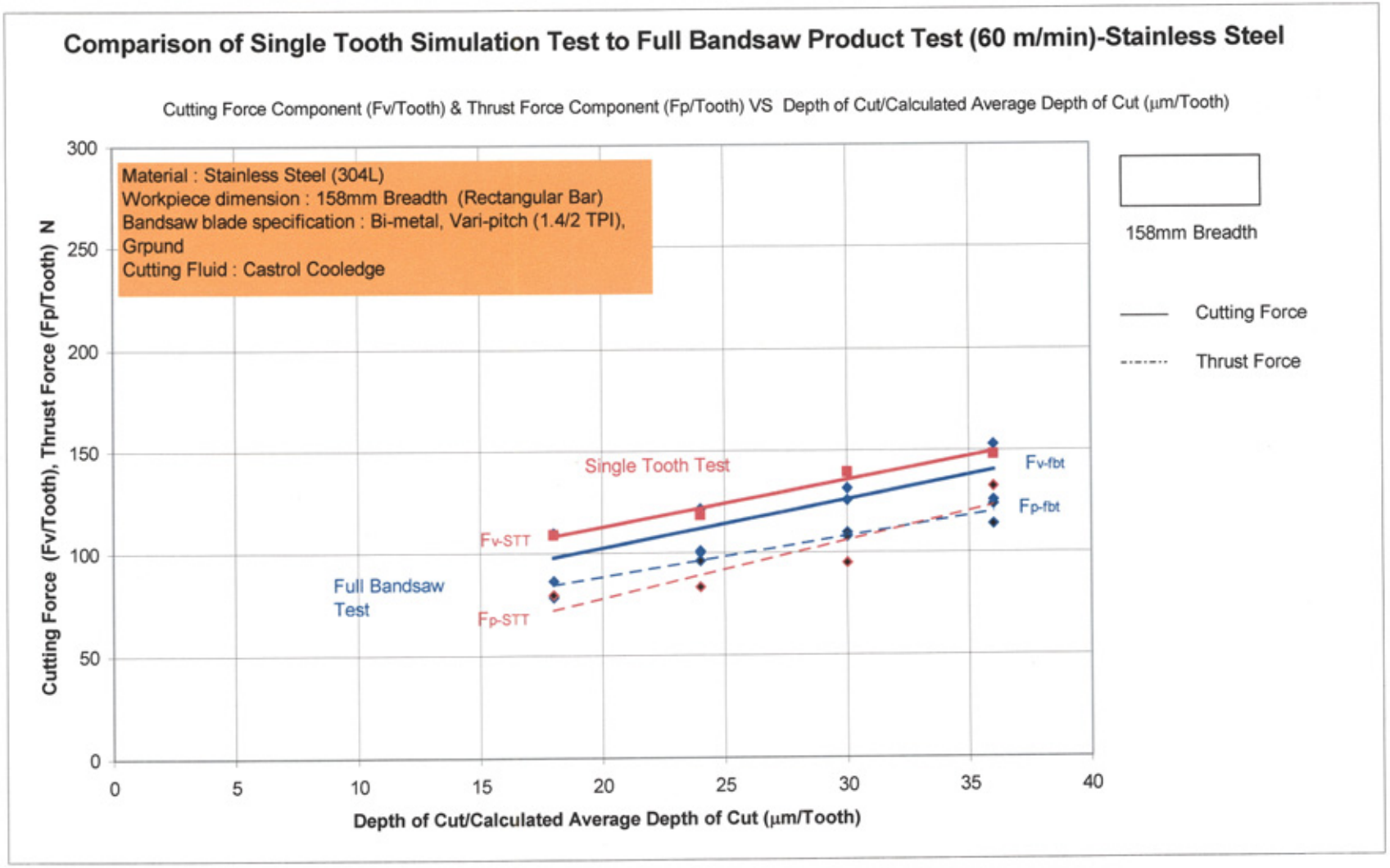

Figure 139 Validation of single tooth test results for Stainless Steel at 60 m/min, using correction factor

APPENDIX A

List of tables

Table 1 Bandsaw machine specification

Machine Model	Behringer HBP650/850A/CNC
Band Length	8800 mm
Band Width	67 mm or 54 mm
Maximum Workpiece Dimension	850 mm x 650 mm
Minimum Workpiece Dimension	20 mm x 20 mm
Cutting Speed	20-300 m/min
Weight	9000 kg
Motor Power	22 kW

Table 2 Test conditions used in the force transducer calibration test.

Cutting speeds (m/min)	31, 40 and 50
Feed per tooth (μm)	1, 3 and 5
Number of repeats for every condition	2

Table 3 Test conditions used for feedrate calibration test

Cutting speeds (m/min)	40 and 70
Feed per tooth (μm)	2, 4 and 6
Number of repeats for every condition	2

Table 4 Nominal chemical compositions (wt.%) and hardness of bandsaw tooth material

Tooth Material	Composition (wt.%)						Tooth Hardness (HV1)
	C	Cr	Mo	W	Co	V	
AISI M42 HSS in Bi-Metal	1.08	3.9	9.4	1.5	8.0	1.3	900

Table 5 Nominal chemical compositions (wt.%) and hardness of bandsaw backing material

Material	Composition (wt.%)						Hardness (HV1)
	C	Mn	Cr	Ni	Mo	Si	
D6A (Backing material)	0.42	0.60	0.90	0.4	0.85	0.10	400

Table 6 Etch agents

Material:	Tool steels	Stainless steel
Etch agent:	Special etch agent (a mixture of 6 gram picric acid, 550 ml ethanol, 40 ml hydrochloric acid, 12 ml acetic acid)	Concentrated hydrochloric acid

Table 7 Nominal chemical composition, weight%, for Stainless Steel workpiece material

Carbon	Silicon	Phosphorus	Sulfur	Chromium	Nickel	Iron
0.030 max	0.6	0.040 max	0.030 max	18.5	8.2	Remainder

Table 8 International Standard

Name	German Werkstoff number	European EN number	British standard number	AISI number
Stainless Steel 304L	1.4301	1.4307	304S11 304S15 304S31	304L

Table 9 Nominal chemical composition, weight%, for Workpiece-X material

Carbon	Silicon	Manganese	Molybdenum	Chromium	Vanadium	Iron
0.3	0.2	0.5	2.2	5	0.6	Remainder

Table 10 Nominal chemical composition, weight%, for Workpiece-Y material

Carbon	Silicon	Manganese	Molybdenum	Chromium	Vanadium	Iron
0.9	0.9	0.5	2.5	7.8	0.5	Remainder

Table 11 Test conditions (Hot Work Tool Steel-Workpiece-X)

Machine	Behringer HBP 600/850, 2-pillar
Coolant	Castrol Cooledge, 5.5% solution oil/water, at 3.8 litres/minute
Work piece material	Workpiece-X (260 HV1) (Rectangular bar 254x77 mm)
Bandsaw Blade	54-1.6 PHG-1.4/2 (Vari-pitch)-8800 (AISI M42 HSS Bi-Metal-Ground)
Tooth Geometry	Rake Angle γ = +10 °, Clearance Angle β= 35 °
Tooth Set Pattern	0-R-L-0-R-L-0
Band Speed	31, 50, 70 and 90 m/min
Nominal Cutting Depth/Tooth	1, 2, 3 and 4 μm
Band Tension	180 MN/m^2

Table 12 Test conditions (Cold Work Tool Steel-Workpiece-Y)

Machine	Behringer HBP 600/850, 2-pillar
Coolant	Castrol Cooledge, 5.5% solution oil/water, at 3.8 litres/minute
Work piece material	Workpiece-Y (250 HV1) (Rectangular bar 254x84 mm)
Bandsaw Blade	54-1.6 PHG-1.4/2 (Vari-pitch)-8800 (AISI M42 HSS Bi-Metal-Ground)
Tooth Geometry	Rake Angle γ = +10 °, Clearance Angle β= 35 °
Tooth Set Pattern	0-R-L-0-R-L-0
Band Speed	31, 40, 50, and 60 m/min
Nominal Cutting Depth/Tooth	1, 2, and 3 μm
Band Tension	180 MN/m^2

Table 13 Test conditions (Stainless Steel 304L)

Machine	Behringer HBP 600/850, 2-pillar
Coolant	Castrol Cooledge, 5.5% solution oil/water, at 3.3 liters/minute
Work piece material	Stainless Steel 304L (210 HV1) (Rectangular bar 254x78mm)
Bandsaw Blade	54-1.6 PHG-1.4/2 (Vari-pitch)-8800 (AISI M42 HSS Bi-Metal-Ground)-Hi/Lo
Tooth Geometry	Rake Angle γ = +10 °, Clearance Angle β= 35 °
Tooth Set Pattern	0-R-L-R-L-R-L-0
Band Speed	31 m/min, 40 m/min, 50 m/min and 60 m/min
Nominal Cutting Depth/Tooth	3 μm, 4 μm, 5 μm and 6μm,
Band Tension	180 MN/m²

Table 14 Tooth Geometry

Tooth Sample	Rake Angle	Clearance Angle	Tooth Width (mm)	Gullet depth (mm)	Pitch
T1	10 °	25 °	1.3	4.24	2 TPI

Table 15 Nominal chemical compositions (wt.%) and hardness of tool material

Material	Tool	Composition						Hardness HV1
		C	**Cr**	**Mo**	**W**	**Co**	**V**	
AISI M42 HSS	T1	1.08	3.9	9.4	1.5	8.0	1.3	880

Table 16 Nominal chemical compositions (wt.%) and hardness of workpiece material

Material	Composition						Hardness HV1
	C	**Cr**	**Mn**	**S**	**Co**	**V**	
Standard Steel (BS 970)	0.4	0.25	1.3	0.12	-	-	140

Table 17 Test conditions used in the single tooth simulation tests

Machine	1609 Dean Smith & Grace lathe machine
Coolant	Castrol Cooledge, 5.5% solution oil/water, at 2.8 liters/minute
Workpiece material	Workpiece-X, Workpiece-Y, Stainless Steel 304L
Bandsaw Blade	54-1.6 PHG-1.4/2 (Vari-pitch)-8800 (AISI M42 HSS Bi-Metal-Ground)-Variable Height
Tooth Geometry	Rake Angle γ = +10 °, Clearance Angle β= 35 °
Tooth Set Pattern	0-R-L-0-R-L-0
Band Speed	31 m/min to 90 m/min
Depth of Cut/Tooth	6μm to 36μm,

APPENDIX 1

Contents

Mapping Test

1. Workpiece-X (full bandsaw blade product test)

2. Workpiece-Y (Full bandsaw blade product test)

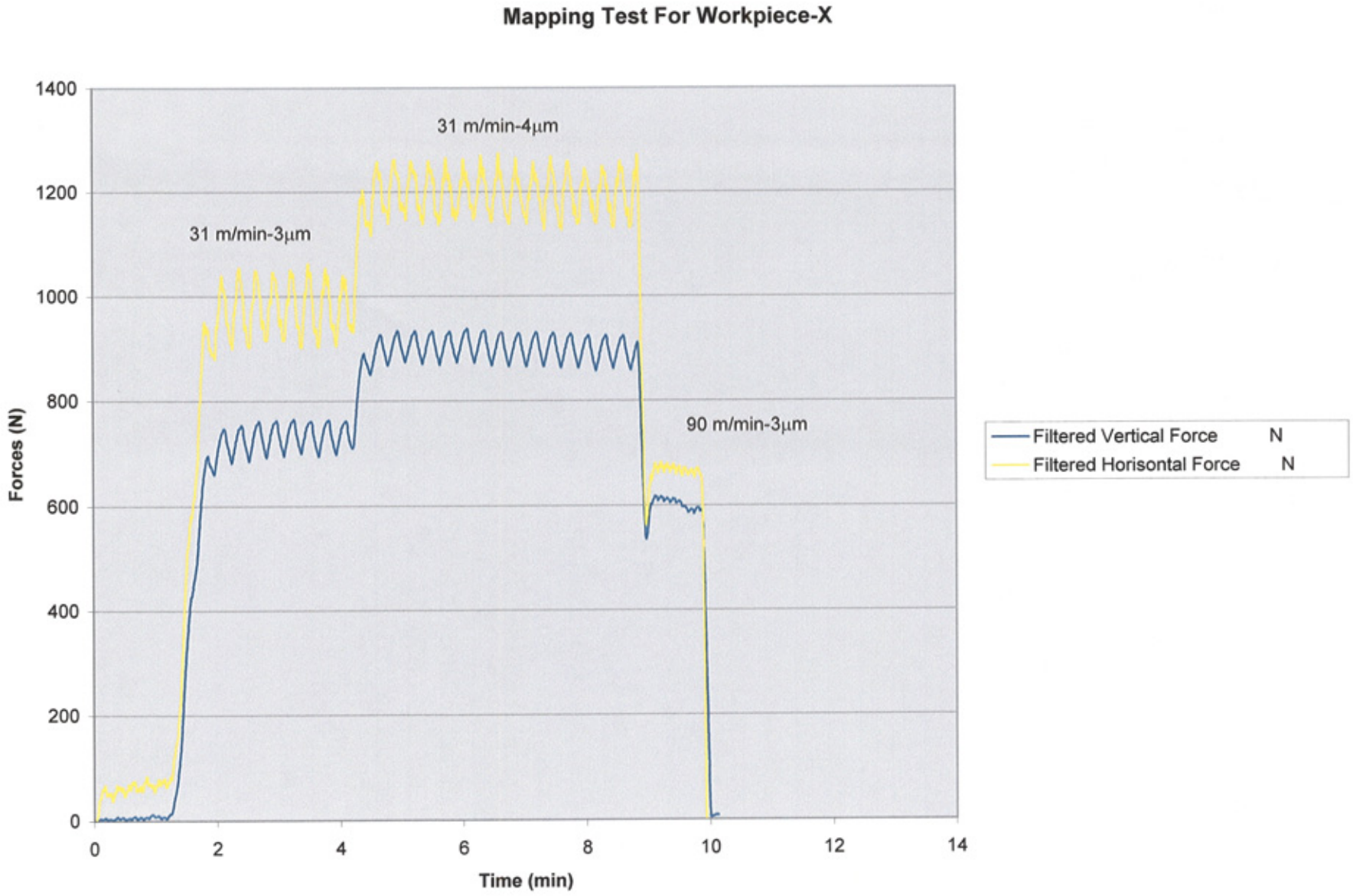
Mapping Test For Workpiece-X
1400
1200
1000
800
600
400
200
0
Forces (N)
0
2
4
6
8
10
12
14
Time (min)
31 m/min-4µm
31 m/min-3µm
90 m/min-3µm
Filtered Vertical Force N
Filtered Horisontal Force N

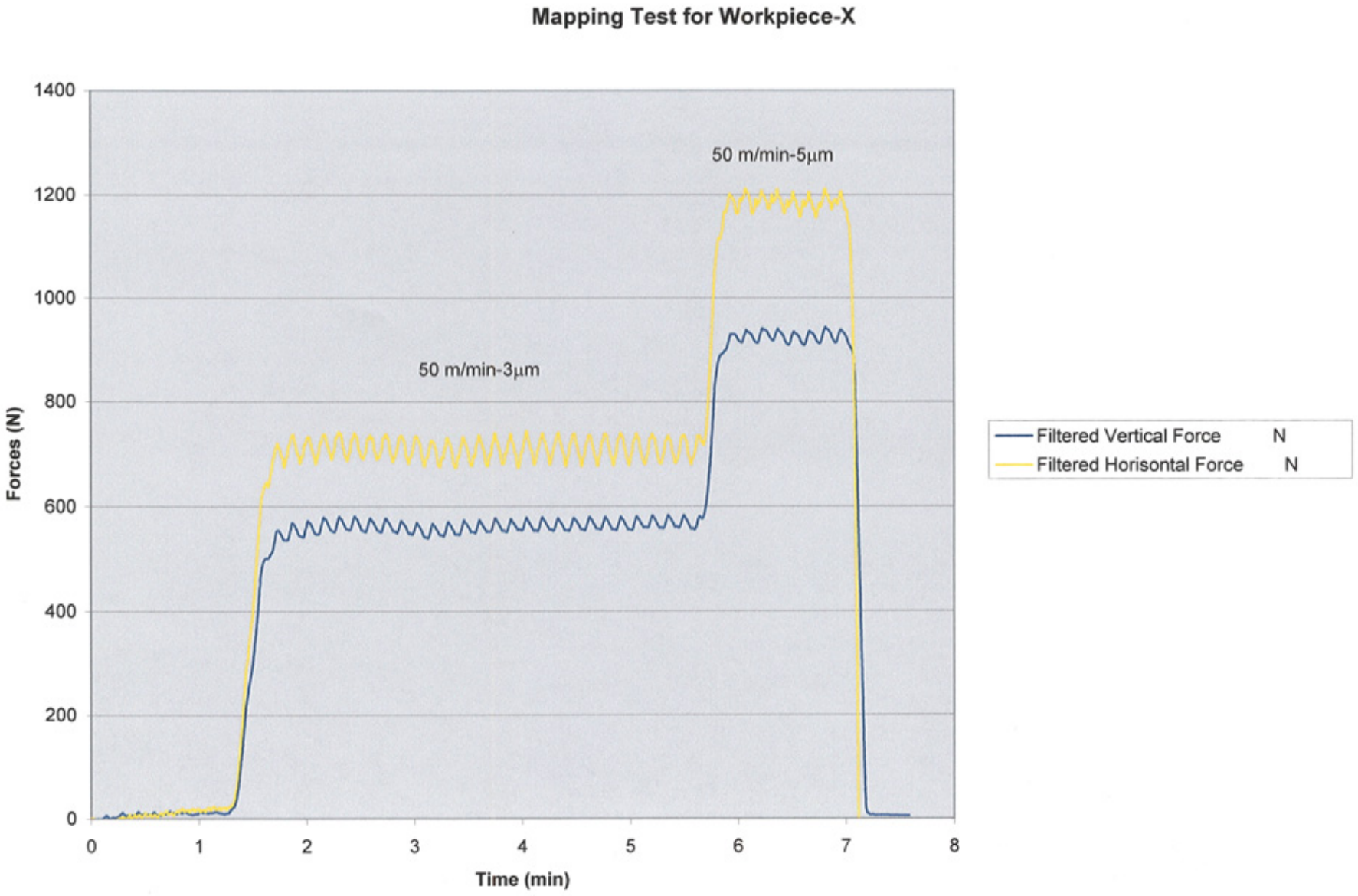
Mapping Test for Workpiece-X
1400
1200
1000
800
600
400
200
0
Forces (N)
0
1
2
3
4
5
6
7
8
Time (min)
50 m/min-5µm
50 m/min-3µm
Filtered Vertical Force N
Filtered Horisontal Force N

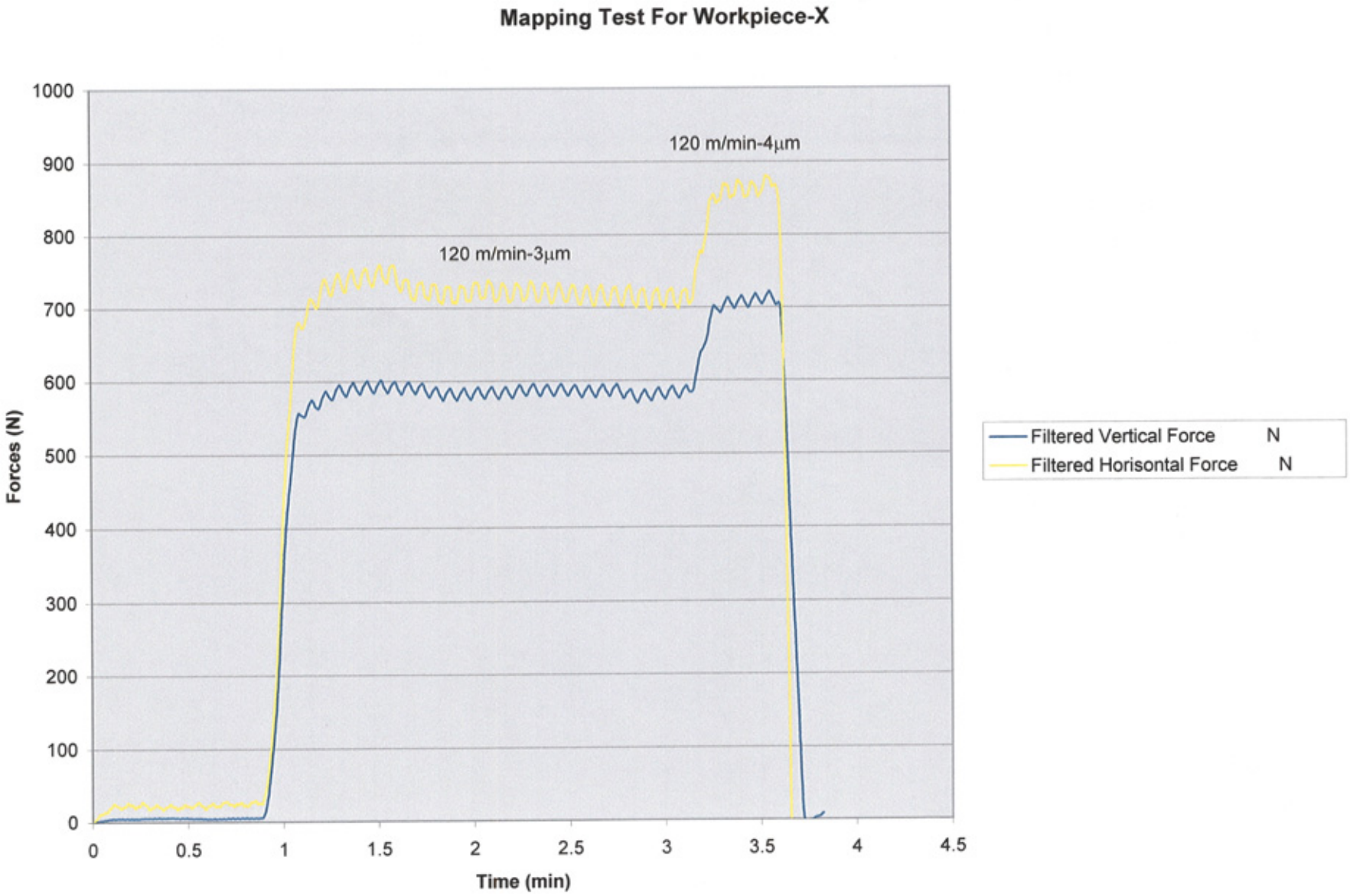
Mapping Test For Workpiece-X
1000
900
800
700
600
500
400
300
200
100
0
Forces (N)
120 m/min-4μm
120 m/min-3μm
0
0.5
1
1.5
2
2.5
3
3.5
4
4.5
Time (min)
Filtered Vertical Force N
Filtered Horisontal Force N

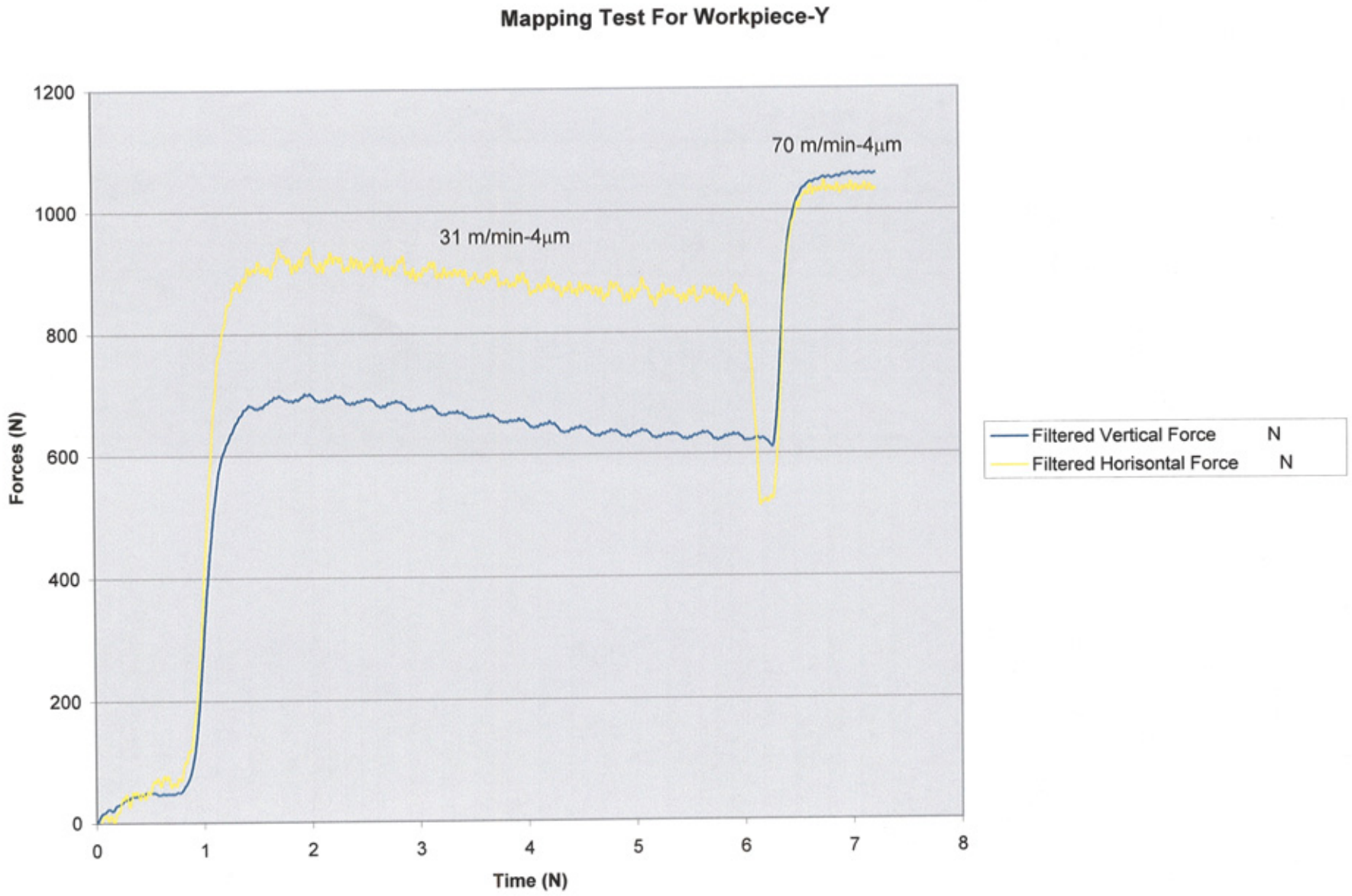
Mapping Test For Workpiece-Y
70 m/min-4μm
31 m/min-4μm
Forces (N)
Time (N)
1200
1000
800
600
400
200
0
0
1
2
3
4
5
6
7
8
Filtered Vertical Force N
Filtered Horisontal Force N

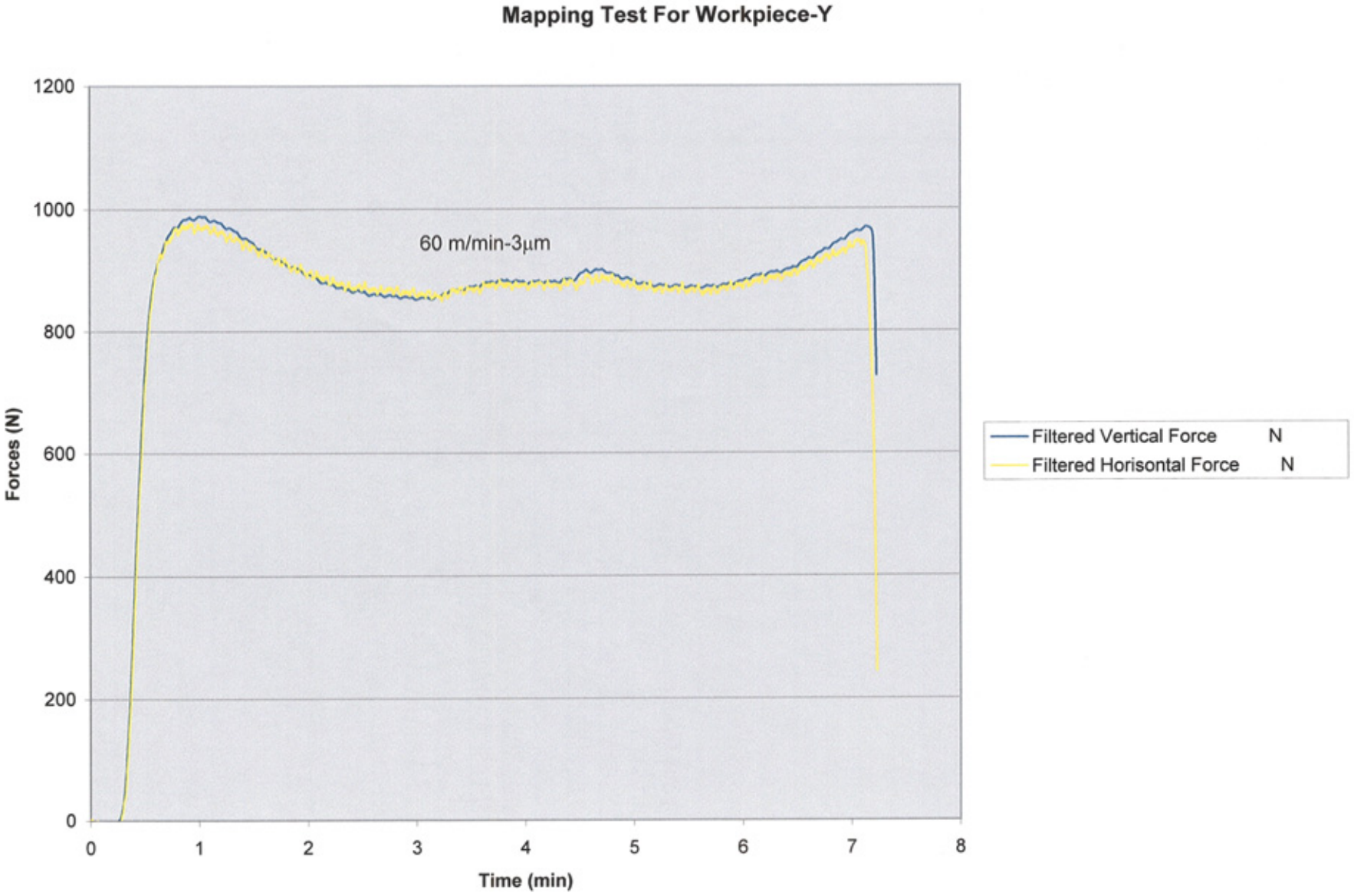
Mapping Test For Workpiece-Y
60 m/min-3μm
Forces (N)
Time (min)
0
200
400
600
800
1000
1200
0
1
2
3
4
5
6
7
8
Filtered Vertical Force N
Filtered Horisontal Force N

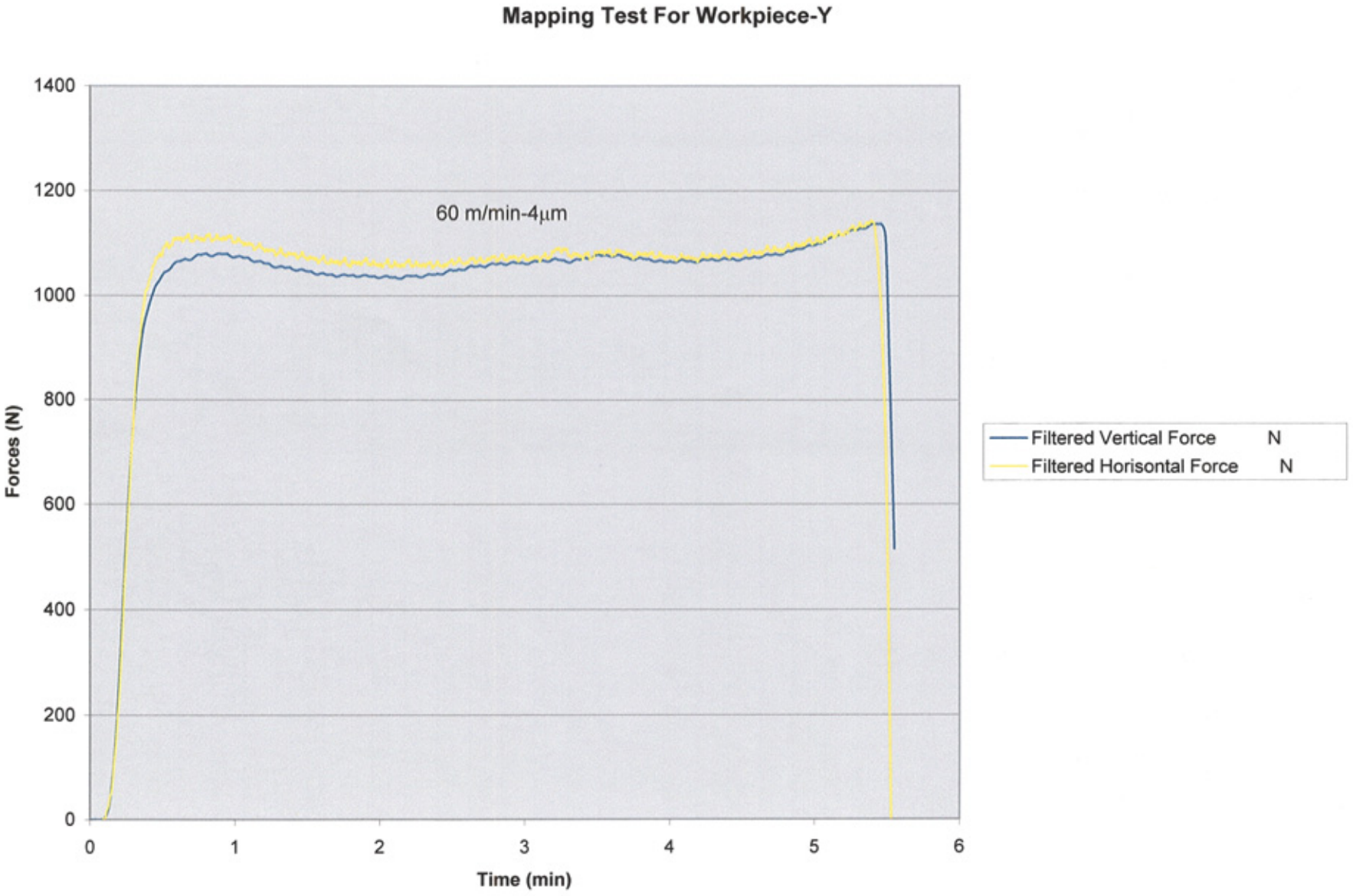
Mapping Test For Workpiece-Y
60 m/min-4μm
Forces (N)
Time (min)
1400
1200
1000
800
600
400
200
0
0
1
2
3
4
5
6
Filtered Vertical Force N
Filtered Horisontal Force N

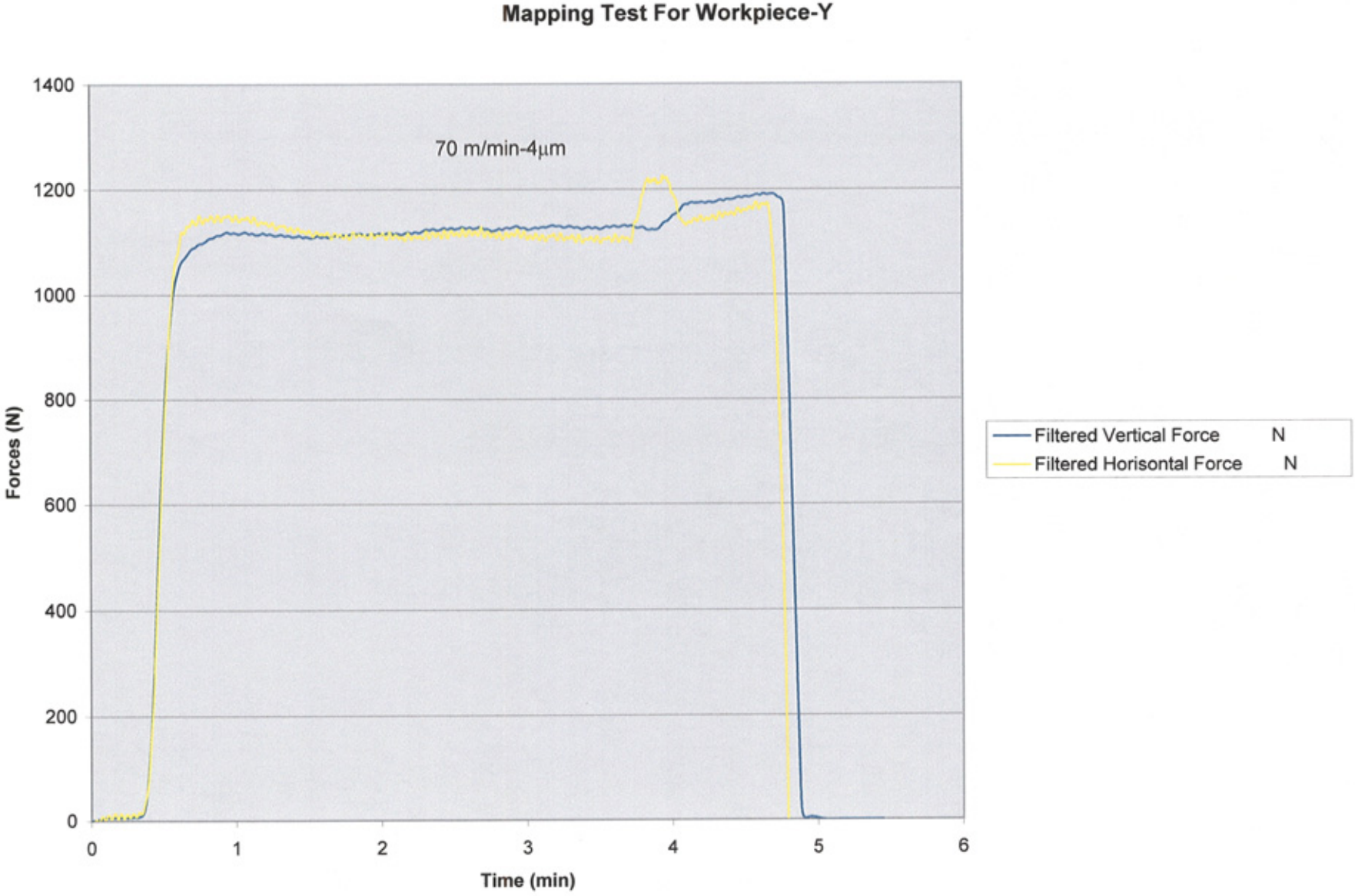
Mapping Test For Workpiece-Y
70 m/min-4µm
Forces (N)
1400
1200
1000
800
600
400
200
0
0
1
2
3
4
5
6
Time (min)
Filtered Vertical Force N
Filtered Horisontal Force N

APPENDIX 2

Contents

TABLE 18-1 DATA SHEET (Workpiece-X)

Workpiece Material : Workpiece-X

Workpiece Dimension : 254mm x 77mm

254 mm

77 mm

Cutting Fluid : Castrol Cooledge, 3.3 liters/min

Bandsaw Blade Specification : HSS, Bi-Metal,Vari Pitch-1.4/2 TPI (Hi-Lo) Ground

Tooth Pattern : 0-R-L-0-R-L-0

Bandsaw Machine : Positive Feed, Hydraulic (Behringer Vertical Pillar)

Band Speed V_b (m\min)	Feed Rate-set (mm/min)	Set Nominal Depth of cut/tooth δ_{as}(μm)	Average Depth of cut/tooth $\delta_{a_{fbt}}$ (μm)	Cutting Force Fv (N)	Thrust Force Fp (N)	Cutting Force/Tooth $F_{v\text{-}fbt}$ (N)	Thrust Force/tooth $F_{p\text{-}fbt}$ (N)	E_{SP} (GJ/m^3)	$E_{SP\text{-}t}$ (GJ/m^3)
31	2.1	1	6	375	322	44.12	37.88	8.48	8.48
31	4.2	2	12	674	576	79.29	67.76	7.62	7.62
31	6.3	3	18	1035	811	121.76	95.41	7.81	7.81
31	8.4	4	24	1154	971	135.76	114.24	6.53	6.53
50	3.4	1	6	339	308	39.88	36.24	7.67	7.67
50	6.7	2	12	570	512	67.06	60.24	6.45	6.45
50	10.1	3	18	870	768	102.35	90.35	6.56	6.56
50	13.5	4	24	1116	936	131.29	110.12	6.31	6.31
70	4.7	1	6	298	269	35.06	31.65	6.74	6.74
70	9.4	2	12	543	464	63.88	54.59	6.14	6.14
70	14.2	3	18	706	604	83.06	71.06	5.32	5.32
70	18.9	4	24	941	768	110.71	90.35	5.32	5.32
90	6.1	1	6	315	288	37.06	33.88	7.13	7.13
90	12.1	2	12	515	441	60.59	51.88	5.83	5.83
90	18.2	3	18	763	626	89.76	73.65	5.75	5.75
90	24.3	4	24	797	641	93.76	75.41	4.51	4.51

TABLE 18-2 DATA SHEET (Workpiece-X)

Workpiece Material : Workpiece-X

Workpiece Dimension : 254mm x 77mm

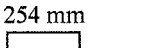

Cutting Fluid : Castrol Cooledge, 3.3 liters/min

Bandsaw Blade Specification : HSS, Bi-Metal,Vari Pitch-1.4/2 TPI (Hi-Lo) Ground

Tooth Pattern : 0-R-L-0-R-L-0

Bandsaw Machine : Positive Feed, Hydraulic (Behringer Vertical Pillar)

Band Speed V_b (m\min)	Feed Rate-set (mm/min)	Set Nominal Depth of cut/tooth δas (μm)	Average Depth of cut/tooth δa_{fbt} (μm)	Cutting Force Fv (N)	Thrust Force Fp (N)	Cutting Force/tooth $F_{v\text{-}fbt}$ (N)	Thrust Force/tooth $F_{p\text{-}fbt}$ (N)	E_{SP} (GJ/m^3)	E_{SP}-t (GJ/m^3)
31	2.1	1	6	386	315	45.4	37.06	8.73	8.73
31	4.2	2	12	674	591	79.3	69.53	7.62	7.62
31	6.3	3	18	868	732	102.1	86.12	6.55	6.55
31	8.4	4	24	1163	973	136.8	14.47	6.58	6.58
50	3.4	1	6	320	270	37.6	31.76	7.24	7.24
50	6.7	2	12	586	535	68.9	62.94	6.63	6.63
50	10.1	3	18	867	767	102.0	90.24	6.54	6.54
50	13.5	4	24	935	812	110.0	95.53	5.29	5.29
70	4.7	1	6	270	260	31.8	30.59	6.11	6.11
70	9.4	2	12	536	483	63.1	56.82	6.06	6.06
70	14.2	3	18	610	545	71.8	64.12	4.60	4.60
70	18.9	4	24	901	808	106.0	95.06	5.10	5.10
90	6.1	1	6	340	330	40.0	38.82	7.69	7.69
90	12.1	2	12	456	366	53.6	43.06	5.16	5.16
90	18.2	3	18	681	597	80.1	70.24	5.14	5.14
90	24.3	4	24	738	602	86.8	70.82	4.17	4.17

TABLE 19-1 DATA SHEET (Workpiece-Y)

Workpiece Material : Workpiece-Y

Workpiece Dimension : 254mm x 84mm

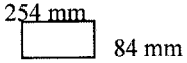

Cutting Fluid : Castrol Cooledge, 3.3 liters/min

Bandsaw Blade Specification : HSS, Bi-Metal,Vari Pitch-1.4/2 TPI (Hi-Lo) Ground

Tooth Pattern : 0-R-L-0-R-L-0

Bandsaw Machine : Positive Feed, Hydraulic (Behringer Vertical Pillar)

Band Speed V_b (m\min)	Feed Rate-set (mm/min)	Set Nominal Depth of cut/tooth δas (μm)	Average Depth of cut/tooth δa_{fbt} (μm)	Cutting Force Fv (N)	Thrust Force Fp (N)	Cutting Force/Tooth $F_{v\text{-}fbt}$ (N)	Thrust Force/tooth $F_{p\text{-}fbt}$ (N)	E_{SP} (GJ/m^3)	$E_{SP\text{-}t}$ (GJ/m^3)
31	2.1	1	6	242	212	32.12	23.29	6.18	6.18
31	4.2	2	12	636	465	62.12	48.12	5.97	5.97
31	6.3	3	18	856	664	81.06	62.47	5.20	5.20
40	2.7	1	6	277	231	35.18	27.65	6.76	6.76
40	5.4	2	12	539	473	63.18	55.65	6.07	6.07
40	8.1	3	18	858	691	100.71	81.65	6.46	6.46
50	3.4	1	6	302	233	29.18	27.41	5.61	5.61
50	6.7	2	12	628	538	77.18	67.76	7.42	7.42
50	10.1	3	18	898	800	97.06	84.35	6.22	6.22
60	4	1	6	362	314	45.53	41.41	8.76	8.76
60	8.1	2	12	686	659	68.24	63.18	6.56	6.56
60	12.1	3	18	852	745	97.18	94.47	6.23	6.23

TABLE 19-2 DATA SHEET (Workpiece-Y)

Workpiece Material : Workpiece-Y

Workpiece Dimension : 254mm x 84mm

254 mm

84 mm

Cutting Fluid : Castrol Cooledge, 3.3 liters/min

Bandsaw Blade Specification : HSS, Bi-Metal,Vari Pitch-1.4/2 TPI (Hi-Lo) Ground

Tooth Pattern : 0-R-L-0-R-L-0

Bandsaw Machine : Positive Feed, Hydraulic (Behringer Vertical Pillar)

Band Speed V_b (m\min)	Feed Rate-set (mm/min)	Set Nominal Depth of cut/tooth δas (μm)	Average Depth of cut/tooth δa_{fbt} (μm)	Cutting Force Fv (N)	Thrust Force Fp (N)	Cutting Force/tooth $F_{v\text{-}fbt}$ (N)	Thrust Force/tooth $F_{p\text{-}fbt}$ (N)	E_{SP} (GJ/m^3)	$E_{SP\text{-}t}$ (GJ/m^3)
31	2.1	1	6	273	198	28.47	24.94	5.48	5.48
31	4.2	2	12	528	409	74.82	54.71	7.19	7.19
31	6.3	3	18	689	531	100.71	78.12	6.46	6.46
40	2.7	1	6	299	235	32.59	27.18	6.27	6.27
40	5.4	2	12	537	473	63.41	55.65	6.10	6.10
40	8.1	3	18	856	694	100.94	81.29	6.47	6.47
50	3.4	1	6	248	233	35.53	27.41	6.83	6.83
50	6.7	2	12	656	576	73.88	63.29	7.10	7.10
50	10.1	3	18	825	717	105.65	94.14	6.77	6.77
60	4	1	6	387	352	42.59	36.94	8.19	8.19
60	8.1	2	12	580	537	80.71	77.53	7.76	7.76
60	12.1	3	18	826	803	100.24	87.65	6.43	6.43

TABLE 20-1 DATA SHEET (Stainless Steel)

Workpiece Material : Stainless Steel 304L

Workpiece Dimension : 158mm x 108mm

158 mm

108 mm

Cutting Fluid : Castrol Cooledge, 3.3 liters/min

Bandsaw Blade Specification : HSS, Bi-Metal,Vari Pitch-1.4/2 TPI (Hi-Lo) Ground

Tooth Pattern : 0-R-L-0-R-L-0

Bandsaw Machine : Positive Feed, Hydraulic (Behringer Vertical Pillar)

Band Speed V_b (m\min)	Feed Rate-set (mm/min)	Set Nominal Depth of cut/tooth δas (μm)	Average Depth of cut/tooth δa_{fbt} (μm)	Cutting Force Fv (N)	Thrust Force Fp (N)	Cutting Force/Tooth $F_{v\text{-}fbt}$ (N)	Thrust Force/tooth $F_{p\text{-}fbt}$ (N)	E_{SP} (GJ/m^3)	E_{SP}-t (GJ/m^3)
31	6.3	3	18	450	350	80.39	66.67	5.15	5.15
31	8.4	4	24	660	480	109.8	101.96	5.28	5.28
31	10.5	5	30	670	575	131.37	109.8	5.05	5.05
31	12.1	6	36	820	590	143.14	129.4	4.59	4.59
40	8.1	3	18	500	390	92.16	76.47	5.91	5.91
40	10.8	4	24	650	550	92.16	86.27	4.43	4.43
40	13.5	5	30	660	560	113.73	109.80	4.37	4.37
40	16.2	6	36	790	630	137.25	121.57	4.40	4.40
50	10.1	3	18	460	390	76.47	68.63	4.90	4.90
50	13.5	4	24	570	480	105.88	96.08	5.09	5.09
50	16.9	5	30	710	570	117.65	101.96	4.52	4.52
50	20.2	6	36	720	610	135.29	119.61	4.34	4.34
60	12.1	3	18	560	440	86.27	78.43	5.53	5.53
60	16.2	4	24	620	515	100	96.08	4.81	4.81
60	20.2	5	30	670	550	125.49	109.8	4.83	4.83
60	24.3	6	36	780	630	125.49	113.73	4.02	4.02

TABLE 20-2 DATA SHEET (Stainless Steel)

Workpiece Material : Stainless Steel 304L

Workpiece Dimension : 158mm x 76mm

Cutting Fluid : Castrol Cooledge, 3.3 liters/min

Bandsaw Blade Specification : HSS, Bi-Metal,Vari Pitch-1.4/2 TPI (Hi-Lo) Ground

Tooth Pattern : 0-R-L-0-R-L-0

Bandsaw Machine : Positive Feed, Hydraulic (Behringer Vertical Pillar)

Band Speed V_b (m\min)	Feed Rate-set (mm/min)	Set Depth of cut/tooth δas (μm)	Actual Depth of cut/tooth δa_{fbt} (μm)	Cutting Force Fv (N)	Thrust Force Fp (N)	Cutting Force/tooth $F_{v\text{-}fbt}$ (N)	Thrust Force/tooth $F_{p\text{-}fbt}$ (N)	E_{SP} (GJ/m^3)	E_{SP}-t (GJ/m^3)
31	6.3	3	18	450	350	88.24	68.63	5.66	5.66
31	8.4	4	24	660	480	129.41	94.12	6.22	6.22
31	10.5	5	30	670	575	131.37	112.75	5.05	5.05
31	12.1	6	36	820	590	160.78	115.69	5.15	5.15
40	8.1	3	18	500	390	98.04	76.47	6.28	6.28
40	10.8	4	24	650	550	127.45	107.84	6.13	6.13
40	13.5	5	30	660	560	129.41	109.8	4.98	4.98
40	16.2	6	36	790	630	154.9	123.53	4.96	4.96
50	10.1	3	18	450	390	88.24	76.47	5.66	5.66
50	13.5	4	24	570	480	111.76	94.12	5.37	5.37
50	16.9	5	30	710	570	139.22	111.76	5.35	5.35
50	20.2	6	36	720	610	141.18	119.61	4.52	4.52
60	12.1	3	18	560	440	109.80	86.27	7.04	7.04
60	16.2	4	24	620	515	121.57	100.98	5.84	5.84
60	20.2	5	30	670	550	131.37	107.84	5.05	5.05
60	24.3	6	36	780	630	152.94	123.53	4.90	4.90

APPENDIX 3

Contents

	1 µm / tooth (set)	2 µm / tooth (set)	3 µm / tooth (set)	4 µm / tooth (set)
31 m/minute	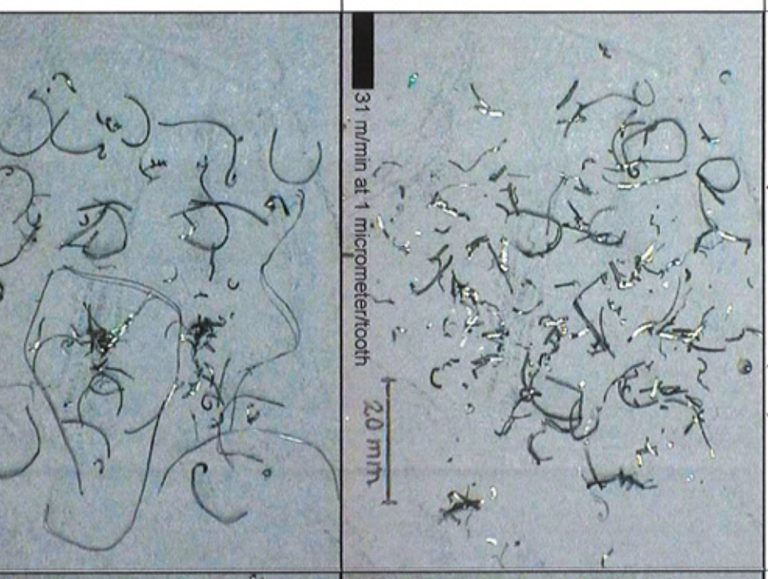	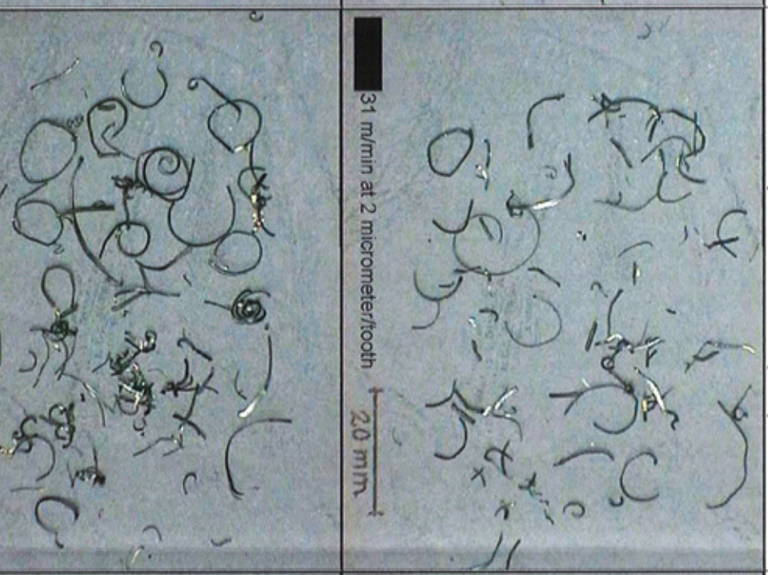	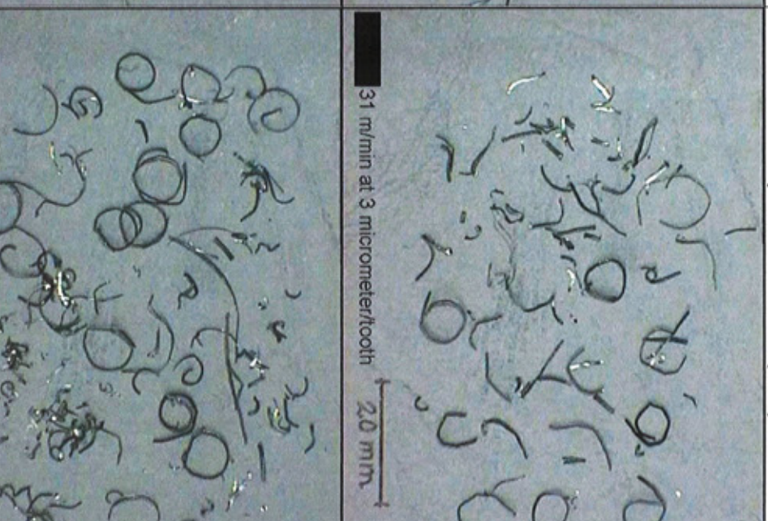	
50 m/minute				
70 m/minute				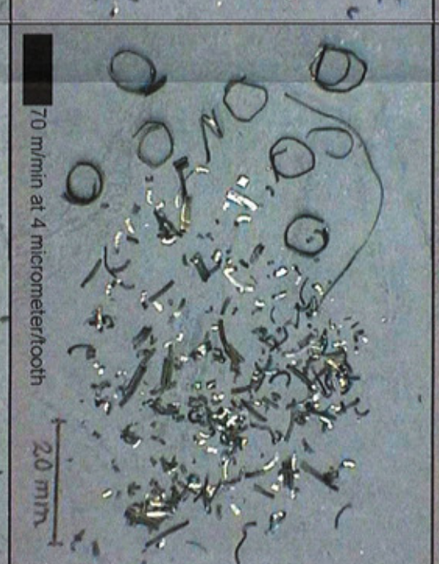
90 m/minute		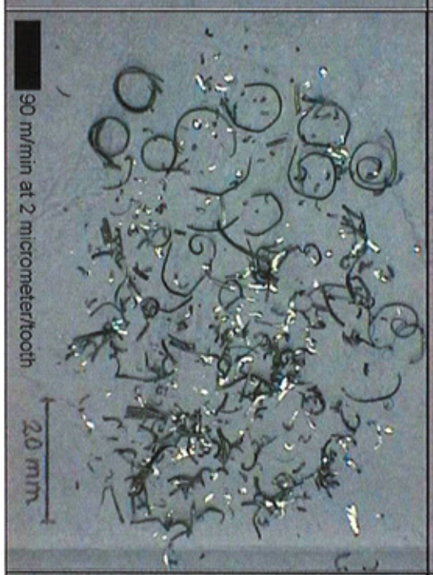		

Material: Workpiece-X Band: 3854-54-1.6-1.4/2-PHG-8900 Workpiece dimension: 254 x 77 mm (w x H)

	1 µm / tooth (set)	2 µm / tooth (set)	3 µm / tooth (set)
31 m/minute			
40 m/minute			
50 m/minute			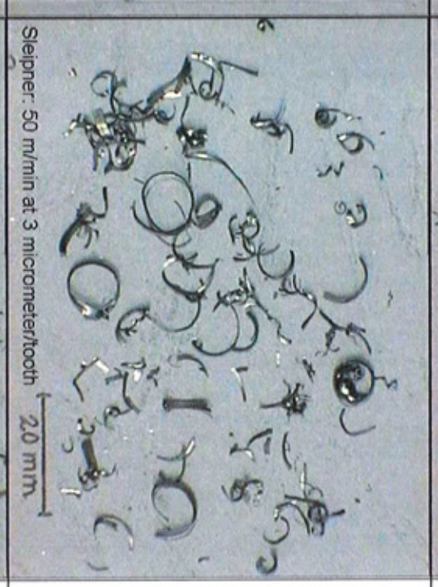
60 m/minute			

Material: Workpiece-Y Band: 3854-54-1.6-1.4/2-PHG-8900 Workpiece dimension: 254 x 77 mm (w x H)

	3 µm / tooth (set)	4 µm / tooth (set)	5 µm / tooth (set)	6 µm / tooth (set)
31 m/minute	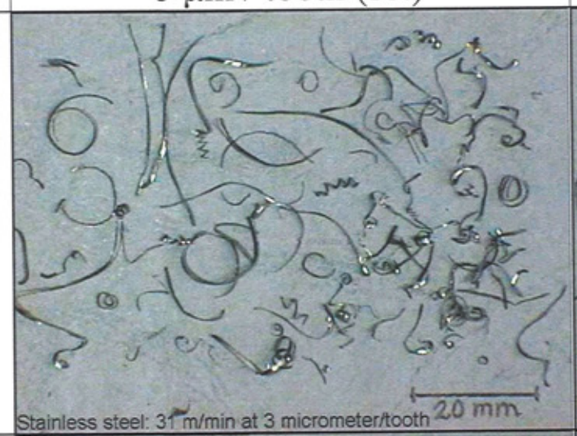	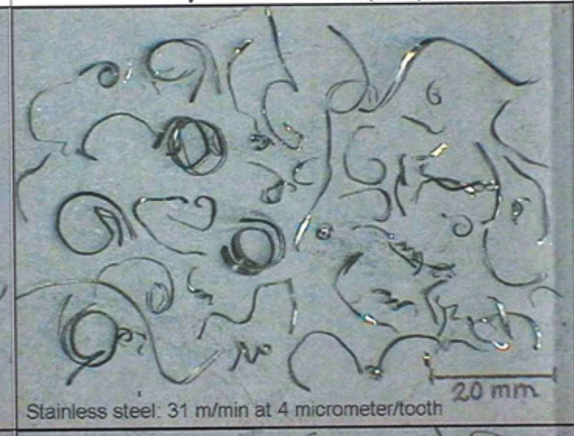	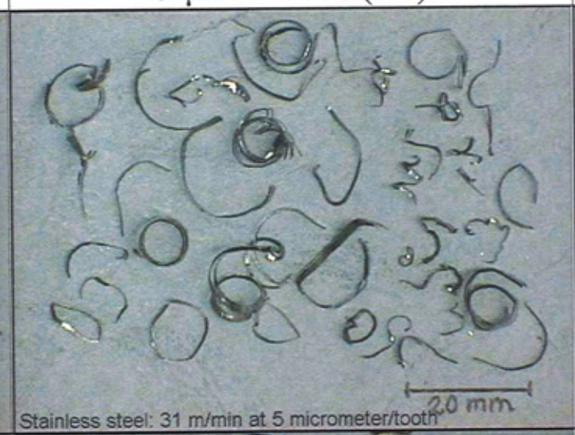	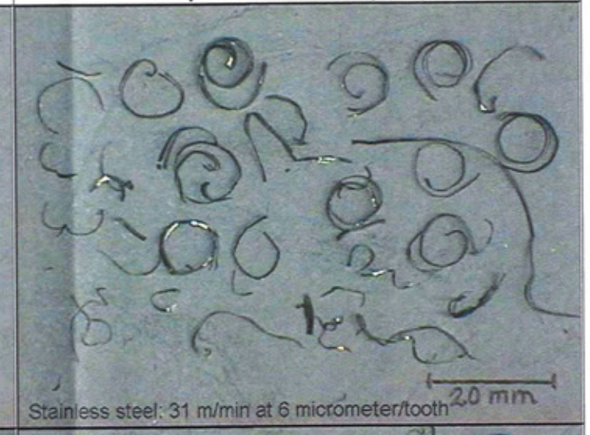
40 m/minute		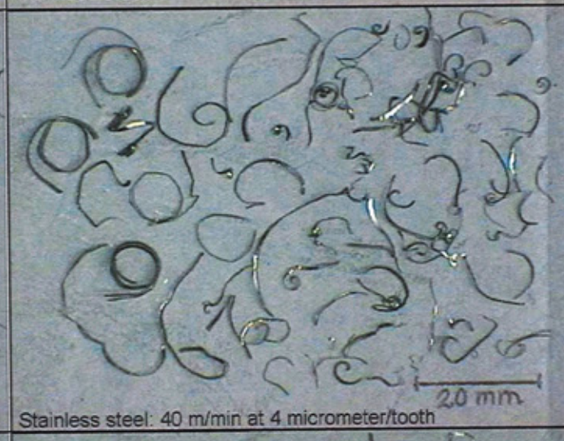	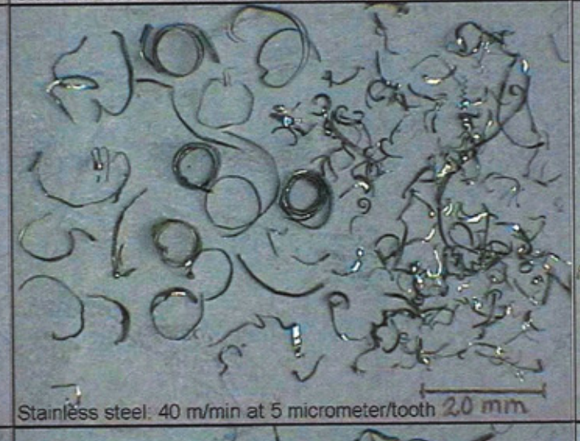	
50 m/minute	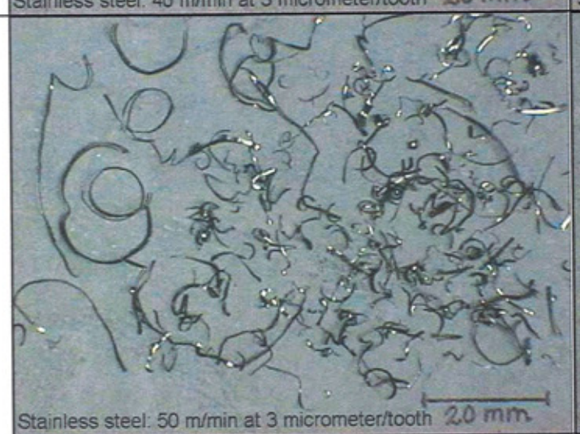		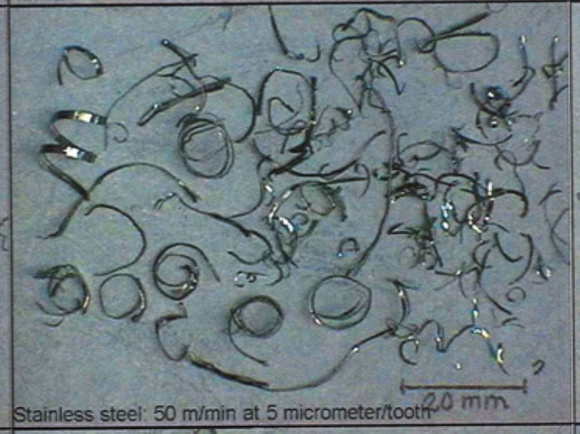	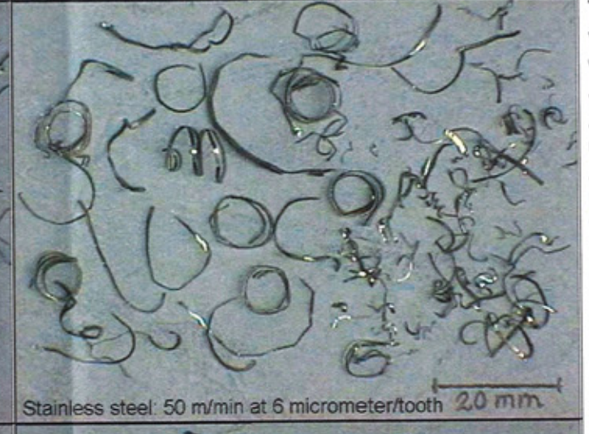
60 m/minute			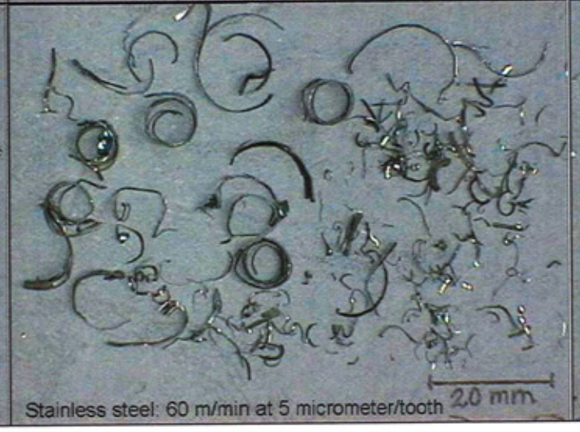	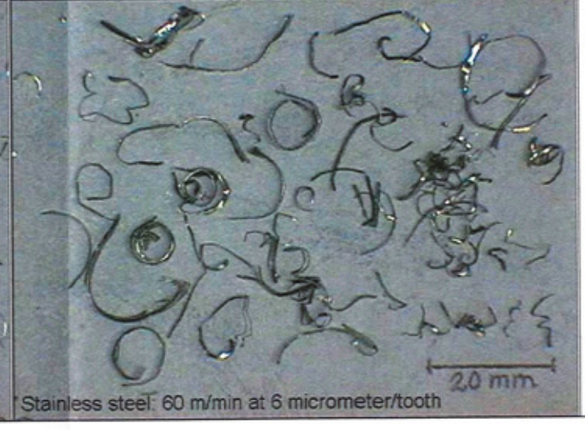

Material: Stainless steel 304L Band: 3854-54-1.6-1.4/2-PHG-8800(ground) dimension: 158 x 76 mm (w xH)

APPENDIX 4

Contents

Table 21 Single Tooth Test Results (STT-1)

Test No.	Chip number	Chip Weight (g)	$h_o = (\rho * W * L_{arc})$ Calculated Depth Of Cut Per Tooth (μm)	F_v Cutting force (N)	F_p Thrust force (N)	$E_{SP} = (F_v / A_c)$ Specific Cutting Energy (GJ/m^3)
1	1	0.02692	54.3	171.5	107.9	2.430
2	2	0.01357	27.4	108.5	-	3.046
3	3	0.01101	22.2	99.75	62.4	3.456
4	4	0.00348	7.02	54.25	39.65	5.945
5	5	0.00578	11.7	61.25	46.65	4.027
6	6	0.00412	8.31	52.5	37.9	4.860
7	7	0.00464	9.36	59.5	41.4	4.89
8	8	0.00363	7.33	52.5	41.4	5.509
9	9	0.00780	15.5	80.5	55.4	3.995
10	10	0.00465	9.38	68.25	44.9	5.597
11	11	0.00363	7.33	47.25	39.65	4.959
12	12	0.00621	12.5	84.0	62.4	5.169
13	13	0.00748	15.1	71.75	50.15	3.655
14	14	0.00544	11.0	63.0	48.4	4.406
15	15	0.00601	12.1	71.75	50.15	4.561
16	16	0.00473	9.55	78.75	50.15	6.343
17	17	0.00500	10.1	54.25	41.4	4.132
18	18	0.00219	4.42	38.5	30.9	6.700
19	19	0.00491	9.91	70.0	58.9	5.434
20	20	0.00732	14.8	63.0	48.4	3.274
21	21	0.00378	7.63	47.25	41.4	4.764
22	22	0.00288	5.81	43.75	34.4	5.792
23	23	0.00244	4.92	38.5	34.4	6.019
24	24	0.00364	7.35	63.0	43.15	6.593
25	25	0.00431	8.7	73.5	51.9	6.50
26	26	0.00203	4.1	42.0	32.65	7.9
27	27	0.00413	8.33	57.75	39.65	5.3
28	28	0.00311	6.3	49.0	30.9	5.98
29	29	0.00457	9.2	56.0	41.4	4.68
30	30	0.00363	7.3	50.75	37.9	5.35

Test No.	Chip number	Chip Weight (g)	$h_o = (\rho * W * L_{arc})$ Calculated Depth Of Cut Per Tooth (μm)	F_v Cutting force (N)	F_p Thrust force (N)	$E_{SP} = (F_v / A_c)$ Specific Cutting Energy (GJ/m^3)
31	31	0.00391	7.9	56.0	37.9	5.45
32	32	0.00160	3.2	42.0	20.4	10.1
33	33	0.00229	4.6	42.0	29.15	7.02
34	34	0.00177	3.6	38.5	29.15	8.2
35	35	0.00490	9.9	56.0	39.65	4.35
36	36	0.00108	2.2	36.75	25.65	12.85
37	37	0.00192	3.9	35.0	27.4	6.90
38	38	0.00158	3.2	42.0	27.4	10.1
39	39	0.00171	3.45	43.75	25.65	9.75
40	40	0.00456	9.2	52.5	36.15	4.39

APPENDIX 5

Contents

SKF Precision Cross-Slide Specification

Selection table for SKF positioning slides and tables

Slide design / Assessment criteria	Linear ball bearing slide	Profile rail slide	Dovetail slide
	 LZ	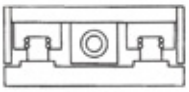 LLB	 S
Stroke			
Load-carrying capacity			
Running accuracy			
Speed			
Acceleration			
Preloading of guide			
Stiffness			
Friction			
Stick slip			
Damping			
Sensitivity to dirt fallout			
Stroke/Overall length			
Price			

Table 2

Precision slides with:			Compact cross table	Degree of Fulfilment 100 %
Crossed roller guides 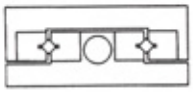 R	Needle roller guides 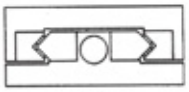 N	Dry sliding liners 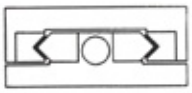 P	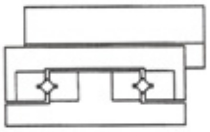 T	
				≥ 2.5 m
				≥ 150 kN
				≤ 3 µ/300 mm
				≥ 200 m/min
				≥ 150 m/m²
				high
				high
				≤ µ 0.002
				none
				high
				insensituve
				1 : 1
				low

Table 2

Characteristic features, speeds, preloading and stiffness

Specific features

Dovetail slides
- robust guides
- high load-carrying capacity
- for high transverse accelerations which make use of guides with rolling elements impossible (e. g. vibrations, shocks).
- excellent vibration damping
- insensitive to dirt fallout
- low preload properties
- danger of stick slip

Precision slides with R-N-P guides
A feature common to all three kinds of precision slide guides are rail guides for limited strokes.

Depending on type, crossed or needle rollers, which serve as rolling elements are housed in plastic or aluminium cages and move between the rails.

For rail guides with dry sliding liners, one of the two rails is laminated with plain bearing material based on PTFE, and the liner surface is ground. A hardened and ground steel rail serves as the opposing sliding area.

R-rail guides with crossed roller assemblies
- robust guidance for most applications
- high load-carrying capacity
- excellent value for the price

N-rail guides with needle roller assemblies
- greater dynamic load-carrying capacity
- greater stiffness
- more suited to short strokes
- less sensitive to shocks

P-rail guides with dry sliding liners
- for high transverse accelerations which make use of guides with rolling elements impossible (e. g. vibrations, shocks).
- for high-frequency or extremely short strokes
- good emergency running properties
- insensitive to dirt fallout
- very good vibration damping properties
- low preload properties

For selection of the slide system which best suits your special application, please see the chapter entitled "Choice of suitable slide system", pages 8 - 11.

Permissible speeds and accelerations

Dovetail slides
The dovetail slide permits speeds of up to **20 m/min** with small loads and adequate lubrication.

Precision slides and compact cross tables
The guides with rolling elements and limited travel incorporated in the **R-N- and T**-slides can be used with travel speeds of up to **2 m/s** and with accelerations of up to **10 m/s²**.

Depending on load, the dry sliding liners incorporated in the **P**-slides permit higher speeds and virtually unlimited accelerations.

If your wish to have even higher speeds and accelerations, please use SKF linear ball bearing and profile rail slides.

Preloading and Stiffness

Dovetail slides
The dovetail guide is aligned with an adjustable gib strip attached to one side of the slide top by means of matched pressure screws with zero play. Alignment is carried out at the factory and the pressure screws are afterwards secured with lacquer. While the stiffness of the dovetail guide can be increased by higher preloading of this adjustable gib strip, this drastically increases the friction factor of the slide and hence the feed force required.

If a system with greater stiffness and hence greater accuracy is required, guides with rolling elements should be used. Slides form the "Precision Slides" series have identical dimensions.

These slide types can be preloaded to a considerably greater extend without any great influence on feed forces.

Precision slides
Depending on guide and slide size, the **R-** and **N-**slides are preloaded exworks with preload screws mounted on one side of the slide top. The preload is around 3% to 10% of the static load rating.

Compact cross tables
Depending on guide an slide size, the T-slides are preloaded exworks with preload screws mounted on one side of the slide top. The preload is around 3% to 5% of the static load rating.

All slide systems
The stiffness of all slide systems can be increased in each individual case by greater preloads. However it should be borne in mind that:
- The size of the increase in stiffness is limited by the need to preserve the stability of the slide components. This applies in particular to the R-, N- and P-slides because of the need to preserve the stability of the slide top.
- Depending on the kind of load, stiffness also depends on deflection of the unsupported slide parts. Thus there can be an improvement if slides with a thick top are used.
- An increased in preloading is at the expense of ease of operation and even running.

Any change in preloading should be carried out only at our works.

Precision tables for motor drive RSS - NSS - PSS (Fig. 22)

For dimensions, please see Tables on pages 52-59.
This range is available in the following designs and widths:

- RSS (crossed roller guides) with width B 50 to 300
- NSS (needle roller guides) with width B 100 to 400
- PSS (dry sliding liner guides) with width B 100 to 300.

The slide top is longer than the base. The stroke is limited by endplates on both sides. It should be noted that the nominal stroke "S" given in the Tables is the maximum effective stroke between the endplates (buffers).

To avoid damage to the screw, this nominal stroke must not be fully used in operation the motor. The effective stroke, for example, between the limit switches must be selected by taking 5-20 mm less, depending on speed.

The slides are equipped with preloaded planetary roller screws which can be selected with various pitches (please see Tables on pages 64-65).

Drive screws are supported at the motor end by preloaded angular contact bearings in the table endplate.

These tables are provided with PUR polyester bellows as standard. As these bellows extend beyond the attachment surface of the bottom, a **base plate GP** can also be fitted. It can serve as:

- **Base plate** for standard assembly (slide bottom underneath)
- **Table plate** for overhead mounting (top above)
- **Intermediate plate** for cross table assembly with toothed belt plate drive

For the dimensions of this GP base plate, please see Table on page 74.

The bellows are overlapped on both sides by two cover sheets in the slide top. Limit and reference switches can be fitted under the right-hand side cover (see "Accessories" on page 69).

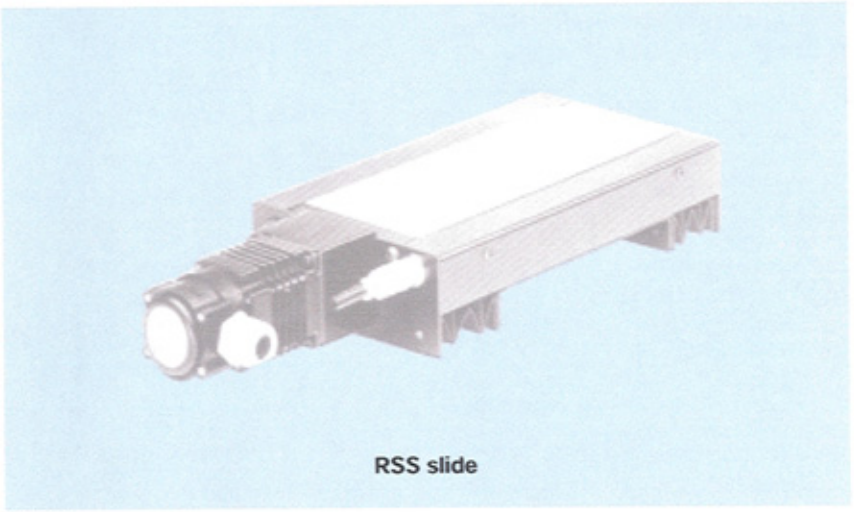

RSS slide

Fig. 22

These slides can be equipped with **standard motor flanges** including torsion-proof couplings (see "Accessories" on pages 76 and 78)

If space restrictions require it, the standard motors can also be attached on the left or right side using a **toothed belt drive** (see "Accessories" on pages 77 and 79).

Attachment of a direct linear measurement system is also possible (see "Accessories" on page 74).

The individual slides can also be assembled in various ways as cross tables or multiaxis units (see in the section on "Accessories", **"Cross table assembly"** on pages 70-71 and **"WG - WW mounting bracket"** on page 68).

R - N - P Precision slides: detailed design
B 50-100 (for product description page, see page 30)

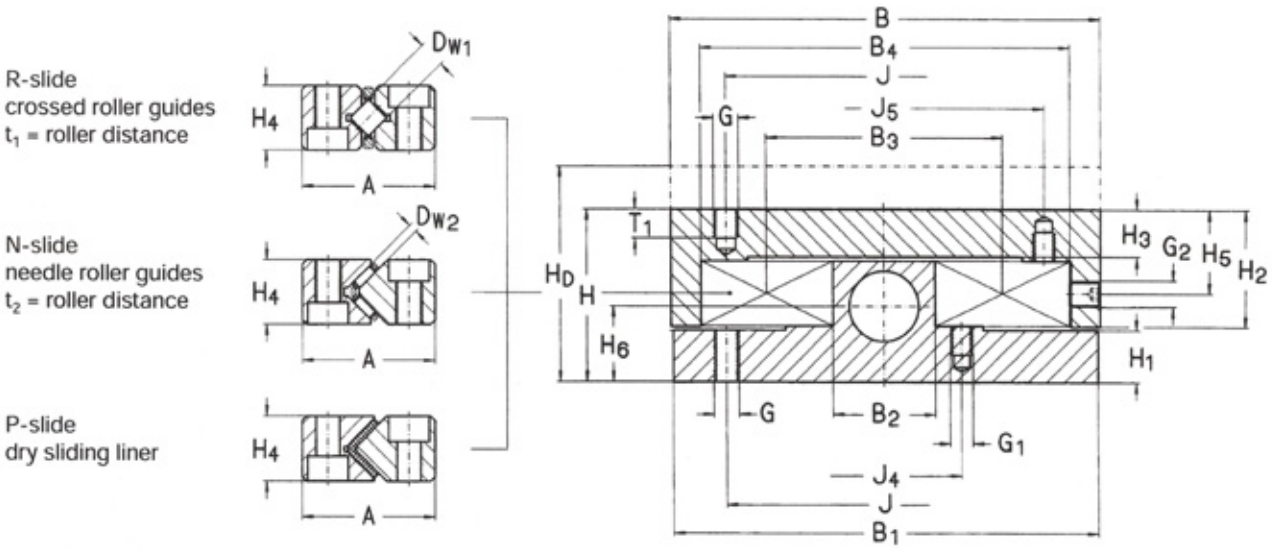

Dimensions

B	B_1	$D_{w1/t1}$	$D_{w2/t2}$	H	H_D [1]	A	B_2	B_3	B_4	H_1	H_2	H_3	H_4	H_5	H_6
mm															
50	49	4/6.25	-	25	35	18	8.5	26.5	44.5	7.5	17	7	8	11.5	12.3
75	74	4/6.25	-	32	44	18	23	41	59	10.5	21	8.5	8	13	15
100	99	8/11	2/3.75	40	50	31	24	55	86	12	27.5	11	15	19.5	15.5

1) Only for "thick" D top

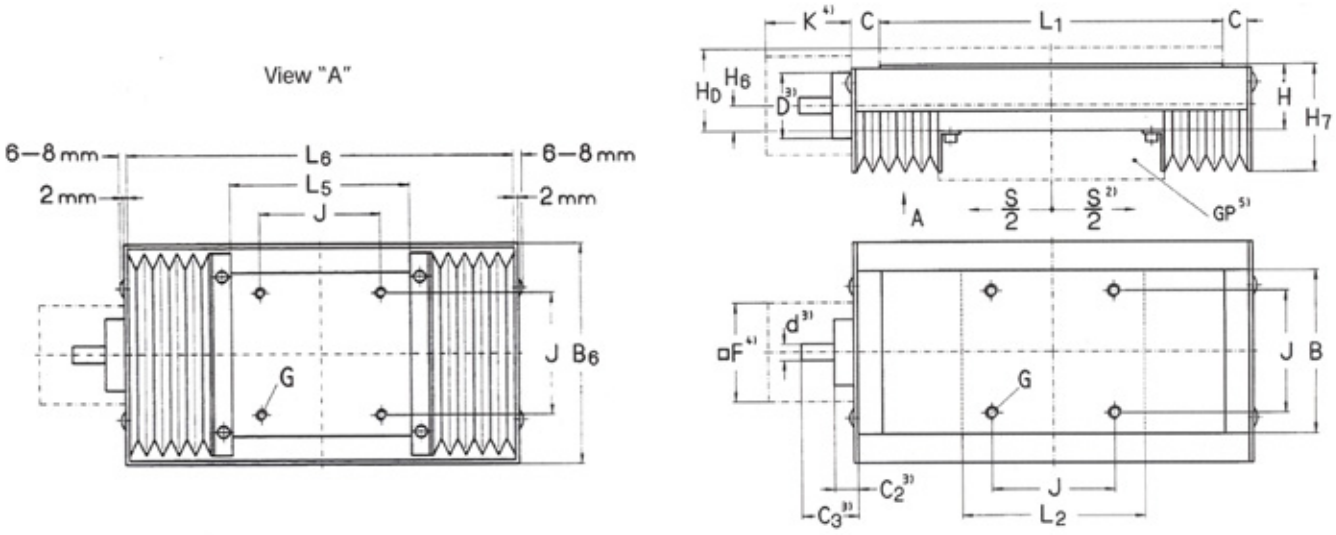

For detailed design, see page 34
For screw selection, see page 64

Dimensions

B	H	H_D 1)	L_1	L_2	Nominal stroke $S^{2)}$	C	B_6	G	H_6	H_7	J	L_5	L_6
mm													
			260	210	**50**							160	290
			310	260	**50**							210	340
			360	310	**50**							260	390
			310	210	**100**							160	340
100	40	50	**360**	260	**100**	15	164	M6	15.5	65	74	210	390
			410	310	**100**							260	440
			360	210	**150**							160	390
			410	260	**150**							210	440
			460	310	**150**							260	490
			460	260	**200**							210	490

1) Only for "thick" top: see order codes
2) Nominal stroke = max. stroke between the end stops.
Effective stroke between the limit switches 5-20 mm shorter, depending on speed
3) For screw abutment dimensions, see page 65
4) For dimensions, see motor flange Table, pages 76 and 78
5) GP = base plate, see page 72

Attachment of limit and reference switches for precision tables
The slides of the series types RSS - NSS - PSS and RSAS - NSAS - PSAS can be equipped with integrated limit and reference switches.

Limit switches
Two limit switches are fitted under the right-hand plate cover of the tabletop on a rail, 5 mm from the mechanical dead ends. They can be adjusted by approximately 20 mm, and are activated by a control cam in the middle of the base.

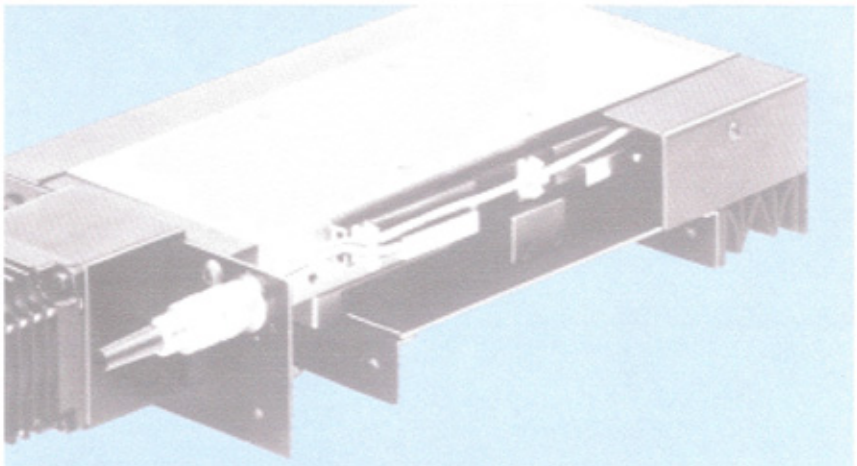

End-switch attachment with inductive switches type EEI 2

Fig. 25

Reference switch
The reference switch is fitted under the same cover and on the same rail as the limit switch. It is 20 mm from the motorside limit switch and is adjustable by around ±20 mm.

A selection is possible from among:
- mechanical limit switches with 2 m free connection cable per switch
- mechanical limit switches, all wired into an 8-pin plug (IP64) on the motor side
- inductive limit or reference switches with 2 m free connection cable per switch
- inductive limit or reference switches all wired into an 8-pin plug (IP64) on the motor side.

Technical Data	Mechanical switch	Inductive switch
Switch accuracy (at const. speed and temperature)	± 0.1 mm	± 0.01 mm
Supply voltage	AC: bis 250V DC: bis 125 V	10 - 30 V DC
Max. switching current	AC: 500 mA DC: 400 mA	200 mA
Normally closed (NC) or normally open (NO)	no restrictions	NC or NO
Output type	-	PNP or NPN
Protection type	IP 67	IP 67
Design	DIN 41635 design B	Special design ☐ 8x40

Warning:
Unless otherwise indicated in the order, we use inductive switches as
- limit switch: PNP/NC
- reference switch: PNP/NO

For order designation: please see order codes, page 94

APPENDIX 6

Contents

Engineering drawings of the single tooth test rig

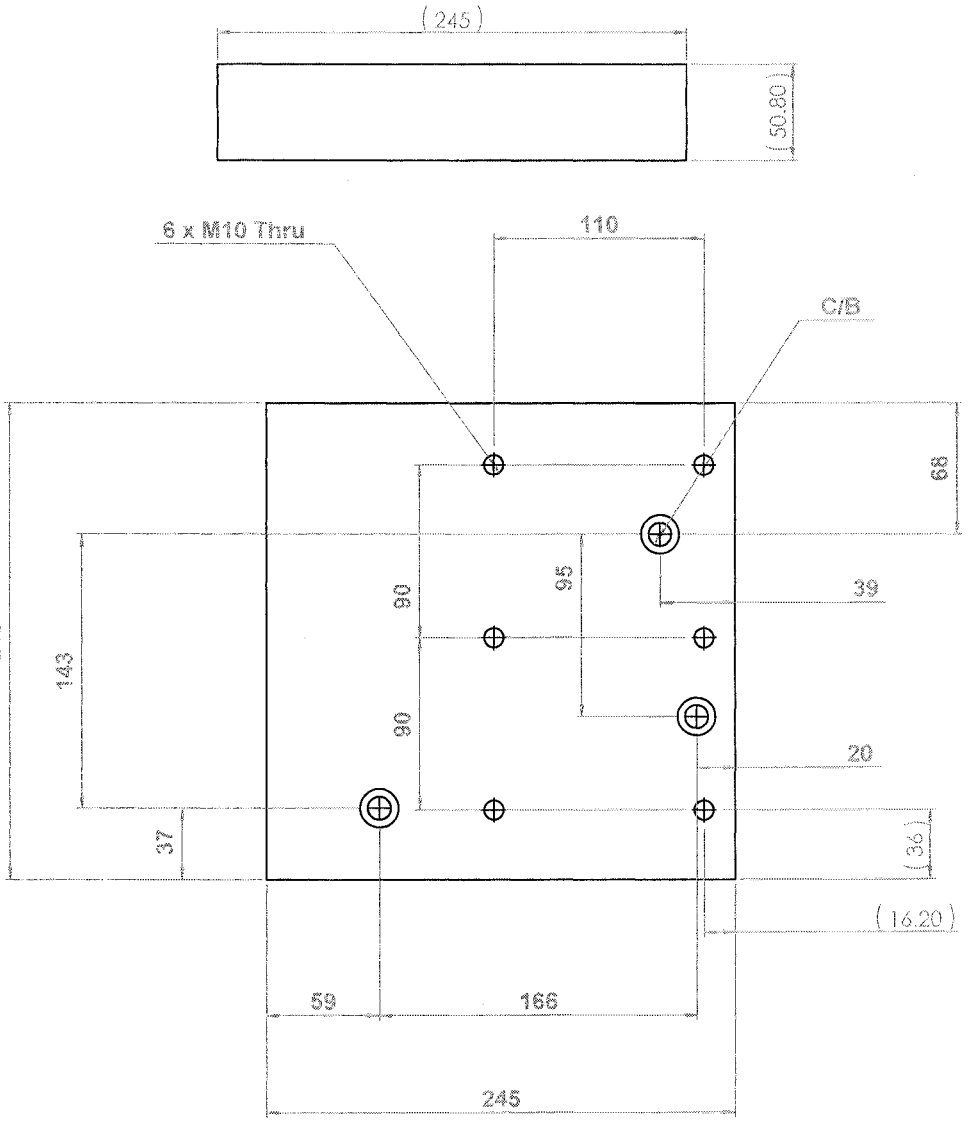

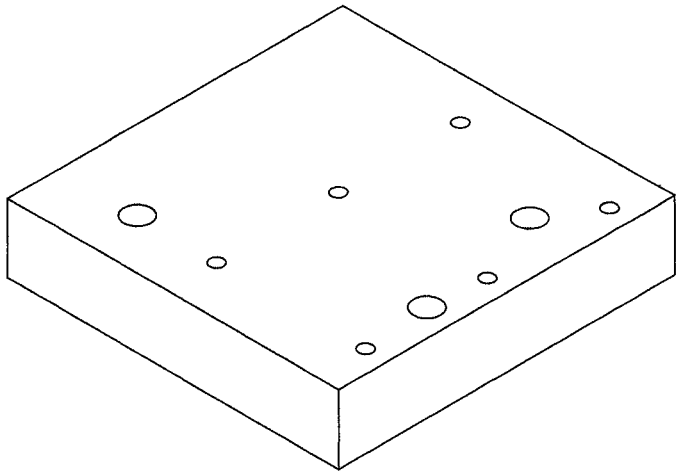

UNLESS OTHERWISE SPECIFIED
DIMENSIONS ARE IN MM
TOLERANCES ARE
± 0.1 MM, ANGLES ±0.25°
ALL M/Ced FACES TO 1.6 um N7

SCHOOL OF ENGINEERING

UNIVERSITY of NORTHUMBRIA at NEWCASTLE

Sheet 1Sheet1

Material :

Scale 1:2.5

Description

A3 Landscape

Date :20/11/2001

Title:
Base Plate

Name

(D)

Third Angle Projection, Dimensions for reference only use CAD Data
All edges, corners with 0.5mm Radius unless stated,
Draft Angle 1°

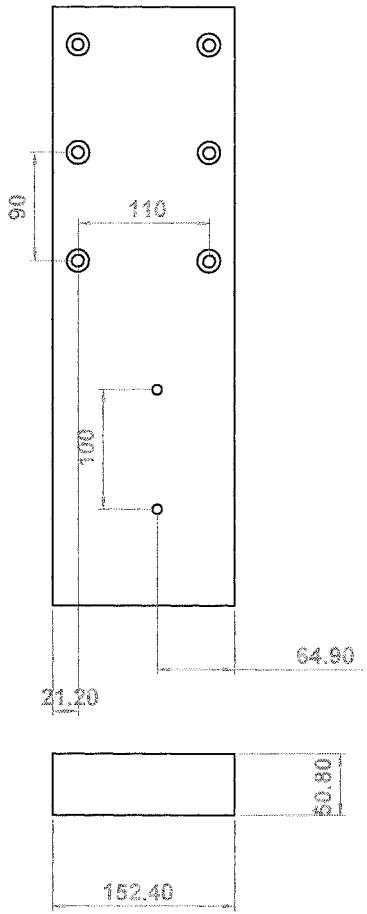

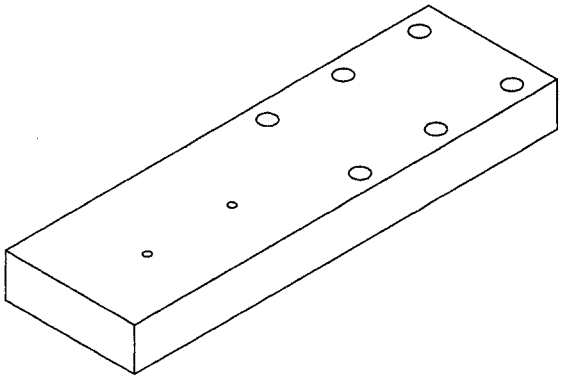

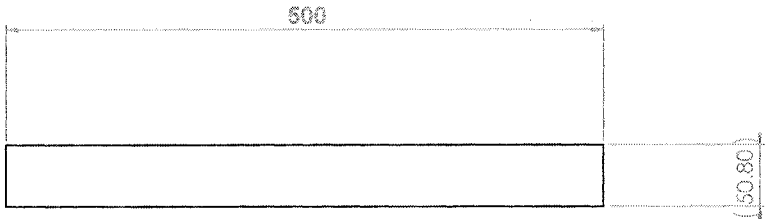

UNLESS OTHERWISE SPECIFIED
DIMENSIONS ARE IN MM
TOLERANCES ARE
± 0.1 MM, ANGLES ±0.25°
ALL M/Ced FACES TO 1.6 um N7

SCHOOL OF ENGINEERING

UNIVERSITY of NORTHUMBRIA at NEWCASTLE

Sheet 1Sheet1

Material :

Scale 1:4

Description

A3 Landscape

Date :20/11/2001

Title:

Mounting Platform

Name

(D)

Third Angle Projection, Dimensions for reference only use CAD Data
All edges, corners with 0.5mm Radius unless stated,
Draft Angle 1°

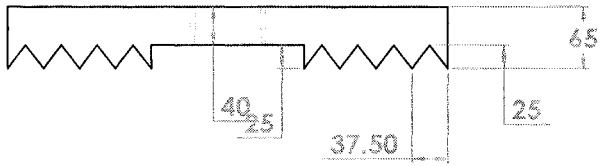

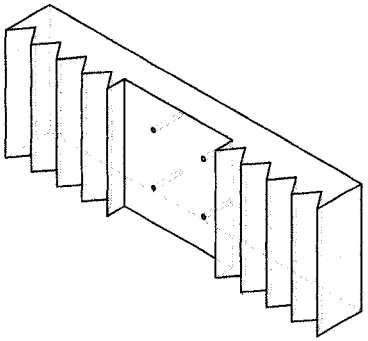

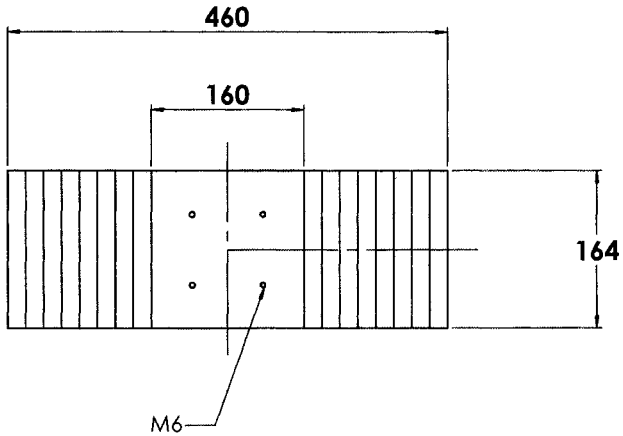

UNLESS OTHERWISE SPECIFIED
DIMENSIONS ARE IN MM
TOLERANCES ARE
± 0.1 MM, ANGLES ±0.25°
ALL M/Ced FACES TO 1.6 um N7

SCHOOL OF ENGINEERING

UNIVERSITY of NORTHUMBRIA at NEWCASTLE

Sheet 1Cross Slide

Material :

Scale 1:5

Description

A3 Landscape

Date : 26/06/2001 FILE:DYNA_DRAWINGS

Title:
Cross Slide

Name

D

SolidWorks Educational License
Instructional Use Only
Third Angle Projection, Dimensions for reference only use CAD Data
All edges, corners with 0.5mm Radius unless stated,
Draft Angle 1°

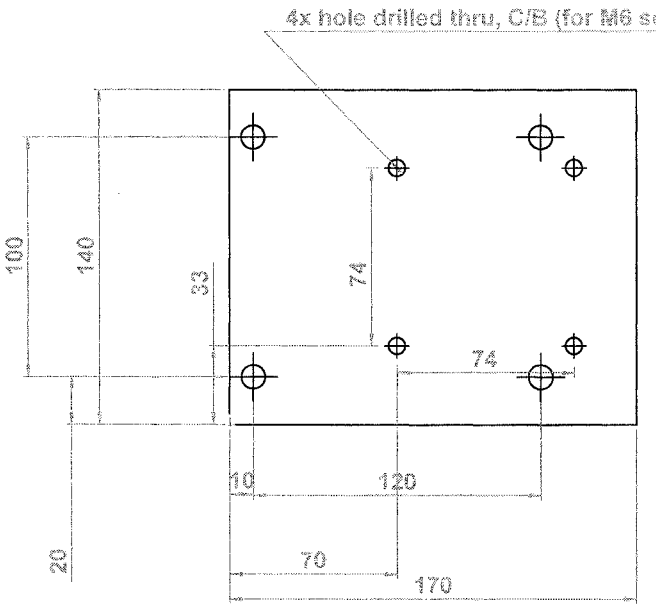

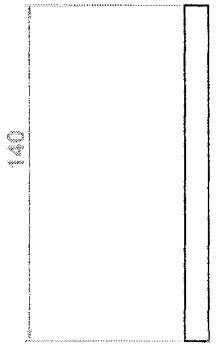

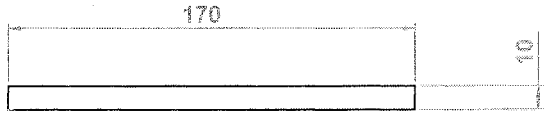

UNLESS OTHERWISE SPECIFIED
DIMENSIONS ARE IN MM
TOLERANCES ARE
± 0.1 MM, ANGLES ±0.25°
ALL M/Ced FACES TO 1.6 um N7

SCHOOL OF ENGINEERING

UNIVERSITY OF NORTHUMBRIA at NEWCASTLE

Sheet 1Dynamometer mounting pla Description

Material : A3 Landscape

Date : 26/06/2001 FILE:dymounting bloc

Title:
Dynamometer mounting plate

Scale 1:2

Name Anand

(D)

Third Angle Projection, Dimensions for reference only use CAD Data
All edges, corners with 0.5mm Radius unless stated,
Draft Angle 1°

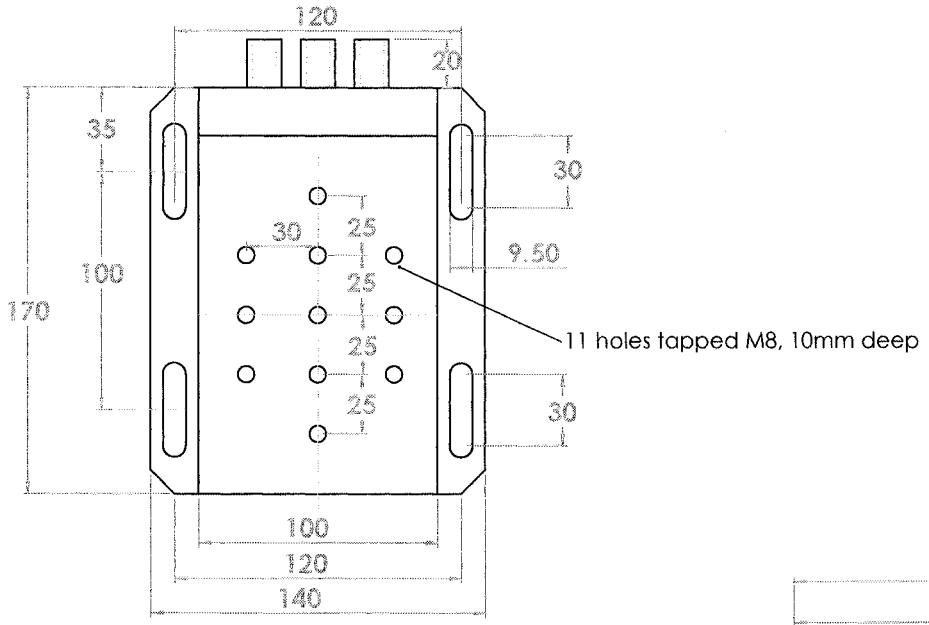

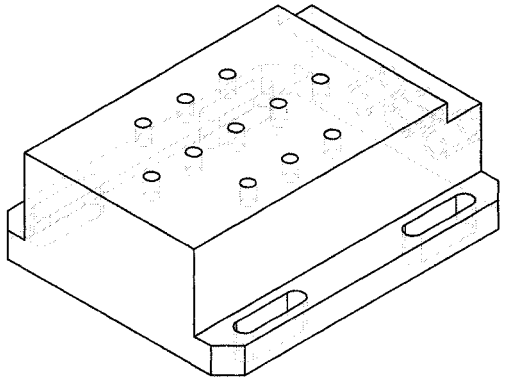

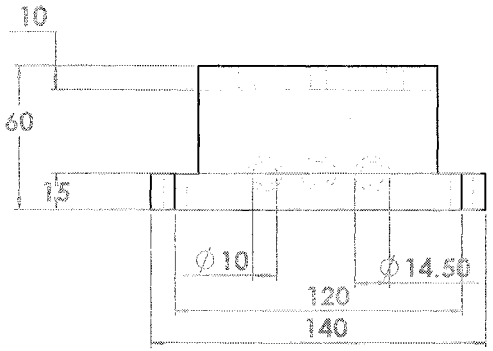

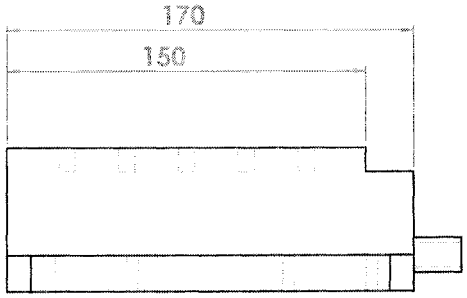

UNLESS OTHERWISE SPECIFIED
DIMENSIONS ARE IN MM
TOLERANCES ARE
± 0.1 MM, ANGLES ±0.25°
ALL M/Ced FACES TO 1.6 um N7

SCHOOL OF ENGINEERING

UNIVERSITY of NORTHUMBRIA at NEWCASTLE

Sheet 1Dynamometer

Material :

Scale 1:2

Description

A3 Landscape

Date : 26/06/2001 FILE:DYNA_DRAWINGS

Title:
Dynamometer

Name

(D)

SolidWorks Educational License
Instructional Use Only
Third Angle Projection, Dimensions for reference only use CAD Data
All edges, corners with 0.5mm Radius unless stated,
Draft Angle 1°

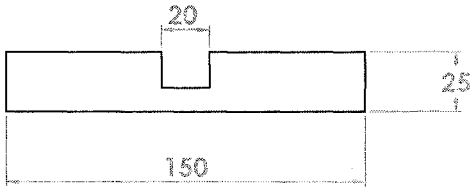

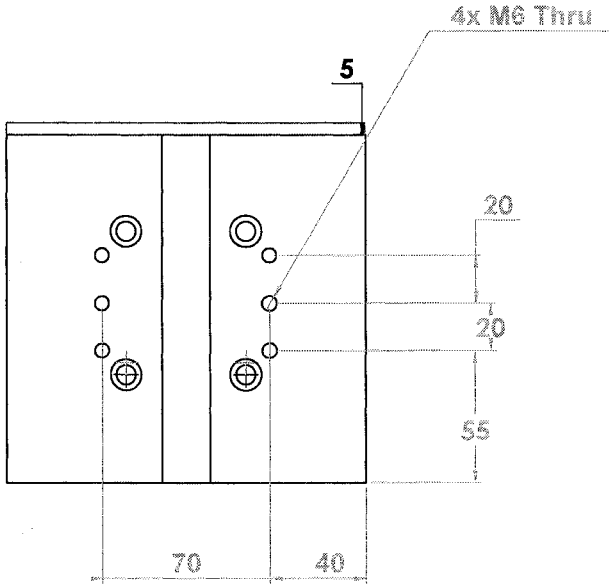

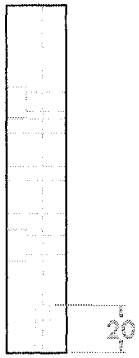

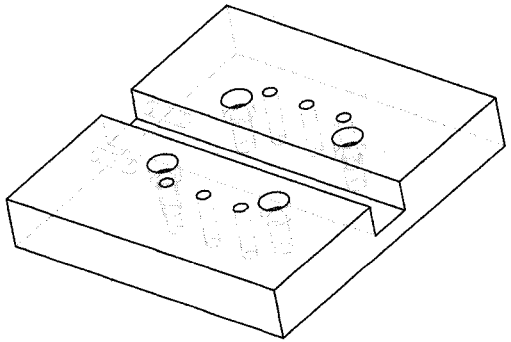

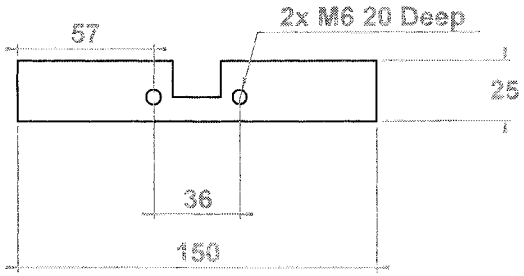

SolidWorks Educational License
Instructional Use Only
Third Angle Projection, Dimensions for reference only use CAD Data
All edges, corners with 0.5mm Radius unless stated,
Draft Angle 1°

UNLESS OTHERWISE SPECIFIED
DIMENSIONS ARE IN MM
TOLERANCES ARE
± 0.1 MM, ANGLES ±0.25°
ALL M/Ced FACES TO 1.6 um N7

SCHOOL OF ENGINEERING
UNIVERSITY OF NORTHUMBRIA at NEWCASTLE

Material : A3 Landscape

Description

Date : 26/06/2001 FILE:DYNA_DRAWINGS

Title: Tool Holder-Part 1

Scale 1:2

Name

D

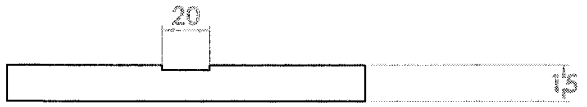

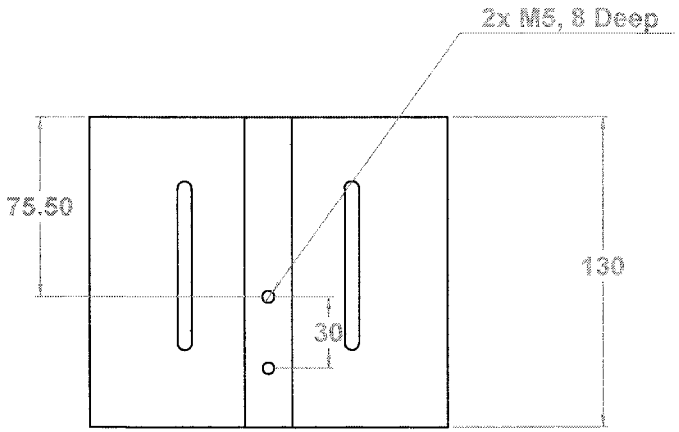

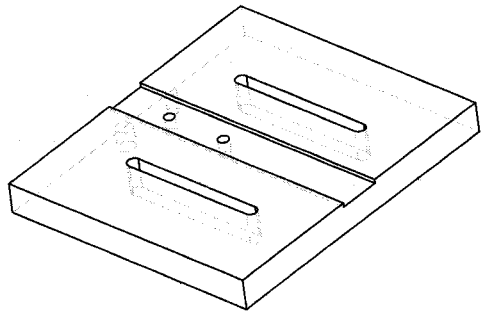

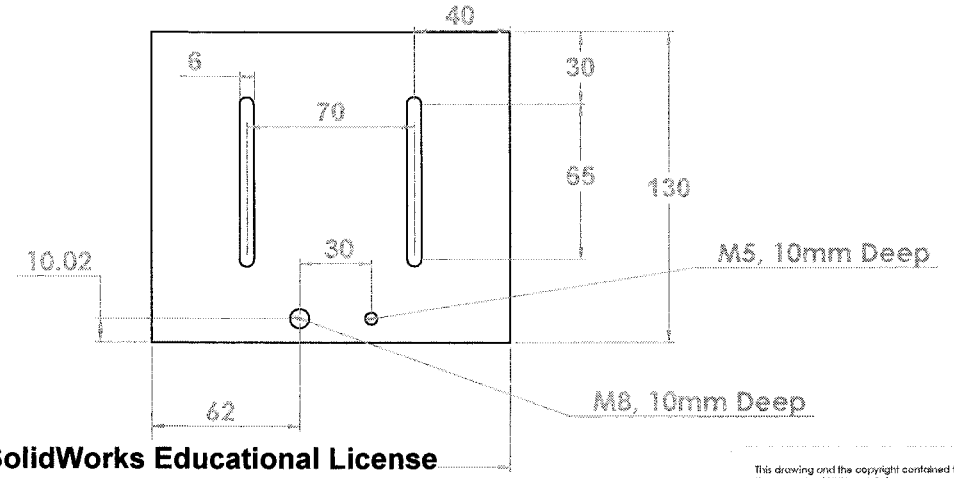

SolidWorks Educational License
Instructional Use Only

Third Angle Projection, Dimensions for reference only use CAD Data
All edges, corners with 0.5mm Radius unless stated,
Draft Angle 1°

UNLESS OTHERWISE SPECIFIED
DIMENSIONS ARE IN MM
TOLERANCES ARE
± 0.1 MM, ANGLES ±0.25°
ALL M/Ced FACES TO 1.6 um N7

SCHOOL OF ENGINEERING

UNIVERSITY of NORTHUMBRIA at NEWCASTLE

Sheet 1Tool Holder-Part2

Material :

Scale 1:2

Description

A3 Landscape

Date : 26/06/2001 FILE:DYNA_DRAWINGS

Title:
Tool Holder-Part2

Name

(D)

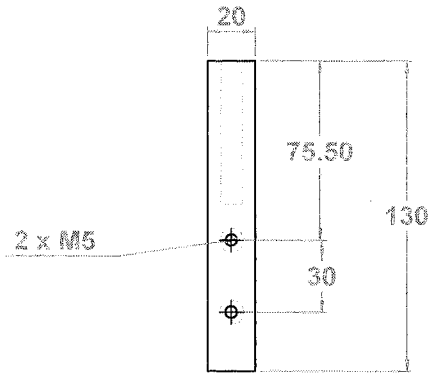

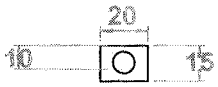

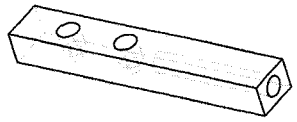

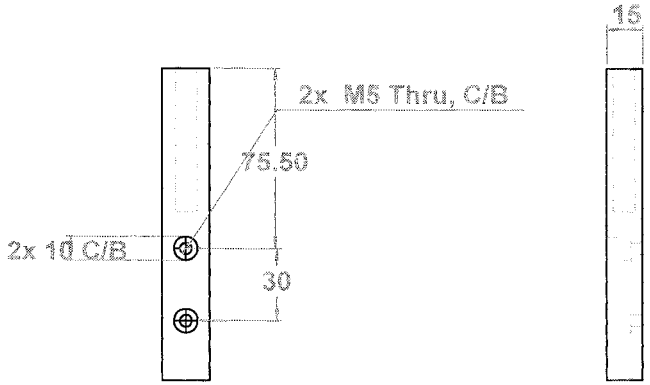

SolidWorks Educational License
Instructional Use Only
Third Angle Projection, Dimensions for reference only use CAD Data
All edges, corners with 0.5mm Radius unless stated,
Draft Angle 1°

UNLESS OTHERWISE SPECIFIED
DIMENSIONS ARE IN MM
TOLERANCES ARE
± 0.1 MM, ANGLES ±0.25°
ALL M/Ced FACES TO 1.6 um N7

SCHOOL OF ENGINEERING
UNIVERSITY of NORTHUMBRIA at NEWCASTLE

Sheet 1Part 2-2-1

Material :

Scale 1:2

Description

A3 Landscape

Date : 26/06/2001 FILE:DYNA_DRAWINGS

Title:
Part 2-2-1

Name

D

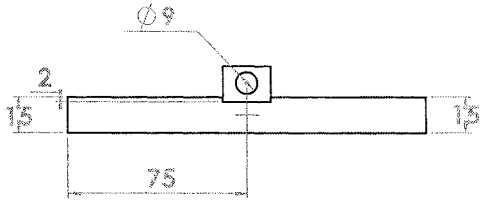

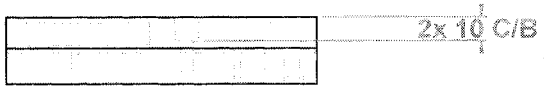

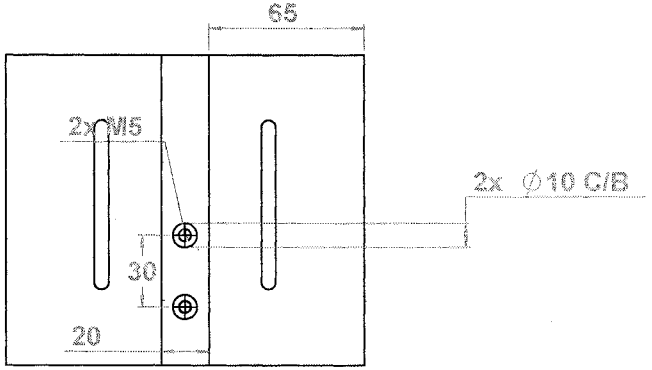

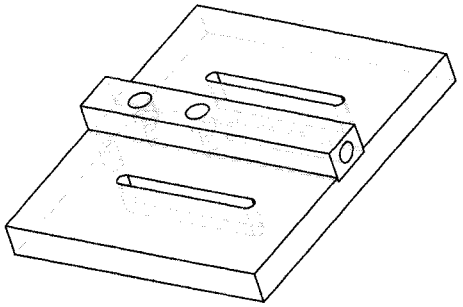

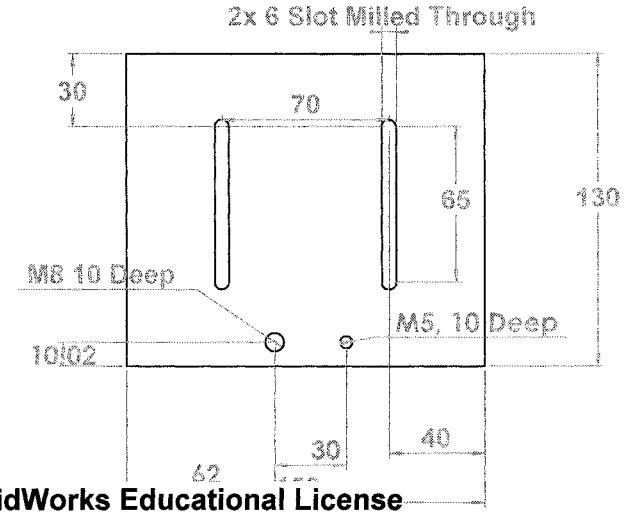

SolidWorks Educational License
Instructional Use Only

Third Angle Projection, Dimensions for reference only use CAD Data
All edges, corners with 0.5mm Radius unless stated,
Draft Angle 1°

UNLESS OTHERWISE SPECIFIED
DIMENSIONS ARE IN MM
TOLERANCES ARE
± 0.1 MM, ANGLES ±0.25°
ALL M/Ced FACES TO 1.6 um N7

SCHOOL OF ENGINEERING

UNIVERSITY of NORTHUMBRIA at NEWCASTLE

Sheet 1Tool Holder Part 2-Assembly

Description

Material : A3 Landscape

Date : 26/06/2001 FILE:DYNA_DRAWINGS

Title:
Tool Holder Part 2-Assembly

Scale 1:2

Name

(D)

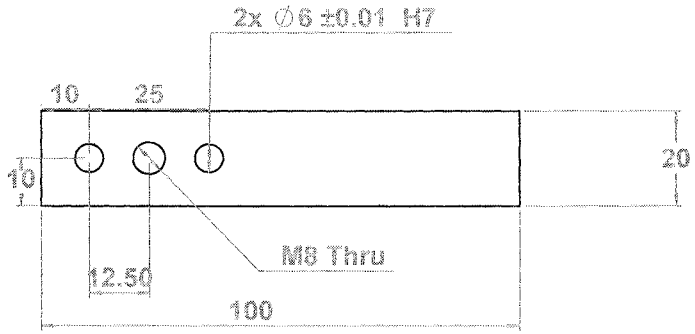

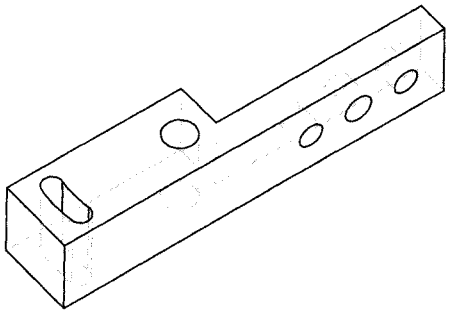

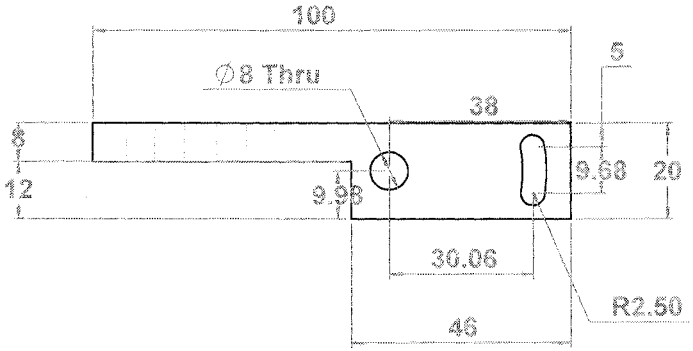

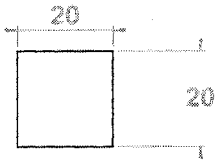

UNLESS OTHERWISE SPECIFIED
DIMENSIONS ARE IN MM
TOLERANCES ARE
± 0.1 MM, ANGLES ±0.25°
ALL M/Ced FACES TO 1.6 um N7

SCHOOL OF ENGINEERING

UNIVERSITY OF NORTHUMBRIA at NEWCASTLE

Sheet 1Tool Holder-Part 3

Material :

Scale 1:1

Description

A3 Landscape

Date : 26/06/2001 FILE:DYNA_DRAWINGS

Title:

Tool Holder-Part 3

Name

(D)

SolidWorks Educational License

Instructional Use Only

Third Angle Projection, Dimensions for reference only use CAD Data
All edges, corners with 0.5mm Radius unless stated,
Draft Angle 1°

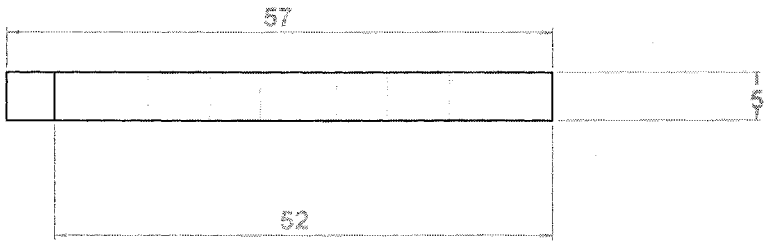

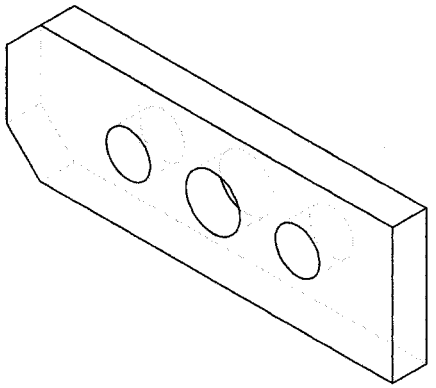

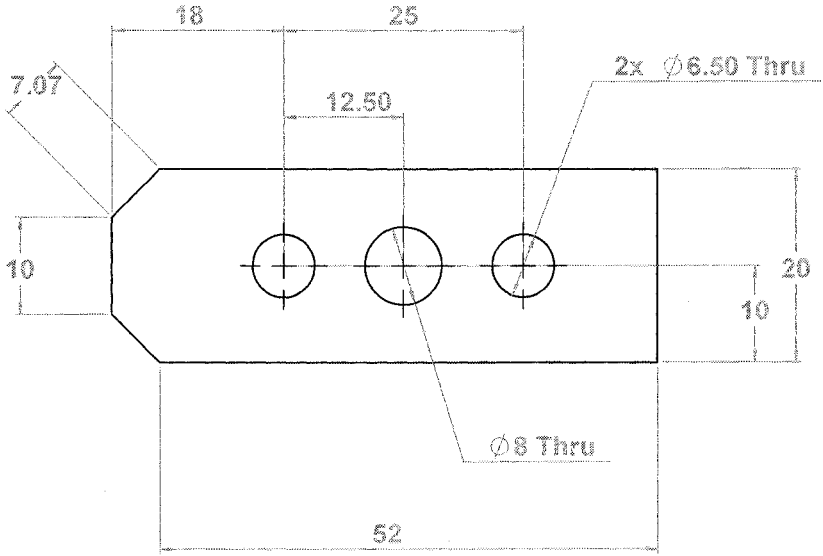

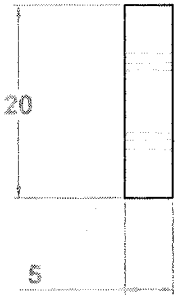

UNLESS OTHERWISE SPECIFIED
DIMENSIONS ARE IN MM
TOLERANCES ARE
± 0.1 MM, ANGLES ±0.25°
ALL M/Ced FACES TO 1.6 um N7

SCHOOL OF ENGINEERING

UNIVERSITY of NORTHUMBRIA at NEWCASTLE

Sheet 1Tool Holder-Part 4

Material :

Scale 2:1

Description

A3 Landscape

Date : 26/06/2001 FILE:DYNA_DRAWINGS

Title:
Tool Holder-Part 4

Name

(D)

SolidWorks Educational License

Instructional Use Only

Third Angle Projection, Dimensions for reference only use CAD Data
All edges, corners with 0.5mm Radius unless stated,
Draft Angle 1°

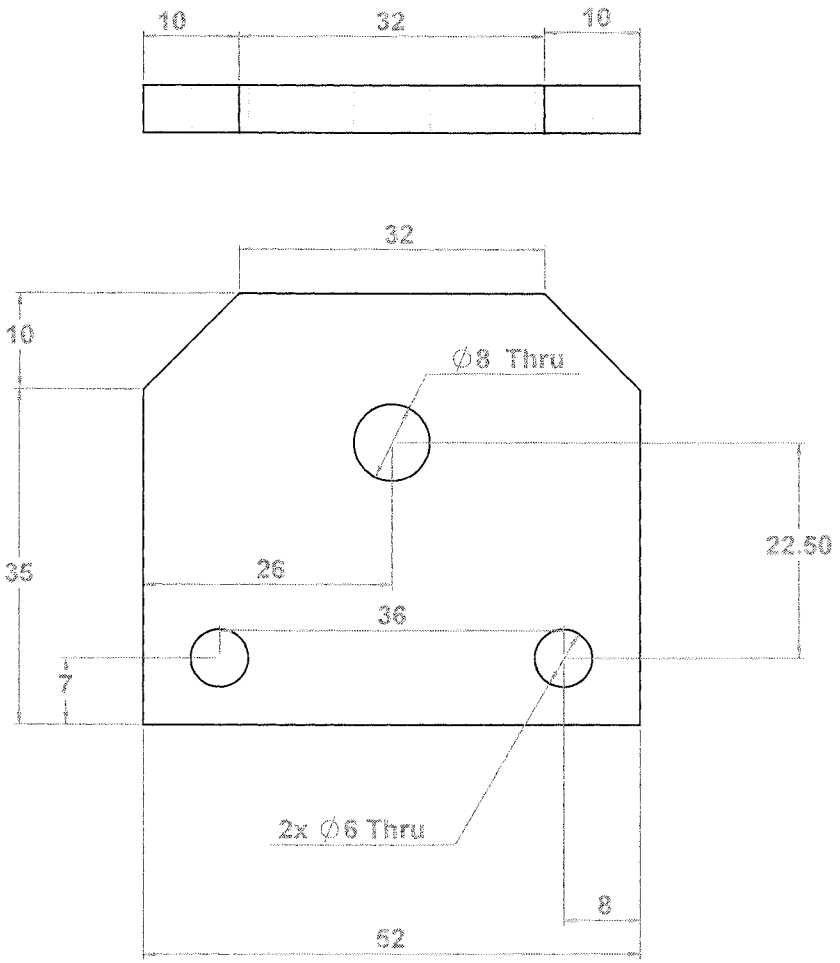

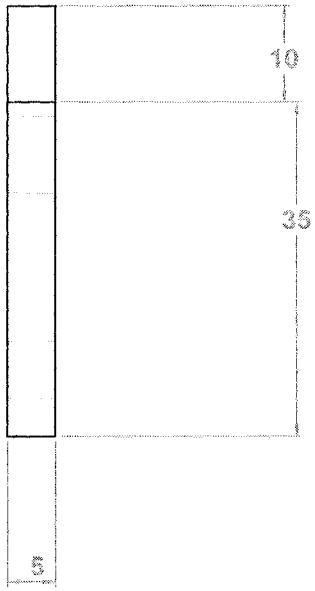

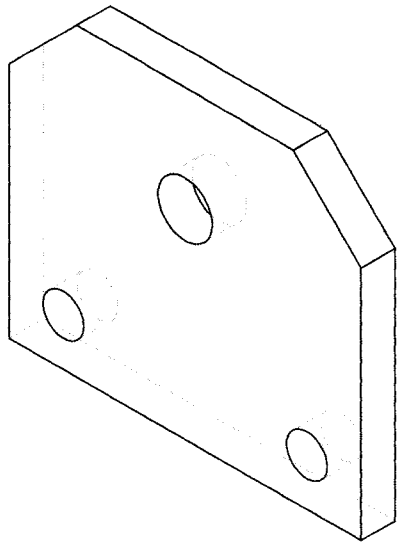

UNLESS OTHERWISE SPECIFIED
DIMENSIONS ARE IN MM
TOLERANCES ARE
± 0.1 MM, ANGLES ±0.25°
ALL M/Ced FACES TO 1.6 um N7

SCHOOL OF ENGINEERING

UNIVERSITY of NORTHUMBRIA at NEWCASTLE

Sheet 1Tool Holder-Part 5

Material :

Scale 2:1

Description

A3 Landscape

Date : 26/06/2001 FILE:DYNA_DRAWINGS

Title:

Tool Holder-Part 5

Name

(D)

SolidWorks Educational License

Instructional Use Only

Third Angle Projection, Dimensions for reference only use CAD Data
All edges, corners with 0.5mm Radius unless stated,
Draft Angle 1°

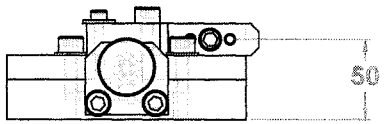

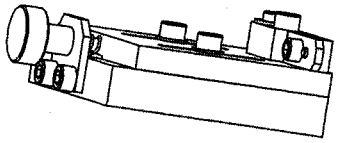

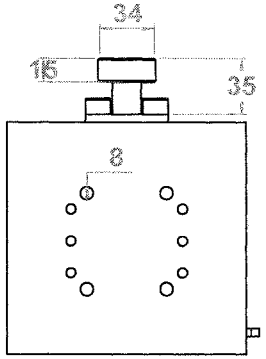

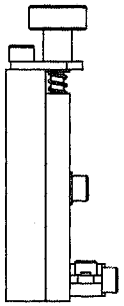

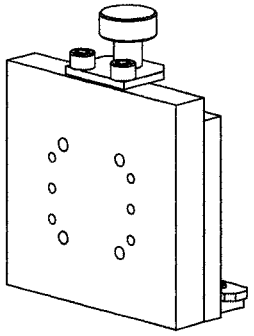

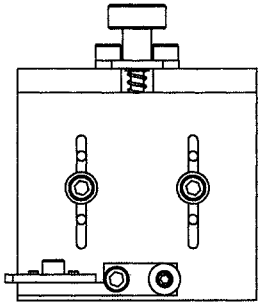

SolidWorks Educational License

Instructional Use Only

Third Angle Projection, Dimensions for reference only use CAD Data
All edges, corners with 0.5mm Radius unless stated,
Draft Angle 1°

UNLESS OTHERWISE SPECIFIED
DIMENSIONS ARE IN MM
TOLERANCES ARE
± 0.1 MM, ANGLES ±0.25°
ALL M/Ced FACES TO 1.6 um N7

SCHOOL OF ENGINEERING

UNIVERSITY of NORTHUMBRIA at NEWCASTLE

Sheet 1Tool Holder Assembly

Material :

Scale 1:3

Description

A3 Landscape

Date : 26/06/2001 FILE:DYNA_DRAWINGS

Title:

Tool Holder Assembly

Name

(D)

APPENDIX 7

Contents

Speed setting on the lathe

Speed setting for single tooth test

Position to place
test-piece on faceplate
to achieve cutting speed

V_b m/min	R.P.M	d mm
30	20	157
40	40	148
50	57	133
60	57	159
70	80	130
90	115	120

d = Workpiece position on faceplate

r.p.m = Spindle speed of lathe

V_b = Cutting speed

APPENDIX 8

Contents

TABLE 22. SINGLE TOOTH TEST DATA SHEET (Workpiece-X)

Band Speed V_b (m\min)	Set Depth of cut/tooth δas (μm)	E_{SP-t} (GJ/m3)	Cutting Force F_{v-fbt} (N)	Thrust Force F_{p-stt} (N)	Cutting force /tooth **(Calculated using Equation 5.5)** F_{v-fbt} (N)	Thrust force/tooth **(Calculated using Equation 5.5)** F_{p-stt} (N)
31	6	13.13	126	106	68.04	57.24
31	12	8.39	161	124	86.94	66.96
31	18	6.60	190	152	102.6	82.08
31	24	5.86	225	190	121.5	102.6
50	6	11.67	112	82	60.48	44.28
50	12	7.71	148	107	79.92	57.78
50	18	6.74	194	146	104.76	78.84
50	24	5.52	212	165	114.48	89.1
70	6	10.10	97	75	52.38	40.5
70	12	7.71	148	107	79.92	57.78
70	18	6.28	181	138	97.74	74.52
70	24	5.49	211	152	113.94	82.08
90	6	9.17	88	72	47.52	38.88
90	12	6.72	129	107	69.66	57.78
90	18	5.56	160	133	86.4	71.82
90	24	5.16	198	142	106.92	76.68

TABLE 23 SINGLE TOOTH TEST DATA SHEET (Workpiece-Y)

Band Speed V_b (m\min)	Set Depth of cut/tooth δas (μm)	E_{SP-t} (GJ/m3)	Cutting Force F_{v-fbt} (N)	Thrust Force F_{p-stt} (N)	Cutting force /tooth **(Calculated using Equation 5.5)** F_{v-fbt} (N)	Thrust force/tooth **(Calculated using Equation 5.5)** F_{p-stt} (N)
31	6	8.13	78	46	42.12	24.84
31	9	7.99	115	77	62.1	41.58
31	12	6.56	126	80	68.04	43.2
31	15	6.46	155	117	83.7	63.18
31	18	6.11	176	120	95.04	64.8
40	6	8.02	77	50	41.58	27
40	9	6.94	100	64	54	34.56
40	12	6.30	121	88	65.34	47.52
40	15	5.88	141	101	76.14	54.54
40	18	5.97	172	124	92.88	66.96
50	6	8.44	81	58	43.74	31.32
50	9	6.88	99	74	53.46	39.96
50	12	7.03	135	109	72.9	58.86
50	15	6.13	147	116	79.38	62.64
50	18	6.01	173	142	93.42	76.68
60	6	8.33	80	61	43.2	32.94
60	9	6.81	98	81	52.92	43.74
60	12	6.67	128	104	69.12	56.16
60	15	5.75	138	111	74.52	59.94
60	18	4.38	126	88	68.04	47.52

TABLE 24 SINGLE TOOTH TEST DATA SHEET (Stainless Steel 304L)

Band Speed V_b (m\min)	Set Depth of cut/tooth δas (μm)	E_{SP-t} (GJ/m3)	Cutting Force F_{v-fbt} (N)	Thrust Force F_{p-stt} (N)	Cutting force /tooth **(Calculated using Equation 5.5)** F_{v-fbt} (N)	Thrust force/tooth **(Calculated using Equation 5.5)** F_{p-stt} (N)
31	18	5.38	155	135	83.7	72.9
31	24	5.00	192	156	103.68	84.24
31	30	4.60	221	168	119.34	90.72
31	36	4.32	249	186	134.46	100.44
40	18	6.56	189	152	102.06	82.08
40	24	5.44	209	163	112.86	88.02
40	30	4.85	233	175	125.82	94.5
40	36	4.17	240	187	129.6	
50	18	6.42	185	161	99.9	86.94
50	24	5.57	214	175	115.56	94.5
50	30	4.94	237	192	127.98	103.68
50	36	4.51	260	200	140.4	108
60	18	7.01	202	147	109.08	79.38
60	24	5.73	220	154	118.8	83.16
60	30	5.38	258	176	139.32	95.04
60	36	4.76	274	245	147.96	132.3

APPENDIX 9

Contents

Chip Chart 1 : Workpiece-X

	30 m/min	50 m/min	70 m/min	90 m/min
6 µm	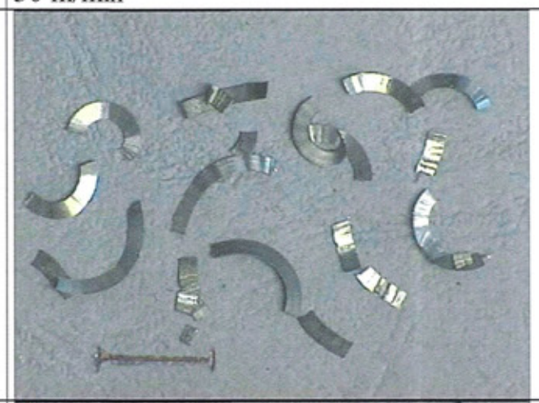	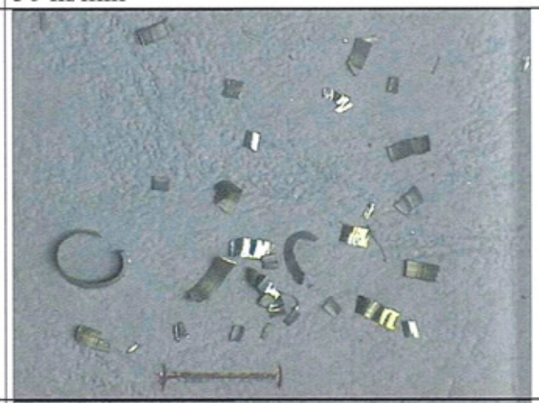		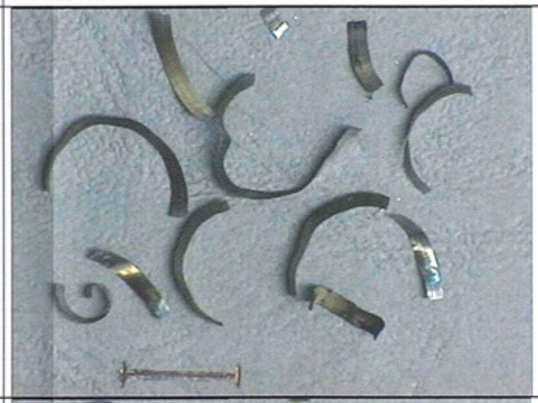
12 µm	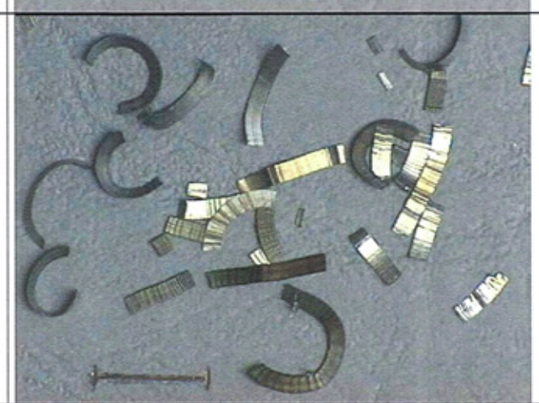			
18 µm		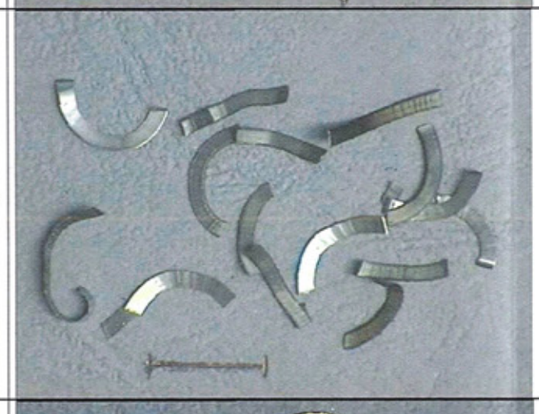		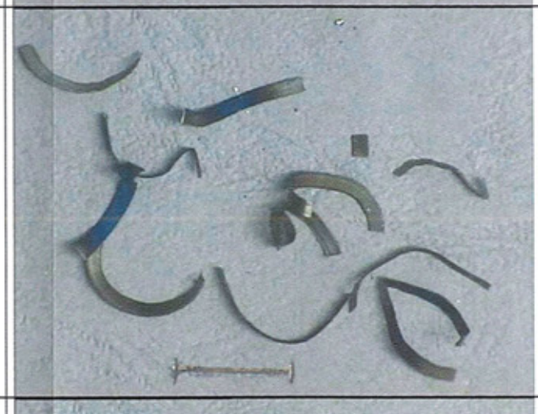
24 µm	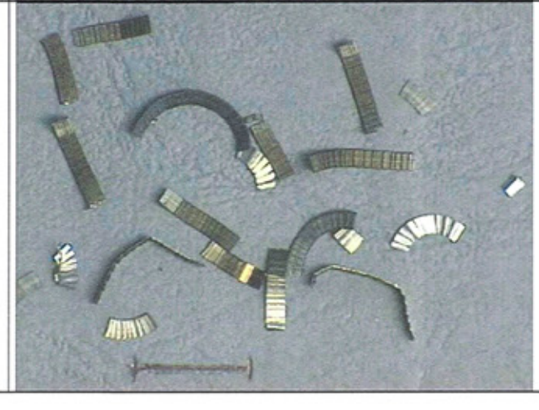	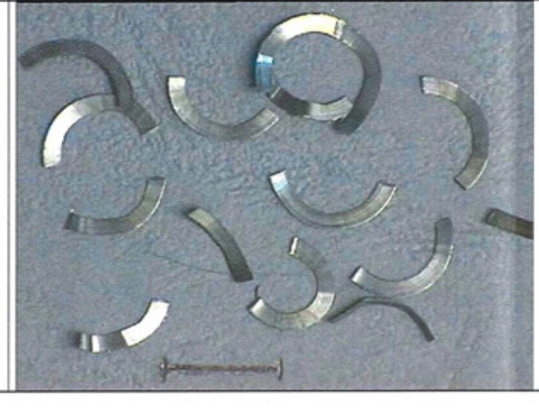	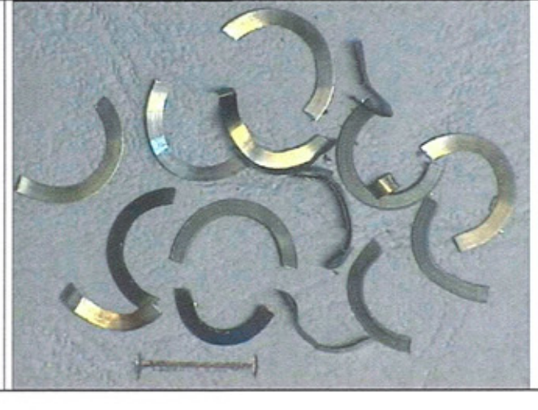	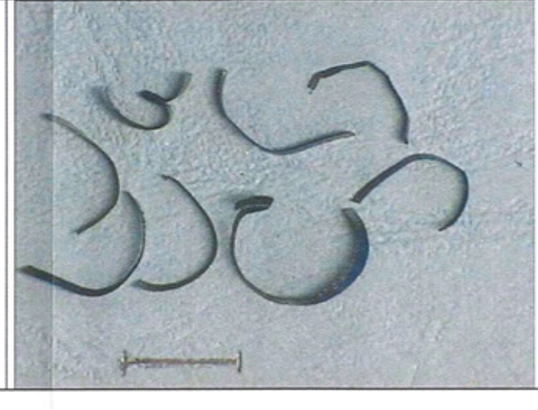

Chip Chart 2: Workpiece-Y

	30 m/min	40 m/min	50 m/min	60 m/min
6 µm	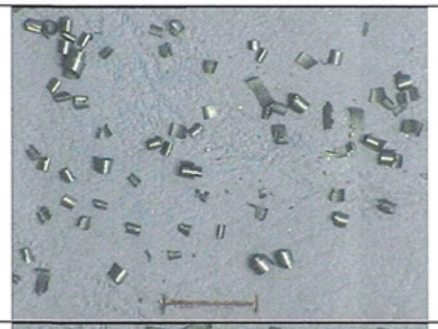	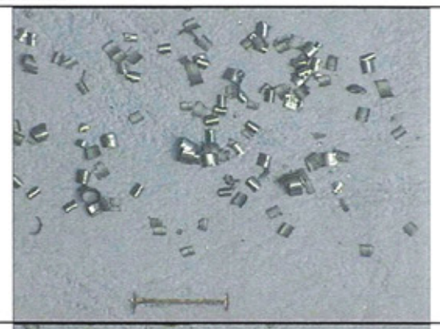		
9 µm	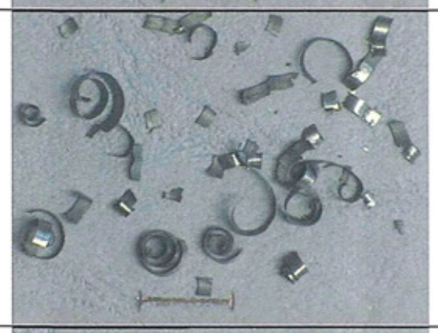	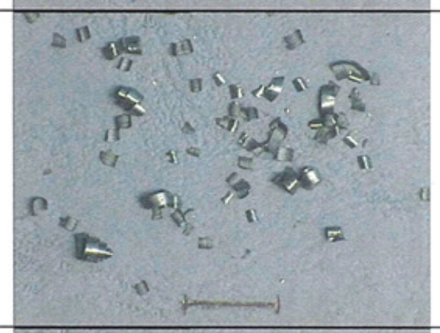	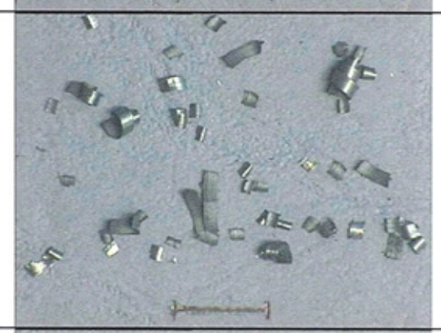	
12 µm				
15 µm	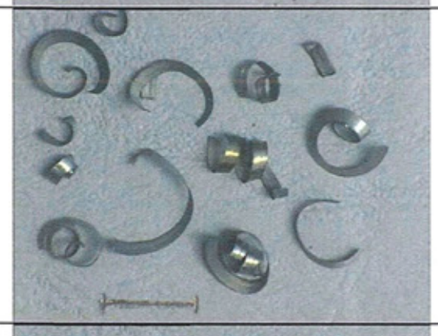	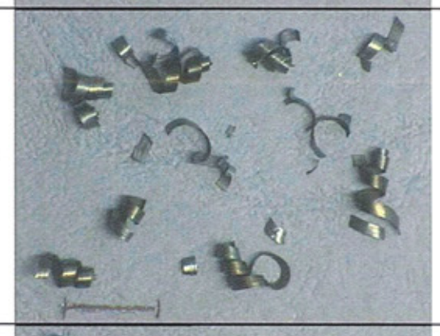	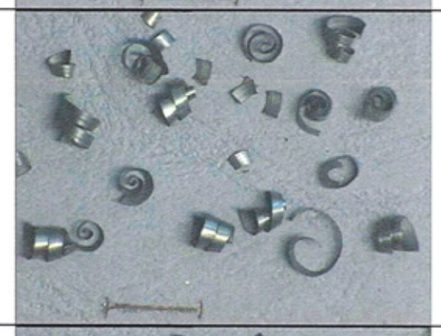	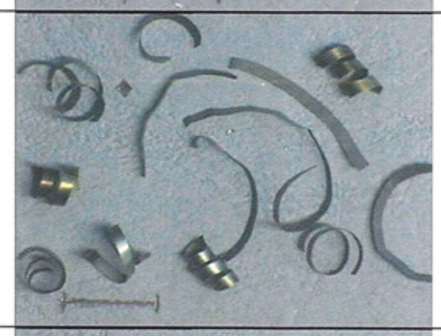
18 µm				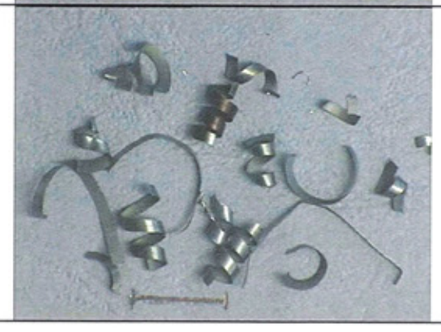

Chip Chart 3: Stainless Steel 304L

	30 m/min	40 m/min	50 m/min	60 m/min
18 µm		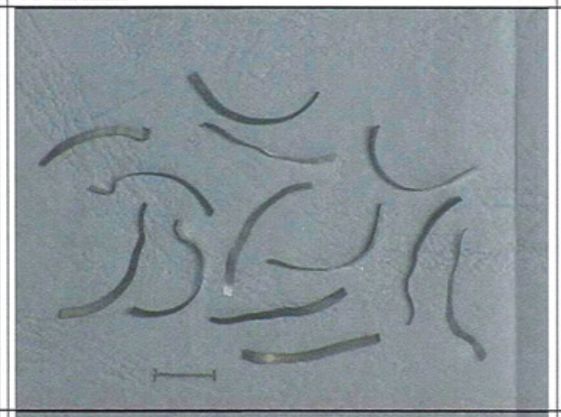		
24 µm				
30 µm				
36 µm			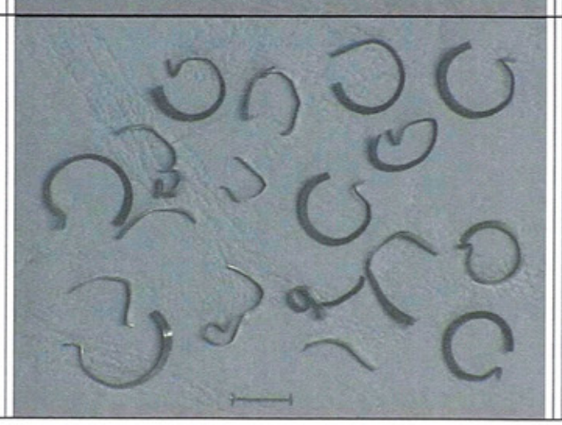	

APPENDIX 10

Published material

1. Sarwar, M; Hellbergh, H; Doraisingam, A.R; Persson, M;
   "Simulation of the intermittent cutting action of a bandsaw blade",
   12th International Conference on Flexible Automation & Intelligent Manufacturing, June 15, 2002

2. Sarwar, M; Hellbergh, H; Doraisingam, A.R; Persson, M;
   "Bandsawing of Ball Bearing steel", Fifth International Conference on the Behaviour of Materials in Machining, Chester, November 2002

3. Sarwar, M; Persson, M; Hellbergh, H; Doraisingam, A.R;
   "Sawability in the band sawing process when machining Hot and Cold work tool steels", Fifth International Conference on the Behaviour of Materials in Machining, Chester, November 2002

Simulation of the Intermittent Cutting Action of a Bandsaw Blade

M.Sarwar*, H. Hellbergh**, A.R. Doraisingam*, M. Persson**

*School of Engineering
University of Northumbria at Newcastle
Newcastle upon Tyne, NE1 8ST, United Kingdom

**BAHCO Metal Saws

ABSTRACT

Bandsawing is fast becoming the most preferred procedure for cutting-off standard workpieces owing to low kerf loss and high metal removal rates. One of the primary problems in evaluating metal bandsaws and developing newer variants, comprising of new saw tooth materials, their heat treatment, or different tooth forms and quality, has been costly and time consuming sawing tests. In order to overcome this, simulation work using a Single tooth test method previously developed was tested and validated. Cutting tests were performed at fine depths of cut (2-10μm) usually found in actual bandsawing process.
The test results showed that the test method adopted could be used to obtain cutting data in 'compressed time'. However, the method requires further improvement to reduce the scatter in the results.

1. INTRODUCTION

Metal sawing is an important primary operation for cutting-off raw material to size, in preparation for the secondary process. Power saws e.g. hacksaws, circular saws and bandsaws, which represent multi-point cutting operations are normally used for cutting-off to size. Recent trends in the manufacturing industry [1,2,3,4] has shown the bandsawing process to be the most preferred procedure for cutting-off standard workpieces to other sawing process (hacksaws, circular saws) owing to low kerf loss and high metal removal rate.

In order to have a better understanding of the mechanics of metal cutting in the bandsawing operation; there is an urgent need to establish fundamental data associated with forces, metal removal rate and specific cutting energy in order to improve the process and blade design. Furthermore demands are being placed on production engineers to cut-off to size new difficult to cut materials being developed to meet the future engineering requirements. In order to cut these effectively and efficiently, knowledge of the cutting conditions (speed, feed, forces and specific cutting energy) are absolutely vital.

Most of the earlier studies [2,3,5,6] concentrated on understanding the cutting action of bandsaws has been rewarding through studying the cutting mechanism of power hacksaw blades. However, this has been through simulation work using single point cutting tools. Although there are obvious differences between hacksaw and bandsaw blades, the geometries of the cutting edges, which primarily control the cutting performance, are very similar.

Sarwar [2,5,6] in his work on blunt tools, found that the depth of cut achieved by each blade tooth was smaller than the cutting edge radius of the saw tooth. As such, the cutting action of a bandsaw blade is classified as a blunt tool. The resulting cutting mechanism removes material by a complex combination of modes of chip formation [5]. In bandsawing operation the edge radius of nominally sharp tools can be in the range of 7μm-20μm. The average depth of cut achieved by each blade can be between 4μm-30μm [6].

One of the primary problems in evaluating metal bandsaws and developing newer variants, comprising of new saw tooth materials, their heat treatment, or different tooth forms and quality, has been costly and time consuming sawing tests. Furthermore, there are no simple ways of quantifying and evaluating the performance and life of these bands during sawing. Normally the time per cut as well as monitoring indirect parameters such as increase in cutting forces, or the amount of run-out of the saw kerf from the vertical plane are often used as performance criteria. This only gives global data, which is difficult to apply to individual teeth. Therefore there is a need to develop a single tooth simulation test which would be representative of a full product performance and give the fundamental data required for optimising the cutting conditions.

Bradbury, Sarwar and Archer [7,8,9], developed a single tooth simulation test using a specially adopted lathe machine. The method was devised to investigate and analyse the characteristics of bandsaw blade performance and design. Experiments [7] were conducted at 10-100 μm depth of cut, and were found to be useful in studying wear characteristics and blade performance. However, the depth of cut per tooth tested was not within the normal operating range, found in actual bandsawing process where depths of cut are between 4-30 μm [6].

This paper presents test results obtained using the Single Tooth Test Method for fine depths of cut cut 2-10 μm. previously not reported [7,8,9]

2. INSTRUMENTATION AND TESTING

The test method uses a lathe machine (1609 Dean Smith & Grace lathe machine) to simulate linear movement of the work-piece with the use of a specially designed work-piece and tool holder. The forces were measured using a three-force component Kistler dynamometer with piezo-electric transducers. This equipment was used to measure the cutting force and feed force components during the metal cutting process. The outputs from the Dynamometer were simultaneously fed into a high frequency amplifier and A/D converter (oscilloscope) where it was stored and presented via a program for visualisation. The experimental set-up is shown in Fig 1.

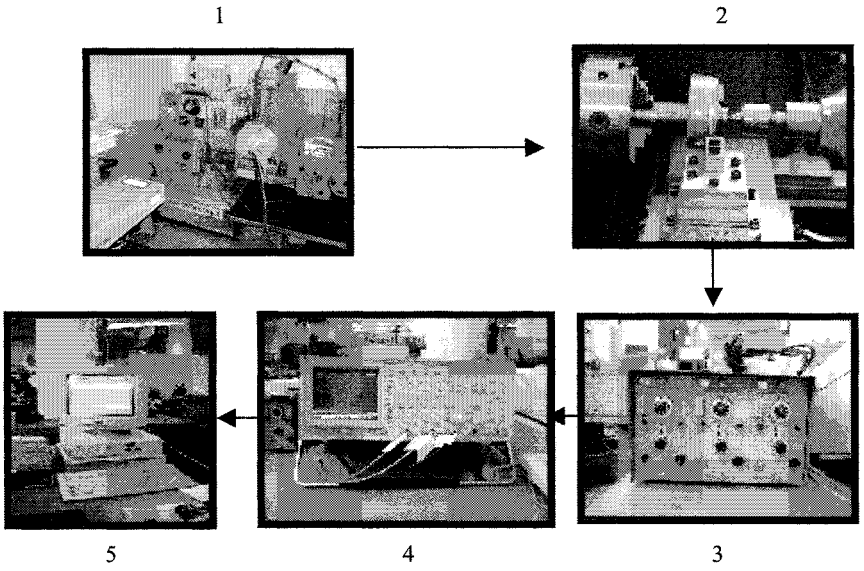

Fig. 1 Equipment used in this experiment.
1. lathe machine. 2. Kistler Dynamometer. 3. Charge amplifier. 4. 20Ms/sec Oscilloscope. 5 Computer

3. TOOTH SAMPLE

The cutting tool used in this experiment to simulate the intermittent cutting process was a single tooth cut out from a bandsaw blade, Fig 2. To prepare samples, blades were cut into two-tooth sections. While maintaining the gullet, one of the tooth tips was ground off, leaving just one tooth to be used in the cutting test, Fig 3. The cutting tools used in the test were un-set saw teeth samples from standard bi-metal, HSS M42, vari-pitch (2/3 TPI) Raker set bandsaw blades, produced using the milling process, Table 1.

Table 1. Tooth Geometry

Rake Angle	Clearance Angle	Tooth Width	Radius R1	Radius R2	Gullet depth	Pitch
10 °	25 °	1.3 mm	2.78 mm	6.30 mm	4.24 mm	2 TPI

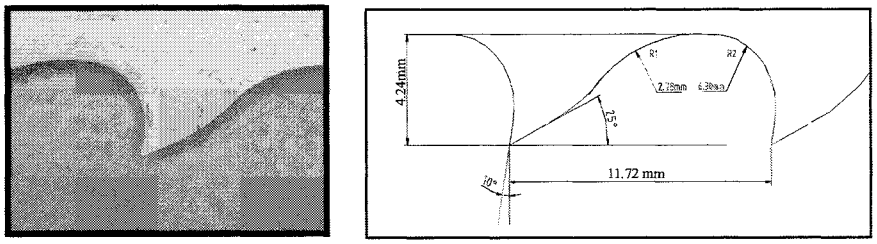

Fig 2. Un-set Tooth Geometry

Table 2. Nominal chemical compositions (wt.%) and hardness of tooth tip

	Composition						*Hardness HV1*
	C	***Cr***	***Mo***	***W***	***Co***	***V***	
AISI M42 HSS	1.08	3.9	9.4	1.5	8.0	1.3	880

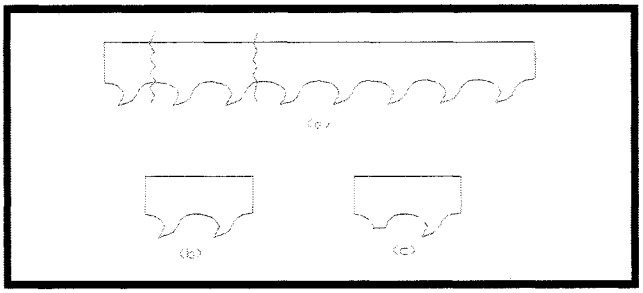

Fig 3. (a) showing section where the bandsaw is cut. (b) Two-tooth section of the bandsaw (c) One tooth is ground off for clearance.

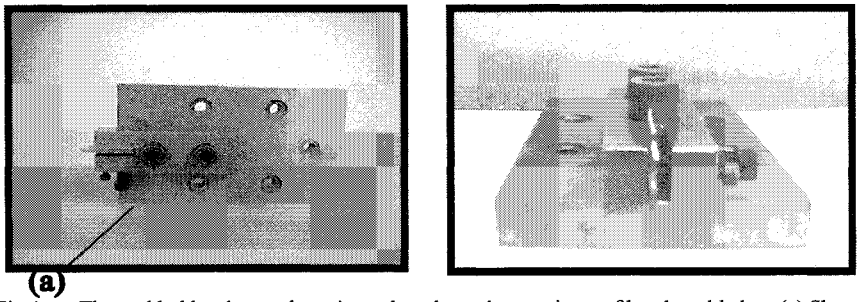

Fig 4. The tool holder shown above is used to clamp the cut pieces of bandsaw blades. (a) Shows where the tool is clamped

4. WORK-PIECE MATERIAL AND HOLDER

Rectangular 48x40x6.5 mm work-pieces were used in the test. The material used was standard steel with a Vickers hardness of 140 HV1, Table 3. For the purpose of the test, a work-piece holder was specially designed, Fig 5. The work-piece holder was a disc of 155 mm diameter with four slots machined on one side to take the workpiece samples, which were clamped to the disc using bolts. The back of the holder has a 90 mm long solid bar, diameter 45mm connection, which was held in a 3-jaw chuck, Fig. 6.

Prior to any test, the test-piece was pre-machined on the periphery using a parting tool. This was carried out in order to provide an arc on the sample workpiece. The diameter of the workpiece holder was of sufficient diameter to represent a linear cut, Fig. 7.

Table 3. Nominal chemical compositions (wt.%) and hardness of workpiece material

Material	*Composition*						*Hardness HV1*
	C	***Cr***	***Mn***	***S***	***Co***	***V***	
Standard Steel (BS 970)	0.4	0.25	1.3	0.12	-	-	140

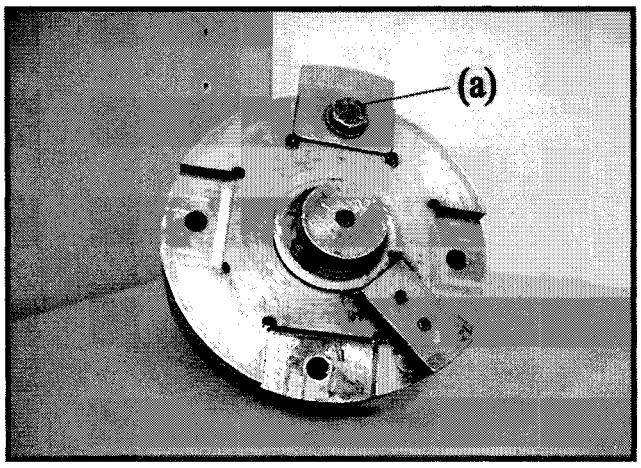

Fig 5. The face of the work-piece holder shows the slots where the test piece is inserted. (a) shows the test piece clamped in the slot

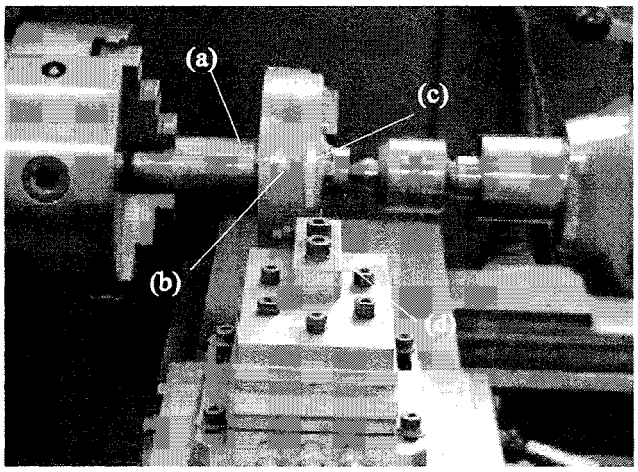

Fig 6. (a) shows the back end of the work-piece holder inserted into the lathe machine (b) work-piece holder (c) work-piece (d) tool holder

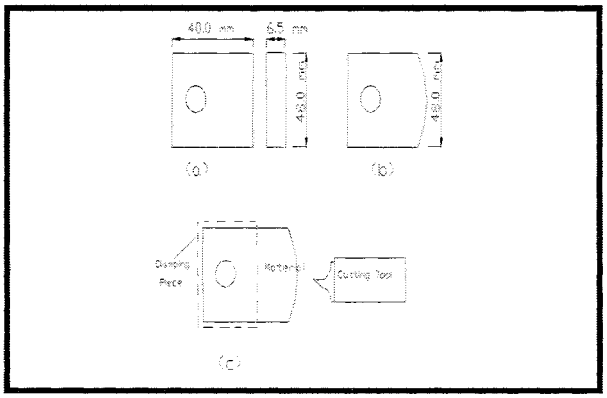

Fig 7, (a) Test material (b) Test material after machining (c) Cutting set-up

5. CUTTING TEST RESULTS

Cutting tests were carried out at depths of cut ranging from 2-50μm at cutting speed of 8 m/min. During each test the cutting force components **Fv** and **Fp** were monitored and recorded for each depth of cut. In order to overcome the stiffness of the tool holder cross-slide, each depth of cut was repeated 3 times and the corresponding chips were collected

weighed and the undeformed chip thickness ($\mathbf{h_0}$) calculated (Appendix 1). The specific cutting energy (**ESP**) was calculated from forces measured using the Kistler Dynamometer (Appendix 1). The results of the test are shown in Fig 8 and Fig 9.

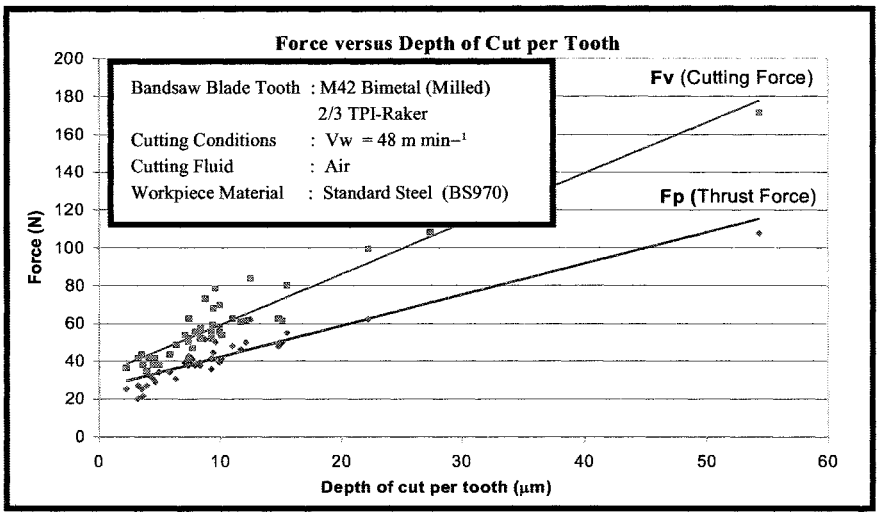

Fig 8. Influence of Depth of Cut on Cutting Force and Thrust Force during Performance Tests (Single Tooth Simulation Test)

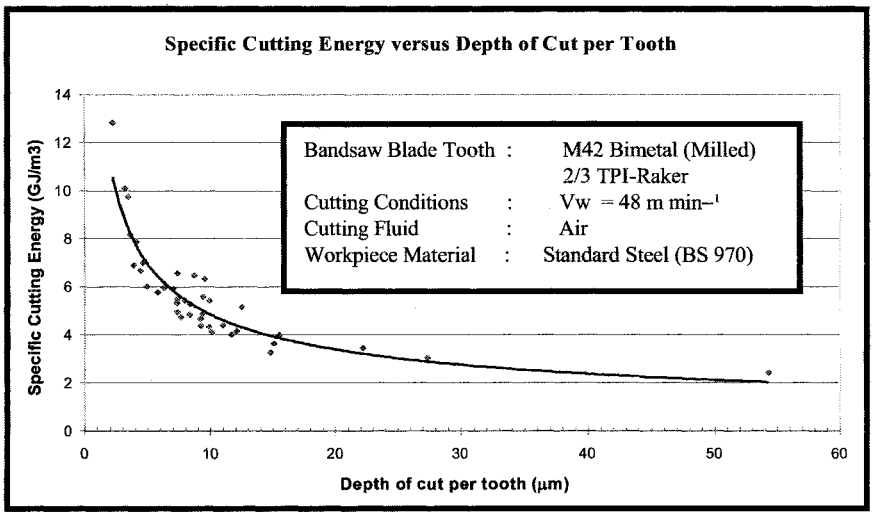

Fig 9. Influence of Depth of Cut on Specific Cutting Energy during Performance Tests (Single Tooth Simulation Test)

6. DISCUSSION

It has been shown that the single tooth test method utilised in the experiment can be used to simulate an actual bandsawing process, when cutting at fine depths of cut (2-10 μm). The forces recorded were between 20-60 N/tooth. This value falls within the range normally found in actual bandsawing process. However, the experiment was time consuming and inconsistent as the tests had to be repeated several times, before the required set depth of cut per tooth was achieved. Due to the stiffness of the tool holder cross-slide system, setting the depth of cut was not possible using the cross-slide dial. Setting was carried out manually and was based on trial and error. The depth of cut for each test conducted was quantified through calculation using the weight of the chip collected.

Cutting force and thrust force graphs plotted against cutting depth of cut per tooth illustrates a linear graph. The cutting force and thrust force components increased when the depth of cut per tooth increased, Fig 8. The variation in specific cutting energy against depth of cut per tooth gives a typical exponential curve. The effect of the edge radius of the cutting tool (saw tooth) is significant at lower depths of cut, giving an inefficient cutting action. When the depth of cut per tooth is increased, the edge radius effect decreases resulting in increased efficiency (low specific cutting energy), Fig 9. The specific cutting energy reaches a steady state at $2GJ/m^3$.

The large scatter in graph 1 and 2 shows that the results obtained are not consistent owing to the fragmented chips produced, and therefore the test method utilised requires further improvements in order to generate consistent and repeatable results.

7. CONCLUSION & RECOMMENDATION

Intermittent cutting using the single tooth simulation method for different depths of cut (2μm to 50μm) proved successful in the study of specific cutting energy and the cutting forces. The cutting depth per tooth achieved was very similar to that found in actual bandsawing process. The large number of results obtained for depths of cut per tooth in the range between 2μm to 15μm show that the testing method adopted can be used to simulate an actual bandsawing process. However, the large scatter in the results show that the testing method requires further improvement with the use of a better feed system. This can be achieved with the use of a precision cross-slide system, results of which will be reported in the future.

REFERENCES

[1] *Owen, J V; "Bandsaws join the mainstream", Manufacturing Engineering, , pp 28-39, Feb. 1997.*

[2] *Sarwar,M; "The mechanics of power hacksawing and the cutting action of blunt tools", Ph.D. thesis at Dept. of Mech. and Prod. Eng., Sheffield City Polytechnic, April 1982.*

[3] *Thompson, P J; "Factors influencing the sawing rate of hard ductile metals during power hacksaw and bandsaw operations", Metals Technology, pp 437-443, 1974.*

[4] *Hogan, J B; "Cutting the tough stuff", Manufacturing Engineering, 2, pp 62-68, 1999.*

[5] *Sarwar,M; Thompson, P J; "Simulation of the cutting action of a single hacksaw blade tooth", The Production Engineer, June 1974*

[6] *Sarwar,M; Thompson,P J; "Cutting action of blunt tools", International MTDR Conference, Manchester,1981*

[7] *Sarwar,M; Bradbury, S.R.; Dinsdale, M; "An approach to computer aided bandsaw teeth testing and design", Proc. 4th Nat. Conf. Prod. Res., Sheffield, Sept. 1998*

[8] *Archer, P M; Bradbury, S R; Sarwar,M; "Evaluation of performance and wear characteristics of bandsaw blades", 5th National Conference on Production Research, Huddersfield Polytechnic, August 1989*

[9] *Bradbury, S.R.; Sarwar, M; " Computer aided stress analysis in the design of bandsaw teeth", 4th International Conference on Computer-Aided Production Engineering, University of Edinburgh, November 1988*

Appendix 1

Cutting depth per tooth **ho,** was obtained by weighing the chip **wo** using a micro balance weighing machine (Sartorius Micro). When the cutting length (arc length $\mathbf{l_{arc}}$ in this case, measured and calculated to be 48.56 mm), cut width assumed to be the width of the teeth (measured to be **Wt**=1.30 mm) and the density (ρ=7850 kg/m^3) of the workpiece material is known, ho can be calculated.

$\rho = \mathbf{w_{chip}} / \mathbf{V_{chip}}$
(where, $\mathbf{V_{chip}}$ = volume of chip) (1)

Since $V_{chip} = ho * Wt * l_{arc}$

Therefore, expression (1) becomes,

$ho = w_{chip} / (\rho * Wt * l_{arc})$ (2)

The specific cutting energy ESP was calculated using the formula

$ESP = F_v / A_c$ (Where, $A_c = ho * Wt$) (3)

Sample calculation for chip 1:

$\mathbf{w_{chip}}$ = 0.02692 g , ρ=7850 kg/m^3 , **Wt**=1.30 mm, $\mathbf{l_{arc}}$ =48.56 mm

1) **ho** = $\mathbf{w_{chip}} / (\rho * \mathbf{Wt} * \mathbf{l_{arc}})$ .....(1)
ho = $(0.02692 \times 10^{-3}) / (7850 \times 1.3 \times 10^{-3} \times 48.56 \times 10^{-3})$
ho = 54.3 µm

2) **ESP** (Specific Cutting Energy) = $\mathbf{F_v}/\mathbf{A_c}$ ($\mathbf{F_v}$=171.5 N, $\mathbf{A_c}$ = **ho * Wt**) (3)
ESP = $171.5 / (54.3 \times 10^{-6})(1.3 \times 10^{-3})$
ESP = 2.4 GJ/m^3

Bandsawing of Ball Bearing Steel

M. Sarwar [a], H. Hellbergh [b], A. R. Doraisingam [a], M. Persson [a]

[a] *University of Northumbria at Newcastle, Ellison Building, Newcastle upon Tyne NE1 8ST, England*
[b] *Bahco Metal Saws AB, Box 833, SE-53118 Lidkoping, Sweden*

Abstract
Recent developments in bandsawing blades and machines are making it possible to saw previously difficult to cut materials. Furthermore material producers and stockholders are required to supply cut-to-size workpieces to the customers and therefore need to have scientific data relating to cutting conditions, tooth geometry and machine parameters which can then be used to optimise the cutting conditions. The work presented here relates to the bandsawing of Ball Bearing Steel (BS 535A99), which is high carbon medium chromium steel using two different teeth set patterns. The results should prove useful to the material producer and the production engineer.

1. Introduction

The development of newer and more accurate bandsawing machines, band materials and tooth designs, has lead to bandsawing becoming the most preferred method used in the manufacturing industry for cutting-off to size workpiece materials, compared to other traditional sawing methods [1]. The technological advancements in the bandsawing industry, such as the use of modern CNC controls has improved the bandsaw machines, allowing better control of the band feed. This has enabled manufacturers to machine difficult to cut materials faster and more accurately, thus reducing the cost [2] and meeting the needs of the supply chain.

In order to meet the present day requirements for high volume production, cutting different materials with high precision and speed, it has been necessary for blade manufacturers to constantly improve and develop their blade materials and tooth design. In the bandsaw blade market there are many different blades for hundreds of different applications [3]. Therefore, it is imperative that when bandsawing workpiece materials, the correct blade having the appropriate geometry is selected. The correct blade will cut faster, increase throughput, and save money [3]. It will also improve the product quality of the workpieces and result in longer band life. On the other hand, selecting the wrong blade can have serious repercussions. The blade can experience rapid wear and this leads to excessive blade changes and machine downtime.

Each material has its own sawing requirements. As such it is vital that bandsaw operators selects the appropriate blade to match the material to the tooth set, pitch, rake angle, gullet and tooth material. This paper presents work related to bandsawing Ball Bearing Steel (BS 535A99) using two different bandsaw blade tooth setting patterns. Both sets of bandsaw blades were produced from the same band coil, having the same tooth geometry (pitch, tooth material, gullet and rake). The only difference between the bandsaw blades was the setting of the teeth. The results of the test should prove useful to material producers and the production engineers when selecting the right bandsaw blade when sawing Ball Bearing Steels.

Nomenclature

0	Un-Set Tooth
R	Right Set Tooth
L	Left Set Tooth
F_P	Total (Maximum) Thrust Force
F_{P0}	Thrust Force Measured From Load Cell 1
F_{P1}	Thrust Force Measured From Load Cell 2
P.D	Positive Deviation
N.D	Negative Deviation

2. Test Methodology

2.1 Sawing Test Conditions

Machine	Behringer HBP420, 2-pillar
Coolant	Castrol Cooledge, 6.5% solution oil/water, at 3 liters/minute
Workpiece Material	Ball Bearing Steel (101 (OD) x 54 (ID) mm hollow bar) 210 HV1
Bandsaw Blade	3851-41-1.6-2/3 (Vari-pitch)-5800 (AISI M42 HSS Bi-Metal)
Tooth Geometry	Rake Angle γ = +10 °, Clearance Angle β= 25 °
Tooth Set Pattern	1. 0-R-L-R-L-R-L-0 (Combo-MM9927-A)
	2. 0-R-L-0-R-L-0-R (Raker-MM9927-B)
Band Speed	80 m/min
Set Depth/Tooth used	3 μm
Band Tension	180 MN/m²

2.2 Bandsaw Nomenclature/Specification

3851	-	41	-	1.6	-	2/3	- 5800
Product code		*Blade width (mm)*		*Blade thickness (mm)*		*Teeth per Inch (TPI)*	*Band length (mm)*

Above represents industrial codes used to describe bandsaw blades

2.3 Tooth profile for Raker and Combo Set

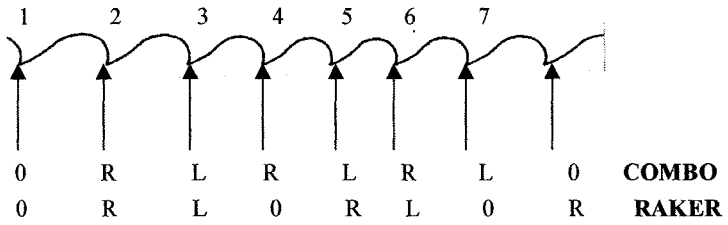

Fig.1 Bandsaw tooth setting

2.4 Bandsaw Blade Specification

The following bandsaw blades were used AISI HSS M42 Bi-Metal blades.

Nominal chemical compositions (wt.%) and hardness of bandsaw tooth material (as supplied by BAHCO)

Tooth Material	*Composition (wt.%)*						*Tooth / Back Hardness (HV1)*
	C	***Cr***	***Mo***	***W***	***Co***	***V***	
AISI M42 HSS Bi-Metal	1.08	3.9	9.4	1.5	8.0	1.3	880 / 480

2.5 Workpiece Material Specification

Bearings used under normal service conditions experience the effects of vibration, shock, misalignment, debris and handling. Therefore the bearing steel used for fabrication must provide toughness, a degree of temper resistance and microstructural stability. The material must also exhibit the obvious requirement of surface hardness for wear and fatigue resistance.

Fig. 2 shows the structure of ball bearing steel, which has been soft annealed in the as received condition. The material structure consists of high-carbon spheroidised cementite and carbides (5-10 %) embedded in a matrix of ferrite (not all the round particles are carbides). This material is prone to cause built up edge as chips adhere to the cutting edge.

Nominal chemical compositions (wt.%) of workpiece material Ball Bearing Steel Hollow Bar

Workpiece Material	*Composition (wt.%)*				
BALL BEARING STEEL (535A99)	**C**	**Si**	**Mn**	**S**	**Cr**
	1.00	0.15/0.30	0.4	0.025	1.30/1.60

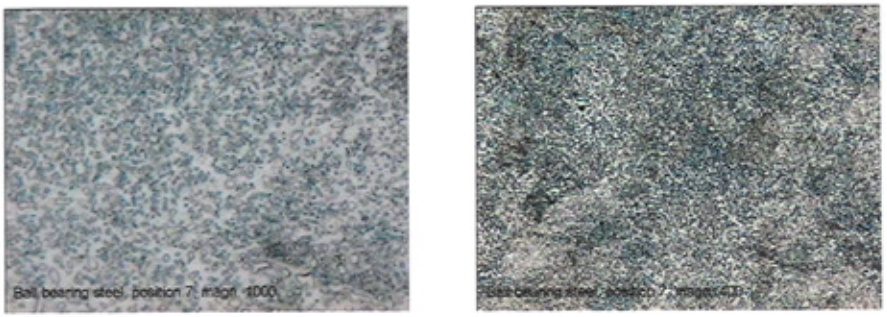

Fig. 2 microscopic examination of polished and etched surface of workpiece material.

3.0 Cutting Tests

Testing of the two bandsaw blades (Combo and Raker) were performed by sawing Ball Bearing Steel work-piece material at a depth of cut per tooth of 3μm at 80 m/min bandspeed. The cutting parameters selected represent typical cutting conditions used by bandsaw machine operators when sawing ball bearing steel hollow bar. The test programme was run, by taking thrust force measurements at the first cut and after every 20 cuts. The sawing tests were continued until the thrust force increased by 50% of the first cut. The bandsaw was removed and cut into 21 tooth sections and the wear flank area of the saw teeth was measured using the SKIM (**S**andvik, **K**loster **IM**) Technique.

3.1 Instrumentation & Experimental Set-up

The test machine used was a 2-Column Behringer Bandsaw Machine, which had capability of measuring only thrust forces. The thrust force was measured using two load cells, which are beam strain gauges (HBM Z6). The readings from the load cells were fed directly into the data logger (HBM Spider8) where it is converted into meaningful data with the use of a software called HBM Catman. The program then gives a graphical representation of the thrust forces measured from the two load cells. The thrust force used for the purpose of this study was the total thrust force **Fp**, which is the sum of the thrust forces measured by the 2 load cells.

4.0 Results & Discussion

4.1 Cutting Tests Results

Sawing of the workpiece material was continued until the thrust force (F_P) increased by 50% of the first cut. The results of the test are shown in the table below, **Fig.3.** The thrust force (F_P) for the Combo set increases faster than the Raker set. The number of cuts that it took for the thrust force (F_P) to increase 50% was 21 cuts with the Combo set and 41 cuts with the Raker set.

Sample	Thrust Force, F_P (N)		
	1st Cut	21 Cuts	41 cuts
COMBO	462	697 (50% of first cut)	
RAKER	468	586	708 (50% of first cut)

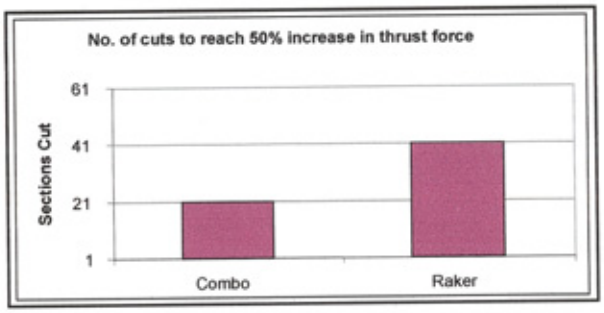

Fig.3 *Wear test results for Combo & Raker tooth setting for 3μm depth of cut per tooth, cutting speed 80 m min^{-1}*

4.2 SKIM Wear Measurement

The wear area measured for the Combo set was in the region between 0.06 mm² to 0.13 mm². The wear area measured for the Raker set was between 0.03 mm² and 0.08 mm². The Combo set in comparison to the Raker set after 41 cuts was shown to exhibit more wear. The effects of tooth setting can be seen to play an important role. To investigate the effects of tooth setting on flank wear, statistical analysis of the measured wear area for both variants were performed. In order to understand how the effects of the tooth setting was influencing the performance of both bandsaw blades, the wear area of the all the teeth in a set was measured. In Combo, there are 7 teeth in a set, 0-R1-L1-R2-L2-R3-L3, the sequence repeats starting again at 0 (straight tooth). For Raker there are only 3 teeth in a set, 0-R-L, this sequence repeats through out the band. The analysis shows a large variation in flank wear area in the Combo set (variation between right/left/unset), **Fig.4 and 5**. This variation can however not be seen in the Raker set, where the flank wear area is almost the same for all types of teeth, **Fig 6**. Variations in flank wear, for the Combo set shows the un-set teeth to

have the most wear followed by the right-set and the left-set. In the Raker set, the right-set teeth has the most wear, however the difference in wear in comparison to the left-set teeth is small. Wear area observed with the Raker set suggests uniform distribution of workload during cutting. This is not observed in the Combo set where the work, is mostly performed by the Un-set tooth, **Fig.4 and 5**

The large wear area observed in the Combo set show that the un-set teeth remove the most work piece material. The setting of the saw teeth causes a shadowing effect, where large parts of the saw teeth edges are blocked by the previously differently set saw teeth, **Fig. 7.** This mainly applies to the regions after the neutral saw tooth where corners of other saw teeth cut instead. The cutting action of the un-set teeth is symmetrical while the right-set and the left-set teeth are subjected to a larger load on the outer corners. **Fig. 7** shows that the distribution of work is more uniform for the Raker set pattern. For the Combo set pattern the second and third right/left-set teeth experiences less wear than the other types of teeth, because the shadowing effect causes these teeth to cut smaller chips. As such the combo set pattern experiences less uniform wear. Thus some of the teeth will be worn more than others.

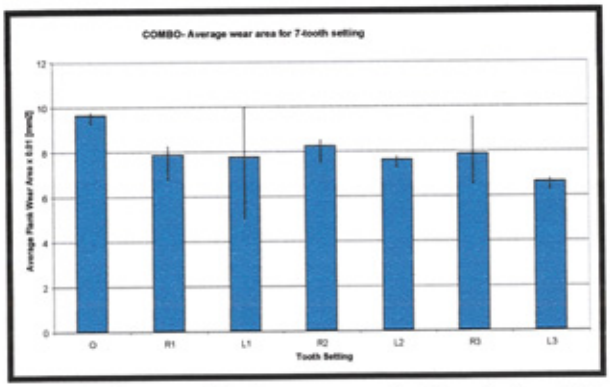

Fig. 4 *Average flank wear area for Combo band for a set of 7 teeth (measured for all the teeth in the band)*

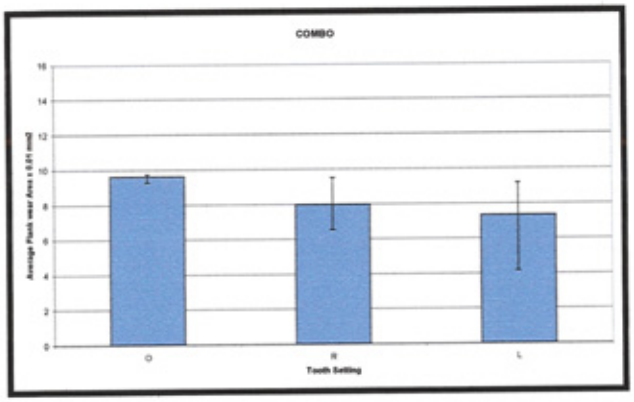

Fig. 5 Variation in average flank wear area in Combo set for un-set, right-set and left-set tooth (measured for all the teeth in the band)

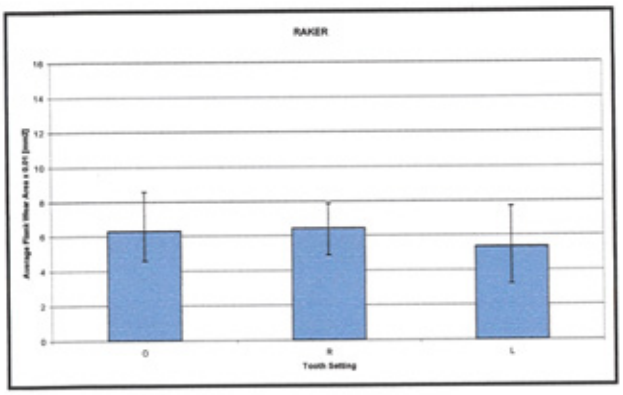

Fig. 6 *Variation in average flank wear area in Raker set for un-set, right-set and left-set tooth (measured for all the teeth in the band)*

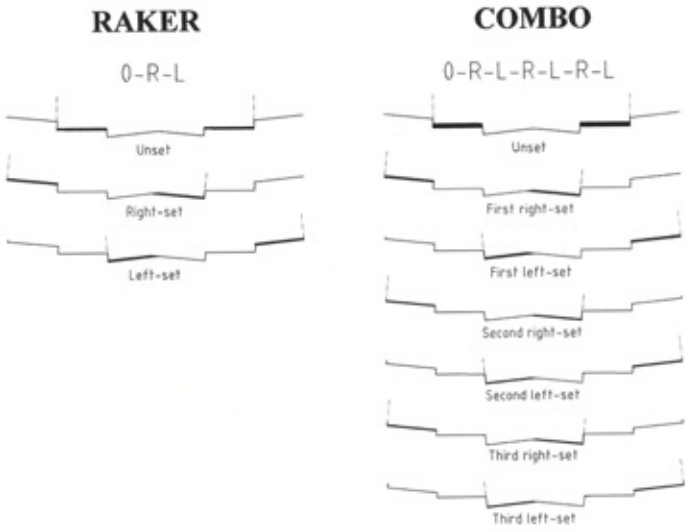

Fig. 7 *Chip cross section removed by the different set teeth during bandsawing*

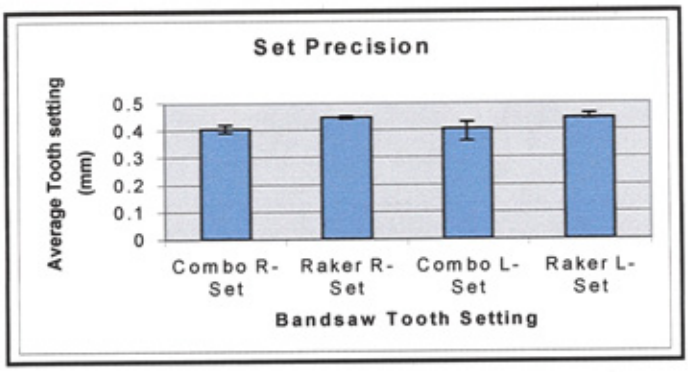

Fig.8 *Comparison of the setting accuracy between Combo and Raker set pattern*

Fig. 8 shows the difference in the setting precision for both variants. The graph shows the Raker set to have a better quality tooth setting than the Combo set, illustrated by the positive and negative deviation. The setting process for the raker set pattern during manufacturing is less complicated and is better controlled as compared to the Combo set pattern. The accuracy in the tooth setting can have a significant effect on the distribution of the workload during sawing. Uneven distribution of the workload causes some teeth in the blade to do more work than others. This causes the blade to wear faster, thus results in shorter band life.

5. Conclusion

The wear test results have shown the Raker set to have a better service life, using 50% increase in thrust force as criteria. Wear measurements for the teeth using the SKIM method showed small wear area, between 0.03 mm^2 to 0.08 mm^2, for the Raker set and between 0.06 mm^2 to 0.13 mm^2 for the Combo. Tooth setting and the setting precision of the bandsaw blade were found to influence band life. The distribution of the workload across each tooth during sawing was shown to have an influence on the wear life of the bandsaw blade. Setting precision of the teeth forms the principal factor that determines the way in which the workload is shared between the teeth. The Raker set was shown to have a better quality tooth setting than the Combo set. As such, the flank wear measured was far less when compared to the Combo set. Another factor, which was found to have a significant effect on wear, was the setting pattern. It was observed in the Combo set, that due to the shadowing effect, most of the work was performed by the un-set teeth followed by the right-set and left-set. In the Raker set, the effect of shadowing was minimal. As such the distribution of the workload during sawing was uniform, resulting in better band life.

Ball bearing steel can be a difficult material to saw due to the abrasive nature of the material as well as being prone to cause BUE. The study performed has shown that by selecting a bandsaw blade with a Raker tooth setting doubles production rate and consequently saves cost.

6. Reference

1. Owen, J V; "Bandsaws join the mainstream", Manufacturing Engineering, Feb. 1997, pp 28-39

2. Hogan, J B; "Cutting the tough stuff", Manufacturing Engineering, 2, 1999, pp 62-68

3. Rozzi, R; "choosing the right blade for your Job", Manufacturing Engineering, Feb.2001, pp 56-60

Sawability in the Bandsawing Process when Machining Hot and Cold Work Tool Steels

M. Sarwar [a], M. Persson [a], H. Hellbergh [b], A. R. Doraisingam [a]

[a] *University of Northumbria at Newcastle, Ellison Building, Newcastle upon Tyne NE1 8ST, England*
[b] *Bahco Metal Saws AB, Box 833, SE-53118 Lidkoping, Sweden*

1.0 Introduction

Bandsawing is an important operation in a variety of industries, particularly steel suppliers, which need to cut-off to size raw material for secondary processes. There is a recent trend for steel stockholders to supply their customers with materials cut-off to size through their specialised cutting centres. Bandsawing offers the advantage of high automation possibilities, high cutting rate, low kerf loss, straightness of cut, reasonably good surface finish and long tool life. Most modern industrial bandsaw machines operate with a constant feed rate that apparently should give the teeth a constant depth of cut throughout the operation. One specific feature of the bandsaw metal-cutting operation is that the depth of cut per cutting edge is small (5μm - 50 μm). The cutting edges themselves are not infinitely sharp but have various edge defects (burrs, radii etc) owing to the manufacturing processes employed. The quality of bandsaws has drastically improved over the last few years by introduction of grinding as a method of producing teeth, resulting in sharper teeth with fewer defects and better tooth height precision.
This paper will present bandsaw performance results for cutting two specific tool steels of importance to manufacturing industry.

2.0 Equipment and experimental details

2.1 Bandsaw machine

The Behringer bandsaw machine used in the experiments is a constant-feed horizontal bandsaw, meaning that it feeds the band vertically (at a constant feed rate) through the workpiece, as seen in **figure 1**. The bandsaw machine has been modified, facilitating cutting and thrust force measurement as well as feed rate measurement. The cutting force (F_V) and thrust force (F_P) components are shown in **figure 1**. Prior to experiments being carried out, the machine was calibrated. The test was carried out using cutting fluid (7% Castrol Cooledge 5 in water) at a flow rate of 3.3 litres/minute.

Table 1. Behringer bandsaw data

Machine Model	Behringer HBP650/850A/CNC
Band Length	8800 mm
Band Width	67 mm or 54 mm
Maximum Workpiece Dimension	850 mm x 650 mm
Minimum Workpiece Dimension	20 mm x 20 mm
Cutting Speed	20-300 m/min
Weight	9000 kg
Motor Power	22 kW

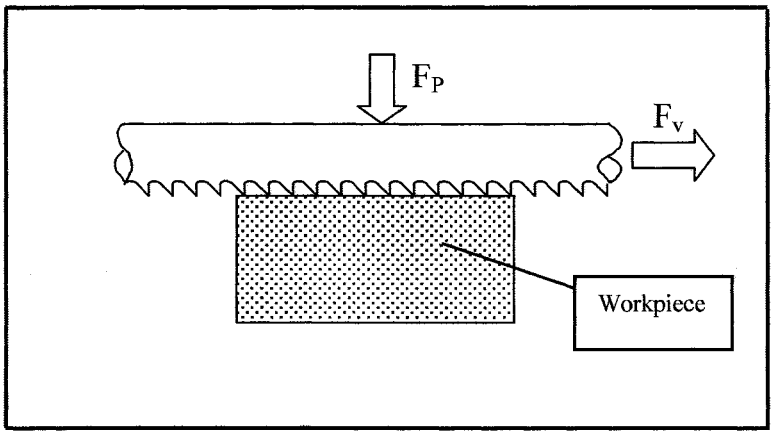

Fig. 1 Horisontal cutting bandsaw. Thrust force F_P and cutting force F_V

2.2 Bandsaw blade

Details about the bimetal bandsaw blade used in testing is shown in **table 2.**

Table 2. Bahco bandsaw blade

Bandsaw product name: Bahco 3854-54-1.6-PHG-1.4/2-8800
Bandsaw body material: Spring steel AISI D6A
Tooth edge material: High speed steel AISI M42
Bandsaw thickness: 1.6 mm
Bandsaw width: 54 mm
Bandsaw length: 8800 mm
Hardness of tooth edge: 900 HV1
Hardness of bandsaw body: 500 HV1

2.3 Workpiece materials

2.3.1 Uddeholm Sleipner, cold work tool steel

Cold work tool steels are used for tools in cold working operations such as forming, blanking, cold drawing, punching, cold rolling, compacting dies, cold extrusion etc.

The nominal chemical composition of the Sleipner material is presented in **table 3.** The material is classed as a general purpose Chromium-Molybdenum-Vanadium alloyed tool steel for medium-run tooling applications. It was recieved in soft annealed condition with nominal physical properties as presented in **table 4.** The workpiece had dimensions 254*84 mm (W*H). The hardness and microstructure was investigated at several positions of the workpiece to assure that it was uniform, these positions are shown in **figure 2.** Hardness of the tested material is presented in **table 5,** where it can be seen that the hardness of the workpiece is fairly uniform, although the centre of the workpiece is slightly softer than the surface. The microstructure consists of ferrite with large (up to 75 μm) carbides embedded in it, as seen in **figures 3 and 4.** There is a difference in carbide size and distribution between the surface and the centre of the workpiece, something that could affect the cutting performance as the bandsaw cuts through the workpiece.

Table 3. Nominal chemical composition of Uddeholm Sleipner, weight%

Carbon	Silicon	Manganese	Molybdenum	Chromium	Vanadium	Iron
0.9	0.9	0.5	2.5	7.8	0.5	Remainder

Table 4. Nominal physical properties, Sleipner

Density at 20 °C, kg/m^3	7730
Youngs Modulus, N/mm^2	205000
Thermal conductivity, W/m*°C (at 400 °C)	25
Specific heat, J/kg*°C (at 20 °C)	460

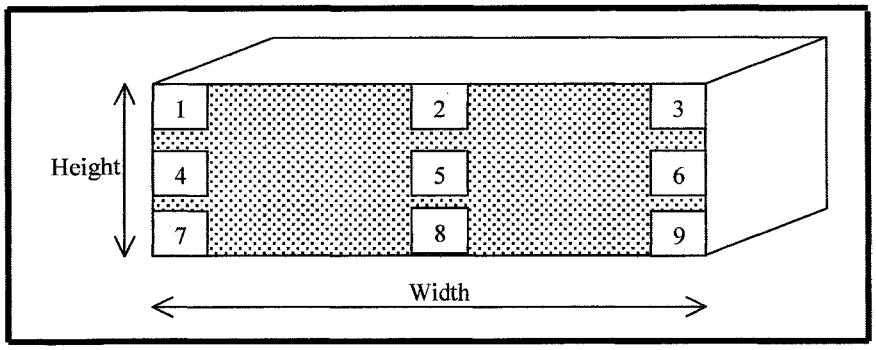

Figure 2. Position of test pieces on workpiece

Table 5. Hardness of Sleipner workpiece

Test piece position:	1	2	3	4	5	6	7	8	9
Average Vickers hardness (HV1):	244	238	234	229	220	240	230	232	228

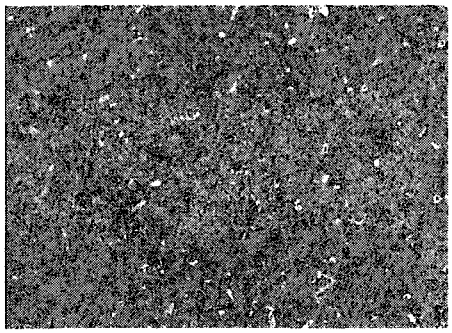

Figure 3. Microstructure of Sleipner, position 1, magnification 100X, etched. Picture size: 625 µm / 470 µm

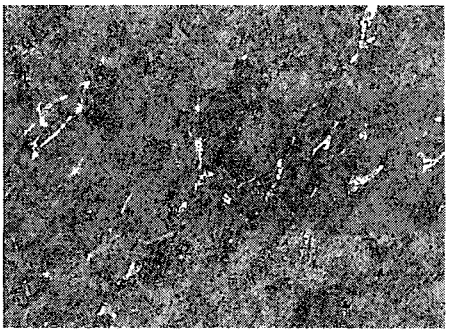

Figure 4. Microstructure of Sleipner, position 5, magnification 100X, etched. Picture size: 625 µm / 470 µm

2.3.1 Uddeholm Dievar, hot work tool steel

Hot work tool steels are used in tools processing molten or heated metal or polymer, as in die casting moulds or hot extrusion nozzles and inserts, operating at high temperatures (500 °C in some extrusion operations). The steel has to maintain its mechanical properties and wear resistance at elevated temperatures. The nominal chemical composition of the Dievar material is presented in **table 6.** The material is classed as a Chromium-Molybdenum-Vanadium alloyed tool steel. The material was recieved in soft annealed condition with nominal physical properties as presented in **table 7.** The workpiece had dimensions 254*77 mm

(W*H). The hardness and microstructure was investigated at several positions of the workpiece, according to **figure 2** in **section 2.3.1**. Hardness of the tested material is presented in **table 8**, where it can be seen that the hardness of the workpiece is uniform. The microstructure, **figures 5 and 6**, consists of ferrite and possibly also small amounts of lamellar pearlite. There are numerous dispersed carbides (not seen in figures) that can be seen at magnification 400X. The microstructure is also uniform in the workpiece, having similar grain size and carbide distribution in the surface and centre of the workpiece.

Table 6. Nominal chemical composition of Uddeholm Dievar, weight%

Carbon	Silicon	Manganese	Molybdenum	Chromium	Vanadium	Iron
0.3	0.2	0.5	2.2	5	0.6	Remainder

Table 7. Nominal physical properties, Dievar

Density at 20 °C, kg/m^3	7800
Youngs Modulus, N/mm^2	210000
Thermal conductivity, W/m*°C (at 400 °C)	31
Specific heat, J/kg*°C (at 20 °C)	not available

Table 8. Hardness of Dievar workpiece

Test piece position:	1	2	3	4	5	6	7	8	9
Average Vickers hardness (HV1):	160	160	157	167	161	162	166	156	155

Figure 5. Microstructure of Dievar, position 1, magnification 200X, etched. Picture size: 313 µm / 235 µm

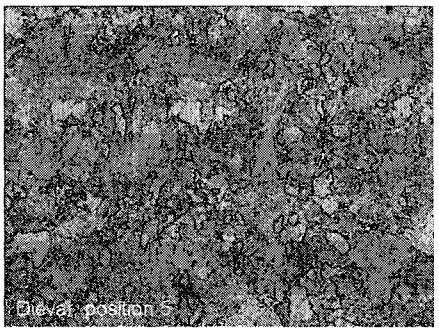

Figure 6. Microstructure of Dievar, position 5, magnification 200X, etched. Picture size: 313 µm / 235 µm

3.0 Results

3.1 Sleipner material (cold work tool steel)

The bandsaw cutting results for the Sleipner material is seen in graphs 1 and 2, showing the results for different cutting speeds to assess the machinability of the workpiece material. These results will be discussed in section **4.1**.

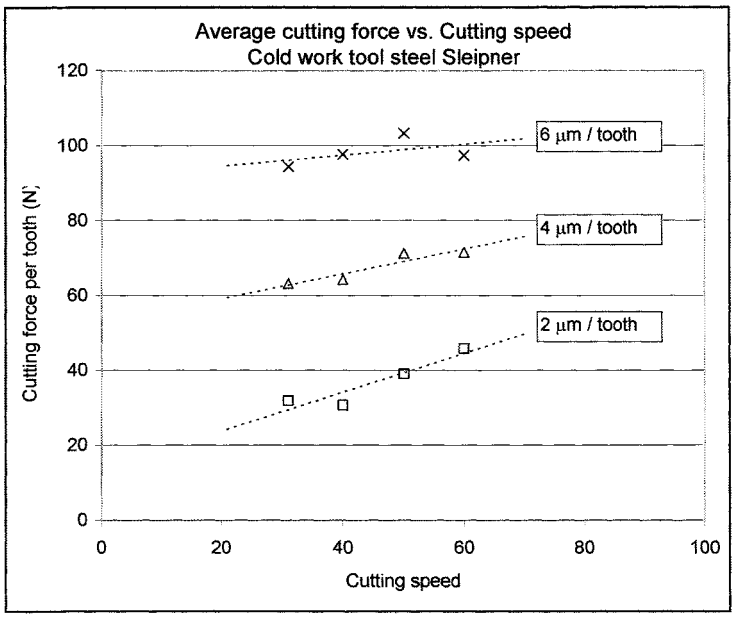

Graph 1 Sleipner material. Average cutting force vs. cutting speed and depth of cut per tooth

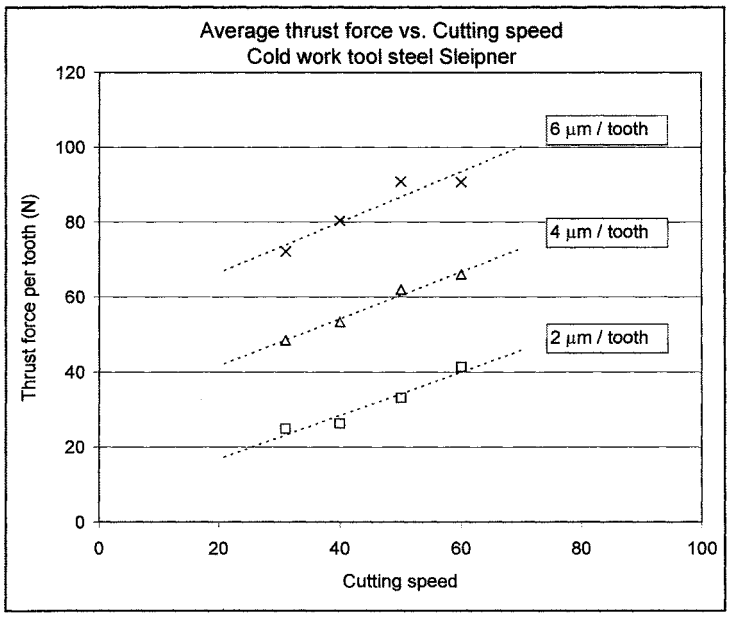

Graph 2 Sleipner material. Average thrust force vs. cutting speed and depth of cut per tooth

3.2 Dievar material (hot work tool steel)

The bandsaw cutting results for the Dievar material is seen in graphs 3 and 4, showing the results for different cutting speeds to assess the machinability of the workpiece material. These results will be discussed in section **4.2.**

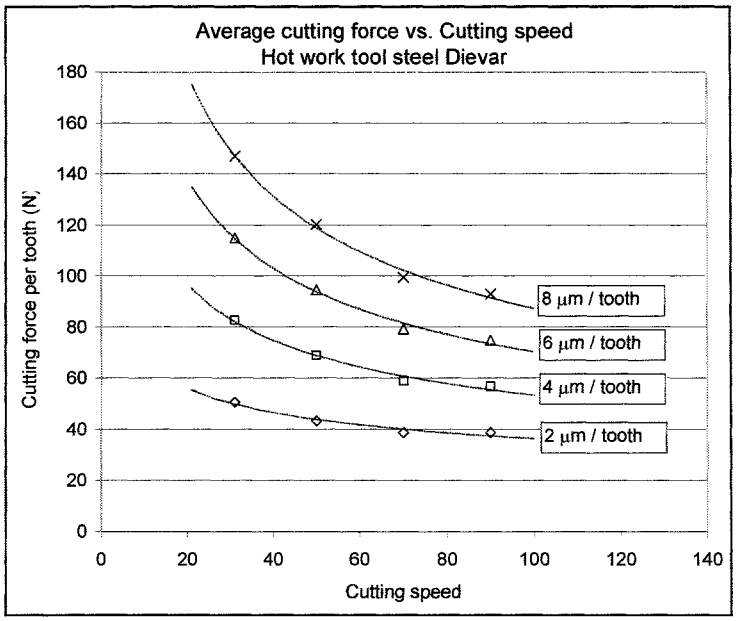

Graph 3 Dievar material. Average cutting force vs. cutting speed and depth of cut per tooth

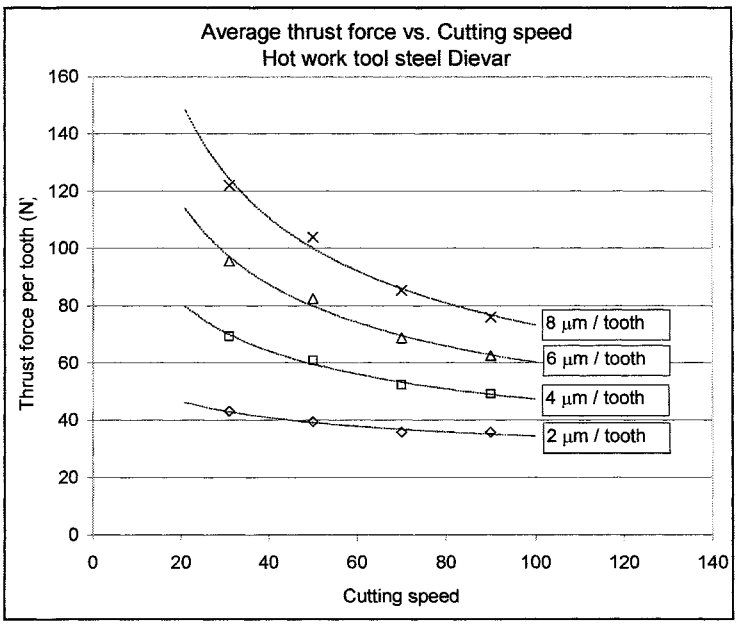

Graph 4 Dievar material. Average thrust force vs. cutting speed and depth of cut per tooth

4.0 Discussion

4.1 Cold work tool steel Sleipner

In graphs 1 and 2, the response to an increasing cutting speed needs explaining. As the cutting speed is increased (with constant depth of cut per tooth maintained), cutting and thrust force increases. Previous bandsaw testing by the author and colleagues (not reported) has shown that for many steel grades, the forces will remain on the same level or decrease with increasing cutting speed.

In the shear zone of the chip formation, increased strain rate (higher cutting speed) will normally result in increased strain hardening, giving increased shear strength of the workpiece material. Higher strain rate also produces more heat, which will soften the material and decrease the shear strength. If the softening from a higher temperature is greater than the hardening from increased strain rate, the cutting force will be decreased as the cutting speed is increased. However in the case of this cold-work tool steel it would seem as if the strain hardening produced is higher than the softening from increased temperature, giving higher forces as the cutting speed is increased. There is also a possibility that there are other mechanisms creating this behaviour.

Looking at the microstructure of the material, some interesting observations can be made. The structure consists of a relatively hard ferrite (appr. 230 HV) due to the high carbon and alloy content. A high-strength ferrite will result in lower machinability, but it will not explain the peculiar strain-rate response.
Also, the microstructure contains relatively large carbide clusters (up to appr. 75 μm). According to the ASM Handbook **[11]**, the abrasive alloy carbides have an adverse effect on machining characteristics, more than the higher hardness of its ferrite matrix would suggest. Since the depth of cut per tooth is small in band sawing, large carbides can probably not be cut but would rather be crushed or "ripped" out of the ferrite matrix. This fact is likely to affect the chip formation and could cause a continuously interrupted chip to take place.

It is difficult to predict what exact effect the above factors (strain hardening, ferrite properties, carbide size/distribution) would have on the cutting and thrust forces. To explain the strain-rate response when band sawing this material, further investigation is required on the effect of matrix hardness, matrix structure and carbide size and distribution.

4.2 Hot work tool steel Dievar

The ASM Handbook **[11]**, states that this hot work tool steel has better machinability than many cold work tool steels. The authors finds this to be true, the Dievar material can be band sawn at higher cutting speed, resulting in a more productive bandsaw operation.
Graphs 3 and 4 show that the response to an increasing cutting speed is the opposite to that of the cold work tool steel. As the cutting speed is increased, the forces decrease. Following the same reasoning used in section 5.1, the strain rate response of the hot work tool steel seems opposite to that of the tested cold work tool steel. If this is so, a higher strain rate causes more softening due to heat than it causes strain hardening.

There are a few significant differences between the materials that can cause the difference in machinability and productivity; one important difference is probably the hardness and strength of the ferrite matrix (Dievar 160 HV, Sleipner 230 HV). Another important difference could be the carbon content and the carbide size and distribution. For the cold work tool steel, a relatively high carbon content (0.9 w%) together with a high alloying content in general produces a ferrite matrix with higher strength than the hot work tool steel (with 0.3 w% Carbon), it also produces large carbides that are relatively widely spaced compared to the Dievar material. In the Dievar material there are no large carbides but instead the carbides are very fine and evenly distributed.

It is not possible to determine the cause of the difference in strain rate response between the two materials, but it can be concluded that when cutting Dievar it is preferable to use a high cutting speed as the cutting and thrust force will decrease with increasing strain rate (for the range of cutting speeds tested).

5.0 List of references

[1] J. V. Owen, Manufacturing Engineering, Feb. 1997, 28-38

[2] M. Sarwar, P.J. Thompson, International MTDR Conference, Manchester, (1981) 295-303

[3] P. Wallén, S. Jacobson, S. Hogmark, Report UPTEC 87 104 R, Uppsala University, Sweden, , 1987

[4] C. Andersson, J.-E. Ståhl, H. Hellbergh, International Journal of Machine Tools and Manufacture, 41 (2001) 237-253

[5] S. Elanayar, Y.C. Shin, Journal of Manufacturing Science and Engineering, 118 (1996) 359-366

[6] D.W. Smithey, S.G. Kapoor, R.E. DeVor, International Journal of Machine Tools and Manufacture, 40 (2000) 1929-1950

[7] P.M. Archer, S.R. Bradbury, M. Sarwar, 5:th National Conference on Production Research, Huddersfield Polytechnic, (1989) 443-451

[8] M.M. Ahmad, B. Hogan, E. Goode, International Journal of Machine Tools and Manufacture, 29 (1989) 173-183

[9] L. Åhman, S. Söderberg, M. Svenzon, Scandinavian Journal of Metallurgy, 11 (1982) 299-308

[10] L. Åhman, S. Söderberg, Report UPTEC 81 72 R, Uppsala University, Sweden, 1981

[11] ASM Specialty Handbook, 1995, Machining of tool steels, 352-376